NASA TN D-1523

TECHNICAL NOTE

D-1523

OPTICAL PROPERTIES OF SATELLITE MATERIALS —

THE THEORY OF OPTICAL AND INFRARED PROPERTIES OF METALS

By Research Projects Division

George C. Marshall Space Flight Center
Huntsville, Alabama

NATIONAL AERONAUTICS AND SPACE ADMINISTRATION

WASHINGTON March 1963

NATIONAL AERONAUTICS AND SPACE ADMINISTRATION

TECHNICAL NOTE D-1523

OPTICAL PROPERTIES OF SATELLITE MATERIALS--

THE THEORY OF OPTICAL AND INFRARED PROPERTIES OF METALS

By Research Projects Division

SUMMARY

The probable effects of solar radiation, primary cosmic rays, van Allen radiation and meteoric dust on the emissive properties of materials are reviewed in the light of recently published data.

Experimental data on the spectral emittance (.25 to 27 microns) of metals with polished and carefully abraded surfaces are presented.

A quantum mechanical theory of optical and infrared dispersion in metals originally developed by T. Holstein* and previously presented in unpublished Westinghouse Research Laboratories Research Reports 60-94698-3-R1 and 60-94698-3-R6 (1954 and 1955) is combined with other existing theories of Umklapp and impurity scattering processes and is shown to successfully account for the optical properties of metals in the entire free electron region at all temperatures of interest.

Detailed calculations are presented for monovalent and some polyvalent metals for which assumption of a symmetric Fermi surface is valid. Polyvalent and transition metals for which interband transitions are important and the Fermi surface is not spherical are also considered. In all, more than a dozen metals, for which reliable experimental data are available, have been successfully treated.

Calculations of the absorption propeties of super-conducting metals are also presented in an attempt to determine the extent to which bulk electron-phonon processes are responsible for infrared absorption by super-conductors.

---

*Holstein's unpublished Westinghouse Research Laboratories Reports are the source of the entire theoretical development presented in Section IV of Chapter 3.

INTRODUCTION

This report is a consolidation of technical summaries on the optical properties of satellite materials prepared and tested by Arthur D. Little, Inc. under contract DA-19-020-ORD-4857.

Chapter 1 presents the effect of satellite environment on the emissivity of material. Chapter 2 discusses the spectral emittance of polished stainless steel, aluminum, and magnesium at 50 degrees centigrade in the 0.25- to 28.0- micron wavelength region. Chapter 3 is devoted to the theory of optical and infrared properties of metals.

DEFINITION OF SYMBOLS

SYMBOL	DEFINITION
A_s	Bulk contribution to the absorption resulting primarily from the electron-phonon interactions
$A\ (\omega,T)$	Total absorptivity
A	Perturbing electromagnetic field
$A\ (x)$	Amplitive function
A_B	Bulk absorptivity
A_s	Diffuse skin absorptivity
A_s	Absorptivity of a superconducting metal
A_n	Absorptivity of a normal metal
m_s	Optical radius of an electron
$m_{j*}(q)$	Phonon annihilation operator
$m_m\ (q)$	Phonon creation operator
α	$\frac{\Theta}{T}$
$\overline{\alpha}$	Complex polarizability
$B\ (\underline{k})$	Expansion coefficient
$B\ (i)$	i-th order terms for an electron which was certain to be at the state $\underline{k}_o$ initially
$B^{s\ \ d}_{(2)\ \ \ (\underline{k})}$	Second order transition coefficient
$b\ (\omega,T)$	$\frac{T\ (\omega,T)}{o\ (T)}$
$b_{ee}\ (\mu)$	Quantum correction factor
$b_{ep}\ (\mu,\alpha)$	Quantum correction factor

SYMBOL	DEFINITION
β	(K T)
c	Speed of light
$\omega\ \theta$	$\frac{k,q}{k,q}$
$\frac{\triangle\ P}{\triangle\ E_2}$	$1 + \frac{\epsilon_o - \epsilon}{\epsilon_o}$ Probability per unit time and unit energy range that an electron at the state E, makes a transition to a range of final states
δ	$\frac{c}{\sqrt{4\pi\ \delta_{ds}\ \omega}}$
δ_I	$\frac{\lambda}{4\pi\ k}$
δ_p	Distance at which the intensity of light of given wavelength falls to $\frac{1}{e}$ of that at the surface
δ_s	Thickness at the metal surface in which most of the optical skin effect is observed
$\underline{E}$	Electric field
$\underline{E}_o$	Maximum amplitude
$\frac{1}{2}\ \underline{F}^2$	Energy density permit volume of the electromagnetic radiation field
E_f	Fermi energy
E_g (T)	Energy gap
$E_{\underline{k}}$	$\frac{k^2\ k^2}{2\ m^*}$
E_q	Energy of a phonon at the state (q)
E_o	Energy at the upper edge of the d-band
F (ω)	Forward scattering amplitude

SYMBOL	DEFINITION
$F(\omega)$	Complex forward scattering amplitude
$F(E)$	Dimensionless electron distribution
$F(E_2')$	Fermi function at the final stage E_2'
$f(E)$	Fermi function
$g(\frac{\theta}{T})$	Grueneisen formula
$g\delta$, $g\epsilon$	Corrections due to electron-electron collisior
g_{sd}	Constant
g	Constant factor representing the strength of the electron-phonon interaction
$_o(T)$	dc damping coefficient
(ω, T)	Damping coefficient
M_o	Electron-impurity scattering frequency
$_{ee}(\alpha)$	dc damping coefficient
(μ,α)	Over-all damping coefficient
$ee\ (\mu,\alpha)$	Electron-electron collision frequency
$\underline{H}$	Magnetic field
H_c	Vertical field strength
$(h\ \underline{k})$	Momentum of an electron
$\underline{J}$	Current density
$(\underline{T}_m\ \overline{F})$	Imaginary part of the scattering amplitude
K	Boltzmann constant
k	Absorption coefficient

SYMBOL	DEFINITION
k_1, k_2	Momentum states
k_d	Fermi momenta for the d-bands
k_s	Fermi momenta for the s-bands
k_d, k_s	Momenta corresponding to the highest occupied levels in the d- and s-bands
ℓ	Mean free path
λ	Wavelength
λ_o	Critical wavelength
M	Mass of the lattice
(M)	Impurity scattering
m	Electron mass
m*	Effective mass of a conduction electron
m^*_1, m^*_2, m^*_3	Three values of effective mass
m_o	Rest mass of an electron
m_d	Effective mass of d-electrons
m_s	Effective mass of s-electrons
m_p	Mass of a photon
μ	Permeability
$\underline{\mu}$	$\frac{h\,\omega}{K\,T}$
N	Complex index of refraction
N_p	$\frac{P_o}{M}$, phonon number density
N (q)	number of phonon states for E_q, which are occupied

SYMBOL	DEFINITION
n	Index of refraction
n_o	Effective number of conduction electrons per unit volume
n_e	Effective number of electrons per unit volume
n_s	Effective number of electrons in the s-band
$\bar{n}_s$	Total number of s-electrons qualified to make transitions to the empty d-states
n_d^o	Number of empty states in the d-band
n_-	Number of paired electrons per unit volume
n_+	Number of unpaired electrons per unit volume
v	Frequency
v_g	Limiting frequency
ω	Angular frequency
ω_o	Frequency characteristic of the electron
ω_q	Phonon frequency
P_s	Power absorbed by a superconducting metal
P_n	Power absorbed by a normal metal
$< P >$	Average of $P(E_1)$
$< P_{(o)}^{(n)} >$	Average probability per unit time
$P(\underline{k} \quad \underline{k} \pm \underline{q} \pm p)$	Probability permit time for the electron to make the indicated transition
$P_{(\pm)}^{(\pm)}(\underline{k}_1 \quad k_2)$	Probability permit time for a conduction electron to make the indicated transition

SYMBOL	DEFINITION
$P_{(o)}^{(n)}\ (\underline{k}_1 \quad \underline{k}_2)$	Probability of a transition by a joint action of the electromagnetic and phonon fields
$P_{(s)}^{(n)}\ (E_1)\ sd$	Probability for an electron initially at the state of energy E_1 in the s-band to make a transition to the final state of energy E_2 in the d-band
$\underline{p}$	Photon mementum
$\psi\ (\underline{x},\ t)$	Perturbed wave function
$\underline{q}$	$\frac{\text{Momentum}}{h}$, phonon wave vector
$R\ (\omega,\ T)$	Reflectivity
R	Total reflectivity
R_s	Surface resistance of superconducting metals
R_n	Surface resistance of normal metals
R_{ep}	Constant
R_{ee}	Constant
R_{ep}^{sd}	Constant
$(R_e\ \overline{F})$	Real part of the scattering amplitude
$\underline{\pi}$	Position vector
π_o	Classical radius of the electron
π_o^*	Effective classical radius of electrons
$\pi,\ s$	$(\pm)$
δ_o	Mass density

SYMBOL	DEFINITION
δ (E)	Density of states function
δ, (E), δ_d (E)	Density of states
δ_n (o)	Density of states function of a normal metal evaluated at the Fermi level
$\underline{S}$	Poynting vector
$\underline{s}$	Electron position coordinate within metal
superscript (-)	Phonon absorption
subscript (-)	Photon absorption
Σ_o	Spontaneous magnetization per gram atom at $0^\circ K$
$\Sigma(T)$	Spontaneous magnetization per gram atom at $T^\circ K$
∂_o	dc electrical conductivity
∂ (w)	Optical conductivity
∂ (O)	$\frac{m_e e^2}{m^*_o}$
∂_n	High frequency conductivity of m normal metal
∂_s	Complex conductivity $\partial_1 + \partial_2$ i of m super conductor
$\partial_s(\omega)$	Total scattering cross section per scattering center
∂_s (ω,T)	Dispersion cross section per electron
T	Absolute temperature
T_1	Superconducting transition temperature
t	Time

SYMBOL	DEFINITION
t_R^o	dc relaxation time
t_R	Relaxation time
$t\ (\underline{k})$	dc relaxation lifetime of an electron
Θ	$\frac{hvg}{K}$ Debye temperature
θ	Angle between the mementa $\underline{k}$, and $\underline{q}$
$V_o(x)$	Original undistorted periodic potential
$U_d\ (x)$	Distorted potential
U_L	Longitudinal phase speed of sound
M_L	Longitudinal phase velocity of sound
V	Sample Volume
V_o	Atomic volume
$V_p\ (x)$	Electron-lattice potential
$V_p = \delta\ U$	Small change in the potential
V_f	Fermi velocity of electron
μ_F	Fermi velocity of electrons
W	Joule heat produced per unit time and unit volume within the conducting medium
$W\ (\omega,T)$	Rate of energy expenditure
$< W >$	Power expenditure due to one electron per unit time
$\overline{W}_{sd}$	Net amount of power absorbed per s-electron

SYMBOL	DEFINITION
$\overline{W}_s$	Power expenditure of a super conductor
$\overline{W}_d$	Weight factor due to the density of states of the d-band
x	$\frac{W'}{\omega_{ep}}$
x_1, x_2, x_3	Principal - axis coordinates
$\Delta (\underline{x})$	Dilatation
ξ	Absorption of a phonon and photon of energy $h\omega$ and $E_{\underline{q}}$, respectively
ξ, ξ', ξ''	Energy terms in resonance factors
y	$\frac{\omega}{\omega_{ep}}$
Z	$E - E_F$
Z_s	Surface impedance of superconducting metals
Z_n	Surface impedance of normal metals
z	Penetration distance into the metal
	$\frac{m^*}{4\pi m_o e^2}$
$R = \tau_o^{-1}$	Relaxation time of a conduction electron

CHAPTER 1

EFFECT OF SATELLITE ENVIRONMENT ON THE EMISSIVITY OF MATERIALS

SECTION I. INTRODUCTION

The space around the earth is permeated by rather strong radiation and particle fluxes of four general types:

1. Electromagnetic radiation from the sun, ranging from radio frequencies to X-rays;

2. Primary cosmic rays, consisting mostly of high-energy protons and α particles;

3. Charged particles trapped by the earth's magnetic field in belts encircling the earth (Van Allen belts);

4. Meteoric dust particles.

The impact of any or all of these types of particles or radiation can alter the optical properties of various materials when applied in a sufficient dose. The effects of radiation and impact damage in three groups of materials, namely, metals, semiconductors and inorganic solids are examined. Organic materials will not be considered in this study.

Table I indicates the nature of radiation damage known to occur in the three selected groups of solids by the types of radiation considered here. The effects tabulated to the right of the heavy line may be expected to be of principal importance in bringing about changes in such optical properties as emissivity, absorptivity and reflectivity.

The occurrence of such changes is contingent upon exceeding a certain threshold dose, specific with each material and each type of radiation. Some of the radiation effects may be reversed by thermal activation. Thus, at any finite temperature above absolute zero only a part of the total effect is retained, another part being lost by concurrent recovery. Upon prolonged exposure most of the radiation damage effects tend to a state of saturation.

The radiation levels existing in the near extraterrestrial space, according to the most recently published data, are reviewed and their special effects upon materials are considered.

TABLE I. TYPES OF OPTICALLY ACTIVE DAMAGE BY VARIOUS RADIATIONS

	Electromagnetic Radiation (Ultraviolet, X-ray and γ-ray)	High-Energy Particle Radiation (Electron, Proton, Neutron)	High-Velocity Projectiles (Micrometeorites)
Metals	Small effect only caused by energetic γ-rays; no effect by softer radiation	Creation of interstitials and vacancies; increase in resistivity; increase in emissivity	Surface abrasion and sputtering; decrease in specular reflectivity
Semiconductors	Photoconductivity; radiation damage only by energetic X- and γ-rays	Removal of carriers, creation of interstitials and vacancies, increase in resistivity	Ditto
Other inorganic solids	Color centers, photochemical effects, increase in absorptivity	Creation of interstitials and vacancies	Ditto

SECTION II. RADIATIONS IN THE EARTH'S ENVIRONMENT

A. ELECTROMAGNETIC RADIATION

The sun is the source of a very large portion of the electromagnetic radiation reaching the earth. In emitting most of this radiation, the sun radiates like a blackbody at a temperature of approximately 5,500° to 6,000°K. The total irradiance at the average distance of the earth from the sun (and outside of earth's atmosphere) is about 2.00 cal/cm^2/min, or 0.140 watt/cm^2. [1] Approximately 25 percent of this radiation lies in the visible spectrum. The region of the spectrum in which the photon energy of the solar radiation is comparable with the ionization energies in solids (a few electron-volts) lies in the ultraviolet (wavelength shorter than 400 mμ). Only 12 to 15 percent of the total solar radiation is contained in the spectral interval from 0 to 400 mμ and of that approximately 10 percent falls in the near ultraviolet from 300 to 400 mμ. Below 340 mμ, direct measurements from high-altitude rockets have yielded the following spectral distribution of ultraviolet radiation [2] :

Wavelength	Spectral Irradiance
340 mμ	110 μw/cm^2/mμ
300	70
260	17
220	3

The irradiance values may be expressed in terms of quantum flux densities (number of quanta of given frequency per cm^2 per second) by recalling that at 200 mμ wavelength one quantum ($h\nu$) has an energy very approximately equal to 10^{-11} ergs. Thus at 200 mμ, a spectral irradiance of 1 μw^{-1}cm^2 corresponds to a quantum flux density of 10^{12} cm^{-2} sec^{-1}.

The extreme ultraviolet region borders on the soft X-ray region which appears in the solar spectrum with a intensity far exceeding that corresponding to the blackbody temperature of the photosphere. This results from the fact that most of the X-ray emission originates in the solar corona at temperatures of the order of 10^6°F. The wavelength of maximum X-ray emission is centered round 50 Å and the total X-ray irradiance in the range between 2 and 100 Å is found to be approximately 0.14 μw/cm^2 [3]; in units customary in X-ray dosimetry this level would correspond to 0.014 rads sec^{-1} cm^{-2} (one rad being equivalent to 100 ergs of X-ray radiation energy absorbed in one gram of matter.)

Because the X-ray quanta are very energetic, the photon flux density

corresponding to this irradiance is relatively low, of the order of $10^9 cm^{-2}$ sec^{-1}.

At times of extreme solar activity (solar flares), the level of X-ray irradiance may increase by a factor of 10 or more, and X-rays of wavelengths as short as 1 to 2 Å may be emitted [4].

In addition to the electromagnetic radiation of solar origin, there is probably a high-energy (γ-ray) component resulting from cosmic ray particle collisions with the residual gas atoms in the upper atmosphere. While no definite data are as yet available, it is generally thought that the total irradiance from this source is extremely small.

B. COSMIC RAYS

Outside the Van Allen radiation belts in outer space [5] the primary cosmic radiation is estimated to consist mostly of protons (80 percent) and α particles (approximately 18 percent); it appears that there are no electrons in the primary cosmic radiation — not counting electrons from the solar corona. There are some neutrons emitted by the sun which reach the earth. The remaining 2 percent of the particle spectrum consists of nuclei of heavier elements, ranging up to iron in atomic weight. Average energies of these primary particles are of the order of 10^9 electron volts (ev), but the distribution extends up to energies of the order of 10^{18} ev. A certain fraction of energetic particles is contributed by solar flares. The interaction of the primary cosmic rays with the upper atmosphere consists of collisions with nuclei of the atmospheric elements, in the course of which a large variety of secondary particles are produced. The secondary particles consist of atomic fragments of various types, and these in turn produce tertiary fragments, and so on. The net result of this process is a nucleonic cascade which, in the case of very energetic primaries, gives rise to extensive showers of particles reaching the earth's surface. A by-product of the interaction of cosmic-ray primaries with the atmosphere may be represented by the Van Allen radiation belts which consist of rather dense belts of charge particles (presumably mostly electrons, but also including protons) trapped by the earth's magnetic field. In the inner belt the particle flux density reaches maximum at an altitude of 2,000 miles from the earth's surface, while in the outer belt the maximum is reached at about 10,000 miles in the equatorial regions. Beyond 10,000 miles, the radiation belts diminish steadily and disappear almost completely beyond 40,000 miles. The maximum particle flux density in each belt is about 40,000 particles cm^{-2} sec^{-1}. The particle flux consists of electrons having energy of at least 0.65 mega electron volts (mev) and protons of energy at least 10 mev. The exact proportion of these two types of particles is not known, nor has their origin been clearly established.

C. MICROMETEORITE FLUX

Particles of meteoric origin come in a very wide range of sizes and flux densities. Direct optical and radar observations indicate that in a mass range between 0.01 and 100 milligrams (mg), there are approximately 10^9 meteors incident on the whole earth's atmosphere per day; this amounts to a total mass of approximately 200 kilograms per day.

Data on the number and size of large meteorites (500 g to 100 mg) are sporadic. On the opposite side of the distribution, terrestrial observations are incapable of recording incidence of particles smaller than about 0.01 mg, although the flux density of such micrometeorites or meteoric dust must be fairly large, as indicated by light scattering phenomena such as zodiacal light. A combination of direct observational data and extrapolations from them as given by Lovell [6] is presented in Table II.

Most of the meteorites are believed to originate in the solar system (asteroidal material, see reference 7). Their velocities are found to lie between approximately 11 to 70 km/sec. The minimum velocity corresponds to the terrestrial escape velocity (11.3 km/sec), the lowest velocity with which a meteoric body from space can strike the earth. The maximum velocity results from the combination of earth's orbital velocity (30 km/sec) and the velocity of escape from the solar system which at the distance of earth is 42 km/sec. Hence the largest velocity with which a meteoric body at its perihelion can make a head-on collision with the earth is 72 km/sec.

The flux density of meteoric particles (number of particles per cm^2 per second) is obtained by multiplying the particle densities Table II, (Column 4) by their velocity. At an average velocity of 40 km/sec the estimated flux density of particles in the 10^{-3} to 10^{-7} mg range is obtained as 4×10^{-5} particles per cm^2 per second.

Direct observations of micrometeorite impacts have been obtained only recently [8]. The results of partial analysis of data from the Explorer I satellite indicate that the average flux density of particles about 4 microns in size (approximately 10^{-10} g mass) is approximately 10^{-6} cm^{-2} sec^{-1} and of particles 10 microns in diameter (approximately 6×10^{-10} g) is about 10^{-7} cm^{-2} sec^{-1}. This appears to be in fair agreement with the data of Table II.

TABLE II. DISTRIBUTION OF SIZE AND FREQUENCY OF METEORS INCIDENT OVER THE ENTIRE EARTH'S SURFACE

	Mass Range	Number/Day	Mass/Day(kg)	Number/cm
Extrapolated	500 to 100 g	~ 300	~ 60	4×10^{-28}
	100 to 10 g	~ 2500	~ 40	3×10^{-27}
	10 to 1 g	$\sim 1.8 \times 10^{4}$	~ 40	2×10^{-26}
	1 to 0.1 g	$\sim 4 \times 10^{5}$	~ 60	5×10^{-25}
Observational data	100 to 10 mg	10^{6}	40	1.5×10^{-24}
	10 to 1 mg	3.6×10^{7}	60	4.5×10^{-23}
	1 to 0.1 mg	1.9×10^{8}	40	2.4×10^{-22}
	0.1 to 0.01 mg	3.3×10^{9}	60	4.1×10^{-21}
	0.01 to 0.001 mg	6.5×10^{10}	60	8.1×10^{-20}
Extrapolated	10^{-3} to 10^{-7} mg	$\sim 10^{19}$	160	$\sim 10^{-11}$
	10^{-7} to 10^{-11} mg	$\sim 10^{29}$	160	$\sim 10^{-1}$

SECTION III. RADIATION DAMAGE IN SOLIDS

A. METALS; GENERAL CONSIDERATIONS

One effect that may conceivably lead to an increase in emmissivity of a metal upon extensive irradiation is the generation of defects that scatter conduction electrons (interstitials and vacancies) and thus increase resistivity. Spectral emissivity of metals at long wavelengths (infrared radiation, $\lambda < 5\ \mu$) obeys fairly accurately the Hagen-Rubens law [9]:

$$E = (4\rho/\lambda)^{\frac{1}{2}} \tag{1}$$

where ρ denotes the resitivity. A relative increase in resistivity ($d\rho/\rho$) will cause (at a constant wavelength) and increase $\frac{1}{2}$ ($dE\lambda/E\lambda$) in emissivity; thus, for example, a 10-percent increase in ρ will cause a 5-percent increase in emissivity. We shall examine in paragraph A2 under what conditions high energy radiations may cause such changes.

Another effect that may increase emissivity of a metal surface exposed to satellite environment is the mechanical damage caused by impacts of micrometeors. Under these impacts the profile of an optically smooth surface may become altered so as to scatter incident radiation diffusely, rather than to reflect it specularly. In addition to the geometrical (profile) effect, it may be expected that the mechanical impacting will also increase the resistivity in a manner similar to that observed in work hardening of metals. We shall not attempt to take the latter effect into account because very little is known at present about the mechanical and thermal phenomena that take place at a point of impact of an extremely fast ($v \approx 10^6$ cm/sec) massive particle upon a metallic surface.

1. Effect of Micrometeors

Spectral emissivity of an optically smooth metallic surface is an intrinsic property of the material, as indicated by the Hagen-Rubens law. Strictly speaking, the emissivity defined by this law is the normal emissivity (emission in the perpendicular direction only); actually, the angular distribution of the emissivity must be considered. The emissivity pertinent to the present problem (radiation from a satellite into the empty space) is the hemispheric emissivity obtained by integration of the angular emissivity over an entire hemisphere. When the analysis is performed [10], it is found that the hemispheric emissivity at low (normal) emissivity values is larger by a factor of 4/3 than the normal emissivity. At higher emissivities the ratio of the two is smaller and becomes 1.0 for a blackbody (see Table III).

TABLE III. RATIO OF HEMISPHERIC TO NORMAL EMISSIVITY OF A METALLIC SURFACE [11]

E_n (normal)	0	0.1	0.2	0.3	1.0
$\frac{E(\text{hemispheric})}{E_n}$	1.33	1.225	1.145	1.075	1.0

When the profile of the originally smooth metallic surface has been changed by numerous pits and indentations, incident radiation is diffusely scattered, and the hemispheric emissivity must again be considered. When the indentations are large compared with the wavelength of radiation emitted and of smooth profile, the hemispheric emissivity of the surface remains essentially unchanged. In a general case, when the size of the indentations is comparable with the wavelength, diffraction effects become significant and a rigorous treatment of the scattering may be quite complex [11, 12].

However, independent of the exact nature of the scattering process, the hemispherical emissivity will be increased by surface indentations under conditions when multiple reflections can occur (cavity effect). This situation can be taken into account by an assumption that each impacting particle forms a crater of an area, A_c, and emissivity, E_c, (larger than the normal emissivity of the surface). Then the resultant emissivity, E_p, of the damage surface is:

$$E_p = N_c A_c E_c + (1 - N_c A_c) E_o \qquad (2)$$

where N_c is the number of indentations per cm^2, and E_o is the emissivity of the original surface (all emissivities are hemispherical). When $N_c = A_c^{-1}$, the surface is completely covered with indentations and E_p becomes equal to E_c.

The choice of an appropriate value for E_c depends to a considerable extent on the geometry of the indentations. If their depth is at least equal to their diameter, the effective emissivity, E_c, of the crater area would tend to the value 1 (one black body). Studies of crater formation in metallic targets made at the University of Utah [13] indicate that, at velocities up to 1.5 km/sec, the volume of the crater is proportional to the energy of the projectile; thus, for instance, in

aluminum, the constant of proportionality is 0.78×10^{-10} cm^3/erg. If the validity of this relation is extrapolated to meteoric velocities, a particle of 10^{-10} gram-mass incident with a velocity of 40 km/sec (800 ergs kinetic energy) would produce a crater of 6.2×10^{-8} cm^3 volume. Assuming a crater area between 12.5 to 79×10^{-8} cm^2 (4 to 10 μ diameter), one obtains for the depth of penetration, values between 0.5 to 0.08 cm, respectively; if this were actually the case, the meteorites would bury themselves very deeply indeed, or even perforate the metal. The extrapolation of the data from Reference [13] may not be justified, however. An alternate way of estimating the volume of the craters may be obtained by equating the energy of impact to the energy required to heat, melt and vaporize the metal occupying the crater cavity (including the projectile). Using the same data as above and taking for:

$$H_{fusion} = 2.6 \text{ k cal/mole and } H_{vap} = 68 \text{ k cal/mole} \qquad (3)$$

one obtains for the volume approximately 1.8×10^{-9} cm^3 and for the depth between 1.5×10^{-2} to 2.3×10^{-3} cm (for the same crater diameters as above); on this estimate, the depth is considerably smaller but the depth-to-diameter ratio is still large enough to justify the use of black body emissivity for the crater area. Preliminary data on cratering by high-velocity microparticles [14] seem to indicate that the diameter-to-depth ratios remain between 1.5 to 2.5 at lower velocities (about 1 km/sec) but rather abruptly change to about 8 to 10 (shallow craters) when the velocity exceeds approximately 10 km/sec. Until more detailed results are reported in full, the simplest assumption compatible with the preceding estimates are used, namely that the crater area radiates as a black body, i. e. $E_c = 1$.

It is now possible to estimate the time in which the existing flux of micrometeorites will cause a measurable increase in emissivity by 10 percent.

Assume the original emisivity is 0.10 and the flux of micrometeorites of 4 μ size is 10^{-6} cm^{-2} sec^{-1} (paragraph B). Assuming a crater diameter of 10 μ (79×10^{-8} cm^2 area), one obtains a full coverage of the surface after approximately 1.3×10^6 impacts per cm^2. This would require 1.3×10^{12} seconds, or approximately 2×10^4 years. At this damage dose, the hemispherical emissivity of the surface would reach a value $E_p = 1$. However, to increase the original emissivity of 0.1 by 10 percent, i.e., by 0.01, only approximately one one-hundredth of the "saturation" dose would be required, i.e., approximately 400 years.

If the smaller, more numerous micrometeorites contribute significantly to the surface damage, or if the area of the individual craters is larger than estimated above, the same increase in emissivity may occur in still shorter time.

2. Effect of High Energy Radiation

The radiation damage effects from the high energy particle component of the cosmic radiation is considered first. No observational data are available regarding their effect upon resistivity and emissivity of metals. In their absence, we will have to extrapolate from the experimental results obtained with deuterons and electrons at energies in the 1 to 15 mev range.

The detailed atomistic picture of the damage process is very complex (see references 15, 16 and 17) and in many respects still not completely clear. The following is a brief description of the process, sufficient for the present purpose. An energetic, charged nucleon of relatively small mass (protion, deuteron, α particle), upon entering the metal, dissipates most of its energy in exciting the orbital electrons and only a small fraction in exciting thermal lattice vibrations. As it passes near the nuclei of the metal, some of the Coulomb encounters are occasionally so close that sufficient energy is transferred to nucleus and it becomes displaced. The threshold energy for such an event is determined by the condition that about 25 ev must be transferred to the lattice nucleon in the collision; however, many displaced atoms acquire energies in collisions which are several times larger than this threshold energy so that they in turn may be able to produce secondary displaced atoms. The entire region along the path of the primary knock-on in which the number of displaced atom-vacancy pairs (Frenkel defects) may reach several percent of the concentration of the normal atoms, is sometimes called a "thermal spike" because of the flash heating effect ($\sim 10^{4}$°K for $\sim 10^{-11}$ sec) that occurs there. When the original particles have extremely high energies, such as encountered in cosmic ray protons ($\sim 10^{9}$ eV), they may first cause spallation reactions in the metal or produce cosmic ray "stars" (a shower of fragments); the secondary fragments may then in turn collide with lattice atoms.

Most of the radiation damage in metals disappears rapidly by recombination and annealing unless the irradiation is effected at temperatures below about 10°K and the sample is maintained at that temperature level after irradiation. Even at low temperatures, the number of displaced atoms does not increase linearly with the total number of bombarding particles which passed through the sample because of self-annealing (radiation annealing). The defect-forming and self-annealing processes compete with each other according to a differential relation:

$$dN = \alpha d\Phi - \beta N d\Phi \qquad (4)$$

in which N denotes the concentration of Frenkel defects, Φ the total flux of particles per cm^2, and α and β are constants. Upon integration, this equation leads to a logarithmic relation which was first derived

empirically by Marx, Cooper and Henderson [18] in a form:

$$\Delta \rho = A \left[1 - \exp(-\beta\Phi)\right] , \qquad (5)$$

describing the observed dependence of increase of resistivity of metals upon bombardment by 12 mev deuterons. For copper, the constants have values $A \approx 0.5$ μ ohm cm and $\beta \approx 4.8 \times 10^{16}$ cm^2/deuteron. After extensive irradiation, $\Delta\rho$ approaches A as a limiting value (saturation).

When copper was irradiated at low temperatures (about 10°K) by 12 mev deuterons to a total dose of 2×10^{17}, D cm^{-2} its resistivity increased by approximately 0.2 μ ohm cm. After annealing to 77°K, only 41 percent of the initial increase remained and, after further annealing to 300°K, only 7 percent of the increase was left, i.e., 0.014 μ ohm cm [19]. Since the resistivity of copper is approximately 1.7 μ ohm cm, the final effect represents an increase of less than 1 percent; at saturation, it would reach about 2 percent after a total dose of approximately 10^{18} D cm^{-2}.

Data for a few other pure metals (Ag, Au, Fe, Co, Ni and W) and alloys (Cu3Au and CuZn) are also available (see reference 16, p. 424). Iron is claimed to suffer larger resistance increase than other metals (however, no data are given), and it appears to retain a larger percentage of it upon annealing to room temperature. No work on alloys of technological importance (e.g., aluminum alloys or stainless steels) and at elevated temperatures has been published as yet.

Since copper has been investigated in greatest detail, we shall base the estimate of the radiation damage effect by the satellite environment on the data for copper as given above.

The principal difference between accelerator particles which have been employed in radiation damage studies and cosmic radiation is in their relative energies; the cosmic ray primaries are much more energetic. In the primary proton flux above the atmosphere, approximately 70 percent of the whole distribution lies between 0.1 to 1 bev, and about 15 percent is between 1 to 100 [20]. The energy of 300 mev is taken as an approximate center of the distribution.

The average energy loss per centimeter of path length of 300 mev protons in copper is about 1/10 that of 10 mev [21]; thus, we may estimate that a radiation damage resulting in 2 percent increase in resistivity would be reached after a total dose of approximately 10^{19} P cm^{-2}. In Section II, paragraph B is given a maximum proton flux density of 4×10^4 P cm^{-2} sec^{-1} in the Van Allen radiation belt. Thus, the total dose for 2 percent increase in resistivity (1 percent increase in emissivity, see Section III, paragraph A) would be accumulated in 2.5×10^{14} sec or approximately 10^7 years.

In view of this low rate of radiation damage, we may consider the effect of cosmic ray electrons that constitute only a small fraction of the total radiation flux as completely negligible.

B. SEMICONDUCTORS: GENERAL CONSIDERATIONS

Semiconductors differ in their optical properties from other solids in that their behavior changes from quasi-metallic to quasi-dielectric in a fairly sharp frequency interval, the position of which depends upon the nature of the particular semiconductor. In the intrinsic semiconductors, this transition (absorption edge) results from excitation of electrons from valency band to the (normally empty) conduction band when the photon energy is equal or greater than the energy gap, $h \geq E_g$. The values of E_g range from 0.14 ev in PbSe to 3.37 ev in ZnO with Ge at 0.72 ev and Si at 1.35 ev near a typical median. Thus with silicon, the absorption edge is located in the near infrared, at a wavelength $\lambda = 1.24/E_g = 0.92\ \mu$. At wavelengths shorter than 0.92 μ, i.e., in the visible spectrum, intrinsic silicon is almost opaque, much like a metal; at longer wavelengths (in the infrared) it becomes transparent. In germanium the absorption edge is at approximately 1.7 μ. In the infrared, beyond the edge, some absorption results from the small number of free carriers normally presents in the conduction band.

While the absorption index,(nk), which is the imaginary part of the dielectric constant, is small in the infrared, the real part $(n^2 - k^2)$ may attain fairly large values; the reflectivity is also fairly large, typically about 0.40 to 0.50 in Si or Ge. Under these conditions it is not permissible to assume that the emissivity is approximately equal to (1-R) as in the case of well-reflecting metals. Instead, a generalized form of Kirchhoff's law for a semi-transparent body must be used. McMahon [22] analyzed the case of a partially absorbing body bound by two parallel planes (a slab) and derived a formula for its spectral emissivity:

$$E_\lambda = (1 - R_\lambda)\ (1 - T_\lambda)\ (1 - R_\lambda T_\lambda)^{-1} \qquad (6)$$

where R_λ and T_λ are spectral reflectivities and transmissivities, respectively. Since $1 - T_\lambda$ is the absorptivity, A_λ, we may also write:

$$E_\lambda = A_\lambda\ (1 - R_\lambda)\ [1 - R_\lambda\ (1 - A_\lambda)]^{-1} = \frac{A(1 - R)}{1 - R(1 - A)} \qquad (7)$$

Most of the optical studies of semiconductors were made by absorption [23] and no data are available on their emissivity; however, we can by means of Equation (6) analyze the existing data. By differentiation we

obtain for a relative change of emissivity:

$$\frac{dE}{E} = \frac{1 - R}{1 - R(1 - A)} \cdot \frac{dA}{A} , \qquad (8)$$

assuming R is independent of A, which is approximately true in the wavelength range considered here. If we take as a typical value R = 0.5, we see that the variation of emissivity resulting from a variation in absorptivity lies between $\frac{1}{3}$ (dA/A) for A = 1 (100 percent absorption) to 1.0(dA/A) for A = 0 (zero absorption). These formulas can be used in evaluating the existing data on radiation damage in semiconductors (Section III, paragraph B2).

1. Effect of Micrometeorites. Since the effect of bombardment by micrometeorites is presumed to consist predominantly in a geometrical change of surface profile, we may expect that the evaluation performed for metals in Section III, Paragraph A1 is applicable also in the case of semiconductors. Thus the time for a 10 percent increase in emissivity would again be of the order of 100 years.

2. Effect of High Energy Radiation. Radiation damage effects have been studied in a great number of investigations; a good review of the present status is given in the 31 papers collected in the special issue of Journal of Applied Physics, August 1959 [24]. Most of the work reported there is concerned with carrier transport properties and complex semiconductors. The variety of experimental detail is overwhelming and not always pertinent to the present problem. Only one paper, Fand and Ramdas [25], deals directly with optical properties (infrared transmission) of a simple semiconductor (silicon) as affected by irradiation by neutrons, deuterons and electrons, and even this case turns out to be quite complex and not yet fully explored. We shall limit the following discussion to this relatively simple case.

Major changes in optical properties of silicon are obtained after a total dose of the order of 10^{18} particles/cm^2 (deuterons or fast neutrons) and saturation is approached after a total dose of about 10^{19} particles/cm^2. The largest effect is observed on the long wavelength side of the absorption edge, where the absorption may increase by several orders of magnitude (at 1.2 μ by a factor approximately 10^3). Farther in the infrared, however, the effect becomes much smaller and eventually reverses, the absorption being actually reduced after irradiation. This reduction is a result of removal (trapping) of carriers by the Frenkel defects.

In the near infrared, on the short wavelength side of the absorption edge the absorption is increased uniformly by a factor of about 2. In addition to these over-all changes, a number of discrete absorption bands

is produced by irradiation, the strongest of which occur at 1.8 μ and 3.9 μ wavelengths; weaker bands are observed at 3.3, 5.5, 6.0, 20.5, 27.0 and 30.1 μ. The radiation damage effects do not anneal out as readily as in the case of metals and most of the effect can be retained at temperatures around 300°K.

In view of this complex behavior it is difficult to give a single figure for the magnitude of the radiation damage effect upon absorptivity and emissivity. We may state only that large changes in emissivity may occur after irradiation by a total flux of about 10^{18} particles/cm^2.

The maximum flux of fast protons in the Van Allen belts is approximately 4×10^4 P cm^{-2} sec^{-1} (Section II, paragraph B), and we may estimate that the radiation damage efficiency of 300 mev protons is about one-tenth of that of 10 mev deuterons for which the experimental data were given above. Thus a time of the order of 10^6 years would be required to obtain the major changes in absorptivity and emissivity (Equation 8), described above. Since at a certain wavelength (say, 1.2 μ) the relative increase may be very large (factor of 10^3 or more) the time requred to observe a small (10 percent) change in emissivity may be shortened by a factor of 10^4 or more, thus bringing the critical exposure time to the order of 100 years.

C. OTHER INORGANIC SOLIDS: GENERAL CONSIDERATIONS

The inorganic solids we shall consider here may be grouped in three classes: (a) ionic crystals such as alkali halides used in infrared optical systems; (b) crystals of high refractive index such as used in white pigments; and (c) non-crystalline solids such as SiO and various glasses.

With ionic crystals, the best known radiation damage effect is the generation of color centers (F-centers) by absorption of photons of sufficient energy ($E_d > 2$ to 5 eV). A comprehensive review of color centers in alkali halides may be found [26]. F-centers may be described as an anion vacancy with a trapped electron attached to it; other types of electron vacancy sites, such as F, V and M centers have also been identified. These color centers give rise to fairly board absorption bands in the visible or ultraviolet spectral regions; their position in the spectrum is determined by the nature of the crystal. In sodium chloride, the center of the F-band is at approximately 400 mμ and its half-width (at 25°C) is approximately 100 mμ. In potassium bromide, the F-band is centered at 630 mμ. Color centers have been studied only by transmission. Emissivity of radiation-colored crystals has apparently never been investigated. It is, however, possible to make reasonable estimates of spectral emissivity by means of the theory of partially absorbing bodies as presented in Section III, paragraph B.

Crystals of high refractive index used as white pigments are mostly of a mixed ionic-covalent type (ZnS, TiO_2, $BaTiO_3$) and thus not so prone to formation of ionic defects such as F-centers. They respond to radiation by solarization and photo-sensitization, i.e., processes involving photo-oxidation or photoreduction of the impurity atoms presents in the host lattice. A most conspicuous example of solarization is coloring of calcium titanate pigment containing copper impurity by ultraviolet light, which may be described as a photoreduction reaction [27].

$$CaO \cdot Ti^{4+}O_2 + h\nu \longrightarrow CaO \cdot Ti^{+2}O + 2e^-, \qquad (9)$$

$$2e^- + Cu^{2+} \longrightarrow Cu \text{ (color center)}.$$

Similar reactions were studied by Weyl [28] and Goodeve [29], largely because of their importance for light resistance of paints. It is now well established that such reactions can be almost completely eliminated by use of very pure materials.

In the third category of solids, we should include silicon monoxide which is being successfully used as a coating for emissivity control of temperature of the Vanguard satellites [30]. Unfortunately, almost nothing is known about the radiation coloration behavior of this material except an isolated observation (in this laboratory) that a transmitted flux of approximately 10 r of 40 kv X-rays is incapable of producing a visible change in the transparency of a SiO film 0.2 μ thick.

Radiation coloration of glasses has been extensively studied and a review with complete bibliography has been given by Sun and Kreidl [31]. Here too the most prominent effects can be attributed to photo-oxidation and reduction of cations capable of change of valency (Mn, Fe, V, Ce). Glasses of high photosensitivity to ultraviolet light have been developed by Stookey [32] for photoengraving purposes; high-energy radiation sensitive glasses (mainly of the K-Ba-Alphosphate type) have been developed for radiation dosimetry.

In the opposite direction, the need for radiation resistant glasses led to the development of cerium oxide compositions that remain colorless in the visible spectrum even after exposures of the order of 10^6 of energetic γ-radiation [33]. They do form, however, strong absorption bands in the ultraviolet. In view of such a variety of behavior of different glass compositions it is obvious that any generalizations are of limited value and each case will have to be considered individually.

Most types of color centers, in particular F-centers, can be destroyed by heat, infrared radiation or visible light. When irradiation is done at moderate temperatures, the competition between rate of production of color centers and their destruction results in saturation of the ultimate

density of centers.

1. Effect of Micrometeorites. In absence of any experimental data on surface damage of crystals and glasses by micrometeors we may use the same arguments as in Paragraphs A1 and B1 of Section III and conclude that the time for a 10-percent increase in emissivity would be probably of the order of 100 years.

2. Effect of Radiation. F-Centers in alkali halide crystals are readily produced by irradiation with short-wave ultraviolet or soft X-ray radiation. A total dose of approximately 100 ergs/cm^3 absorbed energy may produce typically optical absorption at the center of the band of the order of $k = 10\ cm^{-1}$. This is a very strong absorption, corresponding to almost complete opacity in 1 cm thickness; thus a crystal irradiated to this density would presumably possess emissivity near 1.0 at the center of the band.

According to the data given in Section II, Paragraph A, the radiation flux density in the far ultraviolet (at 200 mμ) is of the order of 10 ergs $cm^{-2}\ sec^{-1}$ (per 1 mμ bandwidth). The dose required for intense coloration would therefore be of the order of 10 seconds. The solar X-ray flux would cause the same coloration in approximately 1,000 seconds approximately 17 minutes.

Solarizable crystals (impure pigments) become colored by ultraviolet or X-ray radiation at rates depending upon concentration and type of impurity. No consistent data are available, but the times required to produce visible coloration by solar ultraviolet radiation are of the order of hours to days. Equivalent X-ray levels are of the order of 10^4 to 10^6r. High purity pigments appear to be virtually immune to visible coloration by ultraviolet radiation and X-rays. For instance, a high-quality commercial white paint (DuPont Dulux alkyd base with 95 percent TiO_2 and 5 percent ZnO pigment) was irradiated in this laboratory with 50 cv X-rays at flux density approximately 10^8r); a barely visible darkening was observed which disappeared after three hours exposure to ambient daylight.

A similar high resistance to coloration by X-rays was observed with silicon monoxide (Section III, Paragraph C). Glasses, on the other hand, are usually quite susceptible to coloration by radiation, presumably because of the impurities present. No data are available about the rate of solarization of glasses by ultraviolet radiation. It is well known, however, that visible coloration of commercial container glasses by terrestrial solar radiation may occur within a few decades; this period may be estimated to the order of one year in the extraterrestrial environment. The same effect is obtained by medium energy X-rays after exposure to approximately 10^5 to 10^6r. The corresponding time at the level of 0.014 r $cm^{-2}sec^{-1}$ (Section II, Paragraph A) would be of the order of one to ten years.

TABLE IV

ESTIMATED TIMES REQUIRED TO PRODUCE SIGNIFICANT INCREASE IN EMISSIVITY

BY RADIATION DAMAGE IN SATELLITE ENVIRONMENT

	Electromagnetic Radiations	High Energy Particle Radiations	Micrometeorites
Metals	no effect	$\sim 10^7$ years (for $\Delta E/E = 2\%$)	$\sim$ 400 years (for $\Delta E/E = 10\%$)
Semiconductors	-(1)-	$\sim 10^2$ to 10 years	$\sim$ 100 years
Other inorganic solids	hours in alkali halides days in impure pigments ∞ in pure pigments ∞ in SiO years in comm'l glasses	-(2)-	$\sim$ 100 years

Note 1 Ultraviolet and soft X-ray radiations have probably a small effect. Effect of high-energy γ-rays ($>$ 1 MeV) is similar to that of fast electrons.

Note 2 Effects of high-energy particle radiations are similar to those of low energy electromagnetic radiations. In view of the relatively low level of particle flux density, the rate would be so much slower that it makes a negligible contribution to the entire effect.

SECTION IV. CONCLUSIONS

The effects of the radiation enviroment upon the optical properties of the selected three classes of materials are summarized in Table 4. The figures given there represent best estimates based on available data for typical representative materials. However, selection of a "typical" representative from such highly diversified classes of materials as semiconductors, or "inorganic solids" is highly arbitrary and it must be replaced in final analysis by a careful study of each specific case.

CHAPTER 2

SPECTRAL EMITTANCE OF POLISHED STAINLESS STEEL, ALUMINUM, AND MAGNESIUM AT 50°C IN THE 0.25-28 μ WAVELENGTH REGION

SECTION I. INTRODUCTION

This chapter describes the results of an experimental study of the spectral emittance of polished stainless steel, aluminum, and magnesium in the wavelength range 0.25-27.0 microns, at 50°C. This work was undertaken for the purpose of determining the changes in emission properties accompanying varying degrees of surface roughness of the specific samples under study.

SECTION II. DEFINITIONS AND THEORY

Thermal radiation properties of a particular material are characterized by a dimensionless parameter, hemispherical spectral emittance, $\epsilon(\lambda,T)$, defined as the ratio of the spectral emissive power, $J(\lambda,T)$, (power radiated per unit surface area per unit wavelength interval) of a material at wavelength, λ, and temperature, T, to the spectral emissive power of a black body radiation, $J_b(\lambda,T)$, at the same wavelength and temperature:

$$\epsilon(\lambda,T) = \frac{J(\lambda,T)}{J_b(\lambda,T)} \tag{10}$$

$J_b(\lambda,T)$ for the black body radiator is given by the Planck radiation equation:

$$J_b(\lambda,T) = \frac{c_1\lambda^{-5}}{e^{c_2/T}-1} \tag{11}$$

where c_1 and c_2 are the usual radiation constants. In the ideal case of a perfectly smooth, flat material, this dimensionless parameter becomes the spectral emissivity, and is considered an intrinsic material property. Because surface conditions strongly influence the intensity and spectral distribution of the emitted radiation, the analogous parameter for real materials is defined as emittance. [34]

For opaque materials, Kirchhoff's law relates the emittance, $\epsilon(\lambda,T)$, and reflectance, $r(\lambda,T)$, by the equation:

$$\epsilon(\lambda,T) + r(\lambda,T) = 1 \tag{12}$$

Measurement of spectral emittance is usually carried out at relatively high temperatures by a direct comparison of radiation emitted by the sample with radiation emitted by a black body at the same temperature. In this case, the equation:

$$\epsilon(\lambda,T) = \frac{J(\lambda,T)}{J_b(\lambda,T)} \tag{13}$$

can be employed for evaluation of results. This method of measurement is not applicable at low temperatures, particularly for poor emitters such as metals, since the low intensity radiation emitted by the sample is nearly equal to the radiation from the surrounding environment which is reflected by the sample and also received by the detector. To surmount this difficulty, some form of reflectance method must be employed.

In choosing one of many types of reflectance methods, one must bear in mind the properties of the samples under consideration. The method of using a collimated beam incident on the material and reflected directly to the detector is applicable only to specular reflectors. For the case of partially diffuse reflectors, such as metals of varying degrees of surface roughness, it is essential that one measure the intensity of radiation reflected into the entire hemisphere above the sample. For the wavelength range 0.25 to 2.5 microns, the integrating sphere can be employed; in the infrared region, one must seek other methods.

Before describing the method used in this particular study, for the infrared region one should note an analogous method which has been utilized for measuring diffuse spectral reflectance [35].

The basic components consisted of a heated hohlraum (~ 1500°F), a water-cooled sample (~ 150°F), and an optical system. The sample protruded from the inner wall of the hohlraum which acted as a black body reference. For a given wavelength, the diffuse radiation emitted by the hemispherical wall and reflected normally by the sample was compared to the energy emitted by the black body. The ratio of the net deflections of the recording system is a direct measure of the normal component of diffuse spectral reflectance. The principal problems in this method are:

a. to obtain a strict temperature uniformity over the entire surface of the hohlraum wall,

b. to maintain the hohlraum at a high and very stable temperature, and

c. to keep the sample at a much lower stable temperature inside the hohlraum.

Consideration of these problems directed us to the alternative method now to be described.

The basic principle underlying the method of measurement of spectral emittance employed in this study can be described by referring to FIGURE 1. Consider a sample at constant temperature, T, surrounded by a thermostatically controlled shield at Temperature, T_1. This shield forms a black body which irradiates the sample from all angles within a hemispherical solid angle. The resultant normal component of diffuse radiation emitted by the shield and reflected from the sample emerges through a small circular aperture in the shield and is then imaged onto the detector by a suitable optical system. A gold-plated chopper mirror is mounted in the beam such that the detector alternately receives radiation from the sample and from a reference black body held at temperature, T_o. The net signal received by the spectrometer detector represents the difference in radiant power between the two sources, and can be expressed as:

$$S_1 = \left[\epsilon(\lambda,T)\ J(\lambda,T) + r(\lambda,T_1) + W(\lambda,T') - J(\lambda,T_o) \right] kA\omega t\Delta\lambda \qquad (14)$$

where

$\epsilon(\lambda,T)$ is the emittance of the sample at λ,T

$J(\lambda,T)$ the black body radiant intnesity at λ, T

$r(\lambda,T)$ the reflectivity of the sample

$W(\lambda,T')$ any additional background radiation at same temperature T'

$J(\lambda,T_o)$ the radiation intensity from the blackbody at T_o.

The constants, k, A,ω, t, $\Delta\lambda$, correspond to the sensitivity of the detector, the area of entrance slit, the solid angle of view, the effective transmissivity of the optical system, and the wavelength band passed by the exit slit of the spectrometer, respectively. Note that $r(\lambda,T)$ represents the normal component of diffuse spectral reflectance.

SECTION III. EXPERIMENTAL METHOD FOR THE INFRARED [36]

The actual method consists of two runs per sample:

a. The blackbody shield is held at the same temperature as the sample, T, and

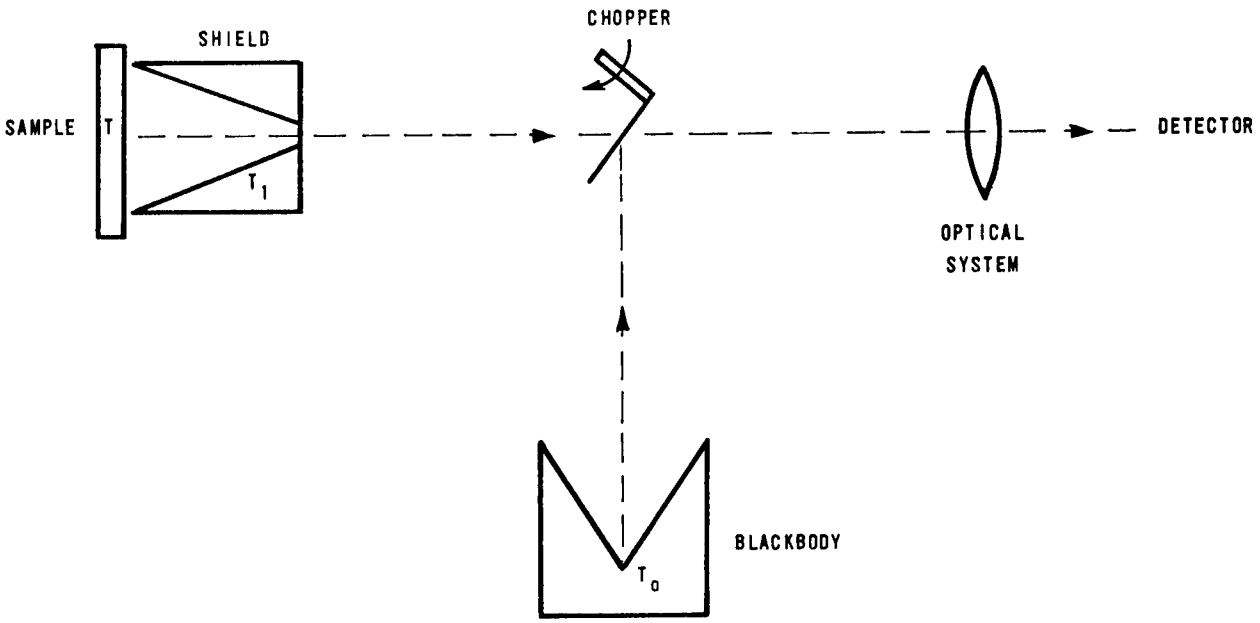

Figure 1. Basic Principle of Operation

b. the blackbody shield is held at a temperature of liquid nitrogen T_2.

Assuming that any additional background radiation is always constant and equal for both runs, we have the expression for the difference in signals between the two runs at λ,T:

$$s = s_1(\lambda,T) - s_2(\lambda,T) = r(\lambda,T)\left[J(\lambda,T) - J(\lambda,T_2) \right] kA\omega t\Delta\lambda \qquad (15)$$

Now if a gold-plated sample with reflectance $\tilde{=} 1$ is used as a reference standard, the expression becomes:

$$\bar{s} = \bar{s}_1(\lambda,T) - \bar{s}_2(\lambda,T) = \left[J(\lambda,T) - J(\lambda,T_2) \right] kA\omega t\Delta\lambda \qquad (16)$$

The ratio of $s/\bar{s}$ gives the normal component of diffuse spectral emittance through Kirchhoff's law.

$$\frac{s}{\bar{s}} = r(\lambda,T) = \epsilon(\lambda,T) \qquad (17)$$

With this method it is important to maintain similar conditions in enviromental temperature for all runs in order that the background radiation term, $W(\lambda,T')$,will always cancel out. Also, careful temperature control of sample blackbody shield and reference blackbody is necessary for accurate reproducible results.

A schematic diagram of the actual system employed for this study is illustrated in FIGURE 2. A sample, s, was mounted in a holder which is heated to the desired temperature by water coils. An iron-constantan thermocouple was inserted through an approximately 0.11-inch diameter hole in the side of the sample to a position close to the front center surface of the sample. With the use of a Leeds and Northrup type K potentiometer and galvanometer, the temperature of the sample was controlled to $\pm$ 0.5°C.

The thermostatically controlled shield consisted of a core wound with two sets of coils. For run No. 1, heated water was circulated through both the sample holder and one set of the shield coils. For run No. 2, the water in the shield was removed, and liquid nitrogen was forced through the other set of coils at a pressure of 5-15 pounds. The sample shield, and mirrors, M_1 and M_2, were enclosed in a dry box which was flushed with nitrogen in order to reduce the water vapor which would enhance the absorption in the water bands of the spectrum in a variable manner.

The reference blackbody, consisted of a dewar flask with a blackened

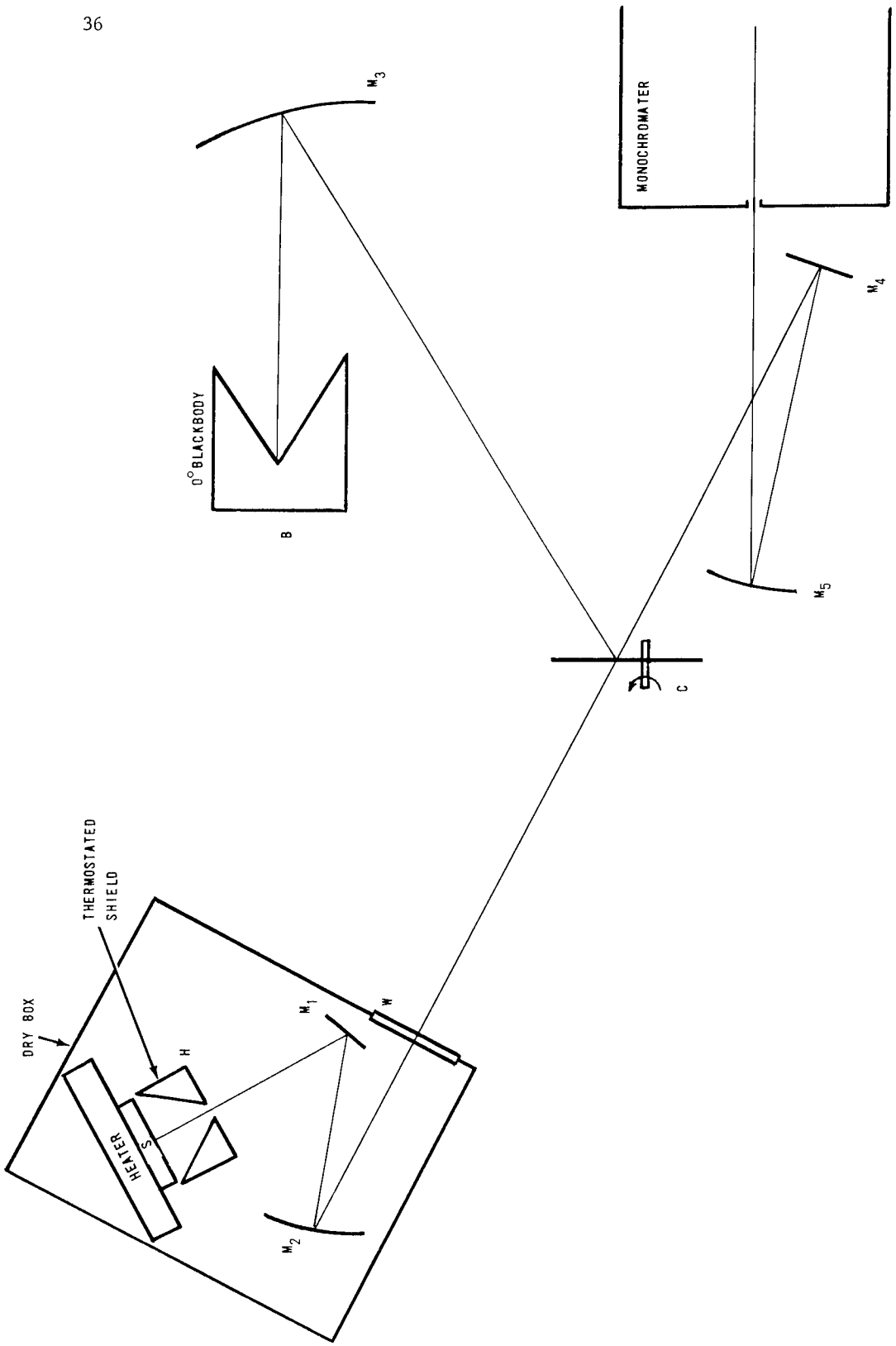

Figure 2. Basic Optics for Room Temperature Spectral Emittance Measurements

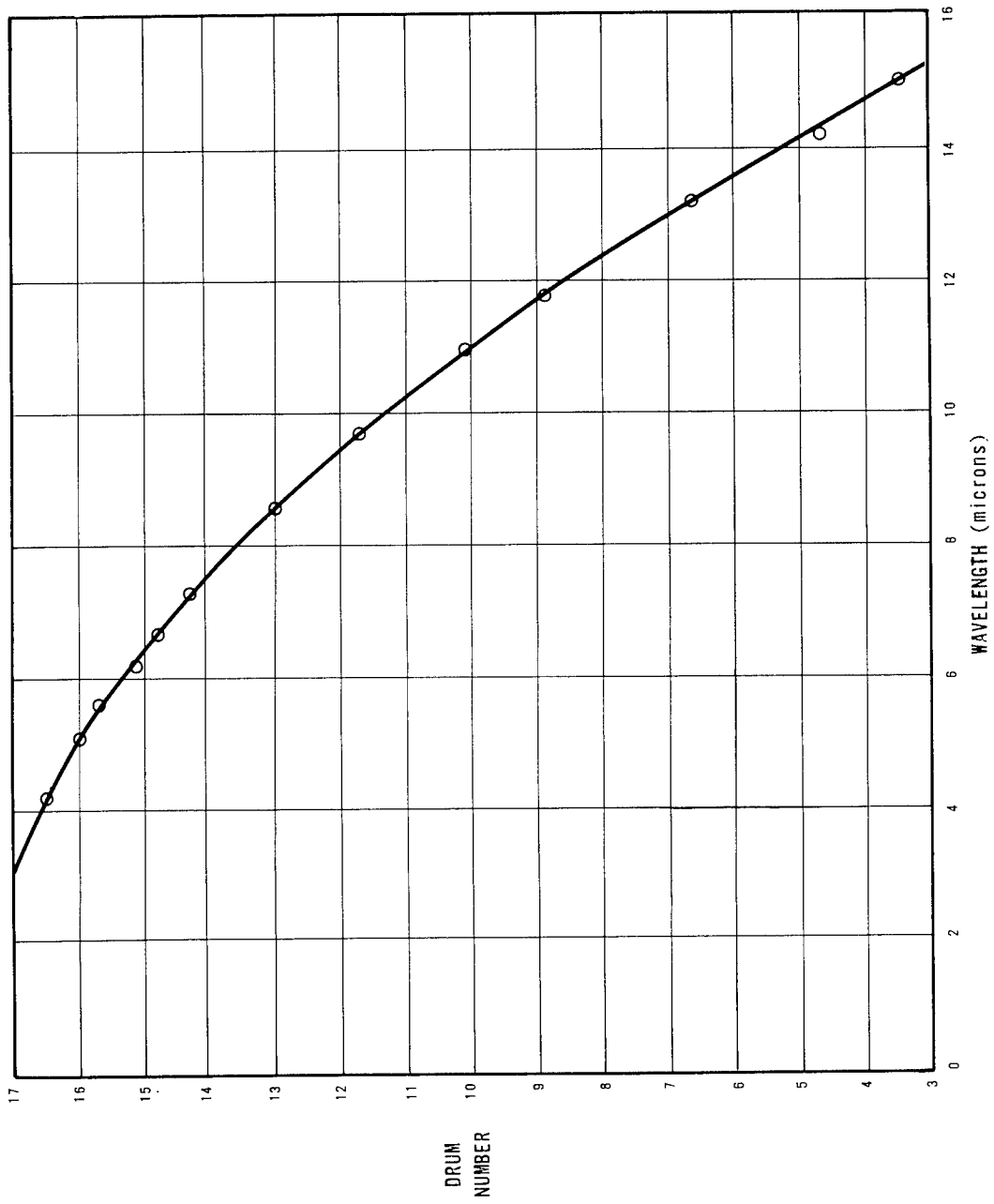

Figure 3. Calibration Curve for NaCl Prism

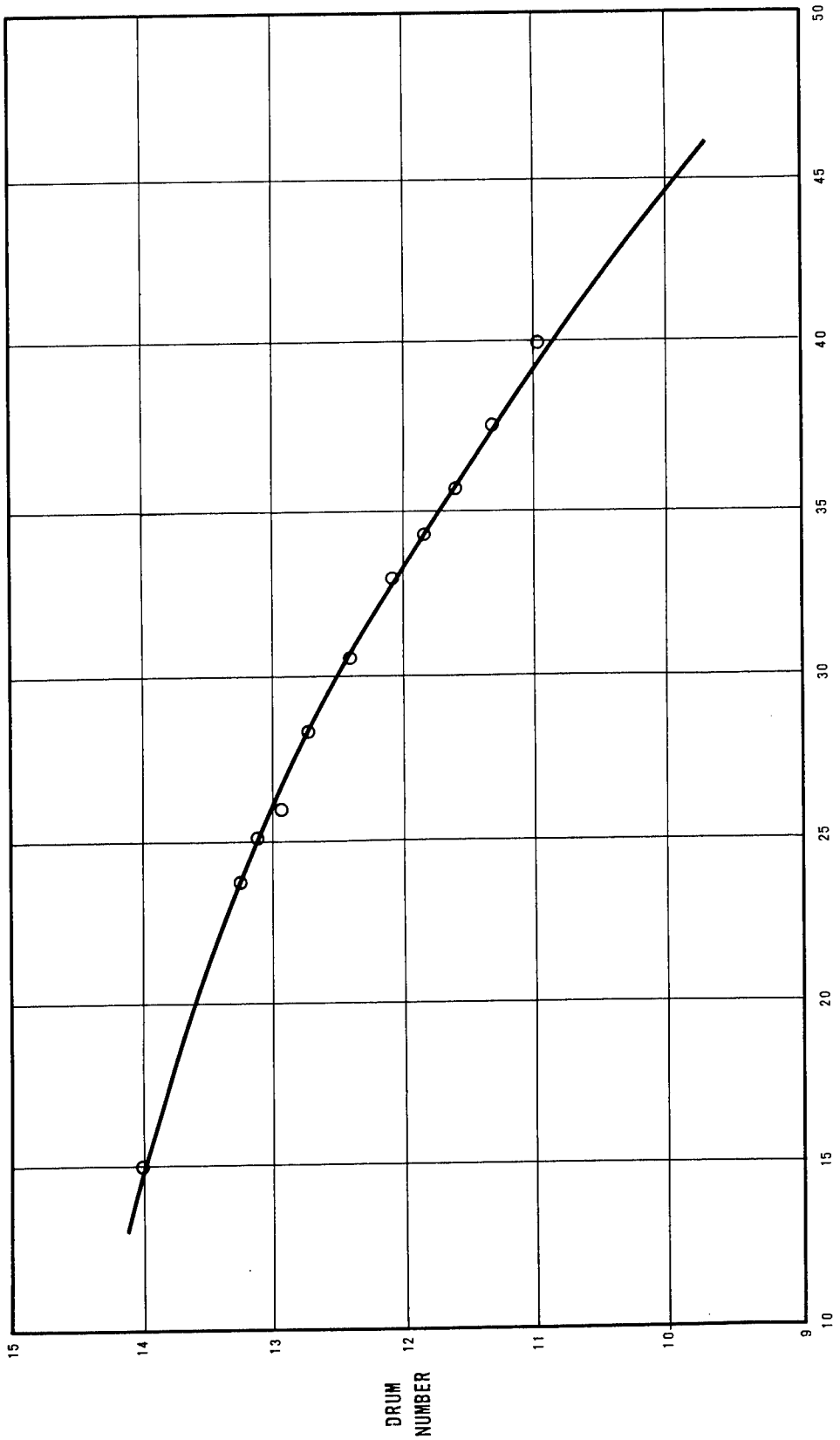

Figure 4. Calibration of CsI Prism with 50°C Source

inside surface and was maintained at ice temperature with crushed ice.

A gold-plated chopper blade was located at the focal point such that radiation from the sample passing through the silver chloride window W and radiation from the reference blackbody at 0°C was alternately focussed by mirrors, M_4 and M_5, on the entrance slit of the spectrometer set at a width of 1000 μ. A sodium chloride prism was used in the 2 to 15 μ wavelength range; for the 14 to 27 μ range, a cesium iodide prism was used, together with a polyethylene film impregnated with carbon black and placed at the entrance slit to filter out stray short wavelength radiation.

During a typical run No. 1, the sample, was allowed to stablize at the desired temperature by monitoring a Sargent Thermonitor temperature control unit which heated a water reservoir. Throughout the run it was necessary to keep a constant check on the sample thermocouple reading and to correct for the lag in water reservoir temperature and sample temperature. Instead of taking a continuous spectrum, the data was recorded as a series of points predetermined from the prism calibration chosen to avoid atmospheric absorption bands as much as possible. This method of recording served as a check on any substantial sample temperature drift as well as representing essentially an average reading for any particular wavelength. All readings were converted to microvolt units and calculations were carried out in accordance with Equations (16) and (17).

SECTION IV. THE INTEGRATING SPHERE AND EXPERIMENTAL METHOD

The reflectance measurements for the 0.25- to 2.5- μ wavelength region were made with a Beckman 24500 Reflectance Unit in combination with a Beckman DK-2 monochromator. The integrating sphere and accessory optics are illustrated in FIGURE 5. For the samples under study, the total reflectance (specular plus diffuse) was measured by passing monochromatic radiation through the sphere's entrance ports directly onto the sample and reference plate at an angle of approximately 5 degrees from the surface normal. The two components of totally reflected radiation are then multiple reflected throughout the interior surface of the integrating sphere. A detector located 90 degrees to the sample surface normal receives the diffuse radiation illuminating the sphere. A tungsten lamp source and lead sulfide detector were used for the 0.45- to 2.5- μ region; for the 0.350- to 0.650- μ region, the tungsten lamp and photomultiplier were used, and for the 0.250- to 0.400- μ region, a hydrogen lamp source and photomultiplier were employed.

In order to determine the 100 percent reflectance signal of a reference, two MgO plates were prepared by coating them with magnesium oxide smoke from a burning magnesium ribbon. Both plates were then mounted in the two exit ports of the integrating sphere and a signal, $r_1'(\lambda)$, was

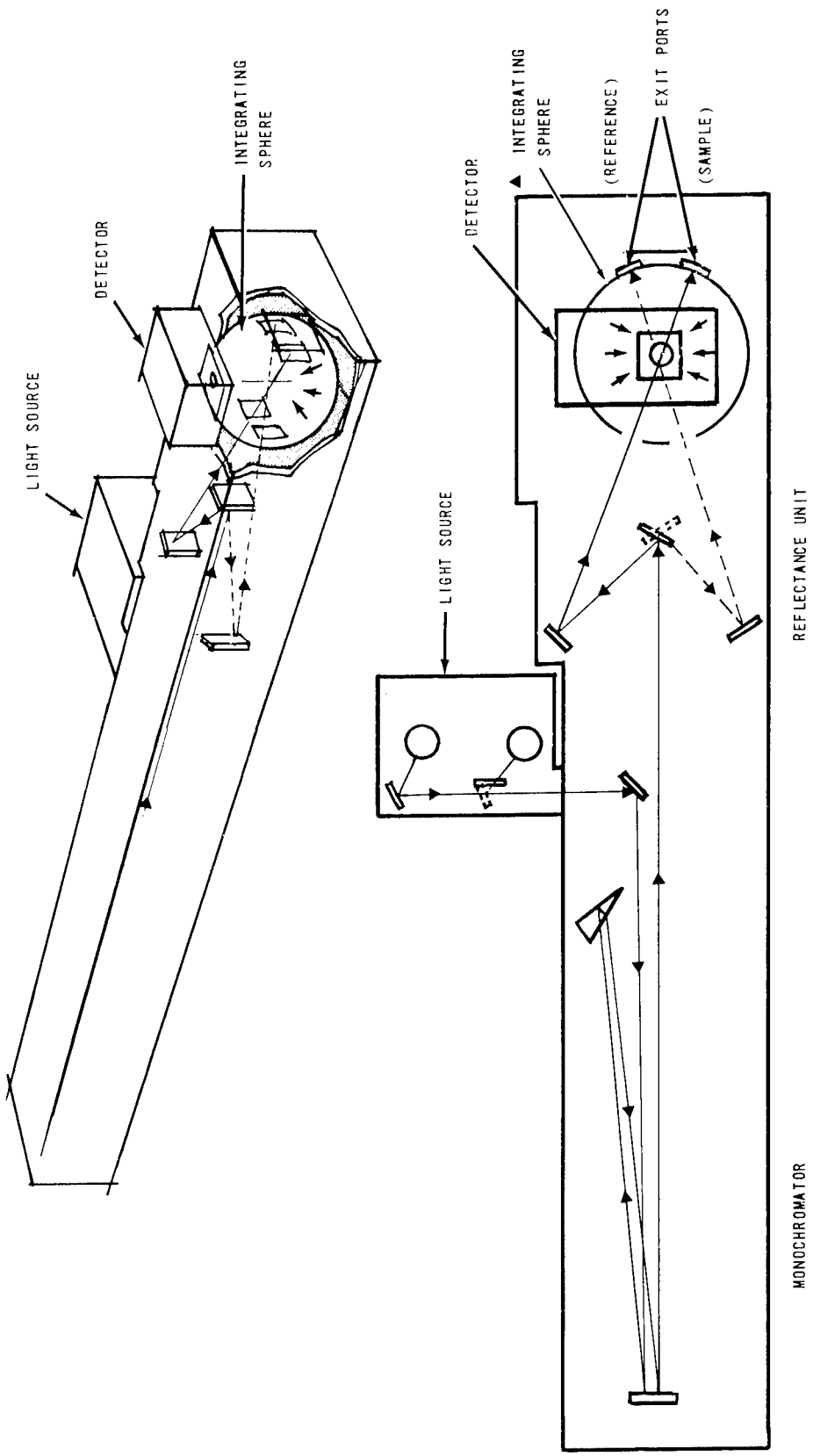

Figure 5. Reflectance Spectrometer Arrangement

recorded throughout the entire spectrum. This signal represents the ratio of intensity reflected by the sample port to that of the reference port.

$$r'_1(\lambda) = \frac{I_{M_1}(\lambda)}{I_{M_2}(\lambda)} \tag{18}$$

This procedure was repeated with the MgO plates in reversed position, giving the term $r'_2(\lambda)$:

$$r'_2(\lambda) = \frac{I_{M_2}(\lambda)}{I_{M_1}(\lambda)} \tag{19}$$

An averaged 100 percent signal for the MgO reference is then expressed as:

$$r'_o(\lambda) = \frac{r'_1(\lambda) + r'_2(\lambda)}{2} = \frac{I_{M_1}^2 + I_{M_2}^2}{2\, I_{M_1}\, I_{M_2}} \tag{20}$$

The difference between the true 100 percent response of the recorder and the MgO 100 percent signal represents a correction term:

$$\Delta r'(\lambda) = 100 - r'_o(\lambda) \tag{21}$$

If a sample now replaces one of the reference plates, one measures the ratio of sample to reference reflectance, r', and when the correction term is included:

$$r(\lambda) = r'(\lambda) + \Delta r'_o(\lambda) = \frac{I_s}{I_{M_o}} \tag{22}$$

If the true reflectance of MgO reported in the literature [38, 39, 40, 41, 42] is denoted as:

$$R_o = \frac{I_{M_o}}{I_o} \tag{23}$$

then the absolute reflectance of the sample is easily calculated as a product of R_o and r.

$$r_o = rR_o = \left[\frac{I_s}{I_{M_o}}\right]\left[\frac{I_{M_o}}{I_o}\right] = \frac{I_s}{I_o} \tag{24}$$

Again utilizing Kirchhoff's law, Equation [20], the spectral emittance in the 0.25- to 2.5- μ range can be determined.

SECTION V. PREPARATION OF SAMPLES

The front surface of all samples were initially roughened with a variety of emery papers. The aluminum and magnesium were then brought to a fine polish with the use of a grinding wheel and alumina powder.

The stainless steel samples were electropolished with a solution consisting of:

300 ml orthophosphoric acid

530 ml glycerine

90 ml water.

After the completion of the experimental measurements the arithmetic average surface roughness in the X and Y direction was determined on a T and H Talysurf-Model 3 instrument. The results, reported as center line average roughness, are listed in Table V. It should be mentioned that the magnesium surface acquired a cloudy appearance due to the formation of an oxide layer.

SECTION VI. EXPERIMENTAL RESULTS

Measurements were made on samples of magnesium, aluminum,and stainless steels of various surface roughness throughout the 0.25- to 27.0- μ wavelength range at 50°C temperature. The stainless steel samples consisted of blocks approximately 2 x 2 x 0.5 inches in size having their front surface electrolytically polished to a bright mirror appearance. "In general, physical and chemical properties which have been determined on mechanically polished surfaces are not characteristic of the bulk metal. However, if the necessary precautions are taken electropolishing methods can produce a brilliant, smooth film-free surface with properties characteristics of the metal rather than of the method of preparation." [43]

The use of electropolishing in the preparation of these samples was made with the intention of removing the amorphous deformed layer (termed the Beilby layer) produced by the initial abrasion treatment. However, as evidence by the surface profile measurements and photomicrographs, the samples still have scratches and pits. The pitting is commonly observed in the case of stainless steel due to the differential attack of the multiphase alloy. From consideration of the physical nature of the reflection

process, one would expect a noticeable effect for short wavelength reflection. In this region the light will be trapped by the grooves and pits and become diffusedly reflected, thus increasing the percentage of diffuse reflection and decreasing the total reflection by trapping. At long wavelength this process does not occur, diffuse reflection becomes negligible and the surface has a greater effective smoothness. Similar blocks of aluminum and magnesium were polished by the usual abrasion methods.

In all the experimental curves this trend toward greater reflectivity (i.e. lower emittance) with longer wavelengths is observed. Also, comparison of samples of the same material but of different surface roughness reveals that they all approach essentially the same value at long wavelengths where the effects of surface irregularities become less important to the reflection process. In regard to most of the reported curves one may note a certain irregularity at approximately 3 μ and 14 μ. At the 3-μ point the Beckman Integrating Sphere data are joined to the Perkin-Elmer data, and it is not unreasonable to expect some slight discontinuity, especially when one notes that the lead sulfide detector response will tend to fall off at this point. (Note also the change in wavelength scale at 3 μ on the graphs.)

The 14-μ region represents the transition from the sodium chloride prism to the cesium iodide prism and the introduction of the polyethylene filter to reduce short wavelength scattered light. Finally, the slight increase in emittance at very long wavelengths (25 μ and greater) in some cases is unreal and probably produced by an increase in scattered light which the detector receives from the enviroment.

Experimental results for three samples of stainless steel 316 are shown in FIGURES 6, 7, and 8; a very rapid decrease in emittance occurs between 0.25 μ and 0.75 μ at which point the curve acquires a much more gradual slope until the region of 26 μ where samples No. 2 and No. 3 assume a value of approximately 0.06 μ; however, sample No. 4 at that point has an emittance of about 0.085 which coincides with the greater roughness of its surface recorded by mechanical measurements.

A sample of stainless steel 304 was also measured and is shown in FIGURE 9. This exhibits the characteristic slope and approaches a probable value of 0.075 at 26 μ. This curve indicates a slight error in the transition region of 2.5 μ to 6.5 μ noted previously. The deviation around 6 μ can be attributed to water vapor absorption. Also the apparent rise at 24 to 28 μ is due to scattered light.

The emittance curves for aluminum 20-24 are shown in FIGURE 10. Measurements throughout the 0.25- to 27.0- μ range were carried out on sample No. 3. The sharp decrease in emittance between 0.25 and 0.5 μ is not quite as striking as for the stainless steel but is still a characteristic at short wavelengths. In the wavelength interval 0.5 to 1.0 μ,

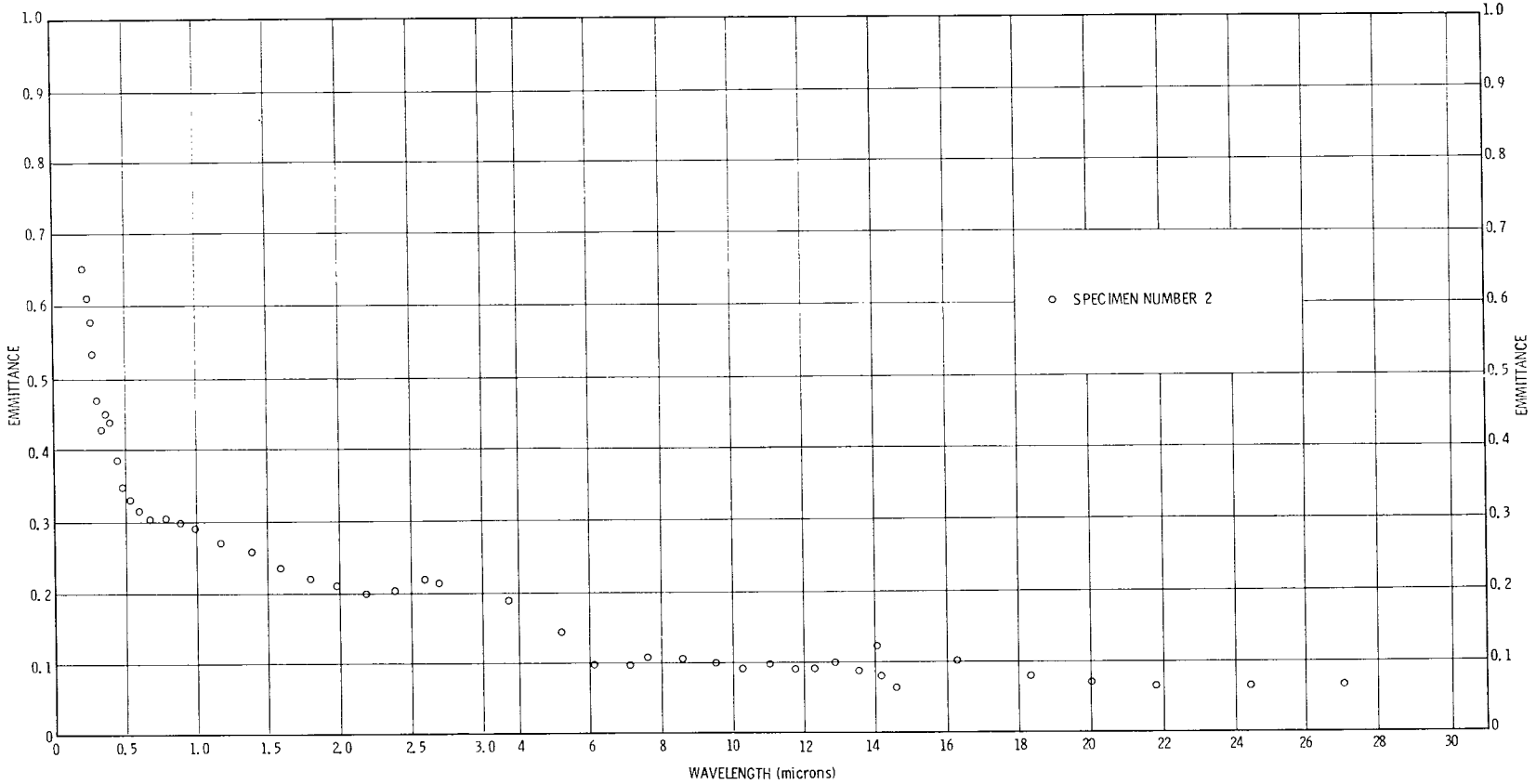

Figure 6. Type 316 Stainless Steel - Specimen Number 2

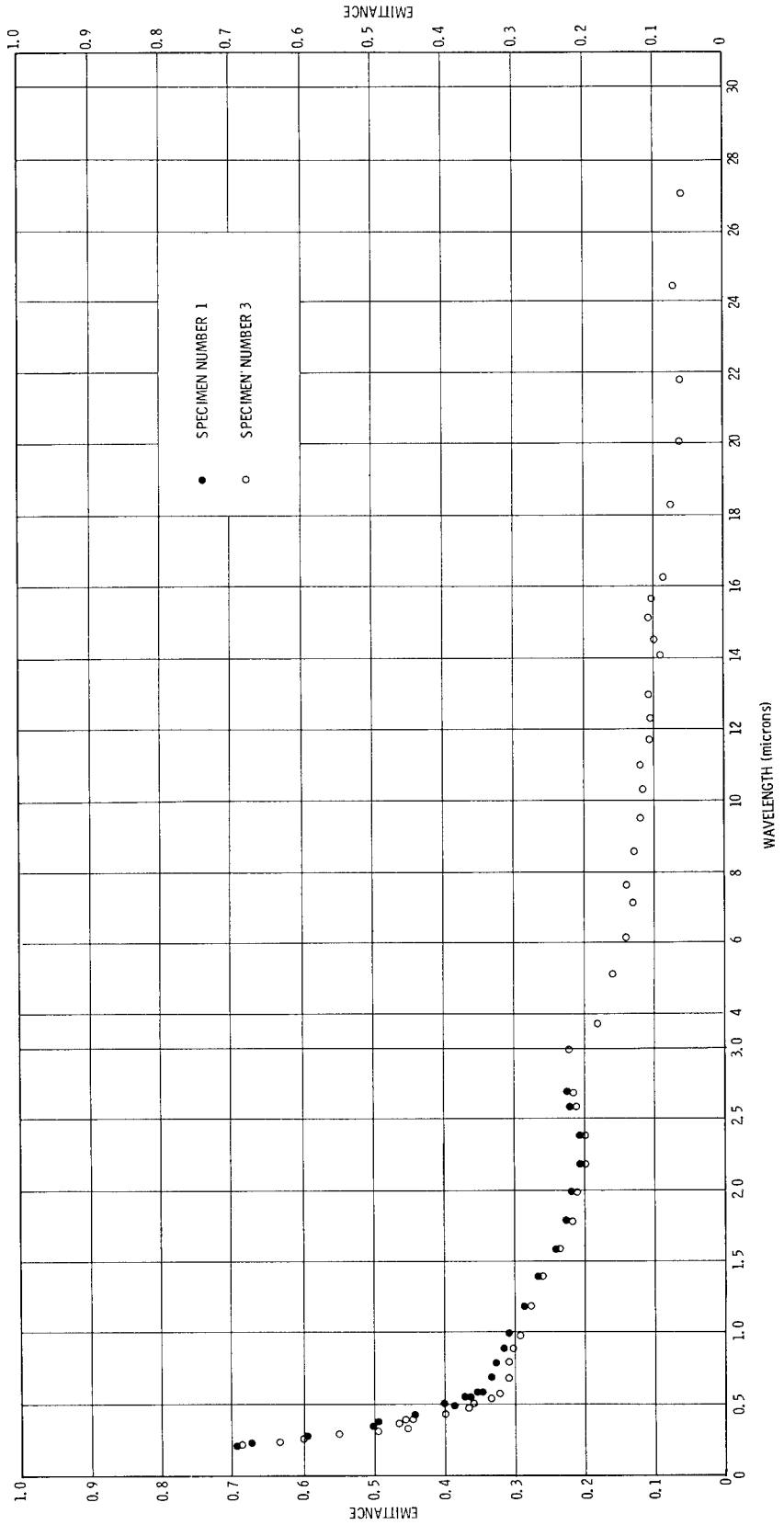

Figure 7. Type 316 Stainless Steel - Specimen Numbers 1 and 3

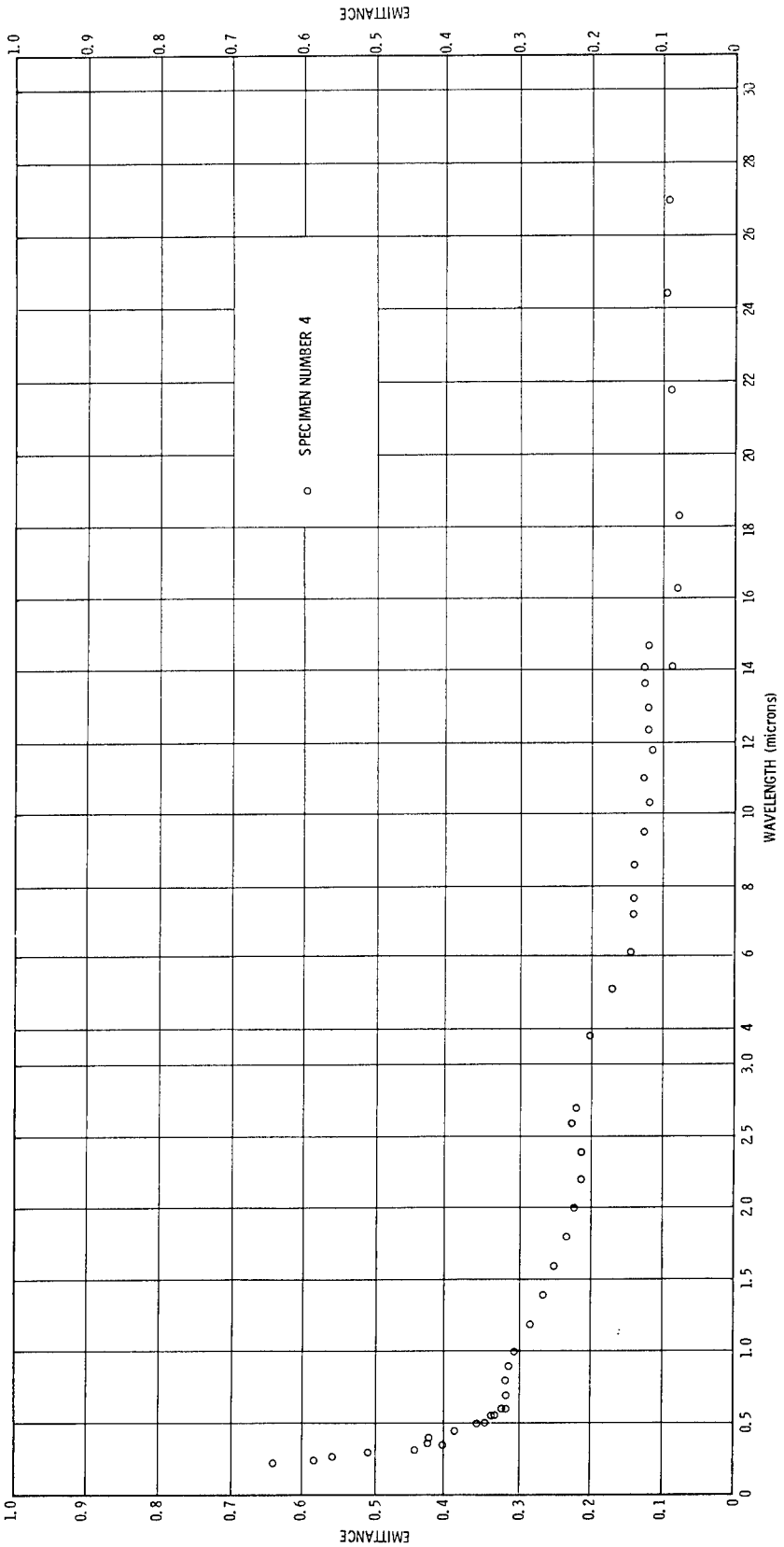

Figure 8. Type 316 Stainless Steel - Specimen Number 4

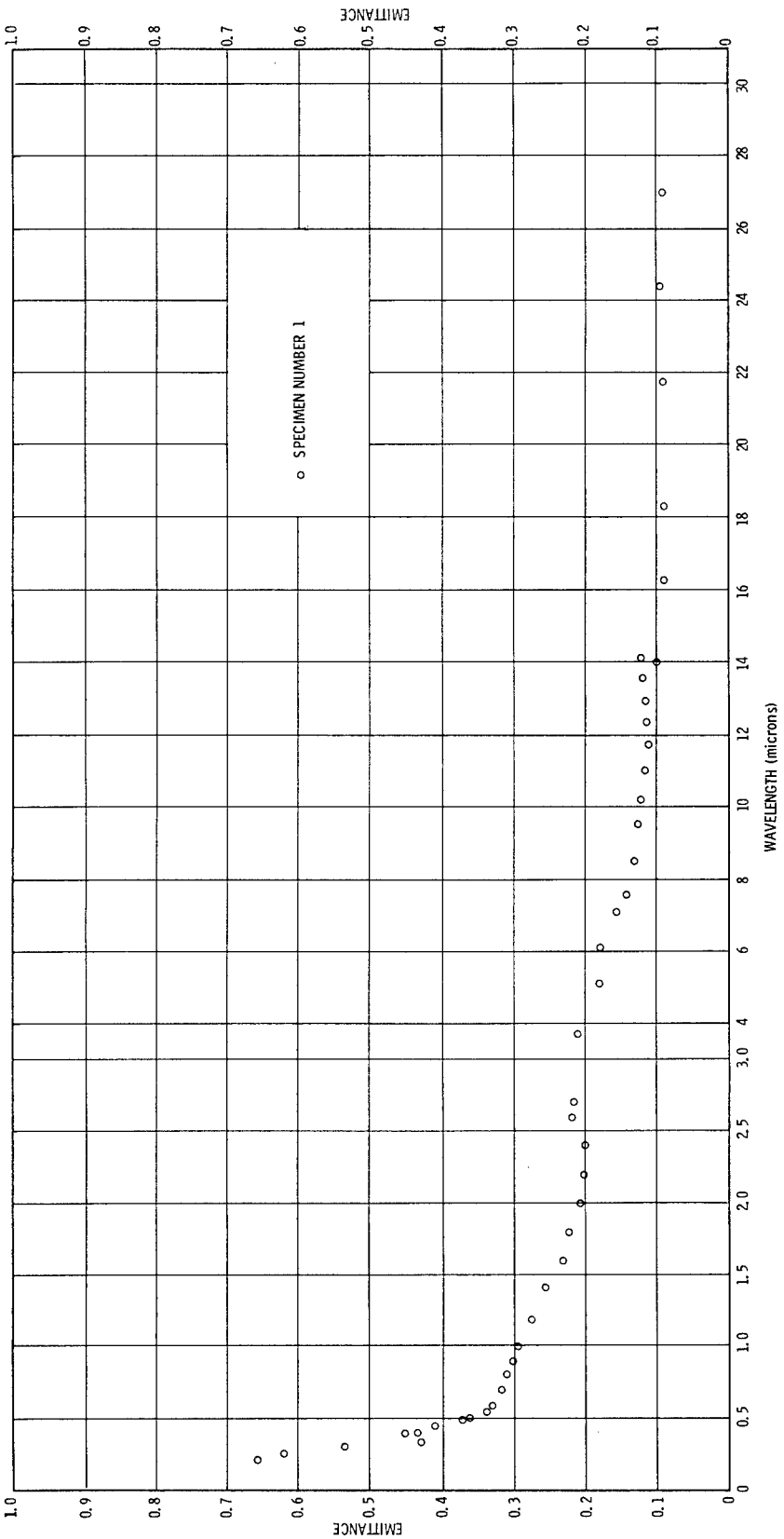

Figure 9. Type 304 Stainless Steel

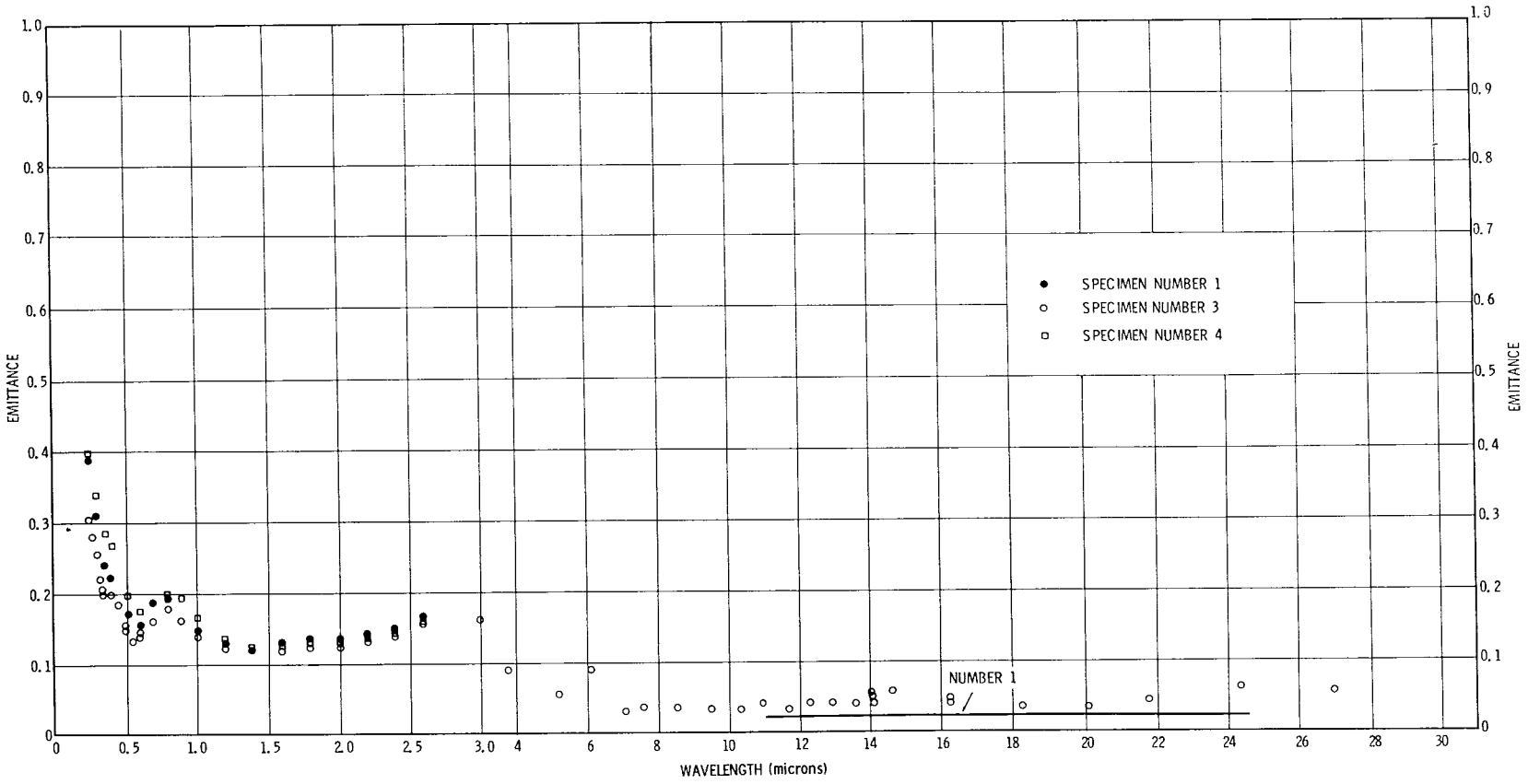

Figure 10. Type 20-24 Aluminum

there appears to be a definite bump (rising from a value of about 0.14 at 0.5 μ to a small peak of 0.18 at 0.8 μ). A thin Al_2O_3 film on the surface indicating an absorption resonance frequency may account for the peak at this point. The curve then continues to decrease with longer wavelengths in the usual manner; the 3-μ transition region occurs as in previous curves. The emittance levels off at a shorter wavelength than that of stainless steel and assumes an average emittance of 0.035 from 8 μ to 27 μ. A curve for No. 1 has been drawn in this region for comparison and one notes its value to be 0.023, indicating a smoother surface. Data for samples Nos. 1 and 4 have also been drawn between 0.25 μ and 2.5 μ. In general, all three samples have nearly the same emittance, with the same bump between 0.5 μ and 1.0 μ. This fact indicates that either the surface roughnesses of all three samples are essentially equivalent, or else an Al_2O_3 film on the three surfaces is covering up any effect of differing surface conditions which otherwise would be observed if the film were absent.

The emittance curves for aluminum 70-75 are shown in FIGURE 11. This exhibits a shape very similar to that of aluminum 20-24, with the typical bump in the 0.5-1.0 μ region. Also, between the wavelengths of 6-27 μ it takes on a fairly level emittance of about 0.035 as in the case of aluminum 20-24. However, in this case, sample No. 3 appears to have a higher emittance than samples No. 1 and No. 4 in the 1.0-3.0 μ region.

The curves for magnesium are shown in FIGURE 12. In the 0.25- to 2.5- μ region one observes a striking decrease in emittance with longer wavelength in addition to a significant difference between the values for samples Nos. 1, 3, and 4. Sample No. 4 has a much greater emittance throughout this region whereas No. 1, although having a larger emittance than No. 3, does approach it around 0.75 μ.

The bump which appeared between 0.5 μ and 1.0 μ in the case of aluminum does not appear in the magnesium curves at all. The measurements out to 27 μ were made on sample No. 3 with greatest attention, although the short wavelength data definitely indicate that all three samples approach a similar value for the longer wavelengths, as would be expected. Between 6 μ and 27 μ the emittance assumes a constant value of approximately 0.055. Again the apparent rise from 22 to 27 μ is unreal and due to scattered light.

SECTION VII. DISCUSSION OF EXPERIMENTAL ERRORS

The chief source of error for the 2-27 μ wavelength range are:

1. Possible error in the true reflectivity of the gold standard;

2. Changes in temperature of the enviroment;

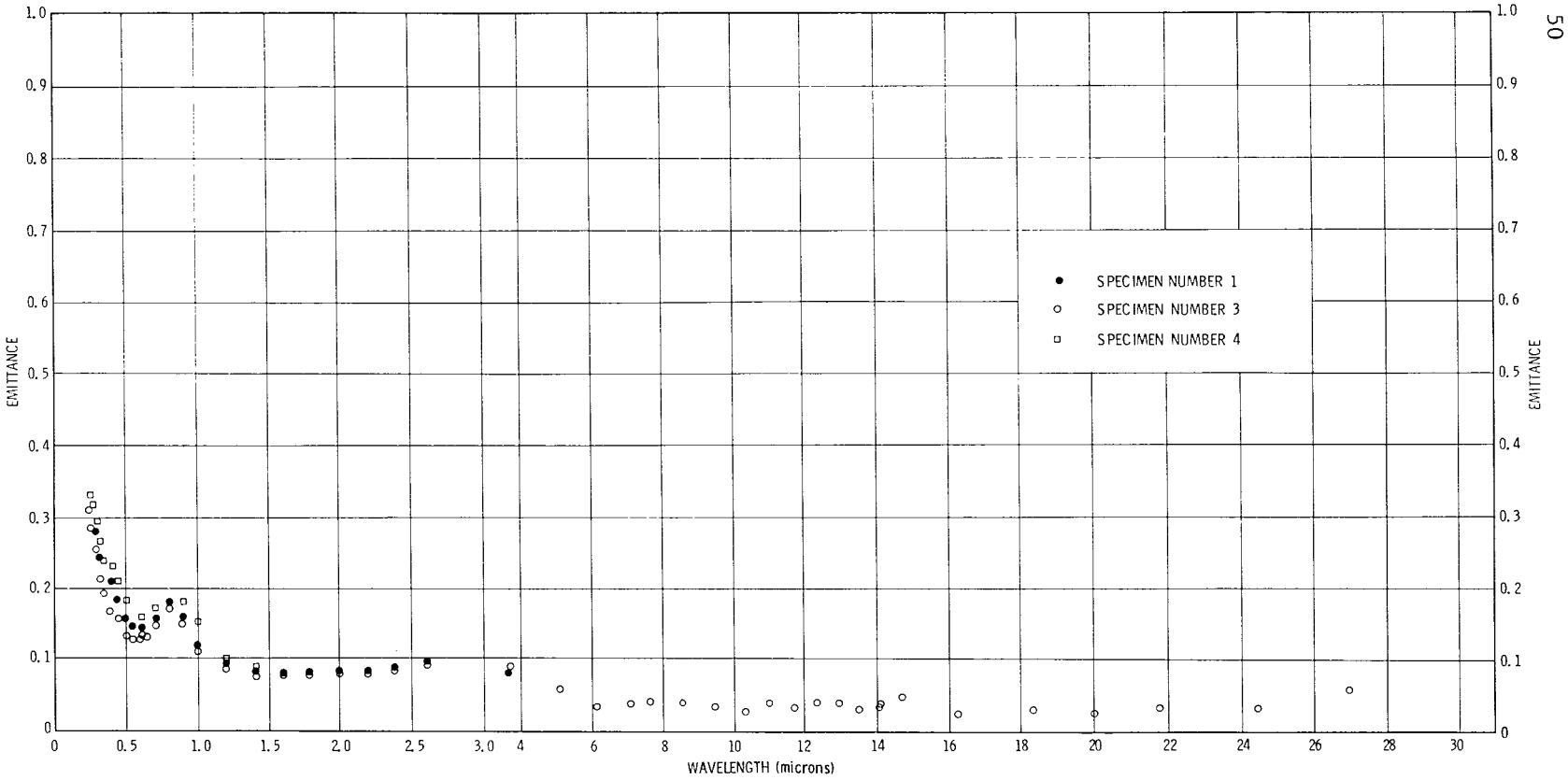

Figure 11. Type 70-75 Aluminum

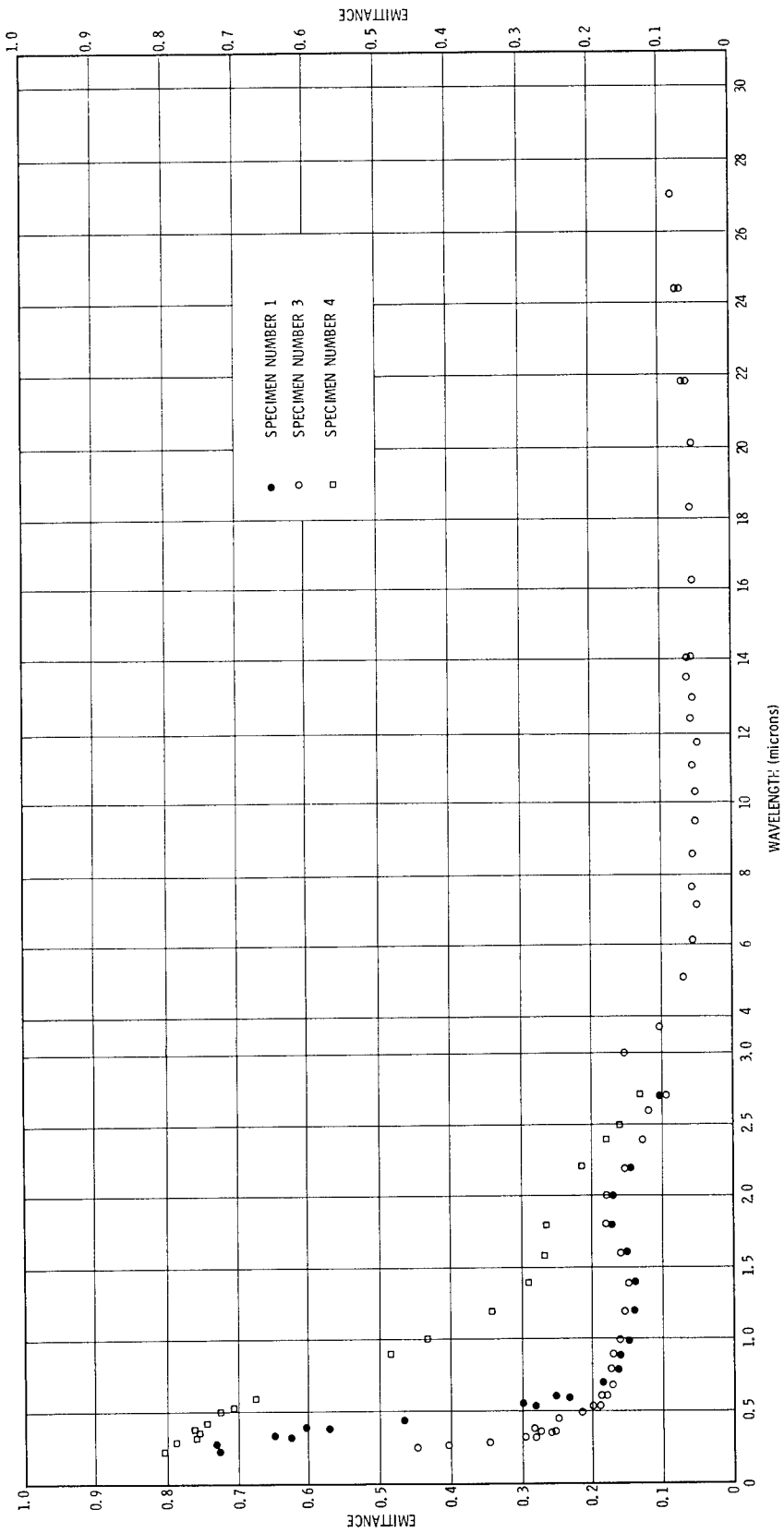

Figure 12. Magnesium Alloy

3. Variations in atmospheric absorption;

4. Sample temperature errors;

5. Use of a large slit width;

6. Prism calibrations;

7. Amplifier drift;

8. Other, such as slight shifts in optical alignment.

The calculations (1 above) were based on the assumption that the gold standard had a reflectivity equal to 1. However, it is known that electrolytically deposited gold has a reflectivity of approximately 0.98 between 7 μ and 14 μ wavelengths [44] (FIGURE 13). A percent error of 2 percent in the calculated reflectivity of a sample will result from a 2-percent error in the assumed reflectivity value for the gold standard. This is easily seen from Equation (17) where $R(\lambda,T)$ is now the true reflectivity of gold, and $r'(\lambda,T)$ equals the measured reflectivity of the sample.

$$r'(\lambda,T) = \frac{s}{\bar{s}} = \frac{r(\lambda,T)}{R(\lambda,T)} \tag{25}$$

Thus, the connected value of reflectivity is given by:

$$r(\lambda,T) = R(\lambda,T)r'(\lambda,T) \tag{26}$$

A. CHANGES IN TEMPERATURE OF THE ENVIROMENT (2 ABOVE)

Changes in the temperature of the environment should also be considered when discussing scattered radiation, since any such change will also affect the intensity and spectral distribution of scattered radiation. These temperature variations were kept to a minimum by carrying out the experiments in a temperature-humidity controlled room. In addition all measurements were made during equivalent time periods each day to maintain similar conditions.

B. VARIATIONS IN ATMOSPHERIC ABSORPTION (3 ABOVE)

Although the experimental equipment was located in a temperature-humidity controlled room, large daily variations in humidity will affect the radiation intensity within the strong absorption bands, and particularly in the 6-μ region. With a large number of data points one can take into account such discontinuities when drawing the curves. For the path length

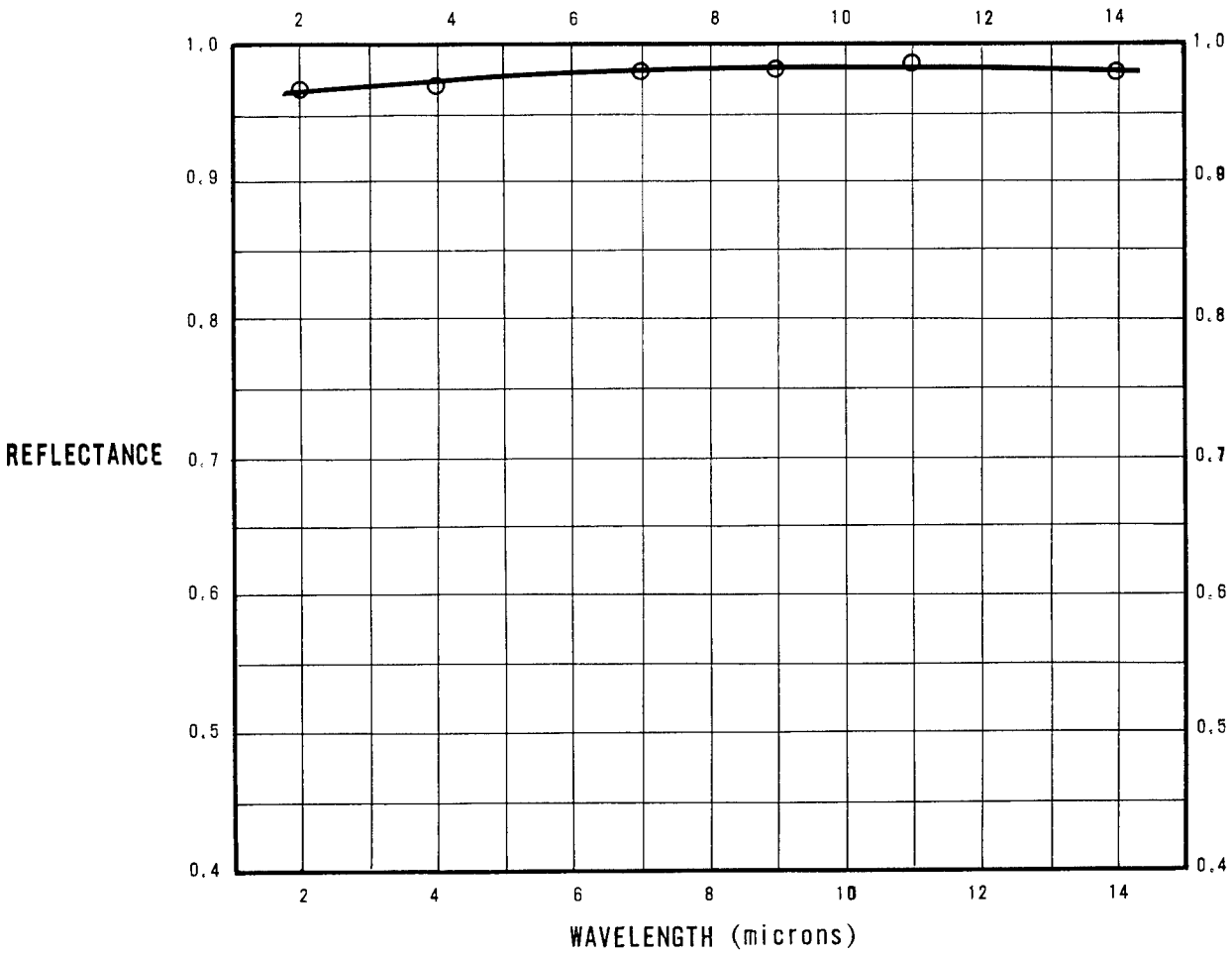

Figure 13. Reflectance of Electrolytically Deposited Gold

REFERENCE Smithsonian Physical Tables, 9th ed., 1954, p. 552.

in air involved, absorption in other regions of the spectrum will change the general level of measured reflectivity to a negligible degree.

C. SAMPLE TEMPERATURE ERRORS (4 ABOVE)

Errors due to sample temperature drift are negligible, the variation being less than $\pm$ 0.5°C, during measurements. Any effects of such temperature variation on the radiation intensity were undetectable at the low temperature level of 50°C.

D. INSTRUMENT ERRORS (5, 6, 7, 8 ABOVE)

Errors arising from items 5, 6, 7 and 8 are difficult to assess. By using a constant slit width throughout measurements, allowing an adequate warm-up time for the electronic equipment, and making careful initial optical alignment and prism calibrations, these errors were minimized. Constant checks on the amplifier gain and zero points indicated that the drift was negligible. From the scatter of data points, the results point to a probable over-all error of $\Delta r = \pm 0.02$. One of the advantages of this method is the elimination of a pyrometer or standard black body which would cause additional errors in experimental results. Also, it eliminates the necessity of absolute flux calibrations and the subsequent tedious calculations.

CHAPTER 3

THEORY OF OPTICAL AND INFRARED PROPERTIES OF METALS

SECTION I. INTRODUCTION

The interactions of metals with an external electromagnetic field manifest themselves in different forms depending on the different spectral ranges that are involved. Two particular examples may be cited, the dc electrical properties which we observe by applying a static electric field, i.e., the zero-frequency limit and the optical and infrared dispersion characteristics which are observed by means of proper optical apparatus where the frequency spectrum extends from the far infrared to the ultraviolet.

The present work is concerned with the normal dispersion characteristics in the optical and infrared range of the spectrum and the manner in which these properties are related to the dc electrical properties and other lattice parameters of metals. Inasmuch as we are concerned with normal dispersion in contrast to anomalous dispersion, the frequency spectrum that is involved in the present work must be sufficiently removed from the anomalous region in which photoelectric resonances of bound electrons become important. Most of the metals that have been studied are found to have their lowest resonances in the wavelength region, $0.3 \sim 1.0$ micron, and normal dispersion is observed for wavelengths longer than these values.

According to the free electron theory of metals, the free valence electrons are responsible for the normal dispersion of optical and infrared waves as well as for electrical conduction.

Ever since the discovery of electrons and Sommerfeld's successful explanation of the phenomenon of thermionic emission based on the free electron picture of metals and on the Thomas-Dirac statistics, it has been a popular notion that both optical dispersion properties and electrical properties may be explained on a common theoretical basis and that these two aspects of metallic properties are interrelated in a rather simple manner. Granted that the simple free electron description of metals is valid, such a notion finds justification in that both the optical dispersion and dc electrical properties are described by the equation of motion of the conduction electrons subject to the general description in terms of Maxwell's equations, the difference between the two aspects of metallic properties arising solely from the different spectral ranges that are involved.

Therefore, it may be expected that various frequency-dependent

optical quantities such as the optical conductivity, $\sigma(\omega)$, and the dielectric constant, $\epsilon(\omega)$, which described the optical dispersion properties, should also describe the dc electrical properties such as the dc electrical conductiveity, σ_o, and dielectric constant, ϵ_o, when we take the limit $\omega \to 0$ in various dispersion equations. On the other hand, the temperature-dependence of various optical quantities may be predicted from the more widely studied electrical properties.

Along with the development of quantum mechanics and quantum statistics, much progress has been made on the theory of electrical conduction in metals during the past 50 years, and current theory is successful in explaining the observed electrical conduction phenomena both qualitatively and quantitatively in most of the noble and alkali metals, and qualitatively in the transition metals. Modern physics is successful in explaining qualitatively some of the salient features found in alloys, e.g., Matthiessen's rule, dependence of resistivity on the relative concentrations of the constituent metal atoms in a random alloy, some unusual properties of the transition metal alloys, etc. Compared with what has been done on the electrical properties of metals, surprisingly little progress has been made on the theory of optical and infrared dispersion in metals. In fact, there is no satisfactory theory available that can predict the dispersion properties in the entire free electron part of the spectrum of even the noble and alkaline metals. Existing theories enjoy a limited success in various segments of the spectrum. However, the less said the better with regard to the transition metals and alloys. This is surprising for theoretically, a description of optical and infrared dispersion properties is expected to be very much like that of electrical properties, at least to the extent that both involved free conduction electrons, and differ from each other only in the extra frequency-dependence appearing in the optical quantities.

Theoretical discussions on the behavior of metallic conductors under the influence of electromagnetic waves were first given by Hagen and Rubens on the basis of the classical Maxwell theory of electrodynamics, and later by Drude on the basis of the free electron description of metals and Maxwell's theory. Drude's theory applies to a wider range of the spectrum than the Hagen-Rubens theory, and the two theories are identical at the longer wavelengths where the optical conductivity, $\sigma(\omega)$, can be replaced by the dc conductivity, $\sigma(0)$.

The limitations that are inherent in these theories have been pointed out in a number of references upon comparison with experimental data. In general, the theories fail in the higher frequency region of the spectrum (i.e., $\hbar\omega \lesssim KT$) and also at low temperatures. The Drude theory has found a qualitative success in a variety of metals in that it offers a good fit to the experimental dispersion curves, and yet

fails quantitatively in that the dc conductivity predicted by the best-fit theoretical curves is always smaller than the measured values. The exceptions are some liquid metals such as mercury and gallium. In any case, the theory fails completely at low temperatures. Despite these limitations, the classical free electron theory of Drude has remained the most successful of the existing theories in the sense that it presents all aspects of dispersion properties in a rather self-contained manner, especially when combined with the Kramers-Kronig relation. Although there have been some attempts made to improve the Drude theory so that it would be applicable to a wider range of the spectrum and to extend it to multivalent and transition metals, they fail to remove the limitations that are inherent in the original Drude theory since these attempts were not made through a rigorous theoretical formulation, but rather by introducing additional unknown parameters.

According to the classical theory, the optical absorptivity (= emissivity) of a pure metal vanishes at very low temperatures in contrast to experimental observations, and a metal can have a nonvanishing absorption or resistivity (Restwiderstand) only if a substantial amount of impurities is present. Although the theory of anomalous skin effect (i.e., anomalous in the sense that the distance traveled by an electron between collisions is larger than the skin depth, $l=v_F \tau > \delta_s$) proposed by Reuter and Sondheimer, and later elaborated by Dingle, has succeeded in explaining a part of the observed absorption at low temperatures, the gap between the theoretical and experimental values still remains to be accounted for and amounts to anywhere between 20 percent ~ 80 percent of the measured values of the total absorptivity.

Practically all of the existing quantum mechanical theories of optical and infrared absorption in metals have been developed since 1954, and were designed to remedy the gap between the classical theoretical values and the observed values of the absorptivity in the near infrared and at low temperatures. However, none of these theories show attempts to formulate different aspects of the optical and infrared dispersion properties in such a self-contained form as is possible in the classical Drude theory. They are confined to derivations of absorptivity as a function of temperature and wavelength in a particular segment of the infrared spectrum. The most outstanding of these theories are those of Holstein, and those developed more recently by Gurzhi and Silin of Russia. It was Holstein who originally suggested that, unlike what is predicted by the theory of anomalous skin effects, a bulk absorption process in which an electron absorbs a photon near the surface and then diffuses into the bulk interior of the lattice emitting a phonon to conserve energy and momentum, may play a significant role at low temperatures. Holstein calculated absorptivity in the near infrared region ($\lambda \sim 1\mu$), and the results were already sufficient to prove that, at low temperatures too, the bulk electron-phonon collisions are not less

important than the skin effects of Reuter, Sondheimer, and Dingle. More recently, Gurzhi made an attempt to formulate the total absorptivity including both the skin effects and the Holstein's bulk mechanism to be applicable to a wider range of spectrum than that defined by $\hbar\omega \gg K\Theta \gg KT$. Gurzhi's result was, at least in its form, more general than that of Holstein's formulas, and will be shown to agree identically with the abosrptivity derived in the present work in the limit, $\hbar\omega \gg K\Theta, KT$. Following the semi-classical calculations by Silin of the contribution by the electron-electron collisions to the absorptivity based on the Fermi-liquid theory of Landau, Gurzhi improved Silin's method by use of a more rigorous Fermi-liquid theory. He pointed out that the electron-electron collisions may be significant at high frequency and at low temperature, and subsequently incorporated these into his previously obtained formula for the total optical absorptivity. The theoretical method used by Gurzhi is essentially that of obtaining perturbation solutions to the kinetic equation for the electron distribution functions taking into account various collision terms. This is very much like what was done by Wilson in his calculations of various dc electrical properties. Holstein used a straightforward quantum mechanical perturbation theory and calculated various transition matrix elements using a semi-classical form of electromagnetic perturbation. There are, of course, other sophisticated theoretical techniques available for calculating the optical properties of metals such as the method of temperature-dependent Green's functions developed by Martin and Schwinger and independently by Kogan, and also the S-matrix formulation which was used by Gurevich and Uritskii in their theory of infrared absorption in crystals, mainly for semi-conductors, in the presence of external magnetic field and in the photoelectric region. However, the remarkable success found in the results obtained by Holstein and Gurzhi in the high-frequency region, and also in the results obtained in the present work for a wider range of spectrum, attest to the fact that a straightforward quantum mechanical perturbation theory is satisfactory for both qualitative and quantitative calculations of the optical properties, at least in the free electron region of the spectrum. On the other hand, a quantitative calculation of optical properties in the resonance region (i.e., for $\lambda \lesssim 1\mu$ for many metals) can be offered when the general results obtained on photoelectric absorption in crystals, such as that by Gurevich and Uritskii, are extended to include the resonance absorption in metals.

The main body of the present work consists of calculations of various optical and infrared dispersion and electrical properties as well as other related lattice parameters based on Holstein's bulk mechanism. In this sense, the theory by Gurzhi is the closest to the present work inasmuch as it is also based on the same mechanism for electron-phonon processes. Although Gurzhi's formula for absorptivity agrees with the present theory identically in the near infrared, where $\hbar\omega \gg K\Theta$, KT, there are some important differences between the two, and the shortcomings

of Gurzhi's theory will be explained.

A theory may be judged on the basis of the following obvious set of criteria:

(a) It has to provide a good fit in frequency-dependence to the optically-observed curves for various optical quantities;

(b) The theory when best fitted to the optical curves should reproduce various dc electrical and lattice parameters in satisfactory agreement with the measured values;

(c) In order to satisfy the correspondence requirement in the classical region, the theory should produce successfully the well-known and time-tested classical formulae for various dispersion properties in the classical case of small $h\omega$ or high temperature; and

(d) As another requirement of the correspondence it should be able to reproduce the well known temperature-dependence of various dc electrical and some thermodynamic properties in the limit of zero frequency or infinite wavelength.

None of the existing quantum mechanical theories succeed in satisfactorily meeting all four of these criteria. Some salient features of the present theory shall be summarized itematically, and it is expected that this will also serve as comparison between the present theory and the existing theory.

In the present theory, the quantum mechanical corrections to the classical dispersion formulae are mostly revealed in the frequency- and temperature-dependence in the over-all damping coefficient, $\Gamma(\omega,T)$. $\Gamma(\omega,T)$ differs significantly from the corresponding dc value, $\Gamma_o(T)$, which is the one used in the classical Drude and Hagen-Rubens theories, only in the spectral and temperature ranges where the quantum effects are important. This is conveniently represented by introducting the relation:

$$\Gamma(\omega,T) = b\ (\omega,T)\,\Gamma_o\ (T) \qquad (27)$$

where the b-factor is particularly important in the quantum mechanical region of high frequency and low temperature. Aside from the appearance of the b-factor, the present theory offers various optical and infrared dispersion formulas which bear very close resemblance to the well-known classical formulas. Thus, it is clear that establishing the frequency- and temperature-dependence of Γ or b will occupy the heart of the present theory. Results for non-transition metals apply mostly to those metals which have $\sim T^5$-dependence on temperature of the electron-phonon part

of the resistivity at low temperature. The transition metals are shown to exhibit, in temperature and frequency dependences, properties distinct from those of non-transition metals. The ferromagnetic and paramagnetic transition metals are investigated independently. It is found that the electron-phonon part of the dispersion formulas for transition metals for which the number of s-electrons is completely compensated by the number of empty states (positive holes) in the d-band, leads to $\sim T^3$-dependence of dc resistivity, while the formulas for those transition metals in which the total number of S-electrons are not sufficient to close the d-band, lead to a negative exponential temperature-dependence at very low temperatures. There are further differences in temperature-dependences between ferromagnetic and paramagnetic transition metals which are offered by the theories of Weiss and Heisenberg, at low temperatures.

Generally, the over-all damping coefficient, $\Gamma(\omega,T)$, is a sum of the contributions by the electron-phonon collisions, electron-electron collisions, and the impurity scattering such that:

$$\Gamma(\omega,T) = \Gamma_{ep}(\omega,T) + \Gamma_{ee}(\omega,T) + \Gamma_{M}(T) \qquad (28)$$

where the subscripts (ep), (ee), and (M) represent the three processes in the order mentioned above, and where the quantum correction factors, $b_{ep}(\omega,T)$ and $b_{ee}(\omega,T)$, may be defined for the first two processes in such a way that:

$$\Gamma_{ep} = \Gamma_{oep}(T) b_{ep}(\omega,T)$$

$$\Gamma_{ee} = \Gamma_{oee}(T) b_{ee}(\omega,T)$$

$$b(\omega,T) = \left(\frac{\Gamma_{oep}}{\Gamma_o} b_{ep}(\omega,T) + \frac{\Gamma_{oee}}{\Gamma_o} b_{ee}(\omega,T) + \frac{\Gamma_M}{\Gamma_o} \right)$$

Among the three processes, only the electron-phonon process is important at ordinary temperatures and in the free-electron region of the spectrum, provided that the metal sample is a reasonably pure one. Many studies have been made on the contributions of the electron-electron collisions and the impurity scattering to optical and infrared absorption in metals. Among the latest developements, the most prominent are the works of Pitaevskii, Silin, and Gurzhi. According to these authors, the electron-electron collisions may contribute significantly either at very low temperatures or in the high-frequency limit of the infrared spectrum, while the impurity scatterings are important at very low temperatures even for a reasonably clean sample. In particular, Gurzhi has derived, a frequency-dependent electron-electron damping coefficient $\Gamma_{ee}(\omega,T)$,

as well as a general formula for the impurity contribution to the damping.

In the present work, a variety of metals, all of which are supposed to be of very small impurity content, have been investigated as to the relative importance of the three mechanisms of damping in the high-frequency region and also at low temperatures. As the result of this investigation, it is found that, although the suggestion of Pitaevskii, Silin, and Gurzhi may apply to some special cases of transition metals, it does not strictly apply to other metals in most of the quantum mechanical region of the free electron spectrum. In fact, the electron-phonon process or the Holstein mechanism alone, in the form that is derived in the present theory, explains quite successfully (viz., up to $2 \sim 5$ percent) the low temperature (4.2°K) near infrared ($1 \sim 1.5\mu$) absorptivity of all the metals for which experimental data are available.

The calculations on transition metals in the present theory suggest that the electron-electron collisions and impurity scatterings are particularly important for those transition metals, and similarly for other multivalent non-transition metals, in which the interband transitions required a non-zero momentum transfer. For a transition metal of this kind, only the phonons of energy larger than a certain non-zero value are effective in the transitions, and as the result of this the electron-phonon, part of the low temperature resistivity has the previously mentioned negative exponential nature. This applies to all the transition metals whose S-electrons are not sufficient to close the d-band, and the low temperature resistivity is due mostly to the electron-electron collisions with the well known T^2-dependence on temperature as well as to the temperature-independent impurity sactterings (Restwider-stand). On the other hand, for those transition metals whose S-electrons are exactly compensated by the positive holes in the d-band such as the triad, Pt, Ni, and Pd, the T^3-dependence of the electron-phonon part plus the T^2-dependence of the electron-electron collision term define the temperature-dependence of the low temperature resistivity to the extent of neglecting an additional T-dependence in the electron-phonon part. This is partly in contrast to the earlier concept that the electron-electron collisions make predominant contributions at low temperatures for all transition metals.

Strictly speaking, the T^2-dependence is predominant in the transition metals other than the traid at temperatures smaller than the value given by:

$$E \cong \frac{\hbar U_L \quad k_d - k_s}{K} : \lesssim 10°K \qquad (30)$$

which is also the lower limit in the summation over the phonon states, where k_d, k_s are the Fermi momenta for the d- and s-bands, U_L is the

longitudinal phase speed of sound, and K is the Boltzman constant.

All the optical dispersion quantities, including the optical conductivity, $\sigma(\omega, T)$, the optical dielectric constant, $\epsilon(\omega,T)$, and absorptivity, $A(\omega,T)$, that are calculated in the present theory, show not only good fit to the corresponding experimental curves throughout the entire free-electron infrared spectrum, but also reproduce various dc electrical properties in excellent agreement with the directly measured values for a number of non-transition and transition metals. They also reproduce exactly the well known temperature-dependence of the dc electrical properties (hence, also of heat capacity and thermal conductivity), such as the famous Grüneisen formula $G\left(\frac{\Theta}{T}\right)$ for non-transition metals. The Grüneisen formula has long been known to describe temperature-dependence in excellent agreement with observations for T not too much larger than Θ.

It is pointed out, as the result of the present theory, that the quantum corrections represented by $b(\omega,T)$-factor can also be significant in a relatively long wavelength region of the infrared, when $\hbar\omega \approx KT$. This is clearly illustrated in the formula for the reflectivity:

$$R(\omega,T) \approx 1 - 2\sqrt{\frac{\omega}{2\pi\sigma_{dc}(T)}}\left[b(\omega,T)\right]^{\frac{1}{2}} \qquad (31)$$

which applies to the Hagen-Rubens limit of the spectrum or, when $\omega^2 \ll \Gamma^2$, where the b-factor, although close to unity in this spectral range, is usually different from unity by a small fraction, and becomes essentially equal to unity when $\hbar\omega \ll KT$ in which case the formula is identically the well-known and time-tested Hagen-Rubens formula. In this sense, Equation (31) may be called the generalized Hagen-Rubens formula.

The present theory also enables us to estimate such lattice parameters as the electron density, the effective mass values of optical electrons, the Fermi energy, the upper edge of the d-band in the transition metal, and longitudinal phase speed of sound, etc. The heat capacity and thermal conduction properties also follow as by-products of the present theory. The impurity content can be estimated from low temperature optical data, even for a sample with such a small impurity content as to be undetectable at ordinary temperatures.

The caluclations for absorptivity at very low temperatures include both normal and superconducting metals. For the superconducting metals, or below the superconducting transition temperature, the calculations are assisted by the theory of superconductivity of Bardeen, Cooper, and Schrieffer. That Holstein's bulk absorption process might be important

in a superconductor was suggested resently by Richards and Tinkham. The calculations in the present work are intended as a check on the said suggestion and to see whether the existing gap between the experimental absorptivity and the predictions of Mattis and Bardeen can be explained by Holstein's mechanism. It may be noted that the absorptivity for light quanta, $\hbar\omega$, smaller than the energy gap (at T 0^{o}K) has been given by Schrieffer and has been shown to agree well with experiments. At the present, no definite conclusion can be provided on the basis of the present calculations because of insufficient experimental data.

Finally, some words need to be said regarding possible limitations in the present theory. The limitations may result mainly from two causes: first, the use of the simple Debye model and second, the assumption of spherical Fermi surfaces.

The first assumption leads to difficulties at very high temperatures ($T \gg \Theta$), where the Umklapp process is important. The same difficulty is found in Gruneisen's formula for dc resistivity at very high temperatures.

Another less serious aspect of limitations in the use of the Debye model is in neglecting the anisotropy among the longitudinal and two transverse directions, whereas in more accurate calculations, one needs to consider three components of the phase velocity of sound as well as three characteristic temperatures instead of the Debye temperature alone. This problem of lattice anisotropy is of no concern for a polycrystalline metal sample. Perhaps the best justification for using the simple Debye model is in the good agreement found between the theoretical and experimental values of heat capacity.

It is well known that the Umklapp processes are important at very low temperatures, especially for those metals in which the interband transitions are important. At very low temperatures, the Umklapp processes enter into various physical quantities through electron-electron collision terms and do not enter into the electron-phonon processes, since the angular deflection involved in an electron-phonon scattering is in the order of $\left(\frac{T}{\Theta}\right)$, which is certainly much less than unity. It is known that contribution by electron-electron collisions to the over-all damping coefficient vanishes when Umklapp processes are not present. In short, at very low temperatures, the Umklapp processes are important to the extent that the electron-electron collisions are important, and hence are automatically taken into consideration in the present theory by incorporating the effects of electron-electron collisions into various dispersion formulas.

The limitations that are associated with the assumption of a

spherical Fermi surface are well known, and are often discussed in the literature. In general, this approximation works well for most monovalent metals, such as the noble metals Ag, Au, and Cu, and also for some multivalent metals for which the interband transitions are not important. On the other hand, the assumption of a spherical Fermi surface is not strictly valid for those non-transition metals in which the Fermi surface touches or almost touches the plane of energy discontinuity and for transition metals in which the interband transitions between the s- and d-bands are most important. In the present theory, the calculations for non-transition metals are carried out on the basis of a spherical Fermi surface, while non-spherical Fermi surfaces have been used for all transition metals. Therefore, it is expected that the results on non-transition metals will not apply strictly to some multivalent metals.

The present work does not include detailed study of the optical and electrical properties of alloys, and also of such other properties of metals as thermoelectricity and magneto-resistive effects. Much has yet to be learned theoretically about the dc electrical properties before it is possible to study rigorously the optical and infrared dispersion properties of alloys.

An attempt has been made to make this thesis self-contained, but, in view of all the relevant work yet to be done in the field of interest, this was impossible. Similarly, an honest effort to give all due credit was made, but it is likely that some work has not been properly cited, such omissions were not intentional.

SECTION II. FUNDAMENTAL RELATIONS BETWEEN OPTICAL AND ELECTRICAL PROPERTIES OF METALS

A. MAXWELL'S EQUATIONS AND KRAMERS-KRONIG RELATIONS

Maxwell's theory of electromagnetism provides us with a set of the most fundamental relations between the optical properties and the electrical properties of metals. These relations, plus the well-known Kramer's Kronig relations between the real and imaginary parts of the complex polarizability, constitute a foundation upon which the interpretation of the optical and infrared behavior of metals in terms of electrical properties is based.

If $\underline{E}$ and $\underline{H}$ are the electric and magnetic fields represented as functions of the coordinate $\underline{r}$ and time t for a given angular frequency:

$$\omega = 2\pi\nu \text{ sec}^{-1} \tag{32}$$

Maxwell's equations for an uncharged conductor are given in cgs units by

$$\nabla \times \underline{H} = \frac{\epsilon}{c} \frac{\partial \underline{E}}{\partial t} + \frac{4\pi\sigma(\omega)}{c} \underline{E} \tag{33}$$

$$\nabla \times \underline{E} = \frac{\mu}{c} \frac{\partial \underline{H}}{\partial t} \tag{34}$$

$$\nabla \cdot \underline{E} = \nabla \cdot \underline{H} = 0 \tag{35}$$

where $\epsilon(\omega)$ is the real dielectric constant, $\sigma(\omega)$ is the conductivity, and μ is the permeability.

At optical and infrared frequencies, $\mu = 1$ for all substances. The magnetic field $\underline{H}$ is eliminated by combining Equations (33) and (34) and we obtain:

$$c^2 \nabla^2 \underline{E} = \epsilon \frac{\partial^2 \underline{E}}{\partial t^2} + 4\pi\sigma \frac{\partial \underline{E}}{\partial t} \tag{36}$$

The solution to this differential equation is given by the typical solution to the usual wave equation:

$$\underline{E} = \underline{E}_o e^{i\omega t \pm i(\epsilon\omega^2 - i4\pi\sigma\omega)^{-\frac{1}{2}} z/c} \tag{37}$$

where $\underline{E}_o$ is the maximum amplitude (i.e., at $z = 0$, $t=0$) and z measures the penetration distance into the metal. Equation (37) takes on the conventional form expressed in terms of the complex index of refraction $\overline{N}$:

$$\underline{E} = \underline{E}_o e^{i\omega(t \pm \overline{N} \frac{z}{c})} \tag{38}$$

if we identify $\overline{N}$ with $[\ldots]^{\frac{1}{2}}\omega^{-1}$ of Equation (37):

$$\overline{N} = (n-ik) = \left[\epsilon - i \frac{4\pi\sigma}{\omega}\right]^{\frac{1}{2}} \tag{39}$$

where n and k represent the index of refraction and absorption coefficient, respectively.

The relation in Equation (39) immediately yields the following two important relations between the electric properties $\sigma(\omega)$ and optical constants (n,k):

$$\epsilon = n^2 - k^2 \tag{40}$$

$$\sigma = nk\omega/2\pi \tag{41}$$

These two relations will be referred to frequently.

The physical significance of $\sigma(\omega)$ for $\omega > 0$ becomes evident when we calculate the rate of energy loss by computing the Poynting vector $\underline{S}$:

$$\underline{S} = \frac{c}{4\pi} \quad (\underline{E} \times \underline{H}) \tag{42}$$

and taking the time average of:

$$-W \stackrel{e}{=} \frac{\partial S_z}{\partial z} \tag{43}$$

where W is the Joule heat produced per unit time and per unit volume within the conducting medium. Then, we obtain as the definition of $\sigma(\omega)$:

$$\sigma(\omega) = \overline{W} / \frac{E^2}{2} \tag{44}$$

which says that σ is the fraction of the energy absorbed or dissipated per unit volume out of the energy density per unit volume $\frac{E^2}{z}$, of the electromagnetic field of frequency ω. It is quite obvious then that $\sigma(0)$, at $\omega = 0$, should be the dc conductivity of the metal. It is a popular pratice to introduce a complex dielectric constant, $\overline{\epsilon}$, and complex polarizability, $\overline{\alpha}$, such that:

$$\overline{\epsilon} = 1 + 4\pi\overline{\alpha} = \overline{N}^2 \tag{45}$$

$$\overline{\alpha} = \alpha - i\alpha' \tag{46}$$

This is analogous to the similar relation for the real quantities:

$$\epsilon = 1 + 4\pi\alpha = n^2 - k^2 : \mu = 1 \tag{47}$$

Then, upon comparing Equations (45 and 46) with Equation (39), we now have:

$$\epsilon = 1 + 4\pi\alpha = n^2 - k^2 \tag{48}$$

$$4\pi\alpha' = \frac{4\pi\sigma}{\omega} = 2nk \tag{49}$$

These two relations enable us to obtain (n, k) values upon knowing the values of the dielectric constant ϵ and conductivity σ at a given frequency, and, conversely, to obtain ϵ and σ values from known values of n and k. In general, the observations in the optical and infrared part of the spectrum are designed to measure the optical constants, (n,k), or

other optical properties such as the reflectivity and emissivity (= absorptivity for metals). Therefore, for the purpose of predicting (n,k) values for a given frequency ω and temperature **T** (°K) from a known set of values of the dc electric properties, $\epsilon(0)$ and $\sigma(0)$, or for the purpose of predicting the dc electric properties from measured values of (n,k), we need to have a set of theoretical equations relating $\epsilon(\omega)$ and $\sigma(\omega)$ to the corresponding dc quantities, $\epsilon(0)$ and $\sigma(0)$. Specifically, the frequency-and temperature-dependence of $\sigma(\omega)$ needs to be specified.

Establishing the correct ω- and T-dependence of σ and ϵ constitutes a major part of the theoretical work explaining the optical, infrared, and the related electrical properties of metals. Fortunately, the solution to the theorectical problem is considerably simplified with the aid of the Kramers-Kronig relation which represents an integral relation between $\sigma(\omega)$ and $\epsilon(\omega)$, or more properly, between the real and imaginary parts of the complex polarizability as follows:

$$\tfrac{1}{2}\alpha(\omega) = -\frac{P}{\pi}\int_0^{\infty} \frac{\omega'\alpha'(\omega')\,d\omega'}{\omega'^2-\omega^2} \tag{50}$$

With the help of Equation (49), this represents a relationship between $\epsilon(\omega)$ and $\sigma(\omega)$ given by:

$$\frac{[\epsilon(\omega)-1]}{4\pi} = -\frac{P}{\pi}\int_0^{\infty} \frac{d\omega'\ 2\sigma(\omega')}{(\omega'^2-\omega^2)} \tag{51}$$

Therefore, it is sufficient to specify the ω - and T-dependence of either σ or ϵ for establishing the complete ω- and T-dependent structure of the optical and electrical quantities that are involved in Equations (15) and (16).

In a more general discussion of the Kramers-Kronig relation, Equation (50) and (51) are equivalently represented in the form:

$$\text{Re}\ [\bar{N}(\omega) - 1] = \frac{P}{\pi}\int_{-\infty}^{+\infty} d\omega\ \frac{\text{Im}[\bar{N}\omega') - 1]}{\omega' - \omega} \tag{52}$$

which may be recognized as the real part of the equation:

$$[\bar{N}(\omega) - 1] = \frac{1}{i\pi}\ P\int_{-\infty}^{+\infty} d\omega'\ \frac{[\bar{N}(\omega') - 1]}{\omega' - \omega} \tag{53}$$

or in the limit of $\eta \rightarrow 0^+$:

$$\left[\bar{N}(\omega) - 1\right] = \frac{1}{2\pi i} \int_{-\infty}^{+\infty} d\omega' \frac{\left[\bar{N}(\omega') - 1\right]}{\omega' - (\omega + i\eta)} \qquad (54)$$

Equation (53), which is the most general representation of the Kramers-Kronig relation, was observed by Kramers as a simple consequence of Cauchy's theorem if we assume that $\bar{N}(\omega)$ is a function of a complex variable ω analytic in the upper half ω-plane which approaches unity at infinity. It was later shown by Kronig that the absence of poles of $\bar{N}(\omega)$ in the upper half ω-plane was both a necessary and sufficient condition for the property that no signal may propagate through a medium with index of refraction $\bar{N}(\omega)$ with a speed greater than that of light.

Sometimes, the optical properties of a medium are expressed in terms of the forward scattering amplitude $F(\omega)$ and the total scattering cross section per scattering center $\sigma_s(\omega)$ rather than in terms of (α,σ) or (n,k).

The equation which shows the relation between the complex forward scattering amplitude $\bar{F}(\omega)$ and the complex index of refraction $\bar{N}(\omega)$ was first offered by Lorentz, namely:

$$\left[\bar{N}(\omega) - 1\right] = n_o \frac{2\pi c^2}{\omega^2} \bar{F}(\omega) \qquad (55)$$

where n_o is the number of scattering centers per unit volume. The same derivation leading to Equation (55) also yields the optical theorem:

$$\sigma_s(\omega) = 4\pi c \ \mathrm{Im}\left(\frac{\bar{F}(\omega)}{\omega}\right) \qquad (56)$$

where $\sigma_s(\omega)$ is the total cross section in cm^2 per scatterer. The above relation also follows very simply upon noting that the intensity of a wave propagating through a medium of refractive index, $\bar{N}(\omega)$, is reduced in a distance by a factor $\left|\exp\left[i \frac{\omega}{c} \bar{N}(\omega) z\right]\right|^2$ and also by $e^{-n_o \sigma(\omega) z}$ according to the definition of $\sigma_s(\omega)$. Comparison of these two expressions gives Equation (56).

Upon comparing Equations (55) and (56) with the relations (45) ~ (49), some useful relations follow..

We have, for instance:

$$n(\omega) = \mathrm{Re}\bar{N}(\omega) = 1 + \frac{2\pi n_o c^2}{\omega^2} \mathrm{Re}\ \bar{F}(\omega) \tag{57}$$

$$k(\omega) = \mathrm{Im}\bar{N}(\omega) = -\frac{2\pi n_o c^2}{\omega^2} \mathrm{Im}\ \bar{F}(\omega)$$

$$= -\frac{n_o c}{2\omega} \sigma_s(\omega) \tag{58}$$

$$\epsilon(\omega) = \mathrm{Re}.\bar{N}^2 = (1 + 4\pi\alpha)$$

$$= \left[\left(1 + \frac{2\pi n_o c^2}{\omega^2} \mathrm{Re}\ \bar{F}(\omega)\right)^2 - \left(\frac{2\pi n_o c^2}{\omega^2} \mathrm{Im}\cdot\bar{F}(\omega)\right)^2\right] \tag{59}$$

$$\sigma(\omega) = -\frac{\omega}{4\pi} \mathrm{Im}\cdot\bar{N}^2 = \omega\alpha$$

$$= -\frac{n_o c^2}{\omega} \left(\mathrm{Im}\cdot\bar{F}(\omega)\right)\left(1 + \frac{2\pi n_o c^2}{\omega^2} \mathrm{Re}\cdot\bar{F}(\omega)\right) \tag{60}$$

where the real and imaginary parts of $\bar{F}(\omega)$ are related to each other through Kramers-Kronig relation:

$$\mathrm{Re}\bar{F}(\omega) = \frac{\omega^2}{\pi} P\int_{-\infty}^{+\infty} d\omega' \frac{\mathrm{Im}\bar{F}(\omega')}{\omega'^2(\omega'-\omega)}$$

$$= \frac{2\omega^2}{\pi} P\int_{o}^{\infty} d\omega' \frac{\mathrm{Im}\bar{F}(\omega')}{\omega'(\omega'^2-\omega^2)} \tag{61}$$

In applying the relations (57) ~ (60) to the infrared dispersion in metals, we need only to remember that n_o is the effective number of conduction electrons per cm^3 and that $\sigma_s(\omega)$ is the total scattering cross section for the conduction electron - external photon interactions including the absorption, emission, and the scattering in the ordinary sense.

B. ABSORPTIVITY (EMISSIVITY) AND REFLECTIVITY

Various optical, infrared and electrical properties may be obtained from measurements of the absorptivity, A, and reflectivity, R, as well

as from n and k. The two quantities are related by the equation:

$$R = 1 - A \tag{62}$$

The relationship between (R,A) and the electrical properties will follow naturally from Equations (48) and (49), when we establish the relationship between (R, A) and (n,k).

The optical theory gives the well-known result that for normal incidence:

$$R = \left| \frac{\bar{N} - 1}{\bar{N} + 1} \right|^2 = 1 - A \tag{60}$$

which defines the reflectivity and absorptivity in terms of the complex index of refraction $\bar{N} = n\text{-}ik$. In particular, for a transparent medium such as glass, we have $\bar{N} = n$, and Equation (63) gives the well-known formula:

$$R = \left(\frac{n-1}{n+1} \right)^2 \tag{64}$$

Equation (63) completely determines R and A in terms of n and k. In order to express R and A in terms of σ and ϵ, it is convenient to follow the simple algebraic method of Price (1949) rather than to use Equations (48) and (49). Upon writing, for the complex polarizability, $\bar{\alpha}$:

$$\left[4\pi\bar{\alpha}\right]^{-1} = (x + iy) \tag{65}$$

The absorptivity is given by:

$$\frac{A^2}{8R} = \frac{A^2}{8(1-A)} = T + (T^2 + Y^2)^{\frac{1}{2}} \tag{66}$$

where:

$$T = x + x^2 + y^2$$

$$1 - \epsilon = 1+k^2-n^2 = x/x^2 + y^2$$

$$\frac{4\pi\sigma}{\omega} = 2nk = -Y/x^2 + y^2 \tag{67}$$

and these are just as well represented in terms of the real and imaginary parts of scattering amplitudes according to the relations (57) ~ (60)

The frequency- and temperature-dependence of R and A will then be determined when the ω- and T-dependent structure of σ or ϵ is obtained theoretically. The spectral and temperature variation of R and A will vary depending on the choice of the particular theoretical model used in calculating the complex polarizability. In particular, if we adopt the classical free electron theory of Drude (1904, 1902), the real and imaginary parts of the complex polarizability are given by:

$$x = -(\omega\uparrow_o)^2$$

$$y = -(\omega\uparrow_R)^2 \qquad (68)$$

where:

$$\uparrow_o = \sqrt{\frac{m^*}{4\pi n_o e^2}} \qquad (69)$$

$\uparrow_R = \Gamma_o^{-1}$ = the relaxation time of a conduction electron

m^* = the effective mass of a conduction electron

e = the electronic charge ($= 4.8 \times 10^{-10}$ e.s.u)

n_o = the effective number of conduction electrons per unit volume

Price (1949) presents an extensive investigation on the qualitative features of the spectral and temperature variations of variations of A and R for metals to which one electron dispersion theory can be applied in the form of Equation (57).

In general, the expressions for x and y will assume different forms for different theoretical models. A brief review on some of the most popular theories on optical and infrared dispersion is presented in the chapter that follows.

SECTION III. EXISTING THEORIES ON OPTICAL AND INFRARED DISPERSION IN METALS

A. HAGEN-RUBENS THEORY

Theoretical discussions on the behavior of metallic conductors under the influence of electromagnetic waves were first given by Hagen and

Rubens (1903) and by Drude (1904) on the basis of classical electrodynamics.

The Hagen-Rubens theory is restricted in its applicability to the long wavelength part of the spectrum where $(\omega \uparrow_R)^2$ is much smaller than unity, $\uparrow_R$ being the relaxation time characteristic of the damping in the electronic motion. The results of the Hagen-Rubens theory follow from Equations (40), (41), and (42) upon taking:

$$\sigma(\omega) \cong \sigma\ (0) = \sigma_{dc} \tag{70}$$

in the long wavelength part of the spectrum. We thus have:

$$nk \approx \left(\sigma_{dc}/\nu\right) \tag{71}$$

It may be shown that $\left(\sigma_{dc}/\nu\right)$ is much larger than unity for the wavelengths for which the approximation (Equation 70) is valid, and hence, approximately:

$$n \cong k \cong \sqrt{\frac{\sigma_{dc}}{\nu}} \tag{72}$$

$$R = 1 - A \approx 1 - 2\sqrt{\frac{\nu}{\sigma_{dc}}} \tag{73}$$

where the latter expression is obtained upon substituting Equation (70) into Equation (53). The formula (73), which is known as the Hagen-Rubens relation, has been compared with the experiment for infrared radiation and for various metals and temperatures (Hagen and Rubens, 1903), and it is in general in fair agreement with the experiment for:

$$\lambda \gtrsim 10\ \mu \tag{74}$$

The approximation represented by Equation (70) is equivalent to taking the current $\underline{J}$ in phase with the applied electric field $\underline{E}$. This will be true only if the relaxation time $\uparrow_R$ of the electron is small compared with the period of the light wave so that the field acting on the electron is approximately constant during the time taken by an electron to traverse its mean free path. For wavelengths shorter than $\sim 10\ \mu$, the current will be out of phase with the field, and it is generally observed that the formulas in Equations (72), (73), and (71) are not even approximately in agreement with the experiment.

B. DRUDE THEORY

A more general theory than that of Hagen and Rubens was given by Drude (1904) by obtaining the solutions to the classical equation of motion for free conduction electrons subject to Maxwell's electromagnetic field.

In contrast to the Lorentz theory (Lorentz 1906) of absorption by dielectrics, which rests on the assumption that bound charges become polarized upon interaction with the electromagnetic wave, Drude (1902, 1904) suggested that consideration of the interaction between the free conduction electrons in the metal and electromagnetic wave. The solution for the conductivity, $\sigma(\omega)$, is obtained upon solving the equation:

$$m^* \ddot{\underline{s}} + m^* \Gamma_o \dot{s} = -e\underline{E}_o e^{-i\omega t} \tag{75}$$

where $\underline{s}$ is the electron position coordinate within the metal, $\underline{E} = \underline{E}_o e^{-i\omega t}$ is the applied electromagnetic field, and Γ_o is the damping coefficient which is also equal to the inverse of the dc relaxation time $\uparrow_R$. Using the effective mass, m^*, in Equation (75) instead of the normal election mass m which was used in the original Drude theory (1904), we have incorporated the later developed effective mass method with the primitive free electron theory of Drude.

Equation (75) yields the expressions for the conductivity $\sigma(\omega)$ and the dielectric constant $\epsilon(\omega)$:

$$\sigma(\omega) = \frac{nk\omega}{2\pi} = \frac{\sigma(0)}{1 + (\omega \uparrow_R)^2} \tag{76}$$

$$\left[1-\epsilon(\omega)\right] = 1 + k^2 - n^2 = \frac{4\pi\sigma(0) \uparrow_R}{1 + (\omega \uparrow_R)^2} \tag{77}$$

where we used the notations:

$$\uparrow_R = \Gamma_o^{-1}$$

$$\sigma(0) = \frac{n_e e^2}{m^*} \Big/ \Gamma_o \tag{78}$$

We see that:

$$\sigma(\omega) \underset{\omega \to 0}{\sim} \sigma(0) \tag{79}$$

so that $\sigma(0)$ is the dc conductivity.

It can be shown readily that the relations in Equations (76) and (77) reduce to the simple relations in Equations (71), (72), and (73) of the Hagen-Rubens theory in the limit:

$$(\omega \uparrow_R)^2 \ll 1 \tag{80}$$

On the other hand, the results of the Drude theory do not apply to that part of the short wavelength region where the contribution of the bound electrons enter (i.e., the reasonance region) through the photo-electric effects. At the shorter wavelengths, the anomalous dispersion occurs due to the contributions of the photo-electric absorption, and also the core polarization becomes important. In this part of the spectrum, the simple free electron thory of Drude is not enough to explain the observed dispersion, and will be modified, for the dielectric constant, as follows:

$$(\epsilon - 1) = n^2 - k^2 - 1 = - \frac{4\pi n_e e^2}{m^* \omega^2} + (\epsilon-1)_c + (\epsilon-1)_p \tag{81}$$

where $(\epsilon - 1)_c$ is the contribution of the core polarization

and $(\epsilon - 1)_p$ of the photoelectric absorption.

In general, the anomalous dispersion is observed at a wavelength well below ~1μ. Ag, Au, and Cu, for instance, have their lowest resonances at 0.27 μ, 0.37 μ, and 0.50 μ (Meier, 1910), respectively. As long as one stays at wavelengths which are long enough to be sufficiently outside the resonance tail, the free electron theory of Drude should be satisfactory. At the high frequency region where the condition:

$$(\omega \uparrow_R)^2 \gg 1 \tag{82}$$

is satisfied, the free electron part of $\sigma(\omega)$ and $\epsilon(\omega)$ are given by:

$$\sigma(\omega) \approx \sigma(0) \Big/ (\omega \uparrow_R)^2 \tag{83}$$

$$\epsilon - 1 \approx - 4\pi n_e e^2 \Big/ m^* \omega^2$$

The values of $(\epsilon-1)$ are available for a variety of metals (Van Vieck, 1959), and are generally independent of frequency (Mott and Jones, 1936). The value of $(\epsilon-1)_p$ may be found either by a direct theoretical calculation, or empirically from the observed data of (n + k) values. The photoelectric part $(nk)_p$ of the observed (n,k) values is

obtained empirically upon subtracting the free electron part (i.e., the Drude part) from the observed (n+k) values making use of the relation in Equation (83). Then, $(\epsilon-1)_p$ is obtained, in turn, upon making use of the Kramers-Kronig relation in Equation (51):

$$(\epsilon-1)_p = \frac{4}{\pi}\int (nk)_p \frac{\omega' \, d\omega'}{\omega'^2 - \omega^2} \tag{84}$$

For wavelengths sufficiently outside the photoelectric region, $(\epsilon-1)_c$ and $(\epsilon-1)_p$ are small enough to be neglected compared with the free electron part. We shall be primarily interested in this part of the spectrum where only the free conduction electrons play a dominant role.

Equations (76) and (77) show that the two Drude equations are related with each other by a rather simple algebraic relation:

$$\sigma/1 - \epsilon = (4\pi\uparrow_R)^{-1} = \Gamma_o/4\pi = nk\nu/1 + k^2 - n^2 \tag{85}$$

This relation enables us to obtain the value of the dc damping coefficient, Γ_o, or the dc relaxation time, $\uparrow_R$, when we have only one pair of (n,k) values at an arbitrary frequency provided that the frequency ω is not too large.

A more exact way of determining the value of Γ_o would be to plot $\sigma(\omega)$ against $(1-\epsilon)$ from a set of (n+k) values, and then determine the slope $(\Gamma_o/4\pi)$ of the resulting straight line. This method was first pointed out by Wolfe (1954, 1955). Any deviation of the curve from the Drude straight line would also provide us with a measure of the validity of the Drude theory at a given frequency.

Beattie and Conn (1955) plotted the Argand diagrams showing $(2nk/\lambda)$ against (n^2-k^2) for Al, Ag, ni and Cu. The values of Γ_o and $\uparrow_R$ determined from the slopes vary greatly depending on the way the metal surfaces are prepared. The best agreements of the dc conductivity values, σ_o, which are obtained upon substituting the Γ_o values into the Drude Equation (76), with the electrically measured values were obtained for evaporated metal films. The results of Beattie and Conn are presented in Table VII. The discrepancy between the measured and calculated (Drude Theory) values of the dc conductivity for evaporated films of Ag, Cu, Ni and Al are found as 40 percent, 100 percent, 40 ~ 50 percent and 40 percent respectively. The calculated values are always smaller than the measured values. These results will be further discussed in a later section, and it will

be shown that the mentioned discrepancy can be explained theoretically upon introducing an additional frequency-dependent factor into the original Drude equation.

For none of the metals that were studied by Beattie and Conn (1955) did the Argand diagrams yield complete straight lines. For Al, for instance, the curve starts to deviate from the straight line at ~8μ. The deviation becomes more pronounced toward the shorter wavelengths as one might have expected. An interesting feature is that the Argand diagrams start to deviate from a straight line long before the wavelength enters the photoelectric resonance tail.

With almost no exception, the dc conductivity, σ_o, calculated according to the Drude Theory from the observed values of optical constants, is always smaller than the measured value even when very carefully prepared metal surfaces are used. Thus, it seems that the classical free electron theory of Drude contains some basic limitations.

Of all the existing theories on the optical and infrared dispersion in metals, the classical free electron theory of Drude (1904, 1902) has been most successful in explaining the experimental results aside from such exceptional cases that will be discussed later.

The Drude Theory has been applied to a large number of metals with varying degrees of success. An excellent review by Schulz (1957-a) and the review by Blau, et al, (1958) gives a detailed account of this work as well as references to many of the original papers. The basis for the relative success of the Drude Theory lies in the fact that, for a number of metals for which sufficient data on (n+k) values are available, Equations (76) and (77) can be fitted to the optically determined curves of $\sigma(\omega)$ and $[1-\epsilon(\omega)]$ upon adjusting Γ_o and $\sigma(0)$ or n_e and m^* to suitable values (Schulz, 1957-a,b,c, 1951, 1954; Beattie and Conn, 1955; Seitz and Turnbull, 1958; and others)

For Au, Ag and Cu, which have their first resonances at 0.37μ, 0.27μ, and 0.5μ, respectively (Meier, 1910), the Drude Equations (76) and (77) can be fitted to the experimental curves with m^* (Cu) = 1.45m, and m^* (Au) = m^* (Ag) = m for $\lambda > 2\ \mu$ (Schulz, 1957-a). The optical behavior of the three simple monovalent metals is clearly consistent with the Drude theory at least so far as the frequency dependence is concerned.

Another example of excellent agreement between theory and experiment is found in the liquid metals Hg and Ga (Schulz, 1957-b). For these metals, the theory fits well for $\lambda \gtrsim 0.3\ \mu$.

TABLE V

	I	II	
Metal	$\sigma_o \times 10^{-16}$ e.s.u. (calculated)	$\sigma_d \times 10^{-16}$ e.s.u. (measured)	$\frac{\sigma_{II}}{\sigma_I}$
Al	11.6	15.0	1.3
Ni	$\begin{pmatrix}3.16\\1.02\end{pmatrix}$	$\begin{pmatrix}4.6\\1.4\end{pmatrix}$	$\begin{pmatrix}1.5\\1.4\end{pmatrix}$

Except for the case of the liquid metals, the success of the Drude theory mentioned above is no more than a qualitative one. For the theory to be quantitatively consistent, the values of the electric properties such as $\sigma(0)$ and $\epsilon(0)$, as well as other lattice parameters, must agree with the measured values when calculated from the measured optical constants. And conversely, the optical constants calculated from the measured values of $\sigma(0)$ and $\epsilon(0)$ should agree with the measured values of the optical constants. However, in practically all cases that have been studied, the dc conductivity values calculated from the best-fit Drude curves are found to be smaller than the handbook values, for monovalent as well as multivalent metals. Such discrepancies occur sometimes by a factor of 2 ~ 10 (see, for instance, Seitz and Turnbull, 1958; Beattie and Conn, 1955).

As it was shown by Beattie and Conn (1955), the dc conductivity calculated according to the Drude theory from the measured values of optical constants depends very strongly on the manner in which the metal surface is prepared. The discrepancy was smallest, being of the order of 40 ~ 100 percent, for the case of evaporated metal films, while for metals prepared in other ways the calculated dc conductivity values were smaller than the handbook values by a large factor of 3 ~ 5. Although the large discrepancies in the case where the surfaces are prepared by a method other than by evaporation may be explained as arising from the crystal structure of the metal surface being disturbed during the process of polishing such as introducing an amorphous layer, the discrepancy for the case of evaporated films is yet to be explained. The only cases where both qualitative and quantitative agreements are found are the

liquid metals Hg and Ga.

In general, the agreement between the theory and experiment for solid, multivalent metals is more incomplete than for monovalent metals such as gold, silver and copper. At best, a partial agreement over a narrow spectral region can be obtained through suitable adjustment of the parameters n_e, m^*, and $\sigma(0)$. This procedure for multivalent metal is justified, as will be explained, when the contribution to $\sigma(\omega)$ and $\epsilon(\omega)$ of the one band is predominant over the second band contribution in a certain range of the spectrum in the two-band description of the free electron theory. In this range of the spectrum, the metal may be treated effectively with the one-electron formula of Drude. By adjusting n_e and $\sigma(0)$, Hodgson (1955) was able to fit measured values of n and k for the divalent metal Zn from 2 to 15 μ. The value of n_e was substantially lower than that calculated, and the value of $\sigma(0)$ substantially lower than that measured. For the trivalent metal Al, Hodgson (1955) and Beattie (1955) could fit the Drude curves to the optical curves in the spectral range of $1 \sim 10$ μ, using suitably reduced values of n_e and $\sigma(0)$.

In spite of the good agreement found in the liquid metals Hg and Ga, it was found (Schulz, 1957-c) that the liquid alloys Hg-In, Hg-Tl, and Ga-In are in complete disagreement with the theory. This is in contrast to the earlier studies of Kent (1919) which pointed out that some liquid alloys follow the Drude theory. But these studies were confined to a very short wavelength range. Some of the early studies on the optical properties of liquid metals (Kent, 1919), bismuth, lead, cadmium and tin, in the spectral range of 0.40μ to 0.579μ shows a remarkable agreement with the Drude theory as shown in Table VII.

C. ELECTRON-LATTICE INTERACTION AND ANOMALOUS SKIN EFFECTS

In the original theory of Drude (1904), the viscous damping coefficient, Γ_o, was used without specified reference to the physical mechanism giving rise to the damping. The introduction of Γ_o was necessary in order to maintain a consistency between the electromagnetic dispersion and the finite dc resistivity on the basis of the free electron model. In this sense, the damping coefficient was used as a parameter whose magnitude was to be determined either from the measured electrical properties or from the measured optical data. Kronig (1927) reconsidered the problem in the frame of the modern theory of metals, showing that if the conduction electrons are treated as moving in a periodic potential perturbed by the thermal agitation of the lattice, they can be held responsible for the optical properties in the infrared as well as for the characteristic absorption and refraction in the visible and near ultraviolet parts of the spectrum. In other words, Kronig attributed the

TABLE VII. LOW TEMPERATURE ABSORPTIVITY OF METALS

Metals	Total Absorptivity A		Bulk Absorptivity (A_β / A) %	Optical Data Used to Calculate A_β, A_s
	Present Theory	Experiment		
Cu	0.0048	0.0050 Biondi(1956)	40%	Beattie Conn (1955) Bor et al (1939) Forsterling + Freederickz (1913)
Al	0.008	____	49%	Golovashkin et al (1960) Motulevich et al (1960)
Ag	0.0046	0.0044 Biondi (1956)	20%	Schulz (1951, 1954) Hodgson (1955) Forsterling + Freederickz (1913)
Hg	0.030 †	____	87%	Schulz (1957)
Ga	0.037 †	____	87%	Schulz (1957)
Zn	A_B= 0.003 *	____	A_B= 0.003	Hodgson (1955)
Sn	A_B= 0.008 *	____	A_B= 0.008	Hodgson (1955)
Ni	0.015	____	86%	Beattie Conn (1955)
Ti	A_B= 0.054 *	____	A_B= 0.054	Hass Bradford (1957)
Pt	0.054	____	94%	Forsterling Freederick (1913)
Ir	0.093	____	95%	Forsterling Freederick (1913)

† These are the extrapolations from the liquid data, and are not strictly valid for solids, except, perhaps, in the order of magnitude.

* The skin absorptivity A_s not computed.

occurrence of finite Γ_o to the mechanism of the electron-lattice interaction.

The mechanism of the electron-Lattice interaction or the electron-phonon interaction as it is popularly interpreted in modern theory, and of impurity scattering when the metal contains a substantial amount of impurities, has shown enormous success in explaining various physical qualities of metals such as the thermal and electric conduction, the Wiedemann-Franz law, the Matthiessen rule, the dependence of the electric resistance on temperature and pressure, and many others. (See, for instance, Wilson, 1936; Mott and Jones, 1936)

The impurity scattering introduces a residual resistance (Restwiderstand) and represents the temperature-independent, additive quantity of resistivity in the Matthiessen rule. A further progress on the behavior of metallic conductors under the influence of electromagnetic waves was made by Reuter and Sondheimer (1948) and was later elaborated by Dingle (1953), Gordon and Sondheimer (1953) and Pitaevski (1958). This work concerns the phenomenon that is popularly referred to as the anomalous skin effect and is important only at low temperatures.

Reuter and Sondheimer (1948), following a suggestion of London (1940), investigated the case, important at low temperatures, that the mean free path of the conduction electrons for collisions with the lattice is of the same order of magnitude as, or even large, compared with the normal penetration depth (skin depth) of the electromagnetic waves in the metal. In this case, the way in which the metal boundary influences the motion of the electrons arriving there becomes important. The authors distinguished two extreme cases: namely, that of the specular reflection at the surface and that of completely diffuse reflection, the latter being at least approximately realized in nature according to the available evidence. Dingle (1952, 1953) added elaboration to the original theory of Reuter and Sondheimer, and showed, in particular, that, especially in the case of diffuse reflection, the values resulting for the absorptivity A(=1-R) of the metallic surface may differ widely from the predictions of standard theory. Qualitatively, this is to say that, in this case, the loss of momentum parallel to the boundary, which an electron suffers when diffusly reflected by it, furnishes a contribution to the real part of the surface impedance of the metal. This contribution remains even if, by lowering the temperature, the bulk resistivity and with it the energy loss in the interior of the metal are reduced. Hence, the metal still retains a non-zero absorptivity when the bulk resistivity is made to vanish by lowering the temperature to 0°K. This conclusion was qualitatively predicted by the experiments of Ramanathan (1952) at the liquid helium temperature. The success of the theory of anomalous skin effect in accounting for the reflectivity of metals has been conclusively demonstrated by Dingle (1953) and Pitaevski (1958).

In its present state of development, the theory of the anomalous skin effect applies strictly to the alkali metals and monovalent metals such as Au, Ag, and Cu. Like the simple Drude theory, the anomalous skin effect does not apply in a region of strong resonance absorption. Table VII shows the values of the absorptivity, A:

$$A = A_v + A_s \tag{86}$$

for Cu and Ag, where A_s is the diffuse skin absorptivity:

$$A_s = \frac{3}{4}\left(\frac{V_f}{c}\right) \tag{87}$$

V_f being the Fermi velocity of electron and c the speed of light, and A_v is the bulk contribution to the absorption resulting primarily from the electron-phonon interactions. The values of A_v for Cu and Ag have been obtained from the formula that will be derived in the calculations of Section IV. It is seen in Table VIII that the bulk and skin effects added together show agreements with the experimental values up to about 2 percent.

Associated with the skin effect is the skin depth which is the thickness at the metal surface in which most of the optical skin effect is observed, and is given by:

$$\delta_s = \left(\frac{m^* c^2}{4\pi n_o e^2}\right)^{\frac{1}{2}} \tag{88}$$

and is in the order of several thousand angstroms. This is not to be confused with the so-called penetration depth δ_p which is a distance characteristic of the surface penetration by light of given wavelength and is the distance at which the intensity falls to $\frac{1}{e}$ of that at the surface.

It is given by:

$$\delta_I = \frac{\lambda}{4\pi k} \tag{89}$$

where k is the absorption index. For sodium at $\lambda = 0.6\mu$, $k \approx 2.6$, and δ_I is approximately 180 Å. In gerneral, δ_I is in the order of several hundred angstroms. The expression of Equation (89) is reminiscent of the similar expression for the penetration depth at radio frequencies:

$$\delta = \frac{c}{\sqrt{4\pi\sigma_{dc}\,\omega}} = \frac{\lambda}{2\sqrt{2\pi}\,k} \tag{90}$$

where σ_{dc} is the dc electric conductivity. The two expressions are essentially the same as far as the qualitative estimations are concerned.

TABLE VI. LIQUID METALS

Metal	Bi	Pb	Cd	Sn	Hg
Ne/atom (calculated)	5.1	5.1	2.4	4.1	2.1
$1/\sigma_o$ (μ ohm/cm) calculated	128	94	33.4	54	87.3
$1/\sigma_{dc}$ (μ ohm/cm) measured	134	98	34	52	94

TABLE VIII LOW TEMPERATURE ABSORPTIVITY OF METALS

Metals	Total Absorptivity A		Bulk Absorptivity (A_β/A) %	Optical Data Used to Calculate A_β, A_s
	Present Theory	Experiment		
Cu	0.0048	0.0050 Biondi (1956)	40%	Beattie Conn (1955) Bor et al (1939) Forsterling & Freederickz (1913)
Al	0.008	---	49%	Golovashkin et al (1960) Motulevich et al (1960)
Ag	0.0046	0.0044 Biondi (1956)	20%	Schulz (1951, 1954) Hodgson (1955) Forsterling & Freederickz (1913)
Hg	0.030+	---	87%	Schulz (1957)
Ga	0.037+	---	87%	Schulz (1957)
Zn	A_B= * 0.003	--- ---	A_B= 0.003	Hodgson (1955)
Sn	A_B= * 0.008	--- ---	A_B= 0.008	Hodgson (1955)
Ni	0.015	---	86%	Beattie Conn (1955)
Ti	A_B= * 0.054	---	A_B= 0.054	Hass Bradford (1957)
Pt	0.054	---	94%	Forsterling Freederick (1913)
Ir	0.093	---	95%	Fosterling Freederick (1913)

+ These are the extrapolations from the liquid data, and are not strictly valid for solids, except, perhaps, in the order of magnitude.

* The skin absorptivity A_s not computed.

SECTION IV. QUANTUM MECHANICAL CALCULATION OF OPTICAL AND INFRARED DISPERSION IN METALS

A. INTRODUCTION

All of the existing theories are based on the common assumption that Maxwell's theory of electromagnetism is valid in the form that was discussed in Section II, and any new theory which is based on the same assumption should necessarily be formulated on the basic grounds laid by the work that has been done in the past.

The classical dispersion equations are simply the solutions to the equations of motion subject to Maxwell's electromagnetic field. Therefore, as long as we confine ourselves to that part of the spectrum where the free electrons are mostly responsible for the dispersion, it is quite natural for us to expect that a new theory which is offered by quantum mechanical calculations should necessarily be a "quantum mechanical free electron theory" which can differ from the classical free electron theory only in specification of the temperature dependence and also of further frequency dependence if any, in the viscous damping and polarizability, etc.

Various quantum mechanical dispersion equations should approach the corresponding classical equations in the limit of low frequency where $\sigma(\omega)$ approaches the value of $\sigma(0)$ of the static case. It is hardly necessary to mention that some of the high-frequency effects, such as the phenomenon of anomalous dispersion arising from the photoelectric resonance of bound electrons and also of the small but important contribution of the core polarization, can be explained rigorously only with the aid of quantum mechanics.

Compared with an enormous amount of qualitative and quantitative applications of quantum mechanics to the properties of metals under the influence of static electric fields, very little progress is found on the optical and infrared dispersive properties of metals beyond what is available from the classical free electron theories and the anomalous skin effects. The less said the better on similar considerations of alloys. However, it is self evident that the noble features of quantum mechanics revealed in the metallic properties under the influence of static electric field provide an indispensable tool for examining the optical and infrared dispersion properties of metals, because as we saw in Section III, the two aspects of metallic properties are intimately linked with each other. This was already qualitatively made use of in the early studies of Mott (1934) and Mott and Jones (1936). Further, much progress that has been made on the optical properties of semiconductors can be extended to metallic conductors with suitable modifications since, after all, the semiconductors and metallic conductors may be

considered as differing from each other more in degree than in kind as far as the respective conduction mechanism and properties are concerned. The qualitative aspects of this feature were already discussed in the early studies of Wilson (1936) and more recently in the work of Bardeen and Shockley (1950).

Some of the considerations that enter in the quantum mechanical calculations may be mentioned as:

(a) the Pauli exclusion principle;

(b) the Fermi-Dirac statistics;

(c) solid band structures;

(d) quantum mechanical interpretations of various interactions that contribute to the viscous damping of conduction electrons;

(e) the effect of core polarization;

(f) the effect of the bound electrons.

The calculations in the frame of the free electron theory involves considering explicitly all of the above except for the last two, in addition to the fundamental relations available from Maxwell's theory of electromagnetism considered in Section II. A qualitative discussion on the effects related with (e) and (f) above was given in Section III, and excellent discussions of these features, as to the mechanism and effects, are presented by Van Vleck (1959) and Mott and Jones (1936) on (e) and (f) above, respectively. A detailed discussion on these points is outside the scope of the present work.

In the theoretical calculations that will follow, it is attempted to find explicitly the ω- and T- dependent structure of the damping coefficient and, hence the polarizability $\bar{\alpha}$ and also the bulk absorptivity A_v (ω,T), in the framework of the free electron theory and with the assumption of spherical Fermi surface. That very little error is involved in assuming a spherical energy surface for most of the body-cnetered, face-centered and hexagonal cubic lattices was pointed out by Wilson (1936) and Mott and Jones (1936), and is shown in the following qualitative expression for dc conductivity (Jones, 1956):

$$\sigma_{dc}^{ij} = + \frac{n_e e^2}{4\pi^3 h^2} \iiint \left(\frac{\partial F(E)}{\partial E} \tau(\underline{k}) \left(\frac{\partial^2 E}{\partial k_i \partial k_j} \right) (d^3\underline{k}) \right. \quad (91)$$

$$(i, j = 1,2,3)$$

where F(E) is the dimensionless electron distribution function at energy E($\underline{K}$) and T($\underline{k}$) is the dc relaxation lifetime of an electron with momentum ($h\underline{k}$). Futhermore, even for a metal which, in a single crystal, has a detectable degree of anisotropy, the spherical approximation of Fermi surface works well for a polycrystalline sample. Some particular cases of metals in which interband transitions make predominant contributions to various electrical and optical properties and for which nonspherical Fermi surface must be used, will be treated in the future section on transition metals.

The results on transition metals should apply equally well to other nontransition, multivalent metals when interband transitions need to be considered.

For metals to which spherical Fermi surface applies, effect of the periodic lattice is incorporated entirely into the effective number of electrons per unit volume and the effective mass. This is in accord with the "effective mass method" which will be discussed in more detail in the following paragraph of this section. Then, for a metal which is free of impurities, the only perturbation to the electronic motion originating from the presence of lattice is the electron-phonon interaction or the interaction between the "free" electrons and the thermal vibrations of the lattice represented by a finite temperature-dependent distortion of the lattice from the perfectly periodic potential of 0°K. Such a perturbation decreases rapidly as temperature is lowered to the absolute zero. The metals with a substantial impurity content and alloys, especially the ones with a random lattice, are exceptions to this picture: there is a finite, temperature-independent perturbation giving rise to a non-zero resistivity at 0°K, the total resistivity being given by this plus an additional temperature-dependent term (Mathiessen's rule), (Mathiessen and Vogt, 1864).

The bulk absorptivity, A_v, the conductivity, $\sigma(\omega)$, as well as the damping coefficient are calculated from the result on the rate of energy expenditure $\overline{W}(\omega,T)$, which is related to $\sigma(\omega)$, according to the free electron theory by:

$$n_e \overline{W} = \frac{E^2}{2} \sigma(\omega) \qquad (92)$$

where $\sigma(\omega)$ is in turn related to the damping coefficient through the typical free electron dispersion equations, and where $(E^2/2)$ is the energy density per unit volume of the electromagnetic radiation field.

Identification of the damping coefficient in the final expression of $\overline{W}$ is straightforward when we compare the result with the corresponding dc expression derived in Wilson's theory of metals (1936). Thus, the

approach adopted in the present work differs from the usual method of finding the damping coefficient directly by calculating the inverse of transition lifetimes (relaxation time) from the transition matrix elements.

TABLE VIII METALS WITH LARGE ANISOTROPY

Metals	Anisotropy in dc resistivity			Reference
	Max.	Min.	Ratio	
Ga (Solid)	55.(5)	7.8 (5)	7	Powell (1949)
Hg (Solid)	23.5	17.8	1.32	Sckell (1930)
Sb	42.6	35.6	1.2	Bridgman (1925)
Cd	8.3	6.8	1.22	"
Te	1.54×10^5	5.6×10^4	2.75	"
Zn	6.05	5.83	1.04	"
Bi	138	109	1.27	"

Powell, Nature 164, 153 (1949)

Sckell, Ann. Physik (5) 6, 932 (1930)

Bridgman, Proc. Amer. Acad. 60, 306 (1925)

B. CALCULATIONAL METHOD AND ASSUMPTIONS ON DAMPING INTERACTIONS

It will be assumed that the predominant contribution to the electron damping comes from the electron-lattice interaction in cooperation with the perturbing electromagnetic field. The contribution by electron-electron collisions, which are important at very high frequencies and at very low temperatures, will be combined with the results of the present section using the formulas obtained by Gurzhy (1958). Further, when metal contains a substantial amount of impurities, the effective damping will be the sum of the contributions by electron-phonon processes, electron-electron collisions and impurity scattering. The additional contribution by impurity scattering is responsible for the temperature-independent residual resistance in the Mathiessen rule. In the present section, calculations will be carried out for a pure metal. However, if the impurity effects need to be considered, a constant term is to be added to the damping coefficient. This additive constant may be calculated from either an optical data (Golovashkin, et al, 1960) or from low temperature measurements of dc resistivity.

In this chapter, only those transitions which take place within a single band in the lowest Brillouin zone will be considered: i.e., intra-band transitions. The case where the interband transitions are involved will be left to a future chapter on transition metals.

Once we adopt the Hamiltonian in a specific form, various transition probabilities can be found by the usual quantum mechanical methods. We shall use the perturbation method similar to that was used by Wilson (1936) and Holstein (1954). Then, the transitions which are responsible for the damping and dispersion are the second order processes in which an electron initially at the momentum state $\underline{k}_1$ makes a transition to the final state $\underline{k}_2$ upon a simultaneous absorptions or emissions of a phonon and a photon.

We define:

$$P_{(\pm)}^{(\pm)}\left(\underline{k}_1 \rightarrow \underline{k}_2\right)$$

as the probability per unit time for a conduction electron to make a transition from the state $\underline{k}_1$ to the final state $\underline{k}_2$ with simultaneous photon and phonon emissions (+) and absorptions (-) when it is certain that the $\underline{k}_2$ state is completely empty and $\underline{k}_1$ state is completely filled and where the superscript (±) designates the phonon processes and the subscript (±) the photon processes.

According to the Fermi-Dirac statistics, the probability that the $\underline{k}$ with the corresponding energy $\underline{E}$ ($\underline{k}$) is filled at temperature T(°K) is given by the Fermi function:

$$f(E) = \frac{1}{1 + e^{\beta(E-E_F)}} \tag{93}$$

where E_f is the Fermi energy and β is $(KT)^{-1}$, K being the Boltzmann constant. Then, the total probability per unit time of an electron initially at the state $\underline{k}_1$ to make a transition to any of the other empty states by either one of the four processes designated by the superscript and subscript $(\pm)$ will be given by:

$$P_{(\pm)}^{(\pm)}\left(\underline{k}_1\right) = 2\sum_{\underline{k}_2}\left[1 - f(E_2)\right] P_{(\pm)}^{(\pm)}\left(k_1 \rightarrow k_2\right) \tag{94}$$

where the factor 2 comes about because, according to the Pauli exclusion principle, two electrons with opposite spins can occupy the state with same $\underline{k}$ and E(k). The appearance of $\left[1-f(E_2)\right]$ embodies the Pauli exclusion principle.

In order to represent the gross manifestations of such microscopic transition processes, we have to average the probability of Equation (94) over all the initially occupied states according to the Fermi-Dirac statistics. The resulting average value of probability (P) per unit time will be in the form:

$$\langle P_{(s)}^{(r)} \rangle = 2\sum_{\underline{k}_1}\sum_{\underline{k}_2} f(E_1)\left[1-f(E_2)\right] P_{(s)}^{(r)}\left(\underline{k}_1 \rightarrow \underline{k}_2\right) \Big/ \left(\sum_{\underline{k}_1} f(E_1)\right) \tag{95}$$

where r, s = $(\pm)$.

Then, following Holstein (1954), the power expended by the electromagnetic radiation field is defined as:

$$\overline{W} = \sum_{r=(\pm)} \hbar\omega \left[P_{(-)}^{(r)} \rangle - P_{(+)}^{(r)} \right] \tag{96}$$

This implies simply that the net power expenditure is the total power absorbed minus the amount which is emitted into the radiation field. There is an analogy between Equation (96) and the corresponding statistical mechanical formula of Wilson (1936).

The relation in Equation (96) is dependent on both the frequency ω and temperature T. A part of the temperature dependence comes from the Fermi-Dirac statistics of the electron distribution and the other

part comes from the Bose-Einstein statistics of the phonon distribution (the thermal vibration of lattice) which enter in the Hamiltonian average over the distribution of phonon states.

Once the T- and ω-dependent expression for $\overline{W}$ is obtained various dispersion formulas follow naturally. For instance, the high frequency conductivity $\sigma(\omega)$ is given by:

$$n_e \overline{W} = \frac{E^2}{2} \sigma(\omega) \tag{97}$$

Thus, it is evident that the main task of theoretical calculations is in finding correct values of $\overline{W}$ or P .

In general, the expression for $\overline{W}$ will vary depending on the particular physical model of the system, the methods of computation, and the particular Hamiltonian that are adopted. According to the effective mass method of Peckar (1946), Slater (1949), Wannier (1937), and James (1949), and to the theorems developed by Bardeen and Shockley (1950), the electrons in the isotropic (cubic) lattice may be considered as free electrons of effective mass m*, and when the lattice is distorted by a small amount resulting in a small change in the potential:

$$V_p = \delta U = U_d(\underline{x}) - U_o(\underline{x}) \tag{98}$$

the amplitude part of the electronic wavefunction $A(\underline{x})$ satisfies the Schrödinger equation:

$$\left[- \frac{\hbar^2}{2m^*} \nabla^2 + \delta U \right] A(\underline{x}) = EA(\underline{x}) \tag{99}$$

where $U_o(\underline{x})$ is the original undistorted periodic potential and $U_d(\underline{x})$ is the distorted potential which depends on the strains ϵ_{ij} that are imparted to the lattice in distortion. If the lattice is not cubic, we must replace $\left(\frac{1}{m^*} \nabla^2 \right)$ by:

$$\left(\frac{1}{m_1^*} \frac{\partial^2}{\partial x_1^2} + \frac{1}{m_2^*} \frac{\partial^2}{\partial x_2^2} + \frac{1}{m_3^*} \frac{\partial^2}{\partial x_3^2} \right) \tag{100}$$

where (x_1, m_2^*, m_3^*) are the three principal-axis coordinates, and (m_1^*, m_2^*, m_3^*) are the three values of effective mass. The amplitude function, $A(\underline{x})$, is a smoothly varying function which does not vary appreciably over the unit cell: If $A(\underline{x})$ does not meet this condition, the method of

effective mass is inadequate without a considerable degree of refinement. In general, wave functions of electrons in metals are rather flat except in the middle of the atom (Mott and Jones, 1936), and the volume within which the wave function is not flat is relatively small, so that the charge density in the flat region is almost exactly $\left(\frac{e}{V_o}\right)$, where V_o is the atomic volume. This flatness of wave function is the reason why the approximation of neglecting the periodic field (free electron approximation) gives good results for metals, and thus Equation (100), should work. According to Bardeen and Shockley (1950), the electron-lattice potential $V_p(\underline{x})$ may be taken in the form:

$$V_p(\underline{x}) = g \triangle(\underline{x}) \tag{101}$$

where g is a constant and $\triangle(\underline{x})$ is the dilation. Neglecting the other terms in the expansion of $V_p(\underline{x})$ in powers of the strain ϵ_{ij} is equivalent to neglecting the dependence of the effective mass on the strain. It was shown that the next largest term in $V_p(\underline{x})$ to that given in Equation (101) is proportional to the square of momentum times the strain:

$$\sim O(k^2 \times \text{strain}) \tag{102}$$

and, for the usual order of magnitude of k^2 involved in metals and for the size of the strain in the thermal agitation of the lattice, this second term can safely be neglected.

C. TRANSITION PROBABILITY CALCULATION

Following Bardeen and Shockley (1950) and Holstein (1954), the Schrödinger equation for a conduction electron interacting with the perturbing electromagnetic field, $\underline{A}$, and the lattice vibration may be written in the form:

$$ih\frac{\partial \psi}{\partial t} = \frac{1}{2m^*}\left(-i\hbar\nabla + \frac{e}{c}\underline{A}\right)^2 \psi + V_p(\underline{x})\psi \tag{103}$$

where $V_p(\underline{x})$ is interpreted as the electron-phonon interaction potential given by:

$$V_p(r) = g \operatorname{div} \underline{u}(r)$$

$$\underline{u}(\underline{r}) = \sum_{\underline{q},j} \hat{e}_{q,j}\left\{a_j(\underline{q})e^{i\left[\underline{q}\cdot\underline{r} - \omega_{\underline{q},j}t\right]} + \text{c.c.}\right\} \tag{104}$$

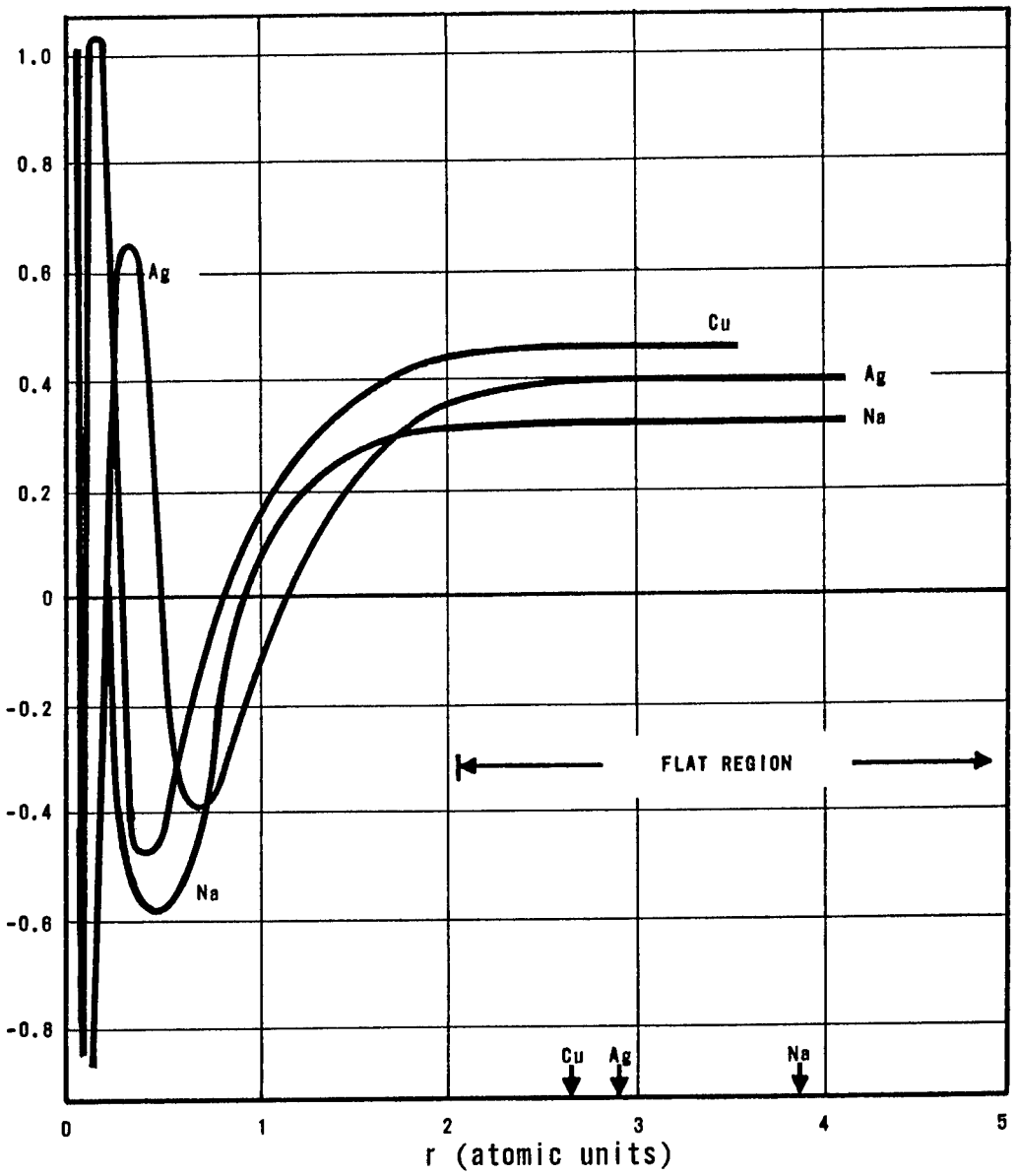

Figure 14. Electronic Wavefunctions of Metals

$$a_j(\underline{q}) = \sqrt{(\hbar N_{\underline{q},j} \quad 2\rho_o V\omega_{\underline{q},j})}$$

$$a_j^*(\underline{q}) = \sqrt{(\hbar [N_{\underline{q},j} + 1] \quad 2\rho_o V\omega_{\underline{q},j})}$$

where $(a_j^*(\underline{q}), a_j(\underline{q})$ are the phonon creation and annihilation operators, ρ_o is the mass density, $\omega_{\underline{q},j}$ is the phonon frequency:

$$\hbar\omega_{\underline{q},j} = E_{\underline{q},j} \tag{105}$$

and $(\hat{e}_{q,j})$ are the orthonormal basic vectors:

$$(\hat{e}_{\underline{q},j} \cdot \hat{e}_{\underline{q},j}) = \delta_{jj'} \tag{106}$$

and g is a constant whose value is of the same order as the electronic energy.

For an isotropic lattice, we have the simpler expression:

$$V_p(\underline{x}) = ig \sum_{\underline{q}} q \left(\frac{\hbar^2}{2N_p MVE_{\underline{q}}}\right)^{\frac{1}{2}} \left[\sqrt{N(\underline{q})}\, e^{i(\underline{q}\cdot\underline{x} - E_{\underline{q}}t/\hbar)} - \sqrt{N(\underline{q})+1}\, e^{-i(\underline{q}\cdot\underline{x} - E_q t/\hbar)}\right] \tag{107}$$

where we have used the following notations:

M : Mass of the lattice

V : The sample volume

N_p : Phonon number density (per unit volume) = $\frac{\rho o}{M}$

$\underline{q}$: Phonon wave-vector (momentum/h)

$E_{\underline{q}}$: Energy of a phonon at the state $(\underline{q})$

$N(\underline{q})$: The number of phonon states for $E_{\underline{q}}$ that are occupied, and is according to Bose-Einstein statistics,

$$N(\underline{q}) = \frac{1}{e^{\beta E \underline{q}} - 1}$$

In practice, it is often possible to distinguish longitudinal and transverse waves in a crystal and discard the latter because of the factor $(\hat{e}_j \cdot \underline{q})$ in Equation (104). This is what has been done in obtaining Equation (107). This is also related to the approximation of taking $E_{\underline{q}}$ dependent only on the magnitude q and using the simple Debye dispersion of phonons when the accoustic branch of phonon spectrum makes predominant contributions. When KT has a value comparable to the discrete quantum of upper branches, the optical branch contributes significantly.

In the present work, the electromagnetic field will be treated purely classically and we will use:

$$\underline{A}(\underline{x}) = \left(\underline{A}(\underline{x}) e^{-i\omega t} + \underline{A}^* (\underline{x}) e^{+i\omega t} \right)$$

$$= -i \frac{e\underline{E}}{2\omega} \left(e^{i(\underline{p}.\underline{x} - \omega t)} - e^{-i(\underline{p}.\underline{x} - \omega t)} \right) \qquad (108)$$

where $\underline{E}$ is the electric amplitude vector which satisfies $(\underline{E}.\underline{p})=0$ when we chose $\underline{A}$ to meet the divergence condition $(\nabla.\underline{A})=0$. The Schrödiger Equation (103) now becomes, upon neglecting the term quadratic in $\underline{A}$:

$$i\hbar \frac{\partial \psi}{\partial t} = - \frac{\hbar^2}{2m^*} \nabla^2 \psi + \left(\frac{e\hbar}{im^*c} \underline{A}. \nabla + V_p \right) \psi \qquad (109)$$

In the absence of the perturbation by the electromagnetic field and the lattice vibration, the stationary states of electrons are represented by the wave functions:

$$\psi_{\underline{k}} (\underline{x},t) = e^{i(\underline{k}.\underline{x} - E_k t/\hbar)} \qquad (110)$$

where:

$$E_{\underline{k}} = (\hbar^2 k^2 / 2m^*) \qquad (111)$$

The perturbed wave function $\psi(\underline{x},t)$ may be expanded into a superposition of the unperturbed, free electron states in the form:

$$\psi(\underline{x},t) = \sum_{\underline{k}} B(\underline{k}) \psi_{\underline{k}} (\underline{x},t) \qquad (112)$$

where $B(\underline{k})$ is the expansion coefficient with an explicit time dependence. By substituting Equation (112) into (109), the equation of motion for $B(\underline{k})$ is obtained as:

$$i\hbar \frac{\partial B(\underline{k})}{\partial t} = \frac{e\hbar\,(\underline{k}\cdot\underline{E})}{2im^*\omega}\left[B(\underline{k}-\underline{p})e^{\,i(E_{\underline{k}}-E_{\underline{k}-\underline{p}}-\hbar\omega)t/\hbar} - B(\underline{k}+\underline{p})e^{\,i(E_{\underline{k}}-E_{\underline{k}+\underline{p}}+\hbar\omega)t/\hbar}\right] \tag{113}$$

$$+ ig\sum_{\underline{q}}\left\{q\left(\frac{\hbar^2}{2N_p MVE_{\underline{q}}}\right)^{\frac{1}{2}}\left[B(\underline{k}-\underline{q})\sqrt{N(\underline{q})}\,e^{i(E_{\underline{k}}-E_{\underline{k}-\underline{q}}-E_{\underline{q}})t/\hbar} - B(k+\underline{q})\sqrt{N(\underline{q})+1}\,e^{i(E_k-E_{\underline{k}+\underline{q}}+E_{\underline{q}})\,t/\hbar}\right]\right\}$$

In the absence of the lattice vibration we would have only the first term [---] in Equation (113) arising solely from the electromagnetic field. In this case, the coefficient $\underline{B}(\underline{k})$ cannot be made to increase indefinitely with time because the energy terms:

$$E_{\underline{k}} - E_{\underline{k}+\underline{p}} \pm \hbar\omega \tag{114}$$

in the exponents cannot be made to vanish. In the language of perturbation theory, the transitions are at most virtual and this corresponds to the fact that a photon cannot be absorbed or emitted by a free electron. Therefore, the electromagnetic perturbation alone cannot explain the damping in optical dispersion (Heitler, 1957). Following the usual procedure of the perturbation method, we write

$$B(\underline{k}) = \delta(\underline{k},\underline{k}_o) + B_{(1)}(\underline{k}) + B_{(2)}(\underline{k}) + \ldots \tag{115}$$

where $B_{(1)}$, $B_{(2)}\ldots$ are the first order, second order, ... terms for an electron which was certain to be at the state $\underline{k}_o$ initially. The electromagnetic and the lattice vibration terms will be considered as the first order perturbations in Equation (109). Then $B_{(1)}$ in Equation (115) will contain only those terms which are in the first power of $\underline{E}$ and g as well as those quadratic in each of $\underline{E}$ and g. The combined action of the electromagnetic field and the lattice vibration is described by that term of $B_{(2)}$ which is bilinear in $\underline{E}$ and g, and we will need only this part of $B_{(2)}$ for our dispersion calculations.

In order to calculate $B_{(2)}$, we need to obtain $B_{(1)}$ first. By substituting Equation (115) into (113) and collecting the terms which are of the first order in $\underline{E}$ and $\underline{q}$, and integrating in time from 0 to t, we obtain the following:

$$B_{(1)}(\underline{k}) = \frac{ie\hbar(\underline{k}.\underline{E})}{2m^*\omega}\left[\delta(\underline{k}_o,\underline{k}-\underline{p})\left(\frac{e^{i(E_{\underline{k}}-E_{\underline{k}-p}-\hbar\omega)t/\hbar}-1}{E_{\underline{k}}-E_{\underline{k}-p}-h\omega}\right)\right.$$

$$-\delta(\underline{k}o,\underline{k}+\underline{p})\left(\frac{e^{i(E_{\underline{k}}-E_{\underline{k}+p}+\hbar\omega)\ t/\hbar}-1}{E_{\underline{k}}-E_{\underline{k}+p}+h\omega}\right)$$

$$-ig\sum_{\underline{q}}\left\{q\left(\frac{\hbar^2}{2N_p MVE_{\underline{q}}}\right)^{\frac{1}{2}}\left[\delta(\underline{k}_o,\underline{k}-\underline{q})\ \sqrt{N(\underline{q})}\left(\frac{e^{i(E_{\underline{k}}-E_{\underline{k}-q}-E_{\underline{q}})\ t/\hbar}-1}{E_{\underline{k}}-E_{\underline{k}-q}-E_{\underline{q}}}\right)\right.\right.$$

$$\left.\left.-\delta(\underline{k}_o,\underline{k}+\underline{q})\ \sqrt{N(\underline{q})+1}\left(\frac{e^{i(E_{\underline{k}}-E_{\underline{k}+q}+E_{\underline{q}})\ t/\hbar}-1}{E_{\underline{k}}-E_{\underline{k}+q}+E_{\underline{q}}}\right)\right]\right\}$$

Using Equation (116) in (113), and collecting only those terms which are bilinear in $\underline{E}$ and g, we obtain:

$$B_{(2)}(\underline{k}\pm\underline{q}\pm\underline{p}) = \left(\frac{\hbar^2q^2}{2N_p MVE_{\underline{q}}}\right)^{\frac{1}{2}}\left(\frac{e\hbar g}{2m^*\omega}\right)\left\{\begin{matrix}N(\underline{q})^{\frac{1}{2}}\\ N(\underline{q})+1\ ^{\frac{1}{2}}\end{matrix}\right\}$$

$$\underline{E}\cdot\left[\left(\frac{\underline{k}\pm\underline{q}}{E_{\underline{k}+\underline{q}}-E_{\underline{k}}+E_{\underline{q}}}+\frac{\underline{k}}{E_{\underline{k}\pm\underline{p}}-E_{\underline{k}}\pm h\omega}\right)\frac{e^{i\xi t/\hbar}-1}{\xi}\right. \qquad (117)$$

$$\left.-\frac{(\underline{k}\pm\underline{q})}{(E_{\underline{k}\pm\underline{q}}-E_{\underline{k}}+E_{\underline{q}}}\times\frac{e^{i\xi' t/\hbar}-1}{\xi'}-\frac{\underline{k}}{(E_{\underline{k}\pm\underline{p}}-E_{\underline{k}}+\hbar\omega)}\ \frac{e^{i\xi''\ t/\hbar}-1}{\xi''}\right]$$

where $\underline{k}$ is now written in place of $\underline{k}_o$, and:

$$\xi = E_{\underline{k}\pm\underline{q}}-E_{\underline{k}}\ \bar{+}\ \hbar\omega\ \bar{+}\ E_{\underline{q}}$$

$$\xi' = E_{\underline{k}\pm\underline{q}\pm\underline{p}}-E_{\underline{k}\pm\underline{q}}\ \bar{+}\ \hbar\omega \qquad (118)$$

$$\xi'' = E_{\underline{k}\pm\underline{q}\pm\underline{p}} - E_{\underline{k}\pm\underline{p}} \mp E_{\underline{q}}$$

The probability per unit time, $P(\underline{k} \;\; \underline{k}\pm\underline{q}\pm\underline{p})$, for the electron to make a transition from $\underline{k}$ to $(\underline{k}\pm\underline{q}\pm\underline{p})$ under the combined action of the electromagnetic and acoustical fields is given by the absolute square of $B_{(2)}$ divided by time,

$$P(\underline{k} \;\; \underline{k}\pm\underline{q}\pm\underline{p}) = \left| B_{(2)} \; (\underline{k}\pm\underline{q}\pm\underline{p}) \right|^2 \Big/ t \qquad (119)$$

$$: \; t \to \infty$$

A significant contribution to Equation (119) comes from those situations where one of the energy denominators contained in Equation (117) becomes zero. Only in such cases does the transition probability per unit time approach a constant nonvanishing value for a large t. The zeros of the energy denominators may be grouped into two categories: those which involve a coincidence of initial and final energies inclusive of the photon energy $\hbar\omega$ and phonon energy $E_{\underline{q}}$, and those which arise from an energy coincidence of an intermediate state with either the initial or final state. The two terms of Equation (117) which contain ξ' and ξ'' will not contribute to the over-all transition probability, since they cancel out in calculations of the energy expenditure. It is easily shown that:

$$\left|\xi'\right| \approx \left| 1 \mp \frac{V_F}{c} \right| \hbar\omega \approx \hbar\omega \qquad (120)$$

On the other hand, the zero, $\xi''=0$, is physically possible and the resonance factor containing ξ'' gives rise to $\delta(\xi'')$ in the expression for the transition probability. However, the terms with ξ' and ξ'' contribute equally to both absorption and emission processes of photons, and the over-all contribution from these terms to the net absorption, which is obtained from:

$$\left(P_{(-)}^{(\pm)} - P_{(+)}^{(\pm)} \right) \qquad (121)$$

cancel out. Therefore, we only need to evaluate the transition probability at the singularity $\xi=0$.

Equation (117) may then be replaced by equation:

$$B_{(2)} \; (\underline{k}\pm\underline{q}\pm\underline{p}) = q \left(\frac{\hbar^2}{2N_p MVE_{\underline{q}}} \right)^{\frac{1}{2}} \left(\frac{\sqrt{N(\underline{q})}}{\sqrt{N(\underline{q})+1}} \right) \frac{e\hbar g}{2m^*\omega} \qquad (122)$$

$$\times \underline{E}\cdot\left(\frac{\underline{k}\pm\underline{q}}{E_{\underline{k}\pm\underline{q}}-E_{\underline{k}}+E_{\underline{q}}}+\frac{\underline{k}}{E_{\underline{k}\pm\underline{p}}-E_{\underline{k}}\mp\hbar\omega}\right)\quad\frac{e^{i(E_{\underline{k}\pm\underline{q}\pm\underline{p}}-E_{\underline{k}}-E_{\underline{q}}\mp\hbar\omega)t/\hbar}-1}{E_{\underline{k}\pm\underline{q}\pm\underline{p}}-E_{\underline{k}}\mp\hbar\omega\mp E_{\underline{q}}}$$

Let us consider the transitions $\underline{k}\rightarrow(\underline{k}+\underline{q}+\underline{p})$ first.

We notice that:

$$\left(E_{\underline{k}+\underline{q}}-E_{\underline{k}}-E_{\underline{q}}\right)+\left(E_{\underline{k}+\underline{p}}-E_{\underline{k}}-h\omega\right)=$$

$$\left(E_{\underline{k}+\underline{p}}-E_{\underline{k}}\right)-\left(E_{\underline{k}+\underline{q}+\underline{p}}-E_{\underline{k}-\underline{q}}\right)+\xi\cong 0 \qquad (123)$$

The quantities of the form $\left(E_{\underline{k}+\underline{p}}-E_{\underline{k}}\right)$ represent the (v/C) corrections, and will be ignored. Furthermore, ξ may be taken equal to zero in Equation (123); a deviation from zero need be considered only in the last factor of Equation (122) representing the resonance factor.

Equation (122) is then replaced by:

$$B_{(2)}\ (\underline{k}+\underline{q}+\underline{p}) = q\left(\frac{\hbar^2}{2N_p MVE_{\underline{q}}}\right)^{\frac{1}{2}}\sqrt{N(\underline{q})}\ \frac{e\hbar g}{2m^*\omega}$$

$$\times\frac{\underline{E}\cdot\underline{q}}{h\omega+E_{\underline{k}}-E_{\underline{k}+\underline{p}}}\times\frac{e^{i\xi t/\hbar}-1}{\xi} \qquad (124)$$

for the transition, $\underline{k}\quad\underline{k}+\underline{q}+\underline{p}$.

The transition probability P $(\underline{k}\rightarrow\underline{k}+\underline{q}+\underline{p})$ may be evaluated readily from Equation (125) upon taking:

$$\left(E_{\underline{k}+\underline{p}}-E_{\underline{k}}-\hbar\omega\right)\cong-\hbar\omega \qquad (125)$$

and following the popular practice (Heitler, 1957):

$$\delta(\xi)=\lim_{t\rightarrow\infty}\frac{\hbar}{2\pi}\ \frac{1}{t}\left|\frac{-i}{\hbar}\int_0^t e^{i\xi t'/j}\,dt'\right|^2$$

$$=\lim_{t\rightarrow\infty}\frac{\hbar}{2\pi}\ \frac{1}{t}\left|\frac{e^{i\xi t/\hbar}-1}{\xi}\right|^2 \qquad (126)$$

We thus have:

$$P\ (\underline{k}\rightarrow\underline{k}+\underline{q}+\underline{p}) = \frac{\pi g^2 N\ (\underline{q}) e^2 \hbar^3 q^2}{4N_p MVE_{\underline{q}} m^{*2}\omega^2} \quad \frac{(\underline{E}\cdot\underline{q})^2}{(\hbar\omega)^2}\ \delta(\xi) \tag{127}$$

Upon introducing the final state momentum, $\underline{k}_2$, as $(\underline{k}+\underline{q}+\underline{p})$ and denoting the initial state $\underline{k}$ as $\underline{k}_1$, and noting also that the argument, ξ, of the delta function, $\delta(\xi)$, represents the absorption of a phonon and and a photon of energy $\hbar\omega$ and E_q respectively, we may rewrite (127) into the form:

$$P_{(-)}^{(-)}\ (\underline{k}_1\rightarrow\underline{k}_2) = \frac{\pi\hbar q^2 N(q) e^2 g^2}{4N_p MVE_q m^{*2}\omega^4}\ (\underline{E}\cdot\underline{q})^2\ \delta(E_2 - E_1 - E_4 - \hbar\omega) \tag{128}$$

where the superscript (-) refers to the phonon absorption and the subscript (-) to the photon absorption.

From now on, the photon momentum, $\underline{p}$, will be neglected for the reason stated previously, and represent the final momentum, $\underline{k}_2$, as:

$$\underline{k}_2 = \underline{k}_1 \pm \underline{q} \tag{129}$$

Then, Equation (128) may readily be generalized to include the emissions (+) of phonons and photons as well, and we have the general formula:

$$P_{(\pm)}^{(\pm)}\ (\underline{k}_1\rightarrow\underline{k}\ ) = \frac{e^2(\underline{E}\cdot\underline{q})^2}{4Vn^{*2}\omega^4}\ G^{(\pm)}(\underline{q})\ \delta(E_2 - E_1 \pm F_{\underline{q}} \pm \hbar\omega) \tag{130}$$

where:

$$G^{(\pm)}\ (\underline{q}) = \frac{\pi\hbar q^2 g^2}{N_p ME_{\underline{q}}} \begin{pmatrix} N(\underline{q}) + 1 \\ N(\underline{q}) \end{pmatrix} \tag{131}$$

which are proportional to the probabilities of absorption (-) and emission (+) of phonons without scattering (Wilson, 1936; Born and Huang, 1956).

Next we evaluate $\langle P_{(s)}^{(r)} \rangle$ $(r,s=\pm)$ from the relations in Equations (94) and (95). Substitution of Equation (130) into (94) gives us:

$$P_{(s)}^{(r)}(\underline{k}_1) = \sum_{k_2} \frac{e^2(\underline{E}\cdot\underline{q})^2}{2Vm^{*}\omega^4}\ G^{(r)}(q)\ \left[1-f(E_2)\right]\ \delta(E_2 - E_1 + rE_{\underline{q}} + s\hbar\omega) \tag{132}$$

The summation over the final momentum states $\underline{k}_2$ may be replaced by corresponding momentum integral,

$$\sum_{\underline{k}_2} \rightarrow \frac{V}{(2\pi)^3} \iiint (d\underline{k}_2) \ \ldots$$

$$d\underline{k}_2 = k_2^2 \, dk_2 d\Omega_2$$

$$= \frac{dE_2}{|\text{grad } E_2|} \, dS_{\underline{k}_2} : dS_{\underline{k}_2} = k^2{}_2 d\Omega_2 \tag{133}$$

In virtue of the relation, $q=\pm(\underline{k}_2-\underline{k}_1)$, the summation over $\underline{k}_2$ is equivalent to summation over the phonon momentum $\underline{q}$ and also to replacing the summation by the corresponding integral in momentum space:

$$\sum_{\underline{q}} \rightarrow \frac{V}{(2\pi)^3} \iiint (d\underline{q}) \ \ldots \tag{134}$$

At the same time, it is expedient to average over the direction of electric field with respect to $\underline{q}$.

One thus obtains:

$$P_{(s)}^{(r)}(\underline{k}_1) = \frac{c^2E^2}{48\pi^3 m^{*2}\omega^4} \int_0^{r_o} q^4 dq \int_{-1}^{+1} d\mu \, G^{(r)}(\underline{q}) \left[1-f(E_2)\right] \tag{135}$$

$$\times \delta\left(\frac{\hbar^2 q^2}{2m^*} + \frac{\hbar^2}{m^*} k_1 q\mu + rE_q + s\hbar\omega\right)$$

where we have taken $\overline{(\underline{E} \cdot \underline{q})^2} = \frac{1}{3} q^2E^2$ and $\mu=\cos\theta$, θ being the angle between the momenta, $\underline{k}_1$ and $\underline{q}$, and $E_2= E_2(\underline{k}_1 \pm \underline{q})$.

The integral over q extends from o to the maximum value q_o where q_o is determined from the Debye temperature Θ and the longitudinal phase velocity of sound u_L by the relation:

$$\hbar u_L q_o = K\Theta \tag{136}$$

where K is the Boltzmann constant. It is also determined equivalently

from the phonon number density N_p per unit volume:

$$N_p = \frac{4\pi}{3} \quad \frac{1}{(2\pi)^3} \quad q_o^3 = q_o^3 \Big/ 6\pi^2 \tag{137}$$

Here we have assumed the simple Debye dispersion of phonons. This approximation is known to be satisfactory at ordinary temperatures, such as in heat capacity calculations. The shortcomings of the Debye model of lattice appear mostly at very high temperatures where the average momentum transfer in electronic processes in considerably larger than the Debye cut-off value, and also at very low temperatures. More complete formulation of phonon dispersion is available; see, for instance, Leighton (1948) on monovalent metals and Bardeen (1937) for a more rigorous form of electron-phonon interaction involving the Umklapp processes important at very high temperatures. The work of Leighton (1948) shows that a more general treatment than Debye's model of the lattice dispersion leads to formulas which are essentially the same as those obtained from the Debye theory, except at very high temperatures. The difference is that the Debye temperature Θ is no more a constant but contains a small temperature-dependence. The deviation of Θ from the value determined from room temperature measurement of heat capacity, for instance, becomes more enhanced at lower temperatures. The temperature-dependence in Θ has also been discussed by Wilson (1936).

In general, the usual Debye temperature value $\Theta\sigma$ (notation used by Wilson) are in the same order of magnitude. It is expected, therefore, that, as long as the Debye cutoff is used as a parameter which is to be adjusted within a small margin in the neighborhood of its room temperature value, the Debye theory is satisfactory in the present formulation. Furthermore, it will be shown that various optical and infrared dispersion properties are not very sensitive to a small variation in Θ,

The delta function in Equation (135) is eliminated by integrating over μ from (-1) to (+1). The existence of a real μ such that the argument of the delta function vanishes for all q between zero and q_o, has been asserted by Wilson (1936) in his calculations of dc conductivity. That the same can be asserted in the present work involving an electromagnetic field is shown in the appendix thus.

$$P_{(s)}^{(r)}(\underline{k}_1 = \frac{e^2E^2}{24\pi^2 m^* \omega^4 h^2 k_1} \int_o^{q_o} q^3 dq \; G^{(r)}(q) \left[1 - f(E_1 - rE_q - s\hbar\omega\right] \tag{138}$$

In obtaining Equations (135) and (138), it has been assumed that $N(q)$, $E_{\underline{q}}$ and hence $G^{(r)}(q)$ depend only on the magnitude q and not on the

angular variables. The only part of Equation (132) where the dependence on the azymuthal angle appears was in $(E\cdot q)^2$ with $\underline{k}_1$ as the polar axis. The argument of f(---) in Equation (138) results from satisfying the delta function after integration over μ. Calculation of $\langle P_{(s)}^{(r)} \rangle$ proceeds by multiplying Equation (138) Fermi function $f(\mathbf{E}_1)$ and summing it up over the initial momentum state $\underline{k}_1$, and dividing the entire expression by the normalization:

$$\sum_{\underline{k}_1} f(E_1) \tag{139}$$

In these calculations, we shall assume that the Fermi energy E_f obeys the condition:

$$E_f \gg \hbar\omega, \quad KT \tag{140}$$

Thus, it is equivalently assumed that, for the frequency range that is of interest, most of the transitions take place in the neighborhood of the Fermi level, and $P_{(s)}^{(r)}(\underline{k}_1)F(E_1)$ differs from zero only in the neighborhood of $E_1 \simeq E_f$. With these assumptions being considered, the density-of-states factor $\sqrt{E_1}$ may be taken out of the integral set equal to $\sqrt{E_f}$. Then, we obtain:

$$\begin{aligned} \langle P_{(s)}^{(r)} \rangle &= \left(\sum_{\underline{k}_1} f(E_1) \right)^{-1} \times \sum_{\underline{k}_1} f(E_1) P_{(s)}^{(r)}(\underline{k}_1) \\ &\cong \frac{e^2E^2}{16\pi^2 m^* \omega^4 \hbar^2 k_o E_f} \int_o^{qo} q^3 dq \, G^{(r)}(q) F_{(s)}^{(r)}(q) \end{aligned} \tag{141}$$

where $F_{(s)}^{(r)}(q)$ is the integral:

$$F_{(s)}^{(r)}(q) = \frac{1}{\beta} \int_{-\infty}^{+\infty} dz \, \frac{e^z}{1+e^z} \cdot \frac{1}{1+e^{z+a}} \tag{142}$$

$$z = \beta(E_1 - E_f - rE_{\underline{q}} - s\hbar\omega)$$

$$a = \beta(rE_q + s\hbar\omega)$$

The integral $F_{(s)}^{(r)}(q)$ can be evaluated exactly, and we have:

$$F_{(s)}^{(r)}(q) = (rE_q + s\hbar\omega) \Big/ \left[e^{\beta(rE_q + sh\omega)} - 1 \right] \tag{143}$$

The power expenditure $\bar{W}(\omega)$ which was defined in Equation (96), can be evaluated using Equations (141) and (143) and:

$$\hbar u_L q = E_q = \hbar\omega_q \tag{144}$$

along with the Relations (136) and (137), and it is in the form:

$$\bar{W}(\omega) = \sum_{r=\pm} \frac{e^2E^2}{16\pi^2 m^* \hbar\omega^3 k_o E_f} \int_o^{q_o} q^3 dq G(r) \left[F_{(-)}^{(r)} - F_{(+)}^{(r)} \right] \tag{145}$$

We substitute $G^{(r)}$ of Equation (131) into (145) and use:

$$N(q) = 1\ e^{\beta E_q} - 1 \tag{146}$$

In order to obtain the power expenditure per unit volume, it is expedient to introduce the effective number of electrons per unit volume, n_e. After some algebraic manipulations, we finally obtain:

$$n_e \bar{W} = \frac{n_e e^2}{m^*} R \left(\frac{T}{\Theta} \right)^5 \frac{E^2}{2\omega^2} Z(\omega,T) \tag{147}$$

where R is constant given by:

$$R = \frac{9\pi^3}{2} \hbar^2 g^2 N_p \Big/ (2m^* E_f^3)^{\frac{1}{2}} MK\Theta \tag{148}$$

and $Z(\omega,T)$ is a function of both ω and T given by:

$$J(\mu,\alpha) = \frac{e^{\mu} \sinh(\mu)}{\mu} \left\{ J_5(\mu,\alpha) - \frac{(e^{\mu}-1)^2}{e^{2\mu}-1} \mu\, J_4(\mu,\alpha) - 2 \frac{(e^{\mu}-1)^2}{e^{2\mu}-1} \mu\, K_4(\mu,\alpha) \right\} \tag{149}$$

$$\mu = \left(\frac{\hbar\omega}{KT} \right) \quad ; \quad \alpha = \left(\frac{\Theta}{T} \right)$$

$$J_n(\mu,\alpha) = \int_o^\alpha y^n dy/(e^Y - e^\mu)\ (e^\mu - e^{-Y}) \tag{150}$$

$$K_n\ (\mu,\alpha) = \int_o^\alpha y^n dy/(e^Y - e\mu)\ (e\mu - e^{-Y})\ (e^Y - 1)$$

This is the basis relation from which important dispersion relations will be obtained in the succeeding parts of this chapter.

A close examination of the relations in Equations (149) and (150) reveals that z (μ,α) approaches values which are independent of μ and hence ω in the limit of $\mu \gg \alpha$ and also when $\mu \to 0$. In particular, when $\mu \to 0$, we have:

$$Z(\mu,\alpha) \sim J_5^{\,o}\ (\alpha) \tag{151}$$

where:

$$J_5^{\,o}(\alpha) = \int_o^\alpha y^5 dy/(e^Y - 1)\ (1 - e^{-Y}) = J_5(\mu,\alpha) \Big]_{\mu=0} \tag{152}$$

This is identified with Wilson's $J_5\left(\frac{\Theta}{T}\right)$, and, more important, with Grüneisen's formula (Grüneisen, 1933) for temperature-dependence of dc resistivity when we multiply by α^{-5}.

The ω-dependent quantity $Z(\mu,\alpha)$ has no precedence in the classical theories and hence constitutes an important consequence of the present theory.

For the coming discussions on dispersion properties, it is convenient to define the quantity $b_{ep}\ (\mu,\alpha)$, the subscript ep signifying the electron-phonon processes, such that:

$$b_{ep}(\mu,\alpha) = \frac{Z(\mu,\alpha)}{Z(0,\alpha)} = \frac{1}{J_5^{\,o}(\alpha)}\ Z(\mu,\alpha) \tag{153}$$

The numerical values of $b_{ep}\ (\mu,\alpha)$ can be obtained when we evaluate the values of $J_n(\mu,\alpha)$ and $K_n\ (\mu,\alpha)$ for arbitrary values of ω and T. The dc quantities $J_n^{\,o}(\alpha)$ and $K_n^{\,o}(\alpha)$ have been discussed in many references and

are available in calculable forms. All types of integrals which enter in evaluation of $b_{ep}(\mu,\alpha)$ are discussed in the appendix, and the results are given as follows (for $n > 0$):

$$J_n(\mu,\alpha) = \frac{1}{e^{2\mu}-1} \sum_{m=0}^{n} \frac{1}{m+1} \mu^{n-m} \binom{n}{m} \left[\frac{(\alpha-\mu)^{m+1}}{e^{\alpha-\mu}-1} \right.$$

$$+ (-1)^{n-m+1} \frac{(\alpha+\mu)^{m+1}}{e^{\alpha+\mu}-1} - (-1)^{m+1} (e^{\mu} + -1^{n}) \frac{\mu^{m+1}}{e^{\mu}-1}$$

$$+ J^{o}_{m+1}(\alpha-\mu) + (-1)^{n-m+1} J^{o}_{m+1}(\alpha+\mu)$$

$$\left. - (-1)^{m+2} J^{o}_{m+1}(\mu) (1 + -1^{n+1}) \right] \qquad (154)$$

$$K_n(\mu,\alpha) = \frac{1}{(e^{2\mu}-1)(e^{\mu}-1)} \left[\sum_{m=0}^{n} \frac{1}{m+1} \mu^{n-m} \binom{n}{m} \left\{ e^{\mu} (-1)^{n-m} \left[\frac{(\mu+\alpha)^{m+1}}{e^{\mu+\alpha}-1} - \frac{\mu^{m+1}}{e^{\mu}-1} \right] \right.\right.$$

$$+ e^{\mu}(-1)^{n-m} \left[J^{o}_{m+1}(\alpha+\mu) - J^{o}_{m+1}(\mu) \right] + \frac{(\alpha-\mu)^{m+1}}{e^{\alpha-\mu}-1} - (-1)^{m+1} \frac{\mu^{m+1}}{e^{-\mu}-1}$$

$$+ \left[J^{o}_{m+1}(\alpha-\mu) + (-1)^{m+1} J^{o}_{m+1}(\mu) \right] - (m+1) e^{\mu} (-1)^{n-m} \zeta_m(\alpha+\mu;\mu)$$

$$\left.\left. - (m+1) \zeta_m(\alpha-\mu;-\mu) \right\} - \frac{(1+e^{\mu})}{n+1} \frac{\alpha^{n+1}}{e^{\alpha}-1} - \frac{(1+e^{\mu})}{n+1} J^{o}_{n+1}(\alpha) \right]$$

$$- (1+e^{\mu}) \zeta_m(\alpha;0) \qquad (155)$$

where $J^{o}_{m+1}(x)$ is the same as what was defined in Equation (152) with the only difference that the upper limit α in Equation (152) is to be replaced by x, and:

$$\zeta_n\,(a;b) = \int_b^a Y^n dy e^{-y} \tag{155}$$

Numerical evaluation of the dc quantities $\left\{J_n^o\,(x)\right\}$ is considerably simplified in the limiting cases, $x \ll 1$ (high temperature) and $x \gg 1$ (low temperature).

For $x \ll 1$, we have:

$$J_m^o\,(x) \cong \int_o^x \left(y^{n-2} - \frac{7}{12}\,y^{n-2} - \frac{7}{12}\,y^n + \ldots\right) dy = \frac{}{n-1}\,x^{n-1} - \frac{7}{12(n+1}\,x^{n+1}x\ldots \tag{157}$$

and for $x \gg 1$:

$$J_n^o\,(x) \cong J_n^o\,(\infty) = n\int_o^\infty \frac{y^{n-1}\,dy}{e^y-1} = n:\sum_{r=1}^{\infty} \frac{1}{r^n} \tag{158}$$

$$(\text{e.g. } J_5^o\,(\infty) = 124.4)$$

D. CALCULATION OF ELECTRON-PHONON DAMPING COEFFICIENT

The damping coefficient which is contributed by the electron-phonon processes or the electron-phonon collision frequency as it is often called, can be obtained in a straightforward way when we compare the expression for $\langle W\rangle$ obtained in paragraph-C with the corresponding, well-known high-frequency dispersion formula which is obtained by solving Drude's equation of motion for a free conduction electron.

It is well known that the power expenditure $\langle W\rangle$ for a free electron system is related to the optical conductivity $\sigma(\omega)$ by the relation:

$$\frac{E^2\sigma(\omega)}{2} = n_e\,\langle W\rangle \tag{159}$$

where $\langle W\rangle$ is the power expenditure due to one electron per unit time and $\frac{E^2}{2}$ is the energy density of the electromagnetic field. Upon comparing Equation (159) with the expression for $\langle W\rangle$ in Paragraph C, we obtain the relation:

$$\sigma_{ep}(\omega) = \frac{1}{4\pi}\,\frac{\omega_o^2}{\omega^2}\,R_{ep}\,\frac{1}{\alpha^5}\,Z(\mu,\alpha) \tag{160}$$

where R_{ep} is a constant independent of temperature and frequency which is determined by the properties of the lattice, and:

$$\omega_o = \left(4\pi \frac{n_e e^2}{m^*}\right)^{\frac{1}{2}} \tag{161}$$

where ω_o is the frequency characteristic of the electron plasma oscillation. ω_o is generally outside the high-frequency limit of the free-electron dispersion spectrum.

At ordinary temperatures, most of the ω-dependence in Equation (160) appears through ω^2 in the denominator as in the case with the high-frequency conductivity of Drude. $Z(\mu,\alpha)$ represents a relatively small variation for changes in ω. According to Equation (151), we have $Z(\mu,\alpha) \sim J_5^o(\alpha)$ when $\mu = 0$. The last three factors in Equation (160) reproduce the well-known Grüneisen formula. It also reproduces the dc damping coefficient derived by Wilson (1936) when we identify our g and N_p with Wilson's C and Δ^{-1} in the expression for R_{ep} given by:

$$R_{ep} = \frac{9\pi^3}{2} \frac{\hbar^2 N_p g^2}{\sqrt{2m^* E_f} MK\Theta} \tag{162}$$

Thus, by making use of the relation:

$$b_{ep}(\mu,\alpha) = \frac{Z(\mu,\alpha)}{J_5^o(\alpha)} \underset{\omega \to o}{\sim} 1 \tag{163}$$

it is natural for us to identify the last three factors in Equation (160) as a damping coefficient, $\Gamma_{ep}(\mu,\alpha)$, similar to its dc equivalent Γ_{ep}^o:

$$\Gamma_{ep}^o(\alpha) = R_{ep} \frac{1}{\alpha^5} J_5^o)\alpha) \tag{164}$$

such that

$$\Gamma_{ep}(\mu,\alpha) = \Gamma_{ep}^o(\alpha)\, b_{ep}(\mu,\alpha) \tag{165}$$

and

$$\Gamma_{ep}(\mu,\alpha) \underset{\mu \to o}{\sim} \Gamma_{ep}(\alpha) \tag{166}$$

In this respect, $b_{ep}(\mu,\alpha)$ shall be named the quantum correction

factor such that:

$$\Delta\Gamma_{ep} = \Gamma_{ep}^{o}\,(b_{ep}-1) > 0 \tag{167}$$

represents the correction for $\omega > 0$.

For the sake of convenience in future applications, we write down $b_{ep}(\mu,\alpha)$ explicitly:

$$b_{ep}(\mu,\alpha) = \left[J_5^o(\alpha)\right]^{-1} \frac{e^{\mu}\sinh\mu}{\mu}\left[J_5(\mu,\alpha) - \mu\,\frac{(e^{\mu}-1)^2}{e^{2\mu}-1)}\,J_4(\mu,\alpha) - 2\mu\,\frac{(e^{\mu}-1)^2}{(e^{2\mu}-1)}\,K_4(\mu,\alpha)\right] \tag{168}$$

The optical conductivity $\sigma(\omega)$ in the form of Equation (160) applies only at $\omega^2 \gg \Gamma_{ep}$. A more general form is obtained when $(\omega^2 + \Gamma_{ep}^2)$ is substituted for ω^2 in the denominator to make it consistent with the dc properties. We thus have:

$$\sigma_{ep}(\mu,\alpha) = \frac{1}{4\pi}\,\Gamma_{ep}^{o}\,b_{ep}(\mu,\alpha)\Big/\left(\frac{\omega}{\omega_o}\right)^2 + \left(\frac{\Gamma_{ep}^{o}}{\omega_o}\right)^2 b_{ep}^2(\mu,\alpha) \tag{169}$$

which gives us the familiar expression for the dc conductivity:

$$\sigma_{ep}(\alpha) = \frac{1}{4\pi}\,\frac{\omega_o^2}{\Gamma_{ep}^{o}(\alpha)} = \frac{n_e e^2}{m^*}\,\frac{1}{\Gamma_{ep}^{o}(\alpha)} \tag{170}$$

when ω is equated to zero.

A quantity which has essentially the same physical significance as the present $b_{ep}(\mu,\alpha)$ has also been obtained by Gurzhi (1958), and is given by:

$$\Phi(\mu,\alpha) = \frac{2}{\mu}\,\frac{1}{\alpha^4}\int_0^{\alpha} dv\, v^4\left[\frac{2\mu}{e^{v}-1} + \frac{v-\mu}{e^{v-\mu}-1} - \frac{v+\mu}{e^{v+\mu}-1}\right] \tag{171}$$

$\Phi \approx 1$ when $\mu \ll \alpha \ll 1$. However, Gurzhi's formula fails to reproduce the correct temperature dependence for dc resistivity and hence for heat capacity in the limit $\mu \to 0$ for arbitrary values of α. It agrees identically with the result of the present theory when $\mu \gg \alpha$. Grüneisen's

formula for resistivity is compared with a heat capacity curve in FIGURE 15, and a good agreement is clearly shown.

A correct theory must be able to reproduce the timetested classical formulas, be they dc properties or optical properties in the classical limit, and the correction factor, such as b_{ep} in the present theory, must approach unity identically when $\mu \to 0$.

E. CORRECTIONS DUE TO ELECTRON-ELECTRON COLLISIONS AND IMPURITY SCATTERING

Contributions to infrared absorption by the processes of electron-electron collisions and impurity scattering have been investigated recently by various authors. Some of the new developments are to be found in the works of the Russian authors, Silin (1958), Pitaevskii (1958) and Gurzhi (1959). Their calculations are based on Landau's theory of Fermi liquids (1957). A metal which is commonly considered to be free of impurities in the order of 10^{-4} or less. For such a metal, the impurity contributions can be safely neglected except at very low temperatures. It is well known that even a small impurity content makes an important contribution to the dc resistivity at very low temperatures through the 'Restwiderstand" of Mathiessen. As for the impurity contributions to various infrared dispersion properties, the investigations in a following chapter revealed that, even at very low temperatures, the impurity contributions can be negligible compared with the contributions by Holstein's mechanism of bulk electron-phonon processes. This is in contrast to common expectations based on our observations of dc properties. It results from the important feature of the present theory that the frequency-dependent damping coefficient, $\Gamma_{ep}(\mu,\alpha)$, retains a large value even at very low temperatures when $\mu \gg \alpha$. On the other hand, for an ω which does not satisfy $\mu \gg \alpha$, Γ_{ep}, at $0^{\circ}K$, decreases rapidly with increase in wavelength, and thus the impurity and electron-electron collisions become important.

Similar conclusions are reached for the electron-electron processes. It will be shown that the electron-electron collisions are insignificant throughout the free electron spectrum, not only at ordinary temperatures, but also at very low temperatures for many metals. Theoretically, the electron-electron processes make more contributions at higher frequencies and at lower temperatures. Except for transition metals and some multivalent metals, the correction amounts to a small fraction of the contribution by electron-phonon processes in the high frequency region of the free electron spectrum.

Thus, the above conclusions on the significance of the two processes

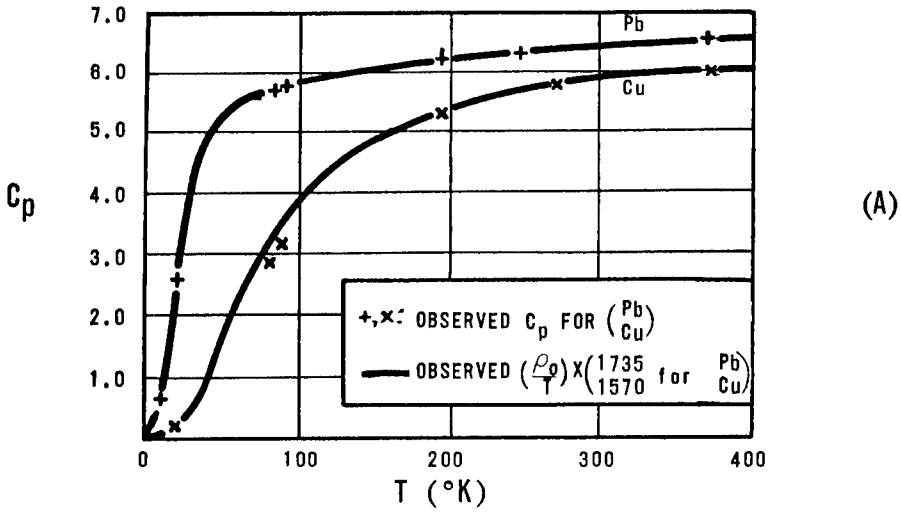

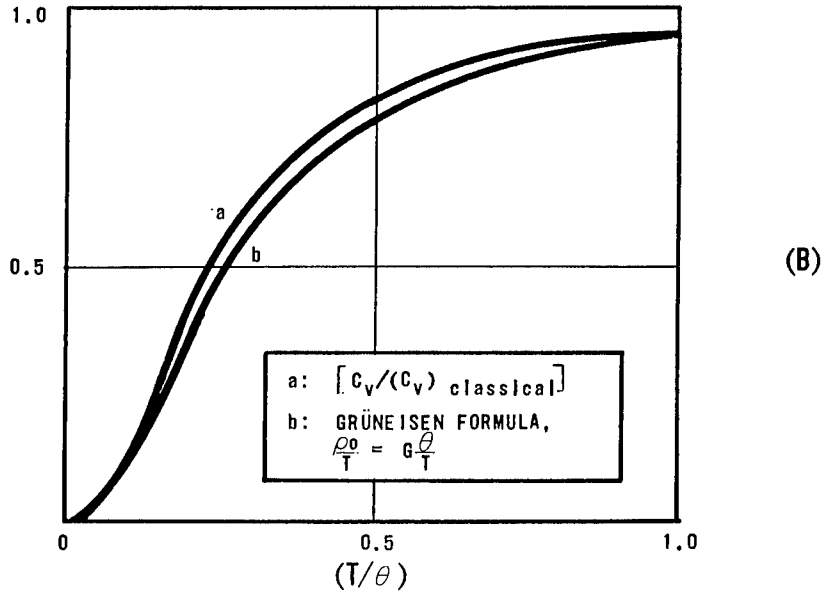

Figure 15. Temperature-Dependence of Heat Capacity and Electric Resistance

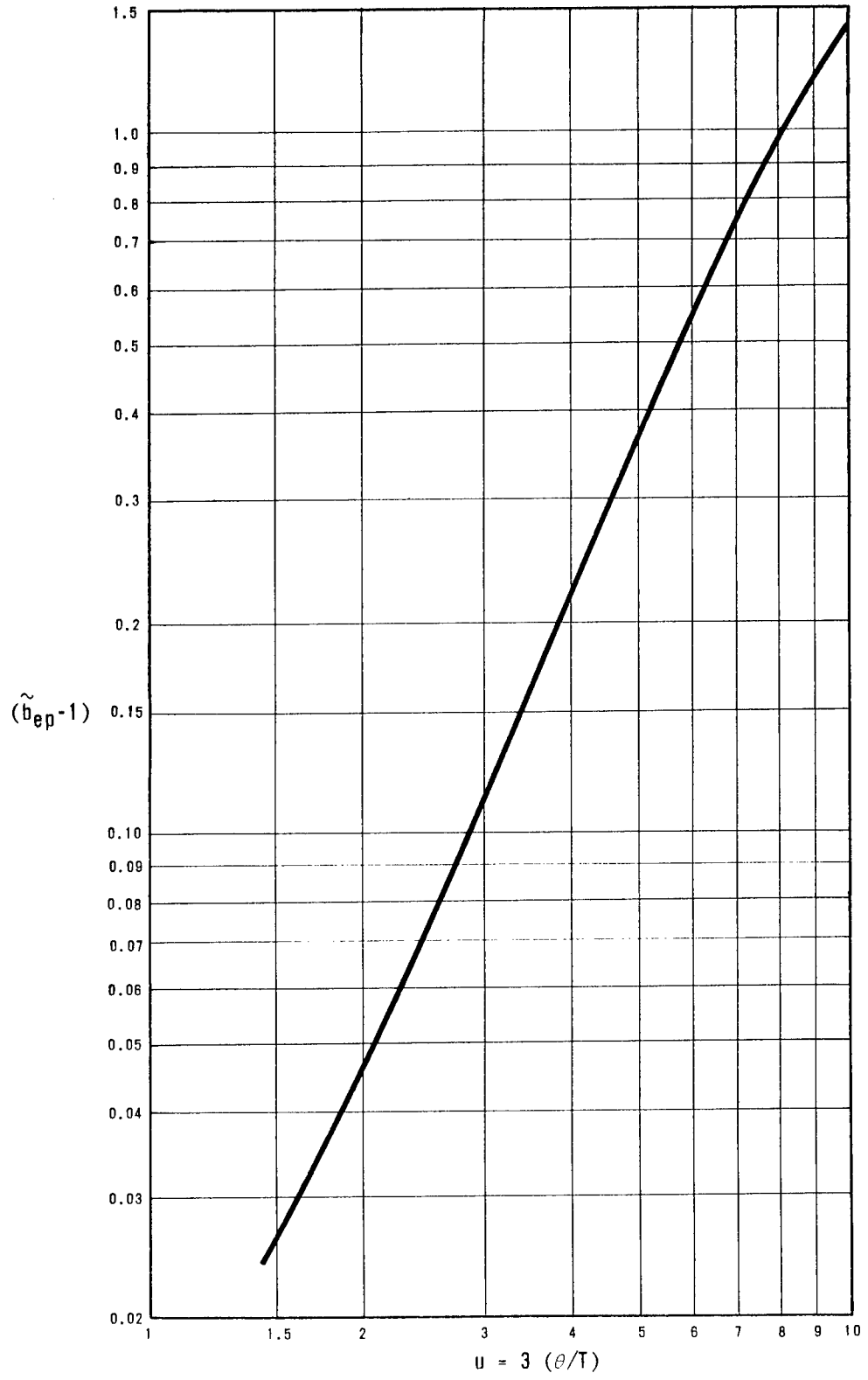

Figure 16. Quantum Correction factor versus $\frac{\theta}{T}$ at Short Wavelengths

are not in exact agreement with the suggestions by Silin (1958), Pitaevskii (1958), and Gurzhi (1959). They suggest that these two processes may be the only predominant contributions for most cases at low temperatures and in the near infrared, and may be important at room temperature as well for some metals.

For our investigations on the relative magnitudes of the contributions by the three processes, we shall use Gurzhi s formula for the electron-electron collision frequency:

$$\Gamma_{ee}(\mu,\alpha) = \Gamma_{ee}^{o}(\alpha) b_{ee}(\mu) \tag{172}$$

$$b_{ee}(\mu) = 1 + \left(\frac{\mu}{2\pi}\right)^2 \tag{173}$$

$\Gamma_{ee}^{o}(\alpha)$ is the dc damping coefficient and is well known to be proportional to $\sim T^2$.

We may write it in the form:

$$\Gamma_{ee}(\alpha) = R_{ee} \frac{1}{\alpha^2} \tag{174}$$

R_{ee} being a constant having the same dimension as Γ_{ee}^{o}. The frequency-dependent factor given by Equation (173) may be considered as a quantum correction factor in the same sense that $b_{ep}(\mu,\alpha)$ has been treated as the quantum correction factor for the electron-phonon collision frequency.

As for the impurity damping, or the electron-impurity scattering frequency as it is often called, it is sufficient to remember that it constitutes a constant, additive quantity, Γ_{M}^{o}, to the over-all damping coefficient, $\Gamma(\mu,\alpha)$, and is independent of both frequency and temperature (or nearly so). Thus, the over-all damping coefficient, with all of its quantum corrections taken into account, now takes the form:

$$\begin{aligned}\Gamma(\mu,\alpha) &= \Gamma_{ep}(\mu,\alpha) + \Gamma_{ee}(\mu,\alpha) + \Gamma_{M}^{o} \\ &= \Gamma^{o}(\alpha)\, b(\mu,\alpha)\end{aligned} \tag{175}$$

$$b(\mu,\alpha) = \frac{\Gamma_{ep}^{o}(\alpha) b_{ep} + \Gamma_{ee}^{o} b_{ee} + \Gamma_{M}^{o}}{\Gamma_{ep}^{o} + \Gamma_{ee}^{o} + \Gamma_{M}^{o}} \tag{176}$$

This is to be used in various dispersion relations where the damping coefficient appears. For the reasons that have been explained in most cases it will be satisfactory to consider only the electron-phonon term $\Gamma_{ep}(\mu,\alpha)$. For example, Γ_{ep} alone yields values of low temperature absorptivity of copper and silver at 4.2°K and $\lambda \cong 1 \sim 1.5\mu$ in excellent agreement with the observed values (up to ~ 2 percent). On the other hand, it is expected that $\Gamma_{ep}(\mu,\alpha)$ will not be sufficient to explain the observed properties of those transition and multivalent metals in which the interband transitions involve a non-zero momentum transfer. Those scattering processes which involve a momentum transfer $|\vec{k}_2 - \vec{k}_1|$ smaller than a certain non-zero minimum do not lead to interband transitions.

Finally, it may be noted that the significance of the electron-electron collision term, Γ^o_{ee}, is directly related to the presence of the Umklapp processes. In fact, it has been pointed out (Gurzhi, 1959) that the electron-electron collision term vanishes if the Umklapp process is not present. The relative importance of the Umklapp processes at low temperatures, as compared with the usual phonon mediated processes may be understood in the following manner. Consider that the average momentum transfer in electron-phonon processes decreases like $\sim \left(\frac{T}{\Theta}\right)$ and the density of phonons also decreases rapidly with decrease in the average momentum transfer. The result of these is the rapid decrease of resistivity, $\sim T^5$, as T is decreased to 0°K, while the electron-electron collisions, activated by the Umklapp processes, have the well-known $\sim T^2$-dependence in resistivity. This should, therefore, be even more true in those transition and other multivalent metals in which the interband transitions are very important. A non-zero lower limit in momentum transfer is present for such transitions.

On the other hand, except for the latter special cases, the above statement is not necessarily valid in that range of the optical or infrared spectrum where the quantum correction factor for electron-phonon processes increases sufficiently fast with decrease in temperature to compensate for decrease in the dc quantity Γ^o_{ep}. For instance, for metals, be they monovalent, multivalent, or transition metals, which involve no non-zero lower limit in momentum transfer, the quantum correction shows the temperature-dependence to be $\sim \frac{1}{T^5}$ while $\Gamma_{ep}(\alpha)$ decreases as $\sim T^5$ when $\hbar\omega \gg K\Theta \gg KT$, thus compensating each other exactly. This is an important consequence of the present theory.

F. CALCULATION OF $\epsilon(\mu,\alpha)$

In Paragraph D, we have taken $\sigma(\mu,\alpha)$ in the form:

$$\sigma = \frac{\omega_o^2}{4\pi} \frac{\Gamma}{\omega^2 + \Gamma^2} \tag{169}$$

where Γ^2 in the denominator comes from Drude's classical equation of motion for free electrons with Γ^o replaced by $\Gamma(\mu,\alpha)$. Upon solving the same equation, the expression for $\epsilon(\mu,\alpha)$ is obtained in the form:

$$\frac{1-\epsilon}{4\pi} = \frac{\omega_o^2}{4\pi} \frac{1}{\omega^2 + \Gamma^2} \tag{177}$$

where the denominator has an additional frequency-dependence, besides ω^2, coming from $b(\mu,\alpha)$ in $\Gamma(\mu,\alpha)$.

Unfortunately, unlike the classical Drude equation, Equation (177) is inconsistent with the Kramers-Kronig relation,

$$\frac{1-\epsilon}{4\pi} = -\frac{2}{\pi} \int_o^\infty \frac{\sigma(\omega')d\omega'}{(\omega'^2-\omega^2)} \tag{178}$$

We shall calculate $\epsilon(\mu,\alpha)$ from Equation (178) for both cases where (i) $\Gamma_{ep}(\mu,\alpha)$ is the only important term and (ii) $\Gamma_{ee}(\mu,\alpha)$ and Γ_M^o need be considered. In any case, an exact solution to the integral is difficult due to the complicated structure of ω-dependence in $b_{ep}(\mu,\alpha)$, and a suitable approximation method has to be used.

When $\sigma(\omega)$ contains only Γ_{ep}, we have:

$$\frac{1-\epsilon}{4\pi} = -\frac{\omega_o^2}{4\pi^2} \int_{-\infty}^{+\infty} \frac{\Gamma_{ep}^o b_{ep} d\omega'}{(\omega'^2 + (\Gamma_{ep}^o)^2 b_{ep}^2)(\omega'^2-\omega^2)}$$

$$= -\frac{\omega_o^2}{4\pi^2} \frac{1}{(\Gamma_{ep}^o)^2} \int_{-\infty}^{+\infty} \frac{b_{ep}(x)\, dx}{(x^2 + b_{ep}(x)^2)(x^2-y^2)} \tag{179}$$

where $x = \left(\frac{\omega'}{\Gamma_{ep}}\right)$ and $Y = \left(\frac{\omega}{\Gamma_{ep}}\right)$, and where we have used:

$$b_{ep}(\mu,\alpha) \equiv b_{ep}(-\mu,\alpha) \tag{180}$$

In order to investigate the property of $(1-\epsilon)$ in the two extreme limits, $\omega^2 \gg (\Gamma^o_{ep})^2$ and $\omega \to 0$, we use the relation:

$$\frac{1}{(x^2+b^2)(x^2-Y^2)} = \frac{(-1)}{(Y^2+b^2)}\left[\frac{1}{x^2+b^2} - \frac{1}{x^2-Y^2}\right]$$

and we have:

$$\frac{1-\epsilon}{4\pi} = \frac{\omega_o^2}{4\pi^2}\,\frac{1}{(\Gamma^o_{ep})^2}\left[\int_{-\infty}^{+\infty} \frac{b(x)\,dx}{(y^2+b^2)(x^2+b^2)} - \int_{-\infty}^{+\infty} \frac{b(x)\,dx}{(x^2-y^2)(y^2+b^2)}\right] \tag{181}$$

where the subscript ep has been dropped for convenience, and b^2's appearing in the integrand are all functions of x and not of y.

Before attempting to solve Equation (181), it may be remembered that $b_{ep}(x)$ is a very slowly varying function of x throughout the entire spectral range except when the temperature is such as to give $1 \ll \mu \ll \alpha$ in the very far infrared, and that $b_{ep}(\mu,\alpha)$ is $\sim 0(\underline{1})$, being always greater than unity for $\omega > 0$.

In the limit of $\mu \gg \alpha$, Equation (181) now becomes:

$$\frac{1-\epsilon}{4\pi} = \frac{\omega_o^2}{4\pi}\,\frac{\tilde{\delta}_{ep}}{\omega^2} \tag{182}$$

where:

$$\tilde{\delta}_{ep} = \frac{1}{\pi}\int_{-\infty}^{+\infty} \frac{b(x)}{(x^2+b^2)}\,dx = \frac{8}{\omega_o^2}\int_0^{\infty} \sigma(\omega)\,d\omega \tag{183}$$

In obtaining Equation (183), it was assumed that $b(x) \equiv b(-x)$ and that b(x) does not have a singularity in the complex x-plane.

We notice in Equation (183) that, when $\sigma(\omega)$ satisfies the sum rule:

$$\frac{2}{\pi}\int_0^{\infty} \sigma(\omega)\,d\omega = \frac{\omega_o^2}{4\pi} \tag{184}$$

we simply have $\tilde{\delta}_{ep} = 1$.

In the limit of $\mu \ll 1$, we obtain from Equation (181)

$$\frac{1-\epsilon_o}{4\pi} = \frac{\omega_o^2}{4\pi} \frac{1}{(\Gamma_{ep})^2} \frac{\tilde{\delta}_{ep}}{\bar{\beta}^2} \tag{185}$$

where:

$$\frac{\tilde{\delta}_{ep}}{\bar{\beta}^2} = \frac{1}{\pi} \underset{\eta \approx 0}{\left(\int_{-\infty}^{+\infty} \frac{dx\, b(x)}{(\eta + b^2)(x^2 + b^2)} - \int_{-\infty}^{+\infty} \frac{dx\, b(x)}{(x^2 - \eta)(\eta + b^2)} \right)} \tag{186}$$

The presence of η in the integrands implies that, in solving the integrals by a contour in complex x-space the zeros of b (x) must be taken as the zeros of the integrands and not as singularities of the integrands, for all $/\!\!>> \eta > 0$. In this case, it is easily shown that the second integral vanishes, and we have:

$$\frac{\tilde{\delta}_{ep}}{\bar{\beta}^2} = \frac{1}{\pi} \left(\int_{-\infty}^{+\infty} \frac{dx\, b(x)}{(x^2 + b^2)(b^2 + \eta)} \right) / \!\!>> \eta > 0 \tag{187}$$

The integrand is taken to vanish at the zeros of b(x).

Upon comparing Equations (182) and (185), we construct one possible form of $(1-\epsilon)$, namely:

$$\frac{1-\epsilon}{4\pi} = \frac{\omega_o^2}{4\pi} \frac{\delta_{ep}}{\omega^2 + (\Gamma_{ep})^2 \bar{\beta}^2} \tag{188}$$

where δ_{ep} and $\bar{\beta}$ may or may not depend on ω, and if δ_{ep} is independent of ω, we simply have:

$$\delta_{ep} = \tilde{\delta}_{ep} = 1 \tag{189}$$

Taking δ_{ep} and β^2 to be independent of ω is essentially equivalent to evaluating the integral (28) by replacing b^2 of denominator by a parameter $\bar{\beta}^2$. In fact, such an approximation is reasonably well justified for $b_{ep}(x)$ is a very slowly varying function of ω for all $-\infty < x < +\infty$, except for

the case of $1 \lesssim \mu \ll \alpha$ (which can occur at very low temperature and in the very far infrared limit). The parameter which best approximates the integrand may be found by a successive approximation, solving the identity equation:

$$\bar{\beta}\,(\alpha) = b_{ep}\,(i\,\bar{\beta}\mu_o,\ \alpha) \qquad (190)$$

$$: \mu_o = \left(\frac{\Gamma^o_{ep}}{KT}\right)$$

where $\bar{\beta}(\alpha)$ is independent of ω.

By such an approximation, Equation (179) is readily solved, and we obtain:

$$\frac{1-\epsilon}{4\pi} \cong \frac{\omega_o^2}{4\pi} \quad \frac{1}{\omega^2 + (\Gamma^o_{ep})^2\,\beta^2} \qquad (191)$$

which applies to all temperatures and ω's except for the case of $1 \ll \mu \ll \alpha$ in which b_{ep} can be a very rapidly varying function of ω, although the over-all magnitude of $(\Gamma^o_{ep}\, b_{ep})$ is generally very small.

It is seen that Equation (191) is identical with Equation (188) when we put $\delta_{ep} = 1$ and take $\bar{\beta}$ as a frequency-independent parameter. Further, the sum rule Equation (184) is automatically satisfied.

The said statement that $b_{ep}(x)$ has zeros but no singularities in the complex x- or $\bar{\mu}$-plane can be understood upon examining the complete expression of $b_{ep}(\bar{\mu},\alpha)$ in the complex $\bar{\mu}$-plane. From Paragraph C, we have the following expression for $b_{ep}(\bar{\mu})$:

$$b(\bar{\mu}) = b^I(\bar{\mu}) + i\,b^{II}(\bar{\mu})$$

$$\bar{\mu} = \mu_1 + i\mu_2$$

$$b^I(\bar{\mu}) = \tfrac{1}{2}\left[\frac{\left(\mu_1(e^{2\mu_1}\cos 2\mu_2 - 1) + \mu_2 e^{2\mu_1}\sin 2\mu_2\right)}{\mu_1^2 + \mu_2^2}\right]\left\{J_5^I\,(\bar{\mu})\right.$$

$$+ J_5^{II}(\bar{\mu}) \quad \frac{\left[\mu_2 (e^{2\mu_1}\cos 2\mu_2 - 1) - \mu_1 e^{2\mu_1} \sin 2\mu_2\right]}{\left[\mu_1 (e^{2\mu_1}\cos 2\mu_2 - 1) + \mu_2 e^{2\mu_1}\sin 2\mu_2\right]} \Bigg\}$$

$$- \Big((e^{\mu_1}\cos\mu_2 - 1)^2 - e^{2\mu_1}\sin\mu_2 \Big) \Big\{ J_4^I(\bar{\mu}) + 2K_4^I(\bar{\mu})$$

$$+ \frac{2e^{\mu_1}\sin\mu_2 \,(e^{\mu_1}\sin\mu_2 - 1)}{\left[(e^{\mu_1}\cos\mu_2 - 1)^2 - e^{2\mu_1}\sin\mu_2\right]}$$

$$\times \Big(J_4^{II}(\bar{\mu}) + 2K_4^{II}(\bar{\mu}) \Big) \Big\} \Big] \tag{192}$$

where we have put:

$$J_n(\bar{\mu},\alpha) = J_n^I(\bar{\mu}) + i\, J_n^{II}(\bar{\mu})$$

$$K_n(\bar{\mu},\alpha) = K_n^I(\bar{\mu}) + i\, K_n^{II}(\bar{\mu})$$

$$J_n^I(\bar{\mu}) = J_n^I(-\bar{\mu}) = \int_o^\alpha y^n dy \, \frac{\left[(e^y + e^{-y})e^{\mu_1}\cos\mu_2 - e^{2\mu_1}\cos 2\mu - 1\right]}{D(\bar{\mu},y)}$$

$$J_n^{II}(\bar{\mu}) = -J_n^{II}(\bar{\mu}) = \int_o^\alpha y^n dy \, \frac{\left[e^{2\mu_1}\sin 2\mu_2 - (e^y + e^{-y})e^{\mu_1}\sin\mu_2\right]}{D(\bar{\mu},y)}$$

$$K_n^I(\bar{\mu}) = K_n^I(-\bar{\mu}) = \int_o^\alpha y^n dy \, \frac{\left[(e^y + e^{-y})e^{\mu_1}\cos\mu_2 - e^{2\mu_1}\cos\mu_2 - 1\right]}{(e^y - 1)\, D(\bar{\mu},y)}$$

$$K_n^{II}(\bar{\mu}) = K_n^{II}(-\bar{\mu}) = \int_o^\alpha y^n dy \, \frac{\left[e^{2\mu_1}\sin 2\mu_2 - (e^y + e^{-y})e^{\mu_1}\sin\mu_2\right]}{(e^y - 1)\, D(\bar{\mu},y)} \tag{193}$$

where:

$$D(\bar{\mu},y) = \left[(e^{y}-e^{\mu_1}\cos\mu_2)^2+ e^{2\mu_1}\sin^2\mu_2\right]$$

$$\times \left[(e^{\mu_1}\cos\mu_2 - e^{-y})^2 + e^{2\mu_1}\sin^2\mu_2\right] \qquad (194)$$

Similarly, the expression for $b^{II}(\bar{\mu})$ is obtained upon replacing (J_n^I, K_n^I) and (J_n^{II}, K_n^{II}) by (J_n^{II}, K_n^{II}) and $(-J_n^I, + K_n^I)$, respectively.

A detailed study of the Expressions (192) and (193) shows that $b(\bar{\mu})$ has no singularity, but has an infinite number of zeros on the real axis of the μ-plane at

$$\mu = \pm i \frac{n}{2}\pi$$
$$n = 1, 2, 3, \ldots. \qquad (195)$$

This implies that in obtaining the solution in Equation (191), we must make sure that only those values of $\bar{\beta}$ which meet the condition:

$$\mu_o\bar{\beta} + \frac{n}{2}\pi \qquad (196)$$
$$: n = 1, 2, 3, 4, \ldots.$$

are considered. We further notice, in Equation (190) which defines $\bar{\beta}$, that any $\bar{\beta}$ which is found from Equation (190) satisfies the condition in Equation (196) automatically. The solution to Equation (190) is obtained upon putting $\mu_1 = 0$ and $\mu_2 = \mu_o\bar{\beta}$ into Equations (192) and (193). We thus have:

$$\bar{\beta}(\alpha) = b_{ep}(i\mu_o\bar{\beta})$$

$$= \frac{1+\sin^2(\mu_o\bar{\beta})}{\mu_o\bar{\beta}\ J_5^{o}(\alpha)}\left[\tan(\mu_o\beta)\ J_5^{I}(\mu_o\bar{\beta})\right.$$

$$\left. + (\mu_o\bar{\beta})\ \frac{1-\cos(\mu_o\bar{\beta})}{\cos(\mu_o\bar{\beta})}\left(J_4^{I} + 2K_4^{I}\right)\right] \qquad (197)$$

where we have used the relation:

$$\frac{J_n^{II}(i\mu_o\bar{\beta})}{J_n^{I}(i\mu_o\bar{\beta})} = \frac{K_n^{II}(i\mu_o\bar{\beta})}{K_n^{I}(i\mu_o\bar{\beta})} = -2\tan(\mu_o\bar{\beta}) \tag{198}$$

and:

$$J_n^{I}(i\mu_o\bar{\beta}) = \int_o^{\alpha} \frac{y^n dy\left[(e^y-\cos\mu_o\bar{\beta})(\cos\mu_o\bar{\beta}-e^{-y}) + \sin^2(\mu_o\bar{\beta})\right]}{\left[(e^y-\cos\mu_o\bar{\beta})^2+\sin^2\mu_o\bar{\beta}\right]\left[\cos\mu_o\bar{\beta}-e^{-y})^2 + \sin^2(\mu_o\bar{\beta})\right]}$$

$$K_n^{I}(i\mu_o\bar{\beta}) = \int_o^{\alpha} \frac{y^n dy\,[---]}{(e^y-1)\,[---]\,[---]} \tag{199}$$

Evaluations of $\bar{\beta}(\alpha)$ in the two limiting cases, $\alpha \gg 1$ and $\alpha \ll 1$, are simplified considerably.

In the limit $\alpha \gg 1$, we have:

$$J_n^{I} \cong \cos(\mu_o\bar{\beta})n!\left[1-\sum_{m=1}^{\infty}\frac{m}{(m+2)^{n+1}}\cos^{m+1}(\mu_o\bar{\beta})\right] \tag{200}$$

$$K_n^{I} \cong n!\cos(\mu_o\bar{\beta})\left[\frac{1}{2^{n+1}}+\frac{1}{3^{n+1}}+\sum_{m=2}^{\infty}\frac{1}{(m+2)^{n+1}}\left(1-\sum_{s=1}^{m-1}s\cos^{s+1}(\mu_o\bar{\beta})\right)\right]$$

For n=4 and n=5, it is safe to take only the first terms of Equation (200), and we have:

$$J_5^{I} \sim 120\cos(\mu_o\bar{\beta}) \quad ; \quad J_4^{I} \sim 24\cos(\mu_o\bar{\beta})$$

$$K_4^{I} \sim \frac{3}{4}\cos(\mu_o\bar{\beta}) \tag{201}$$

$$J_5^{o} \sim 124$$

On the other hand, in the limit $\alpha \ll 1$, it easily follows that:

$$I_n^{I} \cong \frac{\alpha^{n+1}}{8(n+1)}\frac{\cos(\mu_o\bar{\beta})}{\sin^4\left(\frac{\mu_o\bar{\beta}}{2}\right)}$$

$$K_n^I \simeq \frac{\alpha^n}{8n} \frac{\cos(\mu_o\bar{\beta})}{\sin^4\left(\frac{\mu_o\bar{\beta}}{2}\right)} \qquad (202)$$

$$: \mu_o\bar{\beta} \neq \frac{m\pi}{2} \quad (m = 0, 1, 2, \ldots)$$

$$J_5^o \simeq \frac{1}{4}\alpha_4$$

Thus, the identity Equation (197) is reduced to the following two corresponding to the limits, $\alpha \gg 1$ and $\alpha \ll 1$, respectively.

$$\frac{(\mu_o\bar{\beta})^2}{\mu_o} \cong (1 + \sin^2\mu_o\bar{\beta})\left[\sin(\mu_o\bar{\beta}) + \frac{(\mu_o\bar{\beta})}{2}(1-\cos\mu_o\bar{\beta})\right] \qquad (203)$$

$$\frac{(\mu_o\bar{\beta})^2}{\mu_o} \cong \frac{(1+\sin^2\mu_o\bar{\beta})}{4\sin^4\left(\frac{\mu_o\beta}{2}\right)}\left[\frac{1}{3}\alpha^2\sin(\mu_o\bar{\beta}) + \frac{\mu_o\bar{\beta}}{}(1-\cos\mu_o\bar{\beta})\right] \qquad (204)$$

These equations are in a numerically solvable form provided that we know the value of μ_o and hence $\Gamma_{ep}^o(\alpha)$. The solutions to these equations may be obtained with the help of our formula for $\Gamma_{ep}^o(\alpha)$. According to Equation (164) it is seen that:

$$\mu_o \sim \frac{1}{\alpha^4} \ll 1 \qquad (205)$$

in the limit $\alpha \gg 1$, and the only possible solution to Equation (203) exists when $(\mu_o\bar{\beta}) \ll 1$. Thus we find:

$$\bar{\beta} \approx 1 \quad : \alpha \gg 1 \qquad (206)$$

On the other hand, if $\alpha \ll 1$ (high temperature), Equation (164) tells us that $\Gamma_{ep}^o \sim T$ and $\mu_o \sim$constant such that:

$$\mu_o \sim 0\ (1)$$

According to Equation (187), b(x) and $\bar{\beta}$ are $\sim 0\ (1)$. We thus find, from Equation (204):

$$\bar{\beta} \approx \frac{1 + \sin^2(\mu_o \bar{\beta})}{4\sin^2\left(\frac{\mu_o \bar{\beta}}{2}\right)} : \alpha \ll 1 \qquad (207)$$

where $(\mu_o \bar{\beta}) \sim 0\ (1) < \frac{\pi}{2}$.

According to the result shown in Equation (206), the denominator in the dispersion formula for $(1-\epsilon)$ is to be taken as:

$$\left(\frac{1}{\omega^2 + (\Gamma^o_{ep})^2}\right) \qquad (208)$$

when $\alpha \gg 1$, while that of $\sigma(\omega)$ is to be taken as:

$$\frac{1}{\omega^2 + (\Gamma^o_{ep})^2 (\tilde{b})^2} \qquad (209)$$

with $\tilde{b} > 1$.

In the forthcoming applications of the theory to practical cases, we shall in general take $\bar{\beta}$ as a temperature-dependent parameter to be determined by fitting theoretical equations to experimental curves, while b_{ep} is calculated theoretically.

G. CALCULATION OF $\epsilon(\mu,\alpha)$ WITH THE ELECTRON-ELECTRON COLLISIONS AND IMPURITY EFFECTS TAKEN INTO ACCOUNT

We have thus far considered only the part of dispersion which is contributed by the bulk electron-phonon processes. For a more general calculation of $\epsilon(\mu,\alpha)$, we must use the Equations (175) and (176) in the Kramers-Kronig relation. Aside from this, the calculational procedure is similar to that of paragraph E.

For the sake of convenience, we define the following notations.

$$\bar{\Omega}_o(\alpha) = \left(\Gamma^o_{ep}\,\beta_{ep} + \Gamma^o_{ee} + \Gamma^o_M\right) \; ; \; \Omega_o = \left(\Gamma^o_{ep}\, b_{ep} + \Gamma^o_{ee} + \Gamma^o_M\right)$$

$$\left[\Omega_{ee}(\alpha)\right]^{-1} = \left(\frac{\hbar\beta}{2\pi}\right)^2 \Gamma^o_{ee}(\alpha) \qquad (210)$$

$$\bar{\Omega}_{\pm}^{2} = -\tfrac{1}{2}\ \Omega_{ee}^{2}\ \left[\ 1 + 4\ \frac{\Omega_o}{\Omega_{ee}}\ \right]^{\frac{1}{2}}\ \pm\left[\ 1 + 2\ \frac{\Omega_o}{\Omega_{ee}}\ \right]$$

Then, the dispersion denominator in $\sigma(\mu,\alpha)$ can be put into the form:

$$(\omega^2 + \Gamma^2) = \frac{(\omega^2 + \bar{\Omega}_{+}^{2})\ \ (\omega^2 + \bar{\Omega}_{-}^{2})}{\Omega_{ee}^{2}} \tag{211}$$

and we have:

$$\sigma(\mu,\alpha) = \frac{\omega_o^2}{4\pi}\ \ \frac{\Omega_{ee}\left(\ \Omega_o(\omega) + \dfrac{\omega^2}{\Omega_{ee}}\right)}{(\omega^2 + \Omega_{+}^{2})\ \ (\omega^2 + \Omega_{-}^{2})} \tag{212}$$

where Ω's without bars represent quantities of Equation (210) with $\bar{\beta}_{ep}$ replaced by $b_{ep}(\mu,\alpha)$, where $\bar{\beta}_{ep}$ is a temperature-dependent but frequency-dependent parameter similar to $\bar{\beta}$ assumed in Paragraph E. A close examination of $\bar{\Omega}_{\pm}$ in Equation (210) shows that:

$$\bar{\Omega}_{\pm}\ ,\ \ \Omega_{\pm}\ > 0 \tag{213}$$

In solving the Kramers-Kronig relation, we shall again use $\bar{\beta}_{ep}$ in place of b_{ep} in the denominators. This approximation is just as much valid as the same approximation that was adopted in paragraph E. Then we have:

$$\begin{aligned}\frac{1-\epsilon}{4\pi} &= -\frac{\omega_o^2}{4\pi}\ \Omega_{ee}^{2}\int_{-\infty}^{+\infty} d\omega'\ \ \frac{\left(\ \Omega_o(\omega') + \dfrac{\omega'^2}{\Omega_{ee}}\ \right)}{\omega'^2 + \Omega_{+}^{2})(\omega'^2 + \Omega_{-}^{2})(\omega'^2 - \omega^2)} \\ &\approx -\frac{\omega_o^2}{4\pi}\ \ e_{e}^{2}\int_{-\infty}^{+\infty} d\omega'\ \ \frac{\left(\ \Omega_o\ (\omega') + \dfrac{\omega'^2}{\Omega_{ee}}\ \right)}{(\omega'^2 + \Omega^2)\ \ (\omega'^2 + \Omega^2)(\omega'^2 - \omega^2)}\end{aligned} \tag{214}$$

This may be solved by taking the contour integral in the upper half of the complex ω'-plane enclosing the poles on the Im-axis at $\omega' = +i\ \Omega_{+}$ and $+i\ \Omega_{-}$, the semi-circular arc extending from $\omega' = +\infty$ to $+i\infty$ and then to $-\infty$, and the contour being indented above the real points at $\omega' = \pm\ \omega$

We thus obtain:

$$\frac{1-\epsilon}{4\pi} \approx \frac{\omega_o^2}{4\pi} \quad \frac{\Omega_{ee}^2}{\left(\bar{\Omega}_+^2 - \bar{\Omega}_-^2 \right)}$$

$$\times \left[\frac{\left(\frac{\Omega_o \left[i\Omega_- \right]}{\Omega_-} - \frac{\bar{\Omega}_-}{\Omega_{ee}} \right)}{\omega^2 + \bar{\Omega}_-^2} - \frac{\left(\frac{\Omega_o \left[i\,\bar{\Omega}_- \right]}{\bar{\Omega}_+} - \frac{\Omega_+}{\Omega_{ee}} \right)}{\omega^2 + \bar{\Omega}_+^2} \right] \tag{215}$$

In general, we have:

$$\frac{\Omega_o}{\Omega_{ee}} \ll 1 \; ; \quad \frac{\omega}{\Omega_{ee}} \ll 1 \tag{216}$$

for all ω in the free electron region of spectrum, and thus:

$$\bar{\Omega}_\pm \cong \left(\frac{\Omega_{ee}}{\bar{\Omega}_o} \right) \tag{217}$$

$$\left(\Omega_+^2 - \Omega_-^2 \right) \cong \Omega_{ee}^2$$

so that Equation (215) can be reduced to the form:

$$\frac{1-\epsilon}{4\pi} \approx \frac{\omega_o}{4\pi} \quad \frac{1}{\omega^2 + \bar{\Omega}_o^2} \; ; \quad \frac{\Omega_o(i\,\Omega_o)}{\bar{\Omega}_o} = 1 \tag{218}$$

where Ω_o $(i\Omega_o)$ is real since b_{ep} $(ix) = b_{ep}$ $(-ix)$ and the parameter $\bar{\beta}_{ep}$ is found from the identity equation:

$$\bar{\beta} = b_{ep}\,(i\zeta) \tag{219}$$

$$\zeta = h\bar{\beta}(\Gamma_{ep}^o\,\bar{\beta} + \Gamma_{ee}^o + \Gamma_M^o)$$

which becomes identical to Equation (197) in Section IV Paragraph F when Γ_{ee}^o and Γ_m^o are small compared with the electron-phonon contribution. We found

previously that, at low temperatures ($\alpha, \gg 1$), we have:

$$\Gamma^{o}_{ep} \ll 1 \quad ; \quad \bar{\beta}_{ep} \approx 1 \tag{220}$$

while $\Gamma^{o}_{ee}(\alpha)$ decreases relatively slowly, like $\sim T^2$, as T is decreased and Γ^{o}_{M} is the constant, "Restwiderstand" term, so that, in this limit:

$$\zeta \cong \hbar \beta (\Gamma^{o}_{ee} + \Gamma^{o}_{M}) = \zeta_o \tag{221}$$

independent of $\bar{\beta}$. Therefore, fortunately enough, we need not be concerned with evaluating $\bar{\beta}$ at all at low temperatures and $(1-\epsilon)$ is simply given by:

$$\frac{1-\epsilon}{4\pi} \approx \frac{\omega_o^2}{4\pi} \quad \frac{1}{\omega^2 + (\Gamma^{o}_{ee} + \Gamma^{o}_{M})^2} : \alpha \gg 1 \tag{222}$$

On the other hand, at not too low temperatures, Γ^{o}_{ee} and Γ^{o}_{M} are both much smaller than $\Gamma^{o}_{ep}\,\bar{\beta}$ so that the expression for $(1-\epsilon)$ is nearly the same as that obtained in paragraph F.

Similarly, the properties indicated in Equation (216) enable us to write down σ in a reduced form:

$$\sigma = \frac{\omega_o^2}{4\pi} \quad \frac{\Omega_o(\mu,\alpha)}{\omega^2 + [\Omega_o(\mu,\alpha)]^2} \left(1 + \frac{\omega^2}{\Omega_o \Omega_{ee}} \right) \tag{223}$$

which is to be applied whenever Equation (108) is applicable.

It must be remembered that the electron-phonon part of $\Omega_o(\mu,\alpha)$ in Equation (223) is not necessarily smaller than $(\Gamma^{o}_{ee} + \Gamma^{o}_{M})$ because $b_{ep}(\mu,\alpha)$, instead of $\bar{\beta}$, is multiplied to $\Gamma^{o}_{ep}(\alpha)$ in Ω_o. In fact, it is found that the rapid decrease of Γ^{o}_{ep} (i.e., like $\sim T^5$) with decrease in T is exactly compensated by the $\sim \frac{1}{T^5}$ - dependence of $b_{ep}(\mu, \alpha)$ in certain parts of the free electron spectrum.

SECTION V. ABSORPTIVITY, REFLECTIVITY, OPTICAL SIZE OF CONDUCTION ELECTRONS, AND OTHER PROPERTIES OF METALS

A. BASIC FORMULAS FROM SECTION IV

The formulas for optical conductivity, $\sigma(\omega)$, and dielectric constant, $\epsilon(\omega)$, were obtained in the preceding section, first by considering the contribution of only the electron-phonon processes, and second, for the more general case where electron-electron collisions and impurity scattering also need to be taken into account.

In the applications that follow, we shall use the general formulae obtained for the second case.

When the quantity $\left(\frac{\omega^2}{\Omega_{ee}^2}\right)$ is not neglected, the expression for $\sigma(\omega)$ and $\epsilon(\omega)$ take the form:

$$\sigma(\omega) = \frac{\omega_o^2}{4\pi} \frac{\Omega_o^2}{\Omega_1^2} G\sigma\ (\omega) \tag{224}$$

$$\left[1-\epsilon\ (\omega)\right] = \frac{\omega_o^2}{\Omega_2^2} G_\epsilon\ (\omega) \tag{225}$$

where:

$$\Omega_1^2 = \omega^2 + \Omega_o^2$$

$$\Omega_2^2 = \omega^2 + \bar{\Omega}_o^2$$

$$G_\sigma(\omega) = \frac{1 + \frac{\omega^2}{\Omega_o\, \Omega_{ee}}}{1 + \left(\frac{\omega}{\Omega_{ee}}\right)^2}$$

$$G_\epsilon\ (\omega) = \frac{1 + 2\left(\frac{\omega}{\Omega_{ee}}\right)^2}{1 + \left(\frac{\omega}{\Omega_{ee}}\right)^2} \tag{226}$$

$$\Omega_o = \Gamma_{ep}^o\ (\alpha)\ b_{ep}\ (\mu,\alpha) + \Gamma_{ee}^o\ (\alpha) + \Gamma_M^o$$

$$\bar{\Omega}_o = \Gamma^o_{ep}(\alpha)\ \bar{\beta}_{ep}\ (\alpha) + \Gamma^o_{ee}(\alpha) + \Gamma^o_M$$

The multiplicative factors, G_σ and G_ϵ, are corrections due to electron-electron collisions and, in general, are of the order of unity. The entire temperature-dependence in Equations (224) and (225) appears only through Ω_o and $\bar{\Omega}_o$. Only Ω_o shows frequency dependence through the term $b_{ep}(\mu,\alpha)$. The Equations (224) and (225) are more general than Equations (223) and (218), since the latter two neglect $\left(\frac{\omega}{\Omega_{ee}}\right)^2$ which is small compared to unity. In general, $\left(\frac{\omega}{\Omega_{ee}}\right)^2$ is small compared to unity throughout the entire free-electon spectrum (i.e., $\lambda \gtrsim 0.5 \sim 1.0\ \mu$) for all temperatures, so that:

$$G_\epsilon(\omega) \approx 1 \qquad (227)$$

$$G_\sigma(\omega) \approx \left(1 + \frac{\omega^2}{\Omega_o\ \Omega_{ee}}\right)$$

In order to justify this statement, let us compute $\left(\frac{\omega}{\Omega_{ee}}\right)^2$ for a metal which shows a relatively large contribution of electron-electron collisions, and see at what wavelength the relations of Equation (227) are not valid. For this purpose, we write $\Gamma^o_{ee}(\alpha)$ as:

$$\Gamma^o_{ee}(\alpha) = R_{ee}\ \frac{1}{\alpha^2} \qquad (228)$$

where R_{ee} is independent of both T and ω. Then, we have:

$$\left(\frac{\omega}{\Omega_{ee}}\right)^2 = \frac{3.84 \times 10^{-18}}{\lambda^2}\left(\frac{R_{ee}}{\Theta^2}\right) \qquad (229)$$

$$\because \lambda = \frac{2\pi c}{\omega}\ (\mu)$$

For most metals, the values of R_{ee} range from $\sim 10^{10}$ sec^{-1} to $\sim 10^{12}$ sec^{-1} while Θ is of the order of $\sim 10^2$ (°K). Therefore, for $\Theta = 300$°K $R_{ee} = 10^{12}$ sec^{-1}, the wavelength which gives $\left(\frac{\omega^2}{\Omega^2_{ee}}\right) \approx 0.1$ (~10 percent correction) is found as $0.2 \sim 0.3\ \mu$, which is already outside the free

electron region of the spectrum. On the other hand, $\left(\frac{\omega^2}{\Omega_o \Omega_{ee}}\right)$ is not necessarily small, since we have $\left(\frac{\omega}{\Omega_o}\right) \gg 1$ in the near infrared.

In order to predict values of various dispersion properties such as the optical constants, absorptivity and reflectivity, etc., at different temperatures by knowing the values of these quantities at one temperature, it is sufficient to specify the temperature-dependence of Ω_o and $\bar{\Omega}_o$ in addition to the values of the constant parameters entering in Ω_o, $\bar{\Omega}_o$ and Ω_{ee}. At not too low temperatures, Ω_o and $\bar{\Omega}_o$ reduce to:

$$\begin{aligned} \Omega_o &\approx \Gamma_{ep}^{o}(\alpha)\, b_{ep}(\mu,\alpha) \\ \bar{\Omega}_o &\approx \Gamma^{o}(\alpha)\, \bar{\beta}_{ep}(\alpha) \end{aligned} \tag{230}$$

where $\bar{\beta}_{ep}(\alpha)$ and $b_{ep}(\mu,\alpha)$ are given by Equations (197) and (168) respectively, and $\Gamma_{ep}^{o}(\alpha)$ is given by:

$$\Gamma_{ep}^{o}(\alpha) = R_{ep} \frac{1}{\alpha^5} J_5^o(\alpha) \tag{231}$$

In particular, for $\mu = \left(\frac{\hbar\omega}{KT}\right) \gg \alpha = \left(\frac{\Theta}{T}\right)$, we have:

$$b_{ep}(\mu,\alpha) \approx \tilde{b}_{ep}(\alpha) = \frac{1}{5J_5^o(\alpha)}\left[J_5^{o}(\alpha) + \tfrac{1}{2}\alpha^5 + \alpha^5 \frac{1}{e^{(\alpha)} - 1} \right] \tag{232}$$

This relation applies in the spectral range of $\lambda \lesssim 10\ \mu$. At very low temperatures ($\alpha \gg 1$), we may use

$$\begin{aligned} \bar{\Omega}_o &\approx \left(\Gamma_{ee}^{o}(\alpha) + \Gamma_M^{o}\right) \quad ; T > 0 \\ &\approx \Gamma_M^{o} \quad ; T \cong 0 \\ \Omega_o &\approx \bar{\Omega}_o \quad \mu \ll \alpha \\ &\approx \left(\frac{R_{ep}}{10} + \Gamma_M^{o} + \Gamma_{ee}^{o}\right) \quad \mu \gg \alpha \end{aligned} \tag{233}$$

where only Γ_{ee}^{o} retains a temperature-dependence of $\sim T^2$. As the numerical computations in a later section will show, the residual phonon term $\left(\frac{R_{ep}}{10}\right)$ generally has a value which is comparable with the room temperature value of $(\Gamma_{ep}^{o} b_{ep})$ and hence is much larger than Γ_{M}^{o} and Γ_{ee}^{o}. This is clearly in contrast to what might be expected from the classical theory and is also in contrast to the suggestion by Pitaevskii (1958), Silin (1958) and Gurzhi (1959) that, at low temperatures, only the electron-electron collisions and impurity scattering may play a dominant role. On the other hand, it provides strong support for Holstein's suggestion (Holstein 1954) that the bulk electron-phonon processes may make a large contribution to absorptivity even at a very low temperature.

The quantity, Ω_{ee}, entering in the correction factor, $G_\sigma(\omega)$, is independent of both frequency and temperature. For convenience in practical applications, we write G_σ of Equation (227) into the form:

$$G_\sigma(\omega) = \left(1 + \frac{R_{ee}}{\Omega_o} \quad \frac{5.29 \times 10^{+6}}{\lambda^2 \Theta^2}\right) \qquad (234)$$

$$: \lambda \text{ in } \mu$$

It is easily seen that the value of $G_\sigma(\omega)$ remains of the order of unity even at very low temperatures, since according to Equation (233):

$$(G_\sigma - 1) \approx 10 \frac{R_{ee}}{R_{ep}} \quad \frac{5.29 \times 10^{+6}}{\lambda^2 \Theta^2} \; ; \; \mu \gg \alpha$$

$$\approx \frac{R_{ee}}{\Gamma_m^o} \quad \frac{5.29 \times 10^{+6}}{\lambda^2 \Theta^2} \; ; \quad T \cong 0^\circ K \qquad (235)$$

$$\mu \ll \alpha$$

The first equation is not large since $R_{ee} \ll R_{ep}$ and the second is not large since λ^2 is itself large.

In the following part of this section, we shall compute various dispersion properties for different spectral ranges applicable at any temperature. Discussion of these properties for different ranges of temperature is emitted since the preceding discussion on the temperature-dependence of Ω_o, $\bar{\Omega}_o$, and G_σ are sufficient to specify the temperature-dependence of other dispersion properties.

In what follows, the free-electron spectrum is divided into four segments: [i] $\omega^2 \ll \Omega_o^2, \bar{\Omega}_o^2 \ll \omega_o^2$; [ii] $\omega^2 \approx \Omega_o^2, \bar{\Omega}_o^2 \ll \omega_o^2$; [iii] $\Omega_o^2, \bar{\Omega}_o^2 \ll \omega^2 \ll \omega_o^2$; [iv] $\omega^2 \lesssim \omega_o^2$, where ω_o is the frequency characteristic of the electron plasma such that $\epsilon > 0$ for $\omega > \omega_o$ and $\epsilon < 0$ (free electron region) for $\omega < \omega_o$.

B. OPTICAL CONSTANTS, n AND k

The fundamental relations between the optical constants (n,k) and the dispersion properties (σ,ϵ) were derived from Maxwell's theory of electromagnetic fields in section II. They are:

$$\epsilon(\omega) = (n^2 - k^2)$$
$$\sigma(\omega) = \frac{nk\omega}{2\pi} \tag{236}$$

where (n,k) constitute the real and imaginary parts of the complex index of refraction $\bar{N}(\omega)$:

$$\bar{N}(\omega) = (n - ik) \tag{237}$$

Upon inverting the relations of Equation (236), we obtain (n,k) in terms of (ϵ,σ) as follows:

$$n = \sqrt{\frac{|\epsilon|}{2}} \left[\theta(\omega) + \left\{ 1 + \left(\frac{4\pi\sigma}{\omega\epsilon} \right)^2 \right\}^{\frac{1}{2}} \right]^{\frac{1}{2}}$$
$$k = \sqrt{\frac{|\epsilon|}{2}} \left[-\theta(\omega) + \left\{ 1 + \left(\frac{4\pi\sigma}{\omega\epsilon} \right)^2 \right\}^{\frac{1}{2}} \right]^{\frac{1}{2}} \tag{238}$$

where $\theta(\omega)$ has the meaning:

$$\theta(\omega) = \begin{cases} +1 & \epsilon > 0 \quad (\omega_o < \omega) \\ -1 & \epsilon < 0 \quad (\omega_o > \omega) \end{cases} \tag{239}$$

and where ϵ and σ are to be substituted from Equations (224) and (225).

Substitution of Equations (224) and (225) into Equation (238) yields the following expressions of n and k applicable in various spectral ranges where $\omega < \omega_o$:

{i} $\omega^2 \ll \Omega_o^2, \bar{\Omega}_o^2 \ll \omega_o^2$

$$n \approx k \approx \frac{1}{\sqrt{2}} \frac{\omega_o}{\sqrt{\omega \Omega_o'}}$$

$$= \sqrt{\frac{\sigma_{dc}}{\nu}} \left[(b_{ep}-1) \frac{\Gamma_{ep}^o}{o} + 1 \right]^{-\frac{1}{2}} \qquad (240)$$

where:

$$\sigma_{dc} = \frac{\omega_o^2}{4\pi} \frac{1}{o} = \frac{n_e e^2}{m^*} \frac{1}{o} \qquad (241)$$

$$^o = \left(\Gamma_{ep}^o + \Gamma_{ep}^o + \Gamma_M^o \right)$$

At not too low temperatures, we have $\Gamma_{ep}^o \approx \Gamma^o$, and:

$$n \approx k \approx \sqrt{\frac{\sigma_{dc}}{\nu}} b_{ep}^{-\frac{1}{2}} \qquad (242)$$

At very low temperatures:

$$\Gamma^o \approx \Gamma_{ee}^o + \Gamma_M^o \qquad (243)$$

independent of ω, and:

$$\Gamma_{ep}^o \approx R_{ep} \times 124 \left(\frac{T}{\Theta} \right)^5 \qquad (244)$$

{ii} $\omega^2 \approx \Omega_o^2, \bar{\Omega}_o^2 \ll \omega^2$

$$n \approx \frac{1}{\sqrt{2}} \left(\frac{\omega_o}{\Omega_2} \right) \left[\left\{ 1 + \left(\frac{\Omega_o' \Omega_2}{\omega \Omega_1} G\sigma \right)^2 \right\}^{\frac{1}{2}} - 1 \right]^{\frac{1}{2}}$$

$$k \approx \frac{1}{\sqrt{2}} \left(\frac{\omega_o}{\Omega_2} \right) \left[\left\{ 1 + \left(\frac{\Omega_o \Omega_2}{\omega \Omega_1} G_\sigma \right)^2 \right\}^{\frac{1}{2}} + 1 \right]^{\frac{1}{2}} \qquad (245)$$

{iii} $\Omega_o, \Omega_o^2 \ll \omega^2 \ll \omega_o^2$

$$n \approx \tfrac{1}{2} \frac{\omega_o \tilde{\Omega}_o}{\omega^2} \tilde{G}_\sigma \quad : \quad \propto (\lambda^2 + \text{constant}) \tag{246}$$

$$k \approx \left(\frac{\omega_o}{\omega}\right) \quad : \quad \propto \lambda$$

where $\tilde{\Omega}_o$ and $\tilde{G}_\sigma$ represent Ω_o and G_σ with $b_{ep}(\mu,\alpha)$ replaced by $\tilde{b}_{ep}(\alpha)$ given by Equation (8).

{iv} $\omega^2 \lesssim \omega_o^2$

$$n \simeq \left(\frac{\omega_o^2 - \omega^2}{2\omega_o^2}\right)^{\frac{1}{2}} \left[\left\{1 + \left(\frac{\tilde{\Omega}_o \tilde{G}_\sigma}{\omega}\right)^2 \left(\frac{\omega_o^2}{\omega_o^2 - \omega^2}\right)^2\right\}^{\frac{1}{2}} - 1\right]^{\frac{1}{2}}$$

$$k \simeq \left(\frac{\omega_o^2 - \omega^2}{2\omega_o^2}\right)^{\frac{1}{2}} \left[\left\{1 + \left(\frac{\tilde{\Omega}_o \tilde{G}_\sigma}{\omega}\right)^2 \left(\frac{\omega_o^2}{\omega_o^2 - \omega^2}\right)^2\right\}^{\frac{1}{2}} + 1\right]^{\frac{1}{2}} \tag{247}$$

In particular, when $\omega \approx \omega_o$, we have:

$$n \approx k \approx \frac{1}{\sqrt{2}} \left(\frac{\tilde{\Omega}_o \tilde{G}_\sigma}{\omega_o}\right)^{\frac{1}{2}} \ll 1 \tag{248}$$

$$\epsilon \approx 0$$

$$\sigma \approx \frac{\tilde{\Omega}_o}{4\pi}$$

Equations (240) ~ (248), for n and k are plotted qualitatively in FIGURE 15 as functions of λ.

C. ABSORPTIVITY AND REFLECTIVITY

In general, absorption in the free-electron region of the optical

spectrum is attributed to two separate mechanisms; bulk process and the anomalous skin effect. The bulk absorption includes contributions by the electron-phonon processes that was suggested by Holstein (1954) and is the heart of the present theory, as well as the usual electron-electron collisions and impurity scattering. The theory of anomalous skin effects was first offered by Reuter and Sondheimer (1948) and was later elaborated by Dingle (1952, 1953) and Gordon and Sondheimer (1953). Theories which formulate dispersion with consideration of all three, anomalous skin effects, electron-electron collisions and impurity scattering simultaneously, have been developed by Pitaevskii (1958).

Further attempts to formulate the bulk electron-phonon processes have been made and a formula for infrared absorption has been obtained by Gurzhi (1958) by sowing the transport equations for conduction electrons.

The infrared absorptivity obtained by Gurzhi applies mostly in the near infrared, and agrees exactly with the result of the present theory in the same limit of the free-electron spectrum, although the calculational methods adopted are different. The present theory applies to virtually the entire free-electron spectrum for all temperatures.

Denoting the bulk absorptivity, skin absorptivity, and total absorptivity as A_B, A_S, and A respectively, we have:

$$A = A_B + A_S \tag{249}$$

The total reflectivity, R, is simply, (1-A). The skin part of absorptivity is important only at very low temperatures, and will be neglected at all other temperatures. The theory of anomalous skin effects was proposed originally in order to explain the low temperature absorption in metals. That skin effects alone cannot explain the observed low temperature absorption has been made clear in a number of papers, and it was to bridge this gap between theory and experiment that Holstein (1954) offered his mechanism of bulk electron-phonon processes. The results of the present theory not only support Holsteins's suggestion, but also show that such a bulk mechanism, for many metals, is far more important than the skin absorption even at very low temperatures.

It is well known that, when the anomalous skin effect cannot be neglected, it is diffuse rather than specular reflection of electrons at the metallic surface that contributes to low temperature infrared absorption. Thus we shall use the well-known formula:

$$A_S = \frac{3}{4} \quad \frac{\nu_F}{C} \tag{250}$$

as the absorptivity due to the electrons scattered diffusely at the surface, where ν_F is the Fermi velocity of electrons.

We obtained expressions for the optical constants (n,k) in Equation (108) as functions of the parameters $\epsilon(\omega)$ and $\sigma(\omega)$. Therefore, in order to obtain absorptivity of reflectivity as a function of (ϵ,σ), we shall make use of the relation:

$$A_B = \frac{4n}{(n+1)^2 + k^2} \tag{251}$$

where (n,k) contain contributions from the bulk alone. Thus we readily obtain the relation:

$$A_B = \frac{2\left[\theta(\omega) + \left\{1 + \left(\frac{4\pi\sigma}{\omega\epsilon}\right)^2\right\}^{\frac{1}{2}}\right]^{\frac{1}{2}}}{\left[\left[\theta(\omega) + \left\{1 + \left(\frac{4\pi\sigma}{\omega\epsilon}\right)^2\right\}^{\frac{1}{2}}\right]^{\frac{1}{2}} + \sqrt{\frac{|\epsilon|}{2}}\left\{1 + \left(\frac{4\pi\sigma}{\omega\epsilon}\right)^2\right\}^{\frac{1}{4}} + \frac{1}{\sqrt{2\,|\epsilon|}}\right]\right]} \tag{252}$$

Upon substitution Equations (224) and (225) into the above, we obtain the following results for various spectral ranges $\omega < \omega_o$;

{i} $\omega^2 \ll \Omega_o^2, \bar{\Omega}_o^2 \ll \omega_o^2$ (Generalized Hagen-Rubens formula):

$$A_B \approx 2^{3/2}\left(\frac{\omega\,\Omega_o}{\omega_o^2}\right)^{\frac{1}{2}}$$

$$= 2\sqrt{\frac{\nu}{\sigma_{dc}}}\left(1 + \frac{\Gamma_{ep}^o}{\Gamma^o}(b_{ep}-1)\right)^{\frac{1}{2}} \tag{253}$$

where the same remarks apply to the correction factor to the right as in {i} of Section IV, Paragraph B. This correction factor can be significantly larger than unity at low temperatures. At not too low temperatures, we have $\Gamma_{ep}^o \approx \Gamma^o$ so that the correction factor is simply $b_{ep}^{\frac{1}{2}}$. Even at room temperature, this can introduce a correction in the order of 10 ~ 20 percent if:

$$\omega^2 > \left(\frac{K\Theta}{\hbar}\right)^2 \tag{254}$$

Equation (253) is exactly the Hagen-Rubens formula when the correction factor is equated to unity. The original Hagan-Rubens formula for reflectivity has been found to agree well with observed values, and our

formula for reflectivity:

$$R = 1 - 2\sqrt{\frac{\nu}{\sigma_{dc}}}\left(1 + \frac{\Gamma_{ep}^{o}}{\Gamma^{o}}(b_{ep}-1)\right)^{\frac{1}{2}} \qquad (255)$$

is expected to improve the comparison with the experiment. For this reason, we shall call Equations (253) and (255) the "generalized Hagen-Rubens formula":

{ii} $\omega^2 \approx \Omega_o^2$, $\bar{\Omega}_o^2 \ll \omega_o^2$ ($\lambda \lesssim 10\mu$ at T = 300° K)

$$A_B \approx 2^{3/2}\left(\frac{\Omega_2}{\omega_o}\right)\frac{\left[\left\{1 + \left(\frac{\Omega_o \Omega_2}{\omega \Omega_1} G_\sigma\right)^2\right\}^{\frac{1}{2}} - 1\right]^{\frac{1}{2}}}{\left[1 + \left(\frac{\Omega_o \Omega_2}{\omega \Omega_1} G_\sigma\right)^2\right]^{\frac{1}{2}}} \qquad (256)$$

{iii} $\Omega_o^2, \bar{\Omega}_o^2 \ll \omega^2 \ll \omega_o^2$

$$A_B \approx 2\left(\frac{\tilde{\Omega}_o}{\omega_o}\right)\tilde{G}_\sigma(\omega) = \sqrt{\frac{m^*}{\pi n_e e^2}}\,(\tilde{\Omega}_o \tilde{G}_\sigma) \qquad (257)$$

where:

$$(\tilde{\Omega}_o \tilde{G}_\sigma) = \Omega_o + \frac{\omega^2}{\Omega_{ee}}$$

$$= \left(\Gamma_{ep}^{o}\tilde{b}_{ep} + \Gamma_{ee}^{o} + \Gamma_M^{o} + \frac{\omega^2}{\Omega_{ee}}\right) \qquad (258)$$

$$\approx \left(\Gamma_{ep}^{o}\tilde{b}_{ep} + \frac{\omega^2}{\Omega_{ee}}\right) \quad : T \gg 0° \text{ K}$$

At very low temperatures and for $\mu \gg \alpha$, Equation (257) reduces to:

$$A_B \approx \sqrt{\frac{m^*}{\pi n_e e^2}}\left(\frac{R_{ep}}{10} + 5.29 \times 10^{+6}\,\frac{R_{ee}}{\lambda^2 \Theta^2}\right) \quad : \lambda \text{ in } \mu \qquad (259)$$

The skin term A_s of Equation (250) must be added to obtain the total absorptivity. This formula will be used repeatedly in the future in specific applications, and it will be shown that it gives values in excellent agreement with the experiment. A very interesting feature of Equation (259) is the absence of temperature dependence. Further, the dominant term represented by $\left(\frac{R_{ep}}{10}\right)$ does not contain λ-dependence. The values of R_{ep} and R_{ee} are in general of the same order of magnitude as Γ^{o}_{ep} and Γ^{o}_{ee}, respectively, of room temperature so that the quantities within (---) represent a large value while, classically and from some existing quantum mechanical theories, the electron-phonon term is expected to decrease rapidly, like $\sim T^5$, when T is decreased to 0°K.

Now, let us compare the magnitudes of the two terms with the help of some typical numbers. Many metals have $R_{ep} \approx 10^{13} \sim 10^{15}$ sec^{-1} while R_{ee} is of the order of $\sim 10^{9} \sim 10^{11}$ sec^{-1} and, for exceptionally large case, $\sim 10^{12}$ sec^{-1}. Thus, for $R_{ep} = 10^{14}$ sec^{-1}, $R_{ee} = 10^{10}$ sec^{-1}, Θ = 300°K, and $\lambda = 1\mu$, we have:

$$\frac{R_{ep}}{10} = 10^{13} \text{ sec}^{-1} \tag{260}$$

$$5.29 \times 10^{6} \frac{R_{ee}}{\lambda^2 \Theta^2} \simeq (0.06) \times 10^{13} \text{sec}^{-1}$$

In this case, the electron-electron collisions introduce a correction of about ~ 6 percent, while, if we take $R_{ee} = 10^{12}$ sec^{-1}, the correction is as big as 60 percent. Thus, it is clear that, while the electron-electron collision plays a relatively small part even at very low temperatures for many metals, it can be quite significant for some special cases.

{iv} $\omega^2 \lesssim \omega_o^2$

$$A_B \approx \frac{2\left[\left\{1 + \left(\frac{\tilde{\Omega}_o}{\omega}\tilde{G}_o\right)^2\left(\frac{\omega_o^2}{\omega_o^2 - \omega^2}\right)^2\right\}^{\frac{1}{2}} - 1\right]^{\frac{1}{2}}}{\left[\left[\left\{1 + \left(\frac{\tilde{\Omega}_o}{\omega}\tilde{G}_o\right)^2\left(\frac{\omega_o^2}{\omega_o^2 - \omega^2}\right)^2\right\}^{\frac{1}{2}} - 1\right]^{\frac{1}{2}} + \left(\frac{\omega_o^2 \omega^2}{2\omega^2}\right)^{\frac{1}{2}}\left[1 + \left(\frac{\tilde{\Omega}_o}{\omega}\tilde{G}_o\right)^2\left(\frac{\omega_o^2}{\omega_o^2 - \omega^2}\right)^2\right]^{\frac{1}{2}} + \left(\frac{\frac{1}{2}\omega^2}{\omega_o^2 - \omega^2}\right)^{\frac{1}{2}}\right]\right]} \tag{261}$$

In particular, at $\omega^2 \approx \omega_o^2$, this is reduced to:

$$A_B \approx 2^{3/2} \left(\frac{\tilde{\Omega}_o \tilde{G}(\omega_o)}{\omega_o} \right)^{\frac{1}{2}} \tag{262}$$

At such large frequencies, the second term in $G_\sigma(\omega)$ due to electron-electron collisions may become predominant, especially for those metals which have large values of R_{ee}.

The bulk absorptivity and reflectivity are plotted qualitatively in FIGURE 17, where the significance of the correction factor, $G_\sigma(\omega)$, is shown in the high-frequency limit.

D. TEMPERATURE-DEPENDENT SCATTERING CROSS-SECTION, OPTICAL SIZE OF ELECTRONS, AND THE VIRTUAL MASS OF LIGHT QUANTUM

From our formulas for temperature-dependent optical constants, (n,k) or (σ,ϵ), we can define the temperature-dependent scattering amplitude, scattering cross-section per electron, and hence the optical radius of the electron. By scattering cross-section, we mean the effective cross-section of a conduction electron which the external electromagnetic field sees for interaction, including both pure scattering and absorption. In this sense, it may also be called "the dispersion cross-section per electron." If such a cross-section is denoted as $\sigma_s(\omega,T)$ measured in cm^2, the optical radius of an electron, a_s, is defined as:

$$\pi a_s^2 = \sigma_s \tag{263}$$

and is measured in cm.

The concept of "virtual mass of a photon" in metals (and also in dielectric media as well) is a rather new one and its definition is helpful in a qualitative discussion of infrared dispersion in metals. A light quantum of frequency ω, when it enters a medium with index of refraction $n > 1$, behaves as a light quantum of frequency, $\left(\frac{\omega}{n}\right) < \omega$, as if it suddenly gained a nonzero mass m_p and that:

$$\omega^2 = \left(\frac{\omega}{n}\right)^2 + K_p^2 c^2 \tag{264}$$

$$K_p = \left(\frac{m_p c}{\hbar}\right)$$

This is a relation which is often used to obtain the expression of n in dielectric crystals, and is not anything particularly new. A quick glance at the relation reminds us of the familiar expression for relativistic energy of a particle in terms of kinetic and mass terms. Thus, we may conveniently define the first term of Equation (264) as the kinetic term and the second as the mass term, so that:

$$m_p = \frac{\hbar\omega}{c^2} \quad \frac{\sqrt{n^2 - 1}}{n} \geqslant 0 \tag{265}$$

Likewise, we may treat the mass term as a potential term such that an increase in m_p and hence a decrease in the kinetic term correspond to an increase in a potential of some kind. In fact, the physical picture of dispersion properties, at least in the free-electron region, can be better understood in terms of such an argument. For instance, the increase of reflectivity of light by a metal with increase in index of reflection may be explained in analogy with the increase in backward scattering a particle by an increased positive potential step, and hence a smaller kinetic energy in the new potential field. We are essentially applying our knowledge of the elementary particle picture to optical dispersion in contrast to the usual practice of applying optics to massed particles.

We shall now calculate various properties explained above with the help of the relations of Section II. Upon combining Equations (224) and (225) with the dispersion relations for n and k of Section II, we easily obtain the following temperature-dependent expressions for the real and imaginary parts of the scattering amplitudes, $(R_e \bar{F})$ and $(I_m \bar{F})$:

$$R_e \bar{F} = r_o^* \left(\frac{\omega}{\omega_o}\right)^2 \sqrt{2|\epsilon|} \left[\left\{-1 + \left[1 + \left(\frac{4\pi\sigma}{\omega\epsilon}\right)^2\right]^{\frac{1}{2}}\right\}^{\frac{1}{2}} - \sqrt{\frac{2}{|\epsilon|}}\right] \tag{266}$$

$$I_m \bar{F} = r_o^* \left(\frac{\omega}{\omega_o}\right)^2 \sqrt{2|\epsilon|} \left[1 + \left\{1 + \left(\frac{4\pi\sigma}{\omega\epsilon}\right)^2\right\}^{\frac{1}{2}}\right]^{\frac{1}{2}}$$

where r_o^* is the effective classical radius of electrons and is related to the usual classical radius of electron r_o as:

$$r_o^* = \frac{e^2}{m^* c^2} = \left(\frac{m_o}{m^*}\right) r_o \tag{267}$$

where m_o is the rest mass of an electron.

The scattering cross-section, σ_s, and the optical radius, a_s, are obtained from the usual relation:

$$\sigma_s = \pi a_s^2 = \frac{4\pi c}{\omega} I_m \bar{F} \tag{268}$$

The mass of a photon m_p is computed from Equation (265) by using the formulas for $n(\omega)$ that were obtained in Section IV paragraph B. Here again, we shall compute these quantities for various segments of the free-electron spectrum when $\omega < \omega_o$. They are:

{i} $\omega^2 \ll \Omega_o^2, \bar{\Omega}_o^2 \ll \omega_o^2$;

$$R_e \bar{F} \approx I_m \bar{F} \approx \sqrt{2}\ r_o^* \left(\frac{\omega^3}{\omega_o^2 \Omega_o}\right)^{\frac{1}{2}}$$

$$\sigma_s \approx 4\pi \sqrt{2}\ c\, r_o^* \left(\frac{\omega}{\omega_o^2 \Omega_o}\right)^{\frac{1}{2}} \tag{269}$$

$$a_s \approx 2^{\frac{3}{4}} \left(\frac{r_o^* \lambda_o}{\pi}\right)^{\frac{1}{2}} \left(\frac{\omega}{\Omega_o}\right)^{\frac{1}{4}} \tag{270}$$

$$m_p \approx \frac{\hbar\omega}{c^2} \tag{271}$$

where λ_o is the critical wavelength:

$$\lambda_o = \frac{2\pi c}{\omega_o} \tag{272}$$

We notice that $m_p c^2$ is nearly the entire photon energy $\hbar\omega$ meaning that, in this part of the spectrum, the photon may seem nearly motionless to a Fermi electron of speed $F \approx 10^8$ (cm/sec), and hence there is a greater probability of encounter, on the average, between the photon of mass m_p and the conduction electrons during the period of $\left(\frac{2\pi}{\omega}\right)$ (second).

{ii} $\omega^2 \approx \Omega_o^2,\ \bar{\Omega}_o^2 \ll \omega_o^2$

$$R_e\bar{F} \approx \sqrt{2}\, r_o^* \frac{\omega^2}{\omega_o \Omega_2} \left[\left\{ 1 + \left(\frac{\Omega_o \Omega_2}{\omega\, \Omega_1} G\sigma \right)^2 \right\}^{\frac{1}{2}} - 1 \right]^{\frac{1}{2}} \tag{273}$$

$$I_m\bar{F} \approx \sqrt{2}\, r_o^* \frac{\omega^2}{\omega_o \Omega_2} \left[\left\{ 1 + \left(\frac{\Omega_o \Omega_2}{\omega\, \Omega_1} G\sigma \right)^2 \right\}^{\frac{1}{2}} + 1 \right]^{\frac{1}{2}} \tag{274}$$

$$\sigma_s \cong 2\sqrt{2}\, r_o^* \lambda_o \left(\frac{\omega}{\Omega_2} \right) \left[1 + \left\{ 1 + \left(\frac{\Omega_o \Omega_2}{\omega\, \Omega_1} G\sigma \right)^2 \right\}^{\frac{1}{2}} \right]^{\frac{1}{2}} \tag{275}$$

$$a_s \approx 2^{\frac{3}{4}} \left(\frac{\lambda_o r_o}{\pi} \right)^{\frac{1}{2}} \left(\frac{\omega}{\Omega_2} \right)^{\frac{1}{2}} \left[1 + \left\{ 1 + \left(\frac{\Omega_o\, \Omega_2}{\omega\, \Omega_1} G\sigma \right)^2 \right\}^{\frac{1}{2}} \right]^{\frac{1}{2}} \tag{276}$$

$$m_p \lessapprox \frac{h\omega}{c^2}$$

{iii} $\Omega_o^2,\ \bar{\Omega}_o^2 \ll \omega^2 \ll \omega_o^2$

$$R_e\bar{F} \approx 2\, r_o^* \left(\frac{\omega}{\omega_o} \right)^2 \left[\frac{1}{2} \frac{\omega_o\, \tilde{\Omega}_o}{\omega^2} \tilde{G}_\sigma - 1 \right] \tag{277}$$

$$I_m\bar{F} \approx 2\, r_o^* \left(\frac{\omega}{\omega_o} \right) \tag{278}$$

$$\sigma_s \approx 4\, r_o^* \lambda_o \tag{279}$$

$$a_s \approx \frac{2}{\sqrt{\pi}} (r_o^* \lambda_o)^{\frac{1}{2}} \tag{280}$$

$$m_p \approx \frac{\hbar\omega}{c^2} \left[1 - 4 \left(\frac{\omega^2}{\omega_o \tilde{\Omega}_o \tilde{G}\sigma} \right)^2 \right]^{\frac{1}{2}} \tag{281}$$

It is seen that σ_s and a_s are independent of frequency and temperature while we found previously that absorptivity is independent of frequency in this part of the spectrum. Formula (281) for m_p necessitates defining a frequency ω_m such that $m_p = 0$ at $\omega = \omega_m$ given by:

$$\omega_m^2 = \frac{\tilde{\Omega}_o \omega_o}{2 - \frac{\omega_o}{\Omega_{ee}}} > 0 \qquad (282)$$

Strictly speaking, Equation (281) is valid only for ω smaller than ω_m. This corresponds to the point where the index of refraction is identically equal to unity and the light quantum behaves as though the bulk of the metal is not different from vacuum. Photoelectric processes which may be important at such a frequency have been neglected.

{iv} $\omega^2 \lesssim \omega_o^2$

$$R_e\bar{F} \approx 2r_o^*\left(\frac{\omega}{\omega_o}\right)^2\left\{\left(\frac{\omega_o^2-\omega^2}{2\omega_o^2}\right)^{\frac{1}{2}}\left[1+\left\{1+\left(\frac{\tilde{\Omega}_o}{\omega}\right)^2\left(\frac{\omega_o^2\,\tilde{G}\sigma}{\omega_o^2-\omega^2}\right)^2\right\}^{\frac{1}{2}}\right]^{\frac{1}{2}} - 1\right\} \qquad (283)$$

$$I_m\bar{F} \approx 2r_o^*\left(\frac{\omega}{\omega_o}\right)^2\left(\frac{\omega_o^2-\omega^2}{2\omega_o^2}\right)^{\frac{1}{2}}\left[\left\{1+\left(\frac{\tilde{\Omega}_o}{\omega}\right)^2\left(\frac{\omega_o^2\,\tilde{G}_\sigma}{\omega_o^2-\omega^2}\right)^2\right\}^{\frac{1}{2}} + 1\right]^{\frac{1}{2}} \qquad (284)$$

$$\sigma_s \approx 2^{3/2}\,(r_o^*\ \lambda_o)\left(1 + \tfrac{1}{2}\frac{\Delta\omega}{\omega_o}\right)\left(\frac{\tilde{\Omega}_o}{\omega_o}\,\tilde{G}\sigma\right)^{\frac{1}{2}} \qquad (285)$$

$$a_s \approx 2^{3/4}\left(\frac{r_o^*\,\lambda_o}{\pi}\right)^{\frac{1}{2}}\left(1 + \tfrac{1}{4}\frac{\Delta\omega}{\omega_o}\right)\left(\frac{\tilde{\Omega}_o\,\tilde{G}\sigma}{\omega_o}\right)^{\frac{1}{4}} \qquad (286)$$

where $\Delta\ \omega = (\omega - \omega_o)$.

When $\omega \gg \omega_o$, both σ_s and a_s approach very small but constant values of the order, $\left(\frac{\Omega_o}{\Omega_{ee}}\right)$ and $\left(\frac{\Omega_o}{\Omega_{ee}}\right)^{\frac{1}{2}}$, respectively, and vanish identically when there is no Umklapp process present. This is, of course, not strictly true when we consider the contribution of bound electrons which are important in this part of the spectrum.

The scattering cross section σ_s is plotted against λ qualitatively in FIG. 16. The λ-dependence of m_p is also shown. The general pattern in the λ-dependence of σ_s and $\left(\frac{m_c c^2}{\hbar\omega}\right)$ may be compared with those of absorptivity and reflectivity, respectively, of FIG. 17.

SECTION VI. PARAMAGNETIC AND FERROMAGNETIC TRANSITION METALS

A. INTRODUCTION

The calculations presented in the preceding chapters depend on the assumption that the energy surface is spherical. This assumption has been shown to work well for a variety of nontransition metals. However, for many multivalent and transition metals which have been investigated from a theoretical point of view, the surface of the Fermi level cuts through two or more Brillouin zones, and it does not resemble the spherical shape we considered in Sections IV and V.

In particular, the study of ferromagnetic and paramagnetic transition elements represents a special problem from a theoretical point of view, since the metallic properties of these metals have a rather peculiar dependence on the place of the element in the periodic table. These special properties are exhibited in the observed temperature dependences of resistivity as well as of various thermodynamic properties. Behavior of the ferromagnetic transition metals represents an even more special case. Although these metals have been studied rather extensively as to their dc electrical properties based on the quantum mechanical explanations, very little work has been done on the optical and infrared dispersion properties. Some of the qualitative features of the optical properties of transition metals and transition metal alloys were presented by Mott (1936, 1935).

In the transition metals such as Pt, Pd, Ir and Ni, the s-band and d-band overlap and the Fermi level falls in this overlapping region. The most widely investigated metals are the triad, Pt, Pd and Ni, which come before Cu, Ag and Au in the periodic table, and are all face-centered cubic lattices. In palladium, there is about 0.55 to 0.6 electron per atom in 5s states and the same number of holes in the 4d states. In pure platinum, there is about 0.55 to 0.6 electron in 6s states and the same number of holes in 5d states. In nickel, there is about 0.55 to 0.6 electron in 4s states and the same number of holes in 3d states. The density of states $\rho(E)$ of 4s and 3d states of nickel is schematically illustrated in FIGURE 45 and are compared with 4s and 3d states of copper. The large value of energy density of d states compared with s states is qualitatively indicated, and it will be shown that this leads to important consequences.

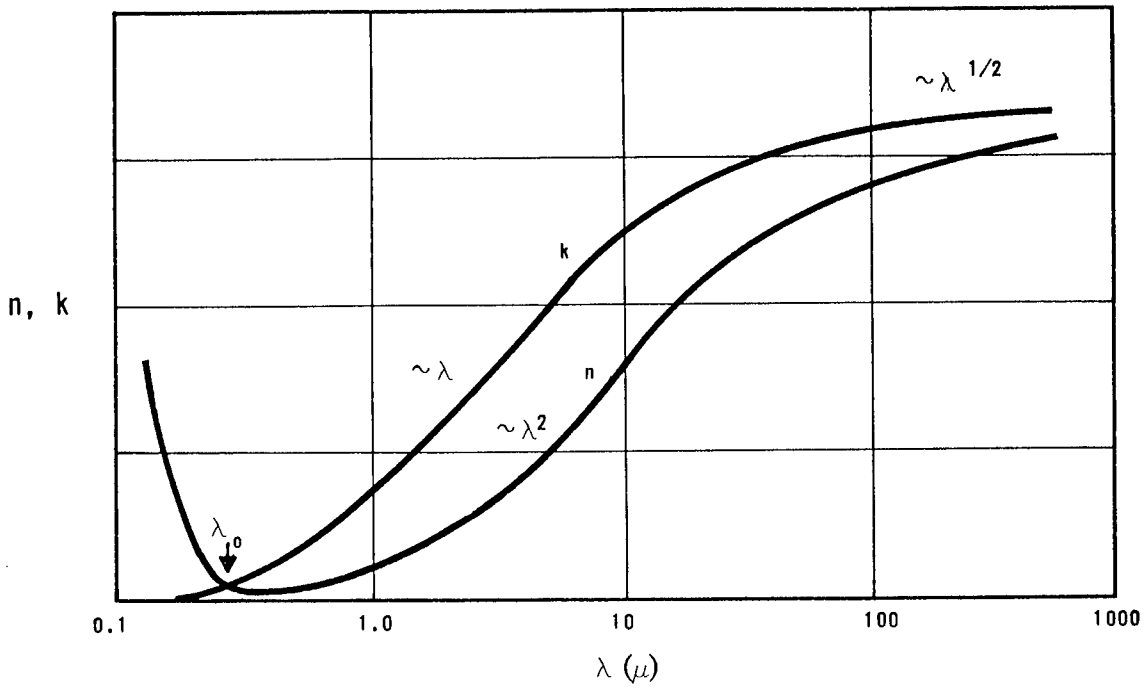

Figure 17. Typical Curves of the Optical Constants n and k versus λ

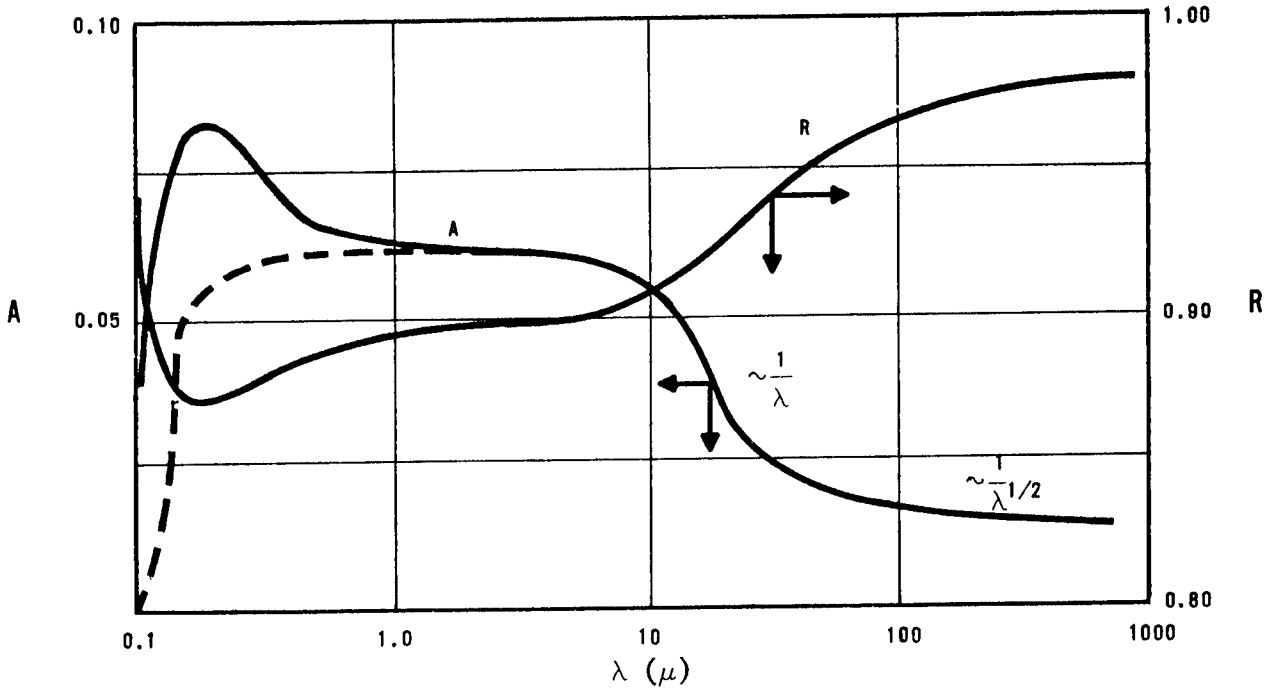

Figure 18. Typical Curve of Absorptivity as a function of Wavelength

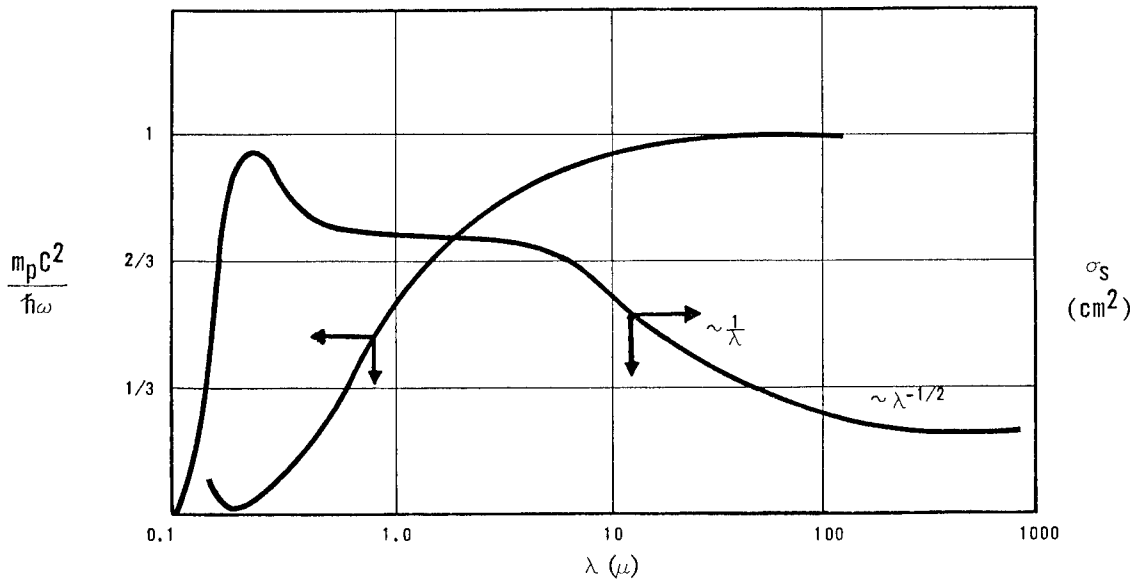

Figure 19. Typical λ-Dependence of the Scattering Cross Section σ_s per Conduction Electron and of the Photon Mass m_p

Some of the important physical consequences of the presence of positive holes in the d-band are:

(a) the ferromagnetism or high paramagnetism shown by these metals;

(b) the low electrical conductivity and anomalous behavior of resistance both at high and low temperatures;

(c) the low reflection coefficient for long wavelengths; and

(d) the high electronic specific heat.

Although all the above properties are mutually related, only the first three will enter explicitly in calculations of optical and infrared dispersion properties. In the language of the optical dispersion theory, the low reflectivity for long wavelengths is the direct consequence of the low electrical conductivity. This may be explained on the basis of the Hagen-Rubens formula for reflectivity R that is applicable at long wavelengths:

$$R \approx 1 - 2\sqrt{\frac{\omega}{2\pi\sigma_{dc}}} \tag{287}$$

where it is seen that a low value of σ_{dc}, the dc conductivity, results in a low value of reflectivity.

The low electrical conductivity is a direct consequence of the large density of states in the d-band. The transition matrix elements that contribute to resistivity or the inverse of the relaxation time, $\uparrow_R$, contains a predominantly large contribution from the s→d transitions, since the probability of such a transition is multiplied by the large value of the density of states of the final d-states. In fact, the interband transitions from s to d states alone account for 90 percent or more of the conductivity because of the large value of the transition probability compared with the other modes of transitions, s→s, d→s, d→d.

For the particular case of the ferromagnetic nickel, three states of electronic configuration are possible: namely, $3d^8\ 4s^2$, $3d^9\ 4s^1$, and $3d^{10}$ states. The wave function for each atom will be a superposition of the atomic wavefunctions corresponding to different electronic configurations. If ψ_2, ψ_1 and ψ_0 are the wavefunctions corresponding to the three configuration states in the order listed above, the wavefunction in an atom of the solid nickel will be in the form:

$$A_2\psi_2 + A_1\psi_1 + A_0\psi_0 \tag{288}$$

where $|A_2|^2$, $|A_1|^2$, and $|A_-|^2$ are constants representing the fraction of occurrence of each of the three configurations. The mean number of electrons in the s-states is then given by:

$$\bar{n}_s = 2 \times |A_2|^2 + 1 \times |A_1|^2 \tag{289}$$

which is equal to $0.55 \sim 0.6$ per atom. This is also equal to the number of positive holes in the d-band. Another consideration enters in the study of nickel on account of the ferromagnetic properties. It is outside the scope of the present work to discuss in detail the mechanism that gives rise to the ferromagnetism. We are only interested in the way the ferromagnetism enters in the optical and infrared dispersion of metal. It is sufficient to note that, in the ferromagnetic nickel, the d-states with one orientation of the electron spin are filled, and the holes occur only for those states of the d-band which correspond to the electron spins oriented antiparallel to these filled states. The electrons in the s-states, however, occur in equal mixture of the two spin states. The result of this is that there is a residual spin component equal to the mean number of positive holes times the electron spin. Since the mean number of holes per atom is exactly equal to the mean number of s electrons, the residual spin per nickel atom at 0°K is:

$$\frac{\hbar}{2} \bar{n}_s = (0.55 \sim 0.60)\frac{\hbar}{2} \tag{290}$$

The residual spin or the spontaneous magnetization decreases gradually as temperature is increased, and the metal turns paramagnetic as temperature is increased further beyond the Curie point.

The important consequence of this property that will be of concern in our calculations is that not all of the s-electrons are qualified to make transitions to the empty d-states: only those s-electrons with the spins antiparalled to the residual spin of the d-states will be able to make transitions because of the Pauli exclusion principle. At 0°K, only $\frac{1}{2}$ of the s-electrons are qualified, while, at a temperature above the Curie point, practically all of the s-electrons are qualified. This explains the large increase in the observed resistivity of Ni above the Curie point (Gerlach, 1932), since the damping contributed by the transitions is directly proportional to the number of d-states which are available for the transitions.

In short, the electrical properties and hence the optical and infrared behavior of a ferromagnetic metal will be a function of both the spontaneous magnetization Σ and temperature.

If we denote the spontaneous magnetization per gram atom at any temperature T°K and at 0°K by $\Sigma(T)$ and Σ_o, respectively, the total number of s-electrons that are qualified to make transitions to the empty d-states may be defined as:

$$\bar{n}_s = \frac{n_s}{2} \chi = \frac{n_s}{2} \left[1 + \frac{\Sigma_o - \Sigma}{\Sigma_o} \right] \qquad (291)$$

$$: 1 \leq \chi \leq 2$$

where n_s is the effective number of electrons in the s-band. This shows immediately that resistivity of nickel has an additional temperature dependence coming from Σ besides the usual temperature dependence coming from the lattice vibrations. The explicit temperature dependence of the factor χ is available from the phenomenological theory of Weiss (1907) at high temperature and the quantum mechanical theory of Heisenberg (1926) at low temperatures. A detailed theoretical and phenomenological discussion on ferromagnetism and paramagnetism is offered by Van Vleck (1959). For the purpose of our calculation that will follow, it is sufficient to note that the phenomenological theory of Weiss shows that $(\chi-1)$ increases with increasing T like

$$e^{-\text{constant}/T}$$

at high temperatures (viz., $T > 400°K$), and that the theory of Heisenberg shows that $(\chi-1)$ decreases like $T^{3/2}$ at low temperatures as T is decreased. The observed and theoretical values of χ and Σ are shown in Table XIV at different temperatures for the ferromagnetic metals, Ni, Co, Fe and others.

In the following part of the present section, probability of the s→d transitions will be calculated by a method similar to that adopted in Section IV for the intraband transitions. All the other modes of transitions, d→d, s→s, and d→s will be neglected compared with the s d transitions.

The weight factor multiplying the s→d transition probability is about 10 times the normal scattering probability according to the evidence provided by the data on the electronic specific heat (Wilson, 1936). This means that neglecting all modes of transitions other than the s-band to d-band transition will introduce an error of about 10 percent in the calculated resistivity. Besides, the results on the intraband transitions are satisfactorily presented by the calculations of Section IV.

Finally, it may be noted that the results that are obtained in the

present chapter should be applicable just as well to interband transitions in other multivalent metals. For nontransition multivalent metals, the interband transitions do not necessarily contribute more than the intraband transitions. Whatever the case may be, it is useful to remember that the total damping coefficient, including both the interband and intraband transitions, can be obtained simply by adding the damping coefficient that is obtained in the present chapter to that obtained in Section IV for intraband transitions.

B. CALCULATION OF TRANSITION PROBABILITY

Because of the large effective mass of the d-electrons their contribution to conductivity will be small and can be neglected compared with that due to the s-electrons. The empty states in the d-band have a considerable effect in that the s-electrons can be scattered not only into energy levels in the s-band but also into the d-band. The large value of the density of states in the final d states makes the s$\rightarrow$d transition probability much larger than the normal s$\rightarrow$s transition probability. Further, the d$\rightarrow$d and d$\rightarrow$s transition probabilities together are even smaller than the s$\rightarrow$s transition probability due to large values of the effective mass, m_d, of d-electrons compared with that of s-electrons, m_s.

For this reason, the following calculations will include only the s$\rightarrow$d transitions. Contribution to the conductivity coming from the s$\rightarrow$d transitions alone explains at least 90 percent of the total conductivity according to the evidence obtained from the data on the electronic specific heat (Wilson, 1936), 1938). In order to obtain the contributions of the s$\rightarrow$s transition, results of Section IV may be used without necessity of modification. Calculations of the s d transition probability involve essentially the same theoretical approach as that adopted in Section IV. The s d transition caused by a joint action of both the electromagnetic field and the phonon field is again a secondorder effect, and may be calculated from the second-order coefficient $B^{s}_{(2)}(\underline{k}^{d})$ representing such a transition. There are eight different processes for the s$\rightarrow$d transitions, four of which involved creation or annihilation of a photon in the s-band, while the other four involved creation or annihilation of a photon in the d-band. These eight processes are illustrated schematically in the accompanying Feynmann diagrams where (A) shows the first four processes and (B) shows the other four processes.

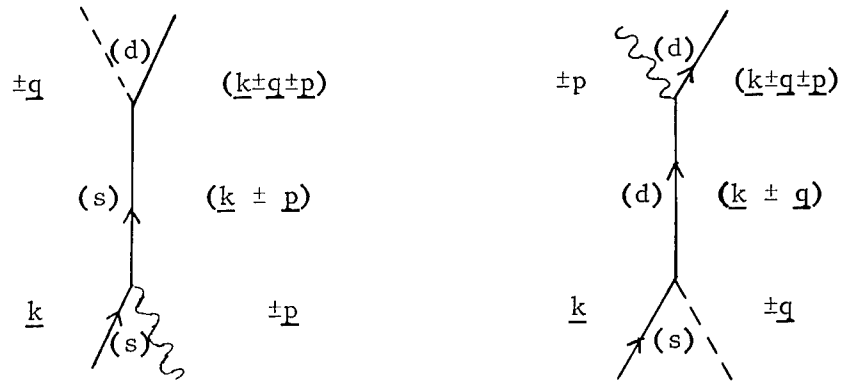

In the diagrams, the solid, curved, and broken lines represent the electron, photon, and phonon, respectively.

The coefficient $B^{s\to d}_{(2)}(\underline{k} \pm \underline{q} \pm \underline{p})$ may be calculated by essentially the same method as that adopted in Section IV. We thus obtain the following two equations corresponding to (A) and (B):

$$B^{s\to d}_{(2)}(\underline{k}\pm\underline{q}\pm\underline{p})\Big|_{(A)} = \mp \left|\underline{q}\right| \left(\frac{\hbar^2}{2N_p MV E_{\underline{q}}}\right)^{\frac{1}{2}} \left(\frac{\sqrt{N_{\underline{q}}}}{\sqrt{1+N_{\underline{q}}}}\right) \frac{e\hbar g^{sd}}{m_s \omega} (\underline{E}\cdot\underline{k})$$

$$\times \frac{(-1)}{E(\underline{k}\pm\underline{p}) - E(k) \mp \hbar\omega} \left[\frac{1-e^{i\xi t/\hbar}}{\xi} - \frac{1-e^{i\xi' t/\hbar}}{\xi'}\right] \tag{292}$$

$$B^{s\to d}_{(2)}(\underline{k}\pm\underline{q}\pm\underline{p})\Big|_{(B)} = \pm \left|\underline{q}\right| \left(\frac{\hbar^2}{2N_p MV E_{\underline{q}}}\right)^{\frac{1}{2}} \left(\frac{\sqrt{N_{\underline{q}}}}{\sqrt{1+N_{\underline{q}}}}\right) \frac{e\hbar g^{sd}}{m_d \omega} \underline{E}\cdot(\underline{k}+\underline{q})$$

$$\times \frac{(-1)}{E'(\underline{k}\pm\underline{q}) - E(k) \mp E_{\underline{q}}} \left[\frac{1-e^{i\xi t/\hbar}}{\xi} - \frac{1-e^{i\xi'' t/\hbar}}{\xi''}\right] \tag{293}$$

where the energy terms denoted as ξ, ξ', and ξ'' in various resonance factors are given by:

$$\xi = \left\{ E'(\underline{k}\pm\underline{q}\pm\underline{p}) - E(k) \mp \hbar\omega \mp E_{\underline{q}} \right\}$$

$$\xi' = \left\{ E'(\underline{k}\pm\underline{q}\pm\underline{p}) - E(\underline{k}\pm\underline{p}) \mp E_{\underline{q}} \right\} \qquad (294)$$

$$\xi'' = \left\{ E'(\underline{k}\pm\underline{q}\pm\underline{p}) - E'(\underline{k}\pm\underline{p}) \mp \hbar\omega \right\}$$

The energy, $E'(\underline{k})$, (with a prime) represents the energy of a d-electron and $E(\underline{k})$, (without a prime) represents the energy of a s-electron with momentum, $(\hbar\underline{k})$:

$$E'(\underline{k}) = E_o - \frac{\hbar^2}{2m_d} k^2$$

$$E(\underline{k}) = \frac{\hbar^2 k^2}{2m_s} \qquad (295)$$

where E_o is the energy at the upper edge of the d-band. The constant factor g^{sd} represents the strength of the electron-phonon interaction which is generally of the same order of magnitude as the energy of an electron and has the same meaning as g which was used in Section IV. As usual taking g^{sd} and also g to be independent of the energy of the electron which is interacting with a phonon is the result of assuming that the electron-ion potential within single unit-cells is reasonably flat, or equivalently that the radius of the atomic core is much smaller than the size of a single unit-cell. This assumption is satisfactory for common applications such as in the present theory. The more general electron-phonon interaction which also includes the deformation of ions was discussed by Bardeen (1937). A further discussion on this problem is offered in the 1958 edition of The Theory of Metals by Wilson.

As in Section IV, we shall ignore the quantities of the order of $\left(\frac{v_f}{c}\right)$, and take:

$$E(\underline{k}\pm\underline{p}) - E(k) \mp \hbar\omega \cong$$

$$E'(\underline{k}\pm\underline{q}\pm\underline{p}) - E'(\underline{k}\pm\underline{q}) \mp \hbar\omega \cong \mp \hbar\omega \qquad (296)$$

Then, of all the terms in Equations (292) and (293), only those which have ξ in the resonance factors need be considered for our calculations, since the others will contribute equally to both the emission and

absorption of a photon and will thus cancel out when we calculate the net absorption term. By combining Equations (292) and (293), and using the relation:

$$\left[\frac{\underline{k}}{E(\underline{k}\pm\underline{p})-E(\underline{k})\mp\hbar\omega}-\frac{m_s}{m_d}\,\frac{(\underline{k}\pm\underline{q})}{E'(\underline{k}\pm\underline{q})-E(\underline{k})\mp E_q}\right]_{\xi=0}\simeq\frac{\underline{k}\left(1+\frac{m_s}{m_d}\right)\pm\frac{m_s}{m_d}\underline{q}}{\mp\hbar\omega} \qquad (297)$$

we now have:

$$B^{s\to d}_{(2)}(\underline{k}\pm\underline{q}\pm\underline{p})\simeq\pm\,q\left(\frac{\hbar^2}{2N_pMVE_q}\right)^{\frac{1}{2}}\left(\frac{\sqrt{N_q}}{\sqrt{1+N_q}}\right)\frac{e\,g^{sd}}{\mp m_s\omega^2} \qquad (298)$$

$$\times\,\underline{E}.\;\;\underline{k}\left(1+\frac{m_s}{m_d}\right)\pm\frac{m_s}{m_d}\underline{q}\;\;\frac{1-e^{i\xi t/\hbar}}{\xi} \qquad (298)$$

It may be noted that the value $\left(\frac{m_s}{m_d}\right)$ of a transition metal is usually very much smaller than unity $\left(\lesssim\frac{1}{10}\right)$ and such a term in Equation (298) can be neglected without any loss in the qualitative merit of our calculations. It is retained in Equation (298), however, because this term can be important when the results are applied to nontransition multivalent metals for which the ratio of the effective mass values is not necessarily small.

The probability for the process in which an electron in the s-band with momentum, $\underline{k}_1$, makes a transition to the d-state with momentum, $\underline{k}_2$, by a joint action of the electromagnetic and phonon fields is obtained from Equation (298) upon using the usual relation:

$$P^{(r)}_{(s)}\;(\underline{k}_1\longrightarrow k_2)\;=\;\lim_{T\to\infty}B^{s\to d}_{(2)}\;(k_1\longrightarrow k_2)\;\;^2\Big/\,T \qquad (299)$$

where we have put $\underline{k}\;\;k_1$ and $k_2=(\underline{k}_1\pm\underline{q}\pm\underline{p})$, and r = (±), s = (±) correspond to emission and absorptions of phonons and photons, respectively. Thus, we obtain:

$$P^{(r)}_{(s)}\;(k_1\longrightarrow k_2)_{s\to d}=\frac{e^2\hbar^4E^2}{12Vm_s^{\,2}(\hbar\omega)^4}\,G^{(r)}_{sd}\;(\underline{q}) \qquad (300)$$

$$\times\left(q^2\left(\frac{m_s}{m_d}\right)^2+k_1^2\left(1+\frac{m_s}{m_d}\right)^2\right)\delta(E_2'-E_1+rE\underline{q}+s\hbar\omega)$$

$$\therefore \quad E_2' = E'(\underline{k}_2) = E_o - \frac{\hbar^2}{2m_d} (k_2)^2$$

where we have taken:

$$\overline{(\underline{E} \cdot \underline{k}_1)\ (\underline{E} \cdot \underline{q})} = 0$$

$$\overline{\frac{(\underline{E} \cdot \underline{k}_1)^2}{k^2}}\ \ \overline{\frac{(\underline{E} \cdot \underline{q})^2}{q^2}} = \frac{1}{3} E^2$$

and

$$G_{sd}^{(r)}(\underline{q}) = \frac{\pi \hbar\, q^2 g_{sd}^2}{N_p M E_{\underline{q}}} \begin{pmatrix} 1 + N_q \\ N_q \end{pmatrix} \tag{301}$$

The probability for an electron initially at the state of energy, E_1, in the s-band to make a transition to the final state of energy, E_2', in the d-band is defined as:

$$P_{(s)}^{(r)}(E_1)_{sd} = 2 \sum_{\underline{k}_2} P_{(s)}^{(r)}(\underline{k}_1 \longrightarrow \underline{k}_2) \left[1 - F(E_2')\right] \tag{302}$$

where the factor 2 is multiplied because two electrons with opposite spins can occupy the state of same momentum, k_2, according to the Pauli exclusion principle, and $F(E_2')$ is the Fermi function evaluated at the final state, E_2'.

The summation over $\underline{k}_2$ may be replaced by the summation over the phonon momentum, $\underline{q}$, and hence by an integral:

$$\frac{V}{(2\pi)^3} \iiint (d\,\underline{q}) \ldots\ldots \tag{303}$$

provided that we are careful in establishing the integral limits in the integral over q since the density of states at the final state now contain a factor

$$\sqrt{E_o - E_2'}$$

instead of $\sqrt{E}$. Occurrence of the factor $\sqrt{E_o - E}$ instead of $\sqrt{E}$ in the density-of-states function leads to the lower limit in the q-integral given by:

$$q_{min} = \left| k_d - k_s \right| \tag{304}$$

where k_d and k_s are the momenta corresponding to the highest occupied levels in the d- and s-bands, respectively, and are given by those at the Fermi level according to the relations:

$$\begin{aligned} k_s &= \left(\frac{2m_s}{h^2} E_F \right)^{\frac{1}{2}} \\ k_d &= \left[\frac{2m_d}{h^2} (E_o - E_F) \right]^{\frac{1}{2}} \end{aligned} \tag{305}$$

Equation (302) is solved by removing the delta function through integration over the angular variable $\cos\theta = \left(\frac{\underline{k}_1 \cdot \underline{q}}{k_1 q} \right)$. In obtaining Equation (300), we have averaged $(\underline{E} \cdot \underline{q})^2$ over the azimuthal angle Φ with $\underline{k}_1$ as the polar axis; similarly, $(\underline{E} \cdot k_1)$ was substituted for being its value that is obtained later on integrating over $(d^3\underline{k}_1)$.

We now have:

$$P^{(r)}_{(s)}(E_1)_{sd} = \frac{e^2 \hbar^2 m_d E^2 \bar{w}_d k_1}{48\pi^2 m_s^2 (\hbar\omega)^4} \left(1 + \frac{m_s}{m_d} \right)^2 \int_{q_m}^{q_o} q \, dq \, G^{(r)}_{sd}(q) \tag{306}$$

$$\times \left[1 + \left(k_1 \frac{q}{} \right)^2 \Big/ \left(1 + \frac{m_d}{m_s} \right)^2 \right] \left[1 - F(E_1 - rE_q - s\hbar\omega) \right]$$

where $\bar{w}_d$ is the weight factor which comes from the density of states of the d-band, and is the same as that used by Wilson (1938), and where $G^{(r)}(q)$ and E_q have been assumed to be independent of the angular variables. As in Section IV, we shall assume that most of the contributions to Equation (306) come from those electrons which are in the neighborhood and k_1^2 in $[\ldots]$ in Equation (306) may be replaced by the Fermi momentum k_s.

Now, we need to average Equation (306) over all the initial occupied

states in the s-band using the Fermi function, $F(E_1)$, for the s-band, and we have:

$$\left\langle P_{(s)}^{(r)}(s\text{---}d)\right\rangle = \frac{\sum_{k_1} P_{(s)}^{(r)}(E_1)_{sd}\, F(E_1)}{\sum_{k_1} F(E_1)}$$

$$= \frac{e^2 E^2 D_{sd}(K\Theta_s)^2}{32\,\pi^2 m_s k_s E_F u_L^5 (\hbar\omega)^4}\left(\frac{m_d}{m_s}\right)\left(1+\frac{m_s}{m_d}\right)^2 \int_{K\Theta_M}^{K\Theta} E_q^2 dE_q \begin{pmatrix} 1+N(q) \\ N(q) \end{pmatrix}$$

$$\times\left[1+\left(\frac{E_q}{K\Theta_s}\right)^2 \Big/ \left(1+\frac{m_d}{m_s}\right)^2\right] F_{(s)}^{(r)}(q) \qquad (307)$$

where:

$$D_{sd} = \left(\frac{\pi\hbar\, g_{sd}^2 \bar{w}_d}{N_p M}\right)$$

$$\beta F_{)s)}^{(r)}(q) = \int_{-\infty}^{+\infty} dz\, \frac{e^z}{1+e^z}\, \frac{1}{1+e^{z+a}}$$

$$= \left(\frac{a}{e^a-1}\right) \qquad (308)$$

$$a = \beta\,(rE_q + s\,h\,\omega)$$

$$K\Theta_m = \hbar u_L \left|k_d - k_s\right|$$

$$K\Theta_s = \hbar u_L\, k_s\ ; \quad \beta = \frac{1}{KT}$$

Equation (307) involves essentially the same types of integrals as Section IV except for the fact that the lower limit of q-integral in Equation (307) is not necessarily equal to zero.

The net amount of power absorbed per s-electron is defined as:

$$\bar{W}_{sd} = \sum_{r=(\pm)} \hbar\omega \left\{ \langle P_{(-)}^{(r)} \ (s \longrightarrow d) \rangle \ - \ P_{(+)}^{(r)} \ (s \longrightarrow d) \right\} \tag{309}$$

If there are $\bar{n}_s$ number of s-electrons per unit volume that are capable of making transitions to the d-band, the power absorbed per unit volume is simply $\bar{n}_s$ times $\bar{W}_{sd}$. As was explained previously, $\bar{n}_s$ of a ferromagnetic metal is not equal to the total effective number (n_s) of s-electrons, but is equal to $\frac{\chi(T)}{2}$ times n_s.

Upon combining Equation (307) with (309), and after some necessary mathematical manipulations, we finally obtain:

(Power expenditure per unit volume)

$$= \bar{n}_s \ \bar{W}_{sd}$$

$$= \frac{E^2}{2\omega^2} \frac{n_s e^2}{m_s} \frac{\hbar^2 N_p g_{sd}^2 \bar{\omega}_d}{\sqrt{2 m_s E_F^3}\, M K \Theta} \left(\frac{\Theta_s}{\Theta}\right)^2 \left(\frac{m_d}{m_s}\right) \left(1 + \frac{m_s}{m_d}\right)^2 \left(\frac{T}{\Theta}\right)^3 \cdot Z(\omega,T) \tag{310}$$

where

$$Z(\omega,T) = \frac{e^{\mu} \sinh \mu}{\mu} \left[\left[\bar{J}_3(\mu,\alpha) - \frac{(e^{\mu}-1)^2}{(e^{2\mu}-1)} \mu \left[\bar{J}_2(\mu,\alpha) + 2\bar{K}_2(\mu,\alpha) \right] \right] \right. \tag{311}$$

$$\left. + \left(\frac{T}{\Theta_s}\right)^2 \frac{1}{\left(1 + \frac{m_d}{m_s}\right)^2} \left[\bar{J}_5(\mu,\alpha) - \frac{(e^{\mu}-1)^2}{(e^{2\mu}-1)} \mu \bar{J}_4(\mu,\alpha) + 2\bar{K}_4(\mu,\alpha) \right] \right]$$

$$; \quad \mu = \beta \hbar \omega \quad ; \quad \alpha = \beta K \Theta$$

where $\bar{J}_n$ and $\bar{K}_n$ are exactly the same as J_n and K_n defined in Section IV except for the fact that we now have the lower limit of these integrals different from zero: the bars represent such a cutoff at the lower limit. Thus, with the definition of the cutoff:

$$\alpha_M = \beta \, K \, \Theta_M \tag{312}$$

we have:

$$\bar{J}_n(\mu,\alpha) = \int_{\alpha_M}^{\alpha} y^n dy/(e^Y - e^{\mu})(e^{\mu} - e^{-y})$$

$$\bar{K}_n(\mu,\alpha) = \int_{\alpha_M}^{\alpha} y^n dy/(e^y - e^{\mu})(e^{\mu} - e^{-y})(e^y - 1) \tag{313}$$

and similarly, we define the functions $\bar{J}_n^o(\alpha)$ and $\bar{K}_n^o(\alpha)$ such that:

$$\bar{J}_n^o(\alpha) = \lim_{\mu \to o} \bar{J}_n(\mu,\alpha) = \int_{\alpha_M}^{\alpha} y^n dy/(e^y - 1)(1 - e^{-y})$$

$$\bar{K}_n^o(\alpha) = \lim_{\mu \to o} \bar{K}_n(\mu,\alpha) = \int_{\alpha_M}^{\alpha} y^n dy/(e^y - 1)^2 (1 - e^{-y}) \tag{314}$$

The dispersion properties that result from Equations (310) and (311) will be obtained in the following part of this section. It will be shown that the dc damping coefficient that is obtained from Equation (310) agrees exactly with that which was obtained in the theory of the dc conductivity by Wilson (1936, 1938).

C. DAMPING COEFFICIENT AND QUANTUM CORRECTION FACTOR FOR INTERBAND TRANSITIONS

Calculations of the damping coefficient $\Gamma_{ep}(\mu,\alpha)$ and $\Gamma_{ep}^o(\alpha)$ for the $s \longrightarrow d$ transitions are carried out in exactly the same way as in Section IV, and therefore various arguments pertaining to the particular method that is employed in the present theory for computing these quantities shall not be repeated.

Upon using Equation (310) in the relation:

$$\frac{E^2}{2}\,\sigma(\mu,\alpha) = \bar{n}_s\,\bar{W}_{sd} \tag{315}$$

we obtain the following expression for the frequency- and temperature-dependent damping coefficient, $\Gamma_{ep}(\mu,\alpha)$;

$$\Gamma_{ep}(\mu,\alpha) = \frac{9\pi^3}{2}\left(\frac{\bar{n}_s}{n_s}\right)\frac{\hbar^2 N_p\, g_{sd}^2\, \bar{w}_d}{\sqrt{2\, m_s E_F^3}\, M\, K\, \Theta}\left(\frac{m_d}{m_s}\right)\left(1+\frac{m_s}{m_d}\right)^2\left(\frac{\Theta_s}{\Theta}\right)^2\frac{1}{\alpha^3}Z(\mu,\alpha) \tag{316}$$

where $(\bar{n}_s/n_s)$ is the ratio of the effective number of s-electrons which are capable of making the s$\longrightarrow$d transitions over the total effective number of s-electrons, and for a ferromagnetic metal, may be expressed generally in the form:

$$\left(\frac{\bar{n}_s}{n_s}\right) = \tfrac{1}{2}\,\chi(T) = \tfrac{1}{2}\left[1+\frac{\Sigma_o-\Sigma}{\Sigma_o}\right] \tag{317}$$

The numerical values of $\chi(T)$ are available in Table XIV and Table XVI for Ni, Fe, Co and others. For a paramagnetic transition metal, $\bar{n}_s$ and $\chi(T) = 2$. The same is true for a ferromagnetic metal when temperature is well beyond the Curie temperature Θ_c. For a ferromagnetic metal, the quantity of Equation (317) is most important at very low temperatures at which it is nearly equal to $(\frac{1}{2})$. As a result of this, a ferromagnetic metal has a smaller resistivity at low temperatures than a paramagnetic metal if both have the same values for other parameters.

Just as in Section IV, the frequency- and temperature-dependent function $Z(\mu,\alpha)$ of Equation (311) has the property:

$$Z(\mu,\alpha) = Z(-\mu,\alpha) \tag{318}$$

and is independent of frequency in the limiting cases of $\mu \ll \alpha$ and $\mu \gg \alpha$, being a slowly varying function of μ for all values of ω and T except for the case of $1 \ll \mu \ll \alpha$. It is easily shown that $Z(\mu,\alpha)$ acquires the following forms in the two limiting cases;

$$Z(\mu,\alpha) \approx \left\{ \bar{J}_3^o(\alpha) + \left(\frac{T}{\Theta_s}\right)^2 \frac{1}{\left(1+\frac{m_d}{m_s}\right)^2} \bar{J}_5^o(\alpha) \right\} ; \ \mu \ll \alpha, 1 \qquad (319)$$

$$\tilde{Z}(\mu,\alpha) \approx \left[\frac{1}{3}\alpha^3 \left\{ 1 - \left(\frac{\alpha_M}{\alpha}\right)^3 \right\} + 2\int_{\alpha_M}^{\alpha} \frac{x^2 dx}{e^x - 1} + \left(\frac{T}{\Theta_s}\right)^2 \frac{}{\left(1+\frac{m_d}{m_s}\right)^2} \right.$$

$$\left. \times \left[\frac{1}{5}\alpha^5 \left\{ 1 - \left(\frac{\alpha_M}{\alpha}\right)^5 \right\} + 2\int_{\alpha_M}^{\alpha} \frac{x^4 dx}{e^x - 1} \right] \right] ; \ \mu \gg \alpha \qquad (320)$$

both of which are independent of μ and hence of ω, where $\bar{J}_3^o(\alpha)$ and $\bar{J}_5^o(\alpha)$ are given by Equation (314). Upon using Equation (319) in (26), the dc damping coefficient, $\Gamma_{ep}^o(\alpha)$, is found as

$$\Gamma_{ep}^o(\alpha) = \frac{9\pi^3}{2}\left(\frac{n_s}{n}\right) \frac{\hbar^2 N_p g_{sd} \bar{w}_d}{\sqrt{2m_s E_F^3}\, M K \Theta} \left(\frac{m_d}{m_s}\right)\left(1+\frac{m_s}{m_d}\right)^2 \left(\frac{\Theta_s}{\Theta}\right)^2 \frac{1}{\alpha^3}$$

$$\times \ \bar{J}_3^o(\alpha) + \left(\frac{T}{\Theta_s}\right)^2 \frac{1}{\left(1+\frac{m_d}{m_s}\right)^2} \bar{J}_5^o(\alpha) \qquad (321)$$

This agrees exactly with that calculated by Wilson (1938) when we take $\left(\frac{m_s}{m_d}\right)$ to be much smaller than unity and equate $(\bar{n}_s/n_s)$ to unity. For most of transition metals, m_s is actually much smaller than m_d and ignoring the terms containing the factor $\left(\frac{m_s}{m_d}\right)$ is well justified: e.g., for the triad of transition metals, Ni, Pt, and Pd, we have $\left(\frac{m_s}{m_d}\right) \sim 0\left(\frac{1}{10}\right)$ and for Nb, $\left(\frac{m_s}{m_d}\right) \sim 0\ (10^{-2})$. Thus, it is sufficient to take $Z(\mu,\alpha)$ and $\Gamma_{ep}(\alpha)$ in the form:

$$Z(\mu,\alpha) \simeq \frac{e^{\mu}\sinh\mu}{\mu}\left[\bar{J}_3(\mu,\alpha) - \frac{\mu(e^{\mu}-1)^2}{(e^{2\mu}-1)} \left(\bar{J}_2(\mu,\alpha) + 2\bar{K}_2(\mu,\alpha) \right) \right] \qquad (322)$$

$$\Gamma_{ep}^{o}(\alpha) \cong \frac{9\pi^3}{2}\left(\frac{n_s}{n}\right)\frac{h^2 N_p g_{sd}^2 \bar{w}_d}{\sqrt{2m_s E_F^3}\, M K \Theta}\left(\frac{m_d}{m_s}\right)\left(\frac{\Theta_s}{\Theta}\right)^2 \frac{1}{\alpha^3}\bar{J}_3^{o}(\alpha) \qquad (323)$$

$$\tilde{Z}(\mu,\alpha) \approx \left[\frac{1}{3}\alpha^3\left\{1-\left(\frac{\alpha_M}{\alpha}\right)\right\} + 2\int_{\alpha_M}^{\alpha}\frac{x^2\,dx}{e^{x-1}}\right] \qquad (324)$$

According to the results of Section IV, that part of the damping which originates in the intraband s⟶s transitions may be written in the form:

$$\Gamma_{ep}^{o}(\alpha)\Big|_{s\to s} = \frac{9\pi^3}{2}\,\frac{h^2 N_p g_{ss}^2}{\sqrt{2}\, m_s E_F^3\, M K \Theta}\cdot\frac{1}{\alpha^5}J_5^{o}(\alpha) \qquad (325)$$

$$= R_{ss}\frac{1}{\alpha^5}J_5^{o}(\alpha)$$

Then, for a comparison of the contributions by the s → d and s → s transitions, we have the ratio:

$$\frac{\Gamma_{ep}^{o}(\alpha)\Big|_{s\to d}}{\Gamma_{ep}^{o}(\alpha)\Big|_{s\to d}} \cong \left(\frac{n_s}{n}\right)\left(\frac{m_d \bar{w}_d}{m_s}\right)\left(\frac{\Theta_s}{T}\right)^2 \frac{\bar{J}_3^{o}(\alpha)}{J_5^{o}(\alpha)} \qquad (326)$$

where we have put $g_{sd}^2 \cong g_{ss}^2$. Since we know that k_s is of the same order of magnitude as q_o, we have $\Theta_s \approx \Theta$ in order of magnitude. At room temperature, the ratio is mostly due to $\left(\frac{m_d \bar{w}_d}{m_s}\right)$ while, at very low temperatures, the ratio can take on a very large value. For nickel, the data on the electronic specific heat show that $\left(\frac{m_d w_d}{m_s}\right) \approx 10$.

By dividing Equation (311 by (319) and ignoring the terms containing $\left(\frac{m_s}{m_d}\right)$ we find the following as the b-factor for transition metals:

$$b_{ep}(\mu,\alpha) = \frac{e^{\mu}\sinh\mu}{\mu\,\bar{J}_3^{o}(\alpha)}\left[\bar{J}_3(\mu,\alpha) - \mu\,\frac{(e^{\mu}-1)^2}{(e^{2\mu}-1)}\left(\bar{J}_2(\mu,\alpha) + 2K_2(\mu,\alpha)\right)\right] \qquad (327)$$

This satisfies the correspondence requirement:

$$\lim_{\omega \longrightarrow 0} b_{ep}(\mu,\alpha) = 1 \tag{328}$$

In the near infrared limit of $\mu \gg \alpha$, we have:

$$\tilde{b}_{ep}(\mu,\alpha) = \frac{2}{3}\left[\left[1 + \frac{}{\bar{J}_3^{\,o}(\alpha)}\left[\frac{1}{2}\alpha^3\left\{1 - \left(\frac{\alpha_M}{\alpha}\right)^3\right\} + \frac{\alpha^3}{e^{\alpha}-1}\left\{1 - \left(\frac{\alpha_M}{\alpha}\right)^3 \frac{e^{\alpha}-1}{e^{\alpha_M}-1}\right\}\right]\right]\right] \tag{329}$$

D. DISPERSION PROPERTIES OF TRANSITION METALS

The results of the preceding section allow us to write down the optical conductivity, $\sigma(\mu,\alpha)$, in the form,

$$\sigma(\mu,\alpha) = \frac{n_s e^2}{m_s} \Gamma_s \Big/ (\omega^2 + \quad_s^2) \tag{330}$$

where $\Gamma(\mu,\alpha)$ is the sum of the electron-phonon damping coefficient, $\Gamma_{ep}(\mu,\alpha)$, which is given by Equation (316), and the damping terms due to the electron-electron collisions, $\Gamma_{ee}(\mu,\alpha)$, and that due to the impurity scattering, Γ_M^o. Equation (330) includes only the contribution of s-electrons; the d-electron contributions as well as the intraband transitions are neglected. When contributions of both s- and d-electrons need be considered, Equation (330) may be replaced by the more general form:

$$\sigma(\mu, \;) = \left(\frac{n_s e^2}{m_s} \Gamma_s \Big/ (\omega^2 + \Gamma_s^2) + \frac{n_d e^2}{m_d} \Gamma_d \Big/ (\omega^2 + \Gamma_d^{\,2})\right) \tag{331}$$

where the electron-phonon contributions to both Γ_s and Γ_d include the intraband transitions as well as $s \rightleftarrows d$ transitions. In general, it is quite sufficient to take $\sigma(\mu,\alpha)$ in the form of Equation (330) and ignore the d-electron contributions as well as the intraband transitions in s- and d-bands. Therefore, it must henceforth be remembered that whenever

we speak of $\Gamma_{ep}(\mu,\alpha)$ of a transition metal, we mean that the one due to the s$\longrightarrow$d transitions.

The over-all b-factor for the total damping coefficient, $\Gamma(\mu,\alpha)$, is again defined as:

$$b(\mu,\alpha) = \left(\frac{\Gamma^o_{ep}}{\Gamma^o} b_{ep}(\mu,\alpha) + \frac{\Gamma^o_{ee}}{\Gamma^o} b_{ee}(\mu,\alpha) + \frac{\Gamma^o_M}{\Gamma^o}\right) \tag{332}$$

where $b_{ee}(\mu,\alpha)$, Γ^o_{ee}, and Γ^o_M were discussed in Section V, and:

$$\Gamma^o = \left(\Gamma^o_{ep}(\alpha) + \Gamma^o_{ee}(\alpha) + \Gamma^o_M\right) \tag{333}$$

The optical dielectric constant, $\epsilon(\mu,\alpha)$, is obtained from Equation (330) by using the Kramers-Kronig relation. The relevant mathematical arguments which were applied in solving the Kramers-Kronig relation in Section V are just as applicable to transition metals, and thus will not be repeated here.

With the definition of the temperature-dependent quantity, $\bar{\beta}(\alpha)$, such that:

$$\bar{\beta}(\alpha) = b_{ep}(i\mu_o\bar{\beta},\alpha) = R_e\, b_{ep}(i\mu_o\bar{\beta},\alpha) \tag{334}$$

the optical dielectric constant is given by:

$$\left[1 - \epsilon(\mu,\alpha)\right] = \frac{\omega_o^2}{\omega^2 + (\bar{\beta}\Gamma^o)^2}$$

$$: \frac{\omega o^2}{4\pi} = \left(\frac{n_s e^2}{m_s}\right) \tag{335}$$

Thus, all relations of Section V should be applicable to transition metals when we replace b_{ep} and β_{ep} of Section IV by those given by Equations (327 and (334), respectively.

The difference between the results of Section IV on non-transition metals and the results of the present section on transition metals are exhibited most strongly at low temperatures and in the near infrared. Some of these properties will be discussed.

E. SOME LOW-TEMPERATURE AND NEAR-INFRARED PROPERTIES OF TRANSITION METALS

For the discussion on low-temperature and near-infrared properties of transition metals and comparison of these properties with the properties of non-transition metals, it is convenient to define a constant R_{ep}^{sd} given by:

$$\frac{9\pi^3}{2} \frac{\hbar^2 N_p g_{sd}^2 \bar{w}_d}{\sqrt{2m_s E_F^3}\, M K \Theta} \left(\frac{m_d}{m_s}\right)\left(1 + \frac{m_s}{m_d}\right)^2 \left(\frac{\Theta_s}{\Theta}\right)^2 \tag{336}$$

Then, the electron-phonon damping coefficient that was obtained in Equation (316) can be written as:

$$\begin{aligned} \Gamma_{ep}(\mu,\alpha) &= R^{sd} \left(\frac{\bar{n}_s}{n_s}\right) \frac{1}{\alpha^3} \; Z\,(\mu,\alpha) \\ &\simeq R^{sd} \left(\frac{n_s}{n_s}\right) \frac{1}{\alpha^3} \; \bar{J}_3^{o}\,(\alpha)\; b_{ep}\,(\mu,\alpha) \end{aligned} \tag{337}$$

where b_{ep} is that given by Equation (327).

First, let us investigate the low-temperature behavior of $\Gamma^{o}(\alpha)$. According to Equation (337), we have:

$$\Gamma_{ep}^{\;o}(\alpha) \simeq R^{sd} \left(\frac{\bar{n}_s}{n_s}\right) \frac{1}{\alpha^3} \bar{J}_3^{o}\,(\alpha) \tag{338}$$

In the limit, $\alpha \gg 1$, this becomes:

$$\begin{aligned} \Gamma_{ep}^{\;o} &\approx R^{sd} \left(\frac{\bar{n}_s}{n_s}\right) \frac{\bar{e}\,\alpha_M}{\alpha^3} \left[\alpha_M^3 + 3\,\alpha_M^2 + 6\,\alpha_M + 6\right] \\ &= 6\, R^{sd} \left(\frac{\bar{n}_s}{n_s}\right)_o \left(\frac{T}{\Theta}\right)^3 \quad : \alpha_M = 0 \end{aligned} \tag{339}$$

$$= R^{sd} \left(\frac{\Theta_s}{\Theta}\right)^3 \left(\frac{\bar{n}_s}{n_s}\right)_o \bar{e}^{\alpha_M} : \alpha_M > 0 \qquad (340)$$

where:

$$\left(\frac{\bar{n}_s}{n_s}\right) = \begin{cases} \frac{1}{2} & : \text{ferromagnetic metal} \\ 1 & : \text{paramagnetic metal} \end{cases}$$

and $\left(\frac{\Theta_s}{\Theta}\right)$ is of the order of unity, since k_s is in general of the same order as the Debye's cut-off value, q_o. For most of transition metals, α_M is not equal to zero, and hence the equation (340) is to be used. For these metals, the electron-phonon damping coefficient vanishes like $\sim \bar{e}^{\alpha m}$, when T is decreased to the absolute zero. The negative exponential factor was also obtained by Wilson (1938). On the other hand, the damping contributed by the electron-electron collisions and the impurity scattering was shown in the previous chapter to be of the form:

$$\left(\Gamma_{ee}^{o}(\alpha) + \Gamma_M^{o}\right) = \left(R_{ee}\left(\frac{T}{\Theta}\right)^2 + \Gamma_M^{o}\right) \qquad (341)$$

where R_{ee} and Γ_M^{o} are nearly independent of T, and R_{ee} is in general much smaller than R_{ep}.

Therefore, for metals with α_M different from zero, the over-all dc damping coefficient at very low temperatures retains only that part which is given by Equation (341), despite the fact that the electron-phonon part alone constitutes the most of $\Gamma^o(\alpha)$ at higher temperatures. This explains the T^2-dependence of resistivity of some transition metals which has been observed by various experimenters. We summarize the above discussion by writing down Γ^o as:

$$\Gamma^o(\alpha) \approx \left(R_{ee}\left(\frac{T}{\Theta}\right)^2 + \Gamma_M^{o}\right) : \begin{pmatrix} \alpha \gg 1 \\ \alpha_M > 0 \end{pmatrix} \qquad (342)$$

The same was found to be true even for a noble metal due to the rapid decrease, $\sim T^5$ of $\Gamma_{ep}^{o}(\alpha)$ with decrease in temperature, although not as rapid as in Equation (340).

Whether there is a transition metal with $\alpha_M = 0$ is a question that is yet to be answered. For such a metal, the s d

transitions at the Fermi level can take place without a finite mometum transfer implying that phonons with the average energy of the order of ~ (KT) are capable of stimulating the s$\longrightarrow$d transitions even at a very low temperature. The following discussion based on a rather qualitative description of the properties of the s- and d-bands suggests that, out of all transition metals and likewise of all multivalent metals for which interband transitions are important, there can exist a metal with $\alpha_M = 0$, if the electrons in the outer band (s- band) are neither more nor less in number than what is required to completely close the empty states of the inner band (d- band) that is involved in the interband transitions. Three transition metals which do satisfy such a condition are the triad, N_i, P_t, and P_d. For nickel, the three possible configurations are ($3d^8$ $4s^2$), ($3d^9$ $4s^1$), and ($3d^{10}$ $4s^0$). For platinum, they are the configurations,($5d^8$ $6s^2$), $5d^9$ $6s^1$), and ($5d^{10}$ $6s^0$). For palladium, they are the configurations, ($4d^9$ $5s^1$) and $4d^{10}$ $5s^0$). In all three metals, the s-electrons plus the d-electrons amount to 10 electrons which can exactly close the d-band. Further, it is known that all three metals have an approximately 0.6 electron per atom in the s-band and the same number of holes in the d-band. That these metals can have $\alpha_M = 0$ and hence

$$k_d = k_s$$

may be shown by computing the total number of empty states in the d-band and the total number of s-electrons from the density-of-states functions of the two bands. At very low temperature, the Fermi function, (F(E), is nearly equal to unity, and we have:

$$n_s = \int_0^{E_F} \rho_s\ (E)\ dE \quad ; \quad n_d^o = \int_{E_F}^{E_o} \rho_d\ (E)\ dE \tag{343}$$

where n_a^o is the number of empty states in the d-band and the density-of-states functions, ρ_s (E) and ρ_d (E), are given by:

$$\delta_s\ (E) = \frac{\sqrt{2}}{\pi^2} \left(\frac{m_s}{h^2}\right)^{3/2} \sqrt{\equiv}$$

$$\delta_d\ (E) = \frac{\sqrt{2}}{\pi^2} \left(\frac{m_d}{h^2}\right)^{3/2} \sqrt{E_o - E} \tag{344}$$

Using these in Equation (343), we obtain:

$$n_s = \frac{1}{3\pi^2}\left(\frac{2\ ms}{h^2}\ E_F\right)^{3/2} = K_s^3/3\pi^2$$

$$n_d^o = \frac{1}{3\pi^2}\left(\frac{2\ md}{h^2}\ (E_o - E_F)\right)^{3/2} = K_d^3/3\pi^2 \qquad (345)$$

Therefore, we find that $k_d = k_s$ for those metals for which n_s is identically equal to n_d^o.

Although the above result may not lead us to a definite conclusion, due to the use of the simplified forms of ρ_s ρ_d, it does permit us to suggest that, if there is any metal which has $\rho_M = 0$, the triad of transition metals N_i, P_t, and P_d, are the most likely ones. In fact, according to the observations by MacDonald and Mendelssohn (1950), the low-temperature resistivity of platinum has been interpreted as having a T^2-dependence on temperature, which, if real, may be attributed to $\Gamma_{ee}^o(\alpha)$. On the other hand, if platinum has $\alpha_M = 0$ so that equation (339) is applicable, the low-temperature resistivity should have both T^2- and T^3-dependence on temperature coming from Γ_{ee}^o and Γ_{ep}^o, respectively. The total damping coefficient will then be given by:

$$\Gamma_{Pt}^o(\alpha) \approx 6\ R^{sd}\left(\frac{T}{\Theta}\right)^3 + R_{ee}\left(\frac{T}{\Theta}\right)^2 + \Gamma_M^o \qquad (346)$$

where the first term is not necessarily much smaller than the rest unless T is very near the absolute zero: e.g. at $\left(\frac{T}{\Theta}\right) = 1/20$, we have:

$$\Gamma_{ep} \sim Rep\ 10^{-3}$$
$$\Gamma_{ee} \sim Ree\ 10^{-3} \qquad (347)$$

and, since R_{ep} is generally larger than R_{ee} by a factor of 10 or more, Γ_{ep}^o is not unimportant even at a temperature as low as $10 \sim 20^oK$.

It is not difficult to see that, even if the low-temperature resistivity exhibits the T^3- term, a clear distinction between T^3- & T^2- terms is not an easy task at low temperatures, and it is thus very possible that this term has been confused with the T^2- term in the past measurements.

Let us investigate the low temperature properties of the quantum-corrected damping coefficient $\Gamma_{ep}(\mu,\alpha)$ in the near infrared, i.e. $\mu \gg \alpha \gg 1$. The low temperature properties of $\Gamma_{ep}(\mu, \alpha)$ in the spectral

ranges, $\mu \ll \alpha$, will be left to the future chapter dealing with the absorption at very low temperatures.

We saw in the previous chapters that, unlike the dc damping coefficient, $\Gamma_{ep}^{o}(\alpha)$, the quantum-corrected damping coefficient maintains a relatively large value in the near infrared even at $0^{o}K$. It will be shown that a similar quality is also found in transition metals, and that this is true for all transition metals regardless of whether α_M vanishes or not provided that α_M is of a much smaller order of magnitude than α.

At very low temperatures, the b-factor for the near infrared spectrum reduces to:

$$\tilde{b}_{ep}(\mu,\alpha) \approx \frac{1}{3\bar{J}_3^{o}(\alpha)}\,\alpha^3\left[1-\left(\frac{\alpha_M}{\alpha}\right)^3\right] \tag{348}$$

When we use this in Equation (337), we obtain:

$$\Gamma_{ep}(\mu,\alpha) \approx \left(\frac{\bar{n}_s}{n_s}\right)_o \frac{1}{3} R^{sd}\left[1-\left(\frac{\Theta_M}{\Theta}\right)^2\right]$$

$$\approx \frac{1}{6} R^{sd} \quad : \text{F. M.}$$

$$\approx \frac{1}{3} R^{sd} \quad : \text{P. M.} \tag{349}$$

which is independent of both ω and T, where we have taken $\Theta_M \ll \Theta$. Thus, unlike $\Gamma_{ep}^{o}(\alpha)$, the negative exponential factor, $e^{-\alpha_M}$, cancels out and the electron-phonon scattering makes large contribution even at very low temperatures. This implies further that the contributions to the damping by the electron-electron collisions and impurity scattering will be important at very low temperatures in the near infrared only if they are important at higher temperatures. When these two processes need be considered, we use the formula:

$$\tilde{\Omega}_o(\mu,\alpha) = \Gamma_{ep}^{o}\,\tilde{b}_{ep} + \Gamma_{ee}(\alpha) + \Gamma_M^{o}$$

$$\cong \frac{1}{6} \times (0)\, R^{sd} + R_{ee}\frac{1}{\alpha^2} + \Gamma_M^{o}$$

$$: \ \alpha \gg 1 \tag{350}$$

while $\bar{\tilde{\Omega}}_o(\alpha)$, which appears in $\epsilon(\mu,\alpha)$, becomes

$$\bar{\tilde{\Omega}}_o(\alpha) \approx R_{ee}\frac{T}{\alpha^2} + \Gamma_M^o$$

$$= \Gamma_M^o : T = 0^\circ K \tag{351}$$

In Equation (350), $\tilde{\Omega}_o$ has a weak T^2- dependence while in Equation (351), $\bar{\tilde{\Omega}}_o(\alpha)$ has a relatively strong T^2 -dependence on temperature, since, in general, $R_{ep} \gg R_{ee} \gtrsim \Gamma_M^o$. As a specific example, let us investigate the near infrared absorptivity at very low temperature. According to Section V, the bulk absorptivity, A_B, is given by:

$$A_B \approx \sqrt{\frac{m_s}{\pi n_s e^2}}\ \tilde{\Omega}_o G_a \tag{352}$$

where:

$$\tilde{\Omega}_o \tilde{G}_\sigma = \left(\tilde{\Omega}_o + \frac{\omega^2}{\Omega_{ee}}\right)$$

$$\Omega_{ee} = \frac{10^{24}}{1.49}\left(\frac{\Theta^2}{R_{ee}}\right) \tag{353}$$

and $\tilde{\Omega}_o$ is given by Equation (350). In general, $R_{sd} \gg R_{ee}$, and when this is true, Ω_{ee} is also much larger than ω_o so that $\tilde{\Omega}_o \tilde{G}_\sigma \approx \frac{1}{6}\chi(0) R^{sd}$ for a reasonably pure sample. Thus the total near infrared absorptivity, A, of a transition metal is:

$$A \approx \frac{1}{3}\chi(0)\frac{R_{sd}}{\omega_o} + \frac{3}{4}\frac{\nu_F}{C} \tag{354}$$

where the second term is the absorption due to the anomalous skin effect and $\nu_F \cong \left(10^{-3} \sim 10^{-2}\right) C$. The numerical value of R_{sd} can be determined from the room temperature value of $\Gamma_{ep}^o(\alpha)$ since the complete temperature-dependence is specified in Equation (238), and $\Gamma_{ep}^o(\alpha)$ is easily found from the optical data and also from dc electric measurements.

The temperature-dependence characteristics that have been discussed

TABLE IX. NUMERICAL VALUES OF $J_5^\circ(\alpha)$

$\frac{1}{\alpha} = \frac{T}{\Theta}$	$J_5^\circ(\alpha)$
0	124.43
0.05	124.42
0.076923	123.14
0.1	116.38
0.125	101.48
0.16667	70.873
0.2	50.263
0.25	29.488
0.33333	12.771
0.5	3.2293
0.66667	1.1199
0.83333	0.47907
1	0.23662
1.25	0.098845
1.52	0.0451

TABLE X. TEMPERATURE-DEPENDENCE OF DAMPING COEFFICIENT IN GOLD

($\Theta = 175^{\circ}K$)

T ($^{\circ}K$)	$\Gamma^{\circ}_{ep}(T) / \Gamma^{\circ}_{ep}(273^{\circ})$ calculated	$\Gamma^{\circ}_{(T)} / \Gamma^{\circ}(273^{\circ})$ observed
273	1	1
87.43	0.2645	0.2551
78.86	0.2276	0.2187
57.8	0.1356	0.1314
20.4	0.00604	0.0058
18.9	0.00346	0.0035
14.3	0.00117	0.00137
12.1	0.00051	0.00048
11.1	0.00033	0.00030
4.2	3×10^{-6}	3×10^{-6}

TABLE XI.

Metals	$\sigma_o \times 10^{-16}$ esu (Present Theory)	$\sigma \times 10^{-16}$ esu (Electrical Meas.)	$\frac{\sigma_o \text{ (Meas)}}{\sigma_o \text{ (Calc.)}}$	Optical Data Used to Calculate Theoretical Value of σ_o
Al	14	15 (Meas. by B. & C.)	1.1	Beattie & Conn (1955)
	18	22 (Meas. by Golovashkin et al)	1.2	Golovashkin et al (1960)
Ni	4.8	4.6 (Meas. by B. & C.)	1.0	Beattie & Conn (1955)
Ga	3.5	3.5 (I.C.T., 1936)	1.0	Schulz (1957)
Hg	0.94	0.94 (I.C.T., 1936)	1.0	Schulz (1957)
Ti	1.6	1.64 (H. & B.)	1.0	Hass & Bradford (1957)
Sn	5	7.8 (Bulk) (Am. Inst. Phys. Hb., 1957)	1.6	Hodgson (1955)
Zn	4*	15 (Bulk) (Am. Inst. Phys. Hb., 1957)	3.8	Hodgson (1955)
Cu	12	13.5 (Meas. by S. & P.)	1.1	Schkliarevskii & Padalka (1959)

*The spectral range in which the optical data are available was too close to the region, and hence this value is not completely reliable.

By "Bulk" is meant that σ_o values quoted are obtained for bulk samples while the optical data were taken with thin layers or mirrors.

TABLE XII

$\frac{T(°K)}{\Theta c}$	F_e		C_o, N_i		$j = \frac{1}{2}$ (theory)	
	$\left(\frac{\Sigma}{\Sigma_o}\right)$	$\frac{1}{2} \chi$ (T)	$\left(\frac{\Sigma}{\Sigma_o}\right)$	$\frac{1}{2} \chi$ (T)	$\left(\frac{\Sigma}{\Sigma_o}\right)$	$\frac{1}{2} \chi$ (T)
0	1	0.500	1	0.500	1	0.500
0.1	0.996	0.502	0.996*	0.502	1.000	0.500
0.2	0.99	0.505	0.99	0.505	1.000	0.500
0.3	0.975	0.512	0.98	0.510	0.997	0.501
0.4	0.95	0.525	0.96	0.520	0.983	0.508
0.5	0.93	0.535	0.94	0.530	0.958	0.521
0.6	0.90	0.550	0.90	0.550	0.907	0.546
0.7	0.85	0.575	0.83	0.585	0.829	0.585
0.8	0.77	0.615	0.73	0.635	0.710	0.645
0.85	0.70	0.650	0.66	0.670	0.630	0.685
0.9	0.61	0.695	0.56	0.720	0.525	0.737
0.95	0.46	0.770	0.40	0.800	0.380	0.810
1.00	0	1.000	0	1.000	0	1.000

* For N_i only

Computed from the Am. Inst. Phys. Hdb.

TABLE XIII. THEORETICAL VALUES OF MICROSCOPIC PARAMETERS

Metals	$N\left(\frac{m}{m^*}\right)$ x 10^{-22} (cm^{-3})	$\mathring{\Gamma}_{ep}$ x 10^{-14} (sec^{-1})	$\tilde{b}_{ep}$	σ_o x 10^{-16} (esu)	$\mathring{\Gamma}_{ee}$ x 10^{-12} (sec^{-1})	v_f x 10^{-8} (cm/sec)	γ ergs. cm^{-3} / deg^2	τ_r^o x 10^{14} (sec.)	ω_o x 10^{-15} ($sec.^{-1}$)
Cu	4.2	0.533	1.2	20	3.1	1,3	483	1.8	12
Ni (I)	1.2	0.625	1.24	4.8	50	0.8	424	0.9	6.2
Ni (II)	0.8	1.1	1.24	2.0	73	0.7	424	0.6	5.1
Al	7.1	1.12	1.2	18	4.2	2.7	718	0.9	15
Al (78^oK)	6.8	0.141	5.94	144	0.3	2.4	734	7	15
Pt	5.7	10.6	1.1	1.4	1.7	1.3	692	0.1	14
Ir	8.1	17.1	1.1	1.2	1.7	1.7	449	0.06	16
Ti	2.2	3.52	1.3	1.6	---	---	---	0.3	8.4
Hg	7.65	21.4	1.00	0.94	1.2	1.55	620	0.05	16
Ga	14.6	10.7	1.07	3.5	0.28	1.88	860	0.1	22

TABLE XIII - Continued.

Metals	$N\left(\frac{m}{m^*}\right)$ $\times 10^{-22}$ (cm^{-3})	Γ^{o}_{ep} $\times 10^{-14}$ (sec^{-1})	$\tilde{b}_{ep}$	$\sigma_o \times 10^{-16}$ (esu)	Γ^{o}_{ee} $\times 10^{-12}$ (sec^{-1})	$v_f \times 10^{-8}$ (cm/sec)	γ ergs. cm^{-3} / deg^2	$\tau^{o}_{r} \times 10^{14}$ (sec.)	ω_o $\times 10^{-15}$ ($sec.^{-1}$)
Zn	1.26	0.94	---	16	---	---	---	1.1	6.4
Sn	6.16	3.0	---	8	---	---	---	0.3	14

C_u, N_i(I): Beattie & Conn (1955)

N_i (II) : Shkliarevskii & Padalka (1959)

All metals for room temperature except for this
γ= Sommerfeld constant for electronic specific heat
For other references on optical data, refer to Tables VI and XI.

TABLE XIV

Elements	Curie Point Θ_c (°C)	Σ_o	Σ (293°K)	$\frac{1}{2}\chi = \frac{1}{2}\left[1 + \frac{\Sigma_o - \Sigma}{\Sigma_o}\right]$ (293°K)
Fe	770	221.9	218.0	0.509
Fo	1131	162.5	161	0.505
Ni	358	57.50	54.39	0.527
Gd	16	253.5	0	1.000
Dy	-168	-----	0	1.00(0)

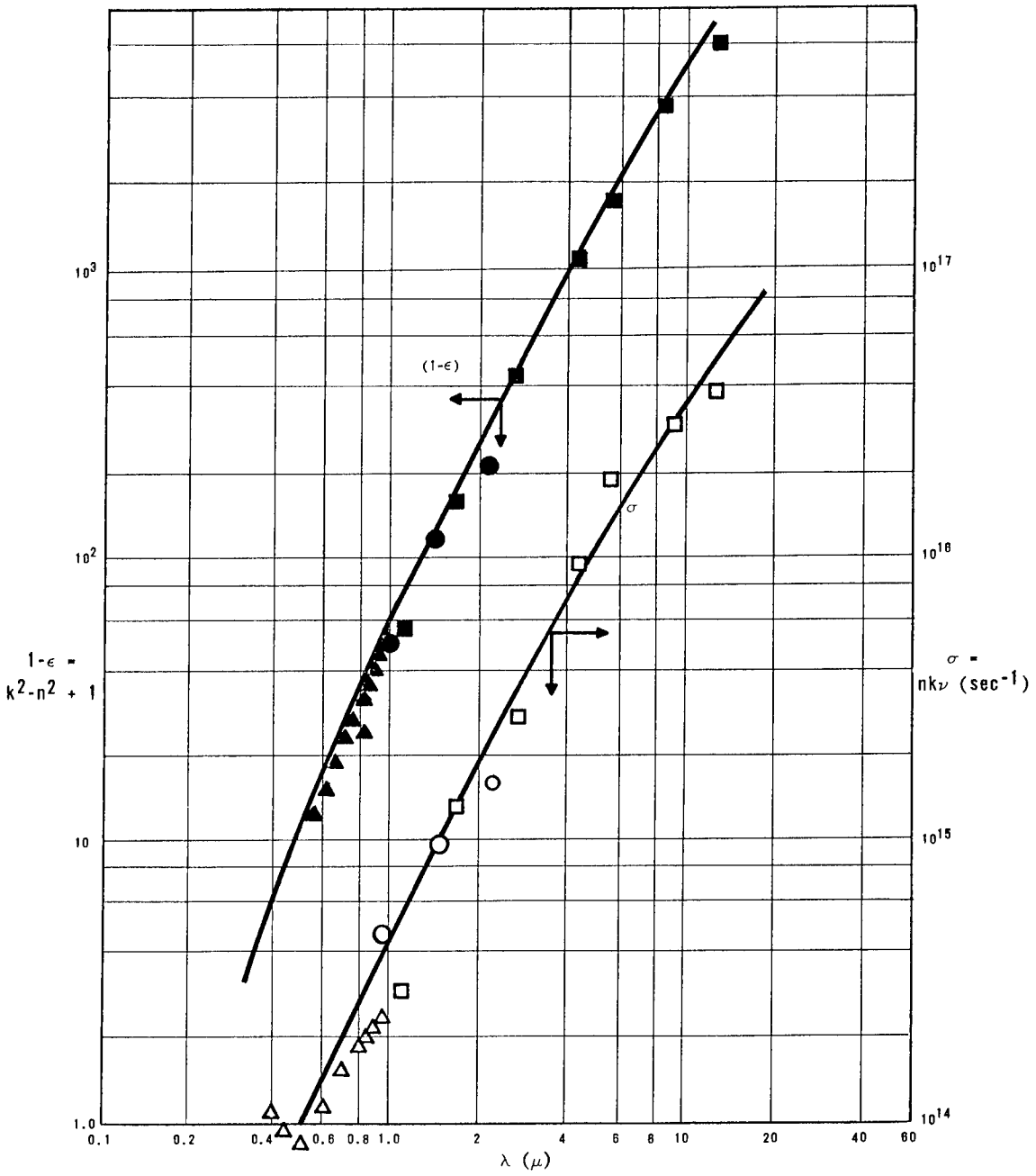

Figure 20. Silver

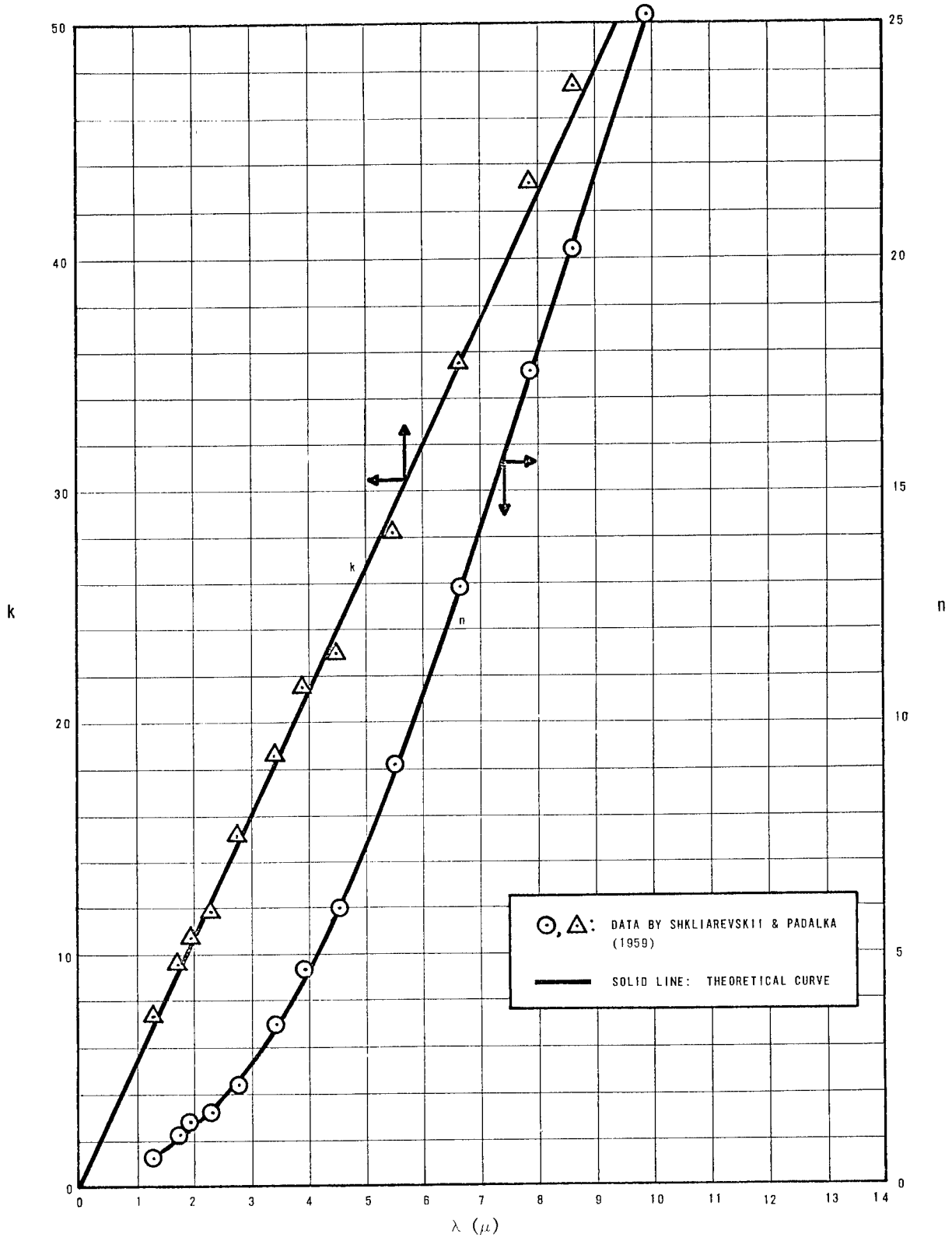

Figure 21. Gold (~ 300°K) n, k versus λ

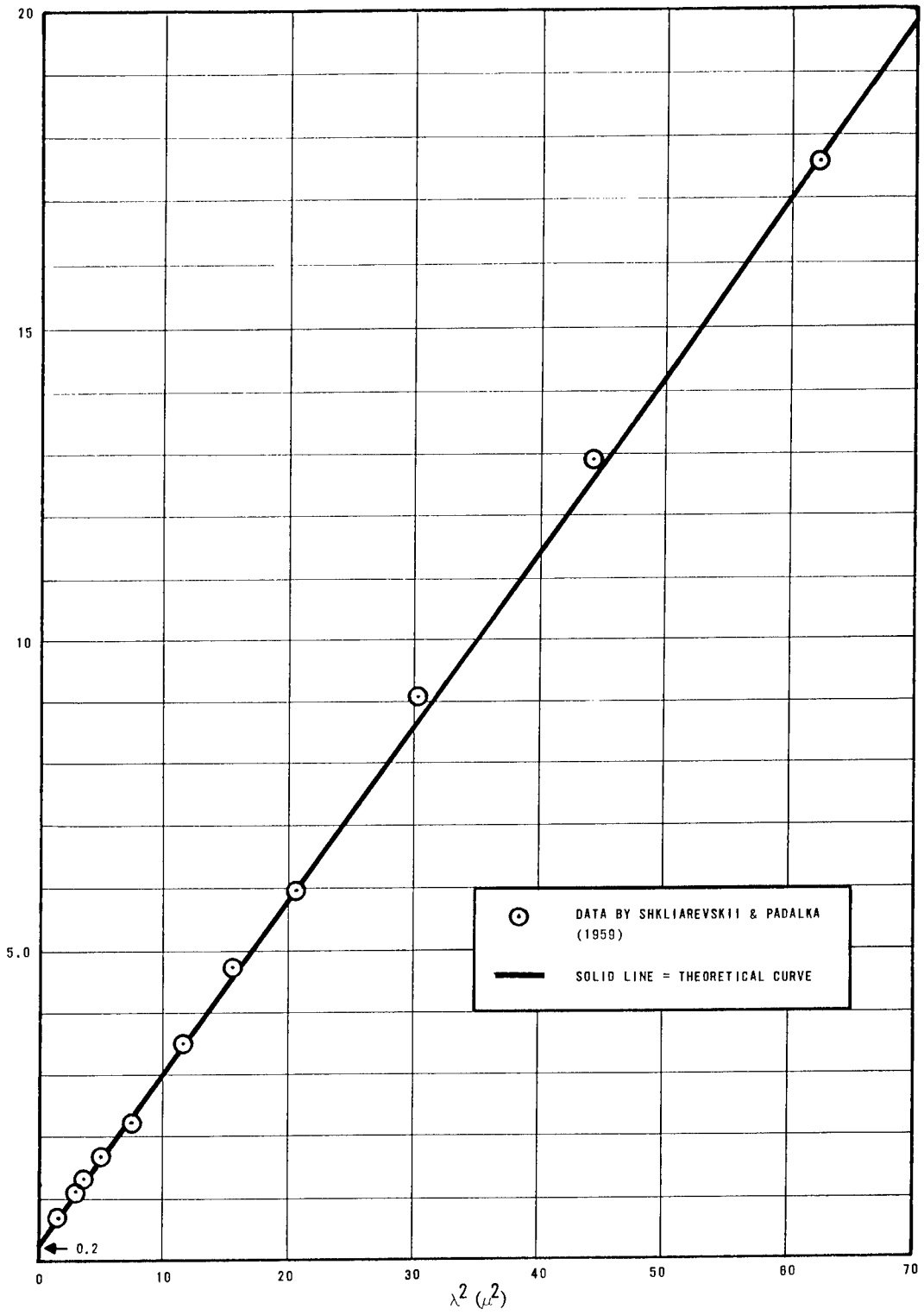

Figure 22. Gold (~ 300°K) n versus λ^2

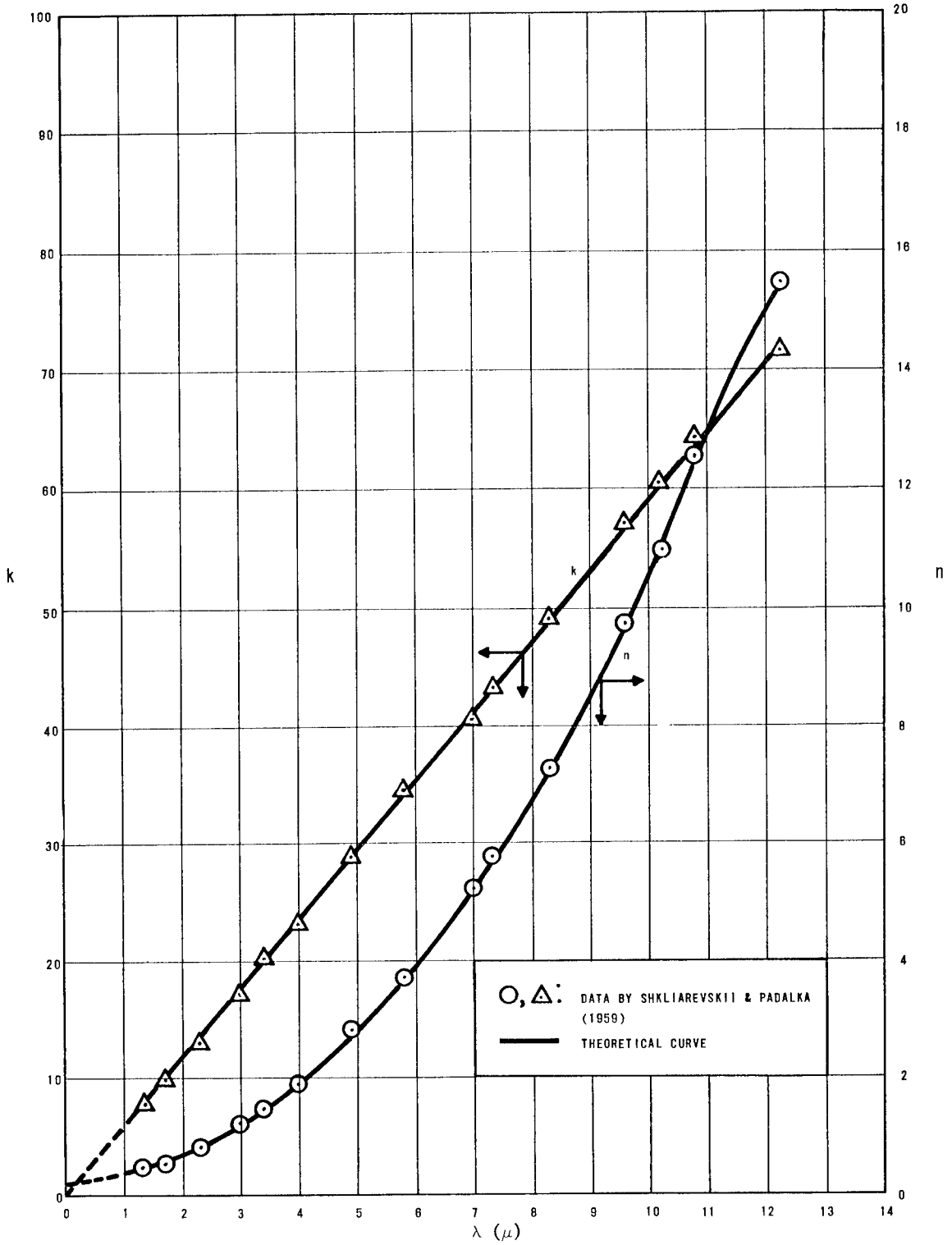

Figure 23. Copper (~ 300°K) n,k versus λ

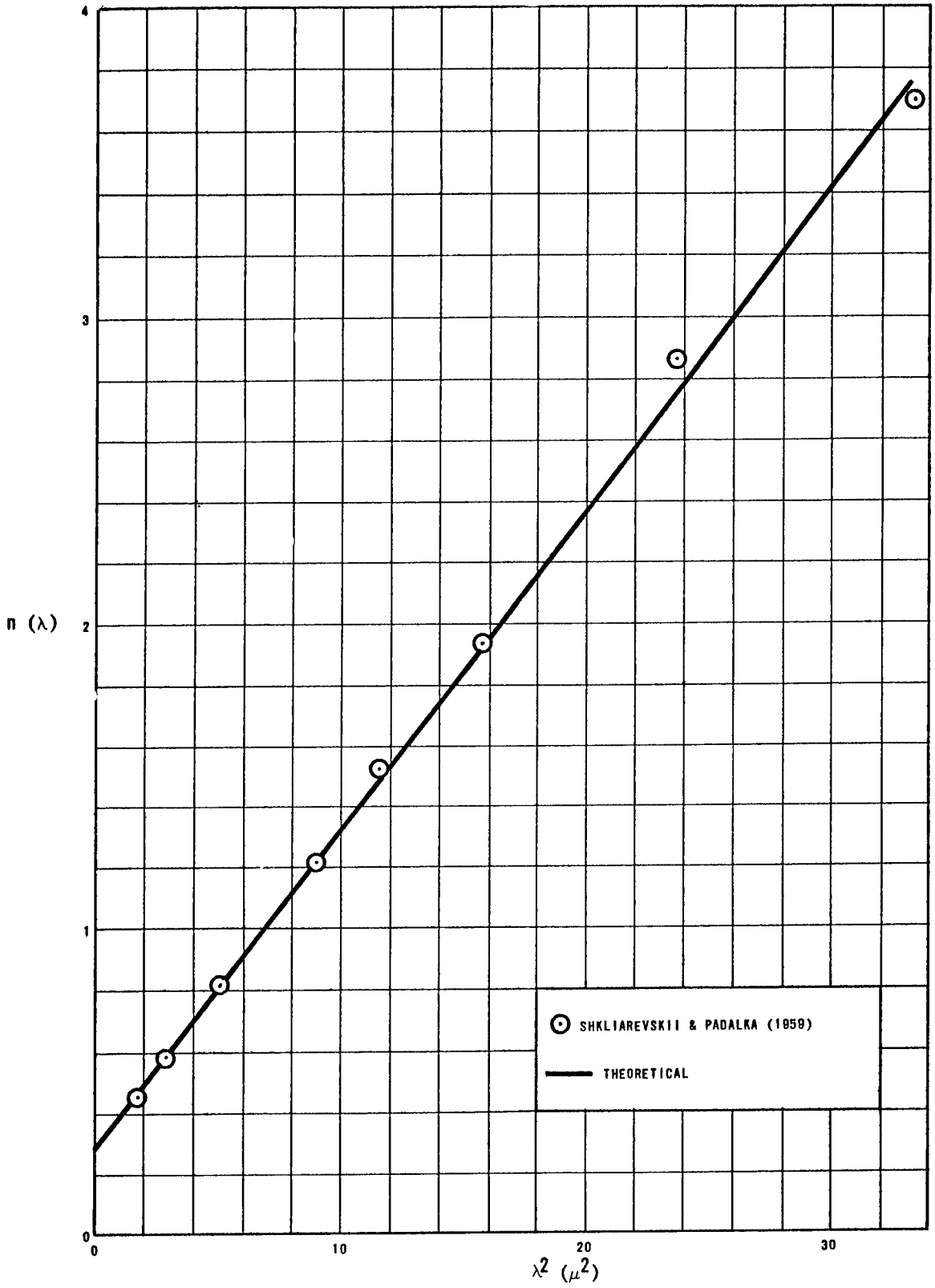

Figure 24. Copper (~ 300°K) n versus λ^2

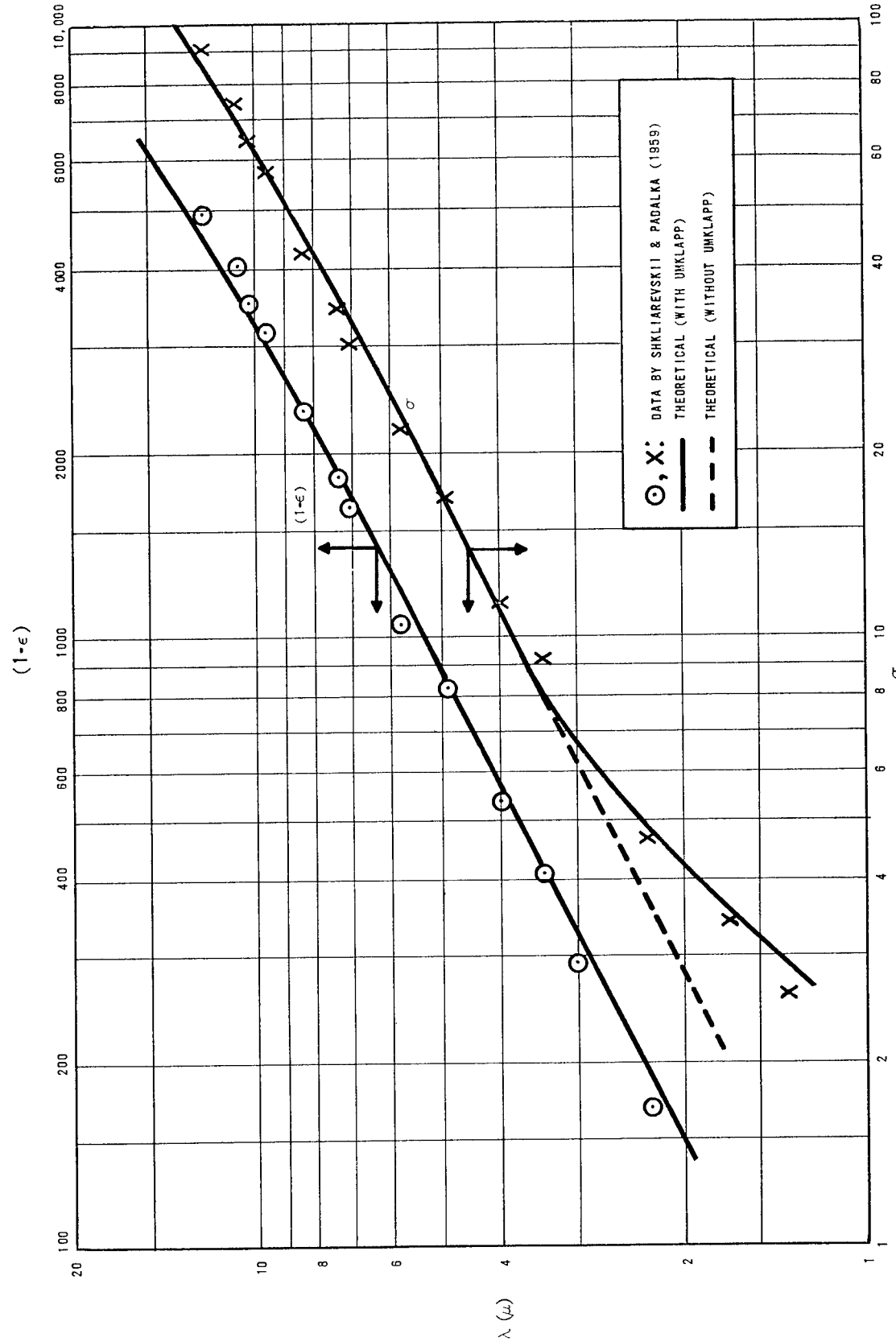

Figure 25. Copper (~ 300°K) (1-ϵ) and $\frac{\sigma}{c}$ versus λ

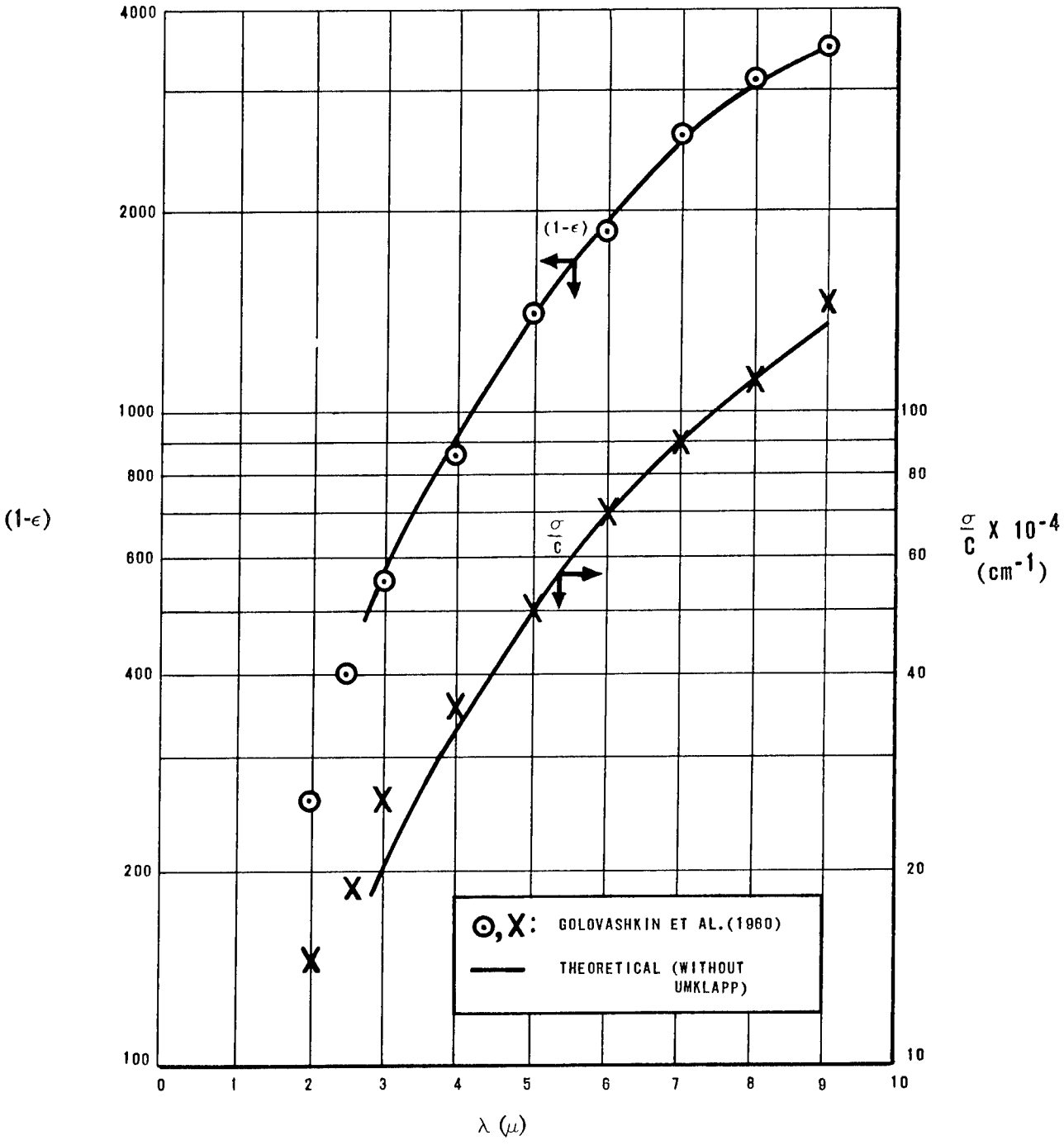

Figure 26. Aluminum (295°K) (1-ϵ) and $\frac{\sigma}{c}$ versus λ

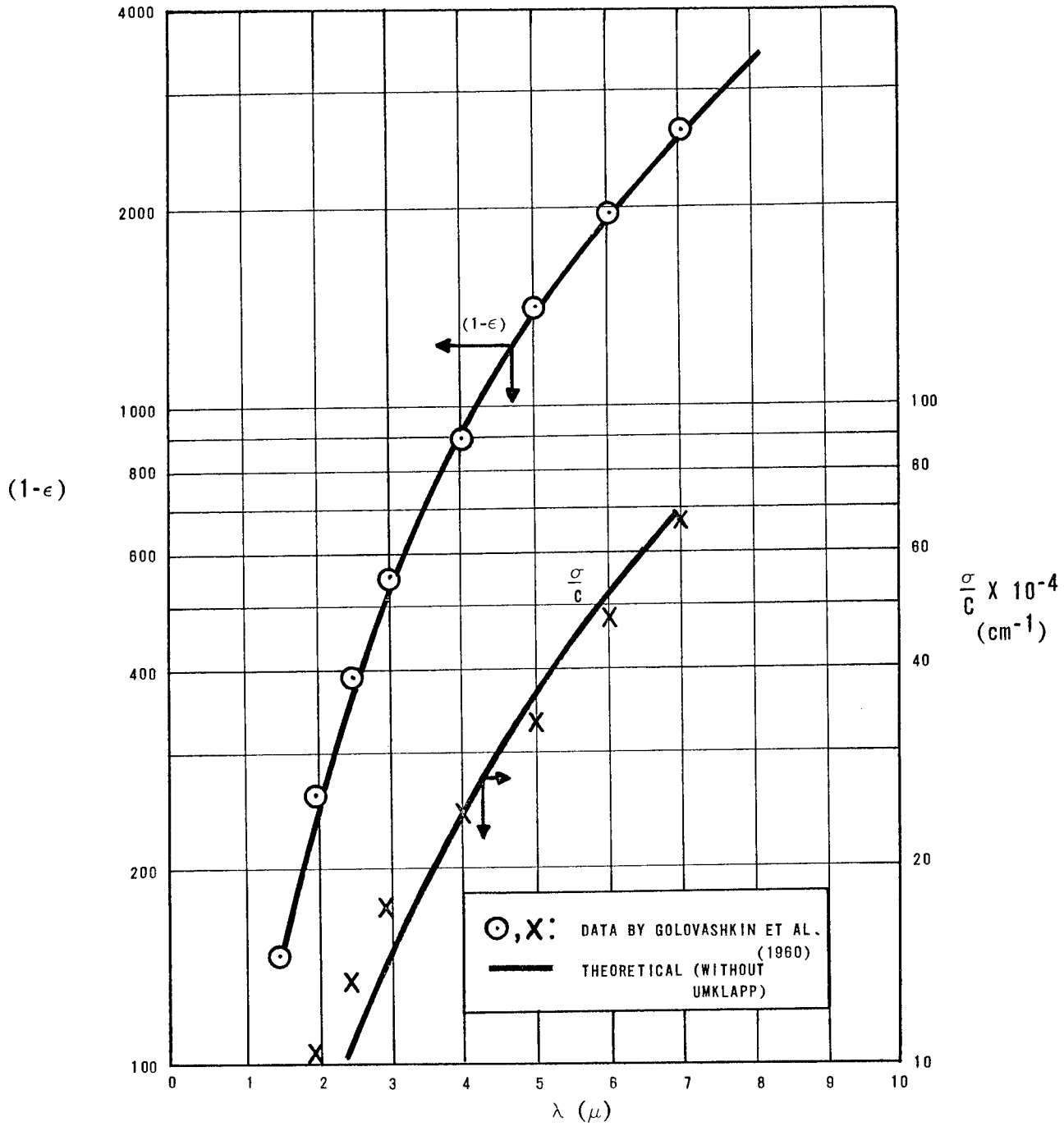

Figure 27. Aluminum (78°K) (1-ϵ) and $\frac{\sigma}{c}$ versus λ

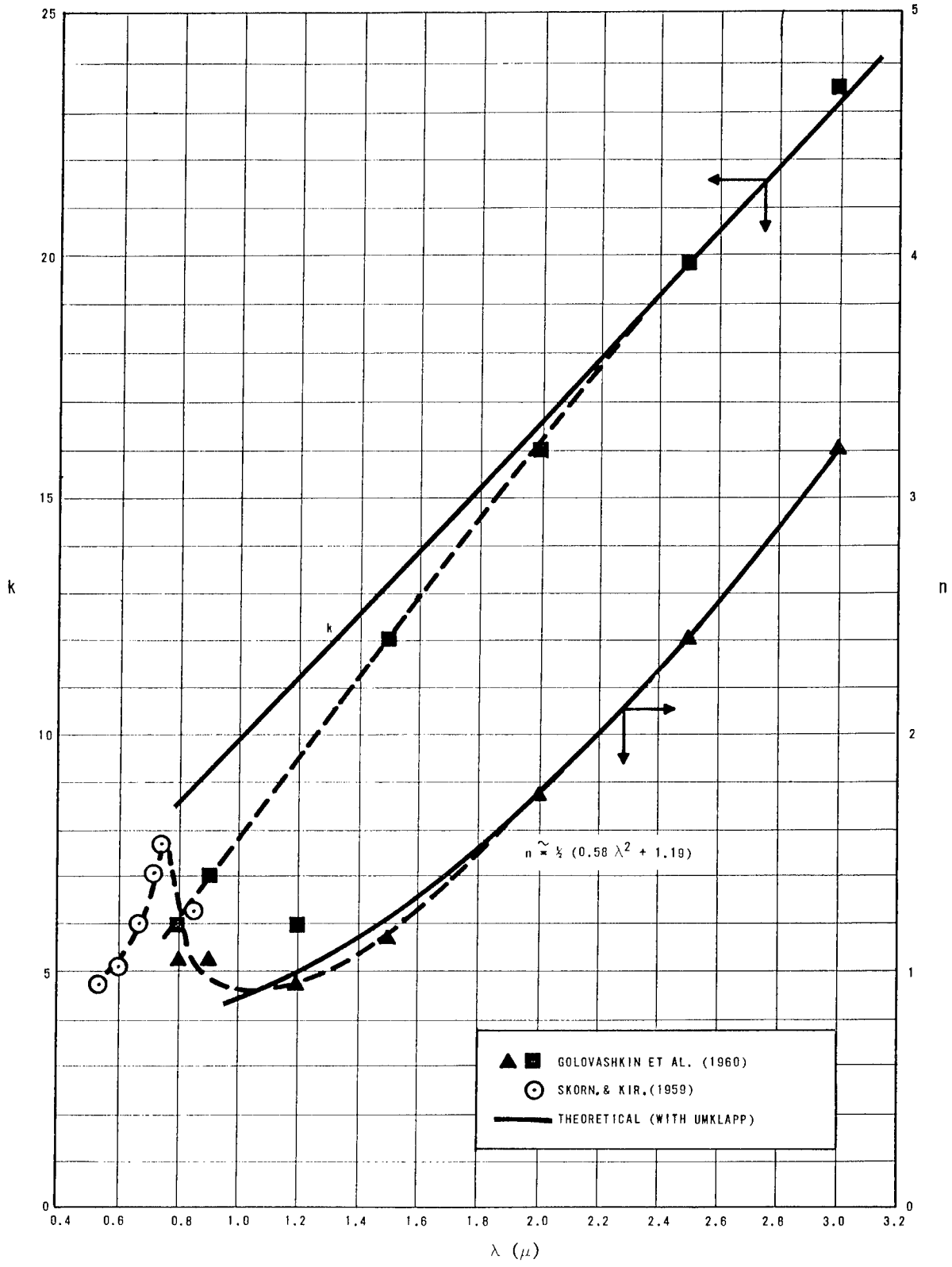

Figure 28. Aluminum (295°K) n, k versus λ

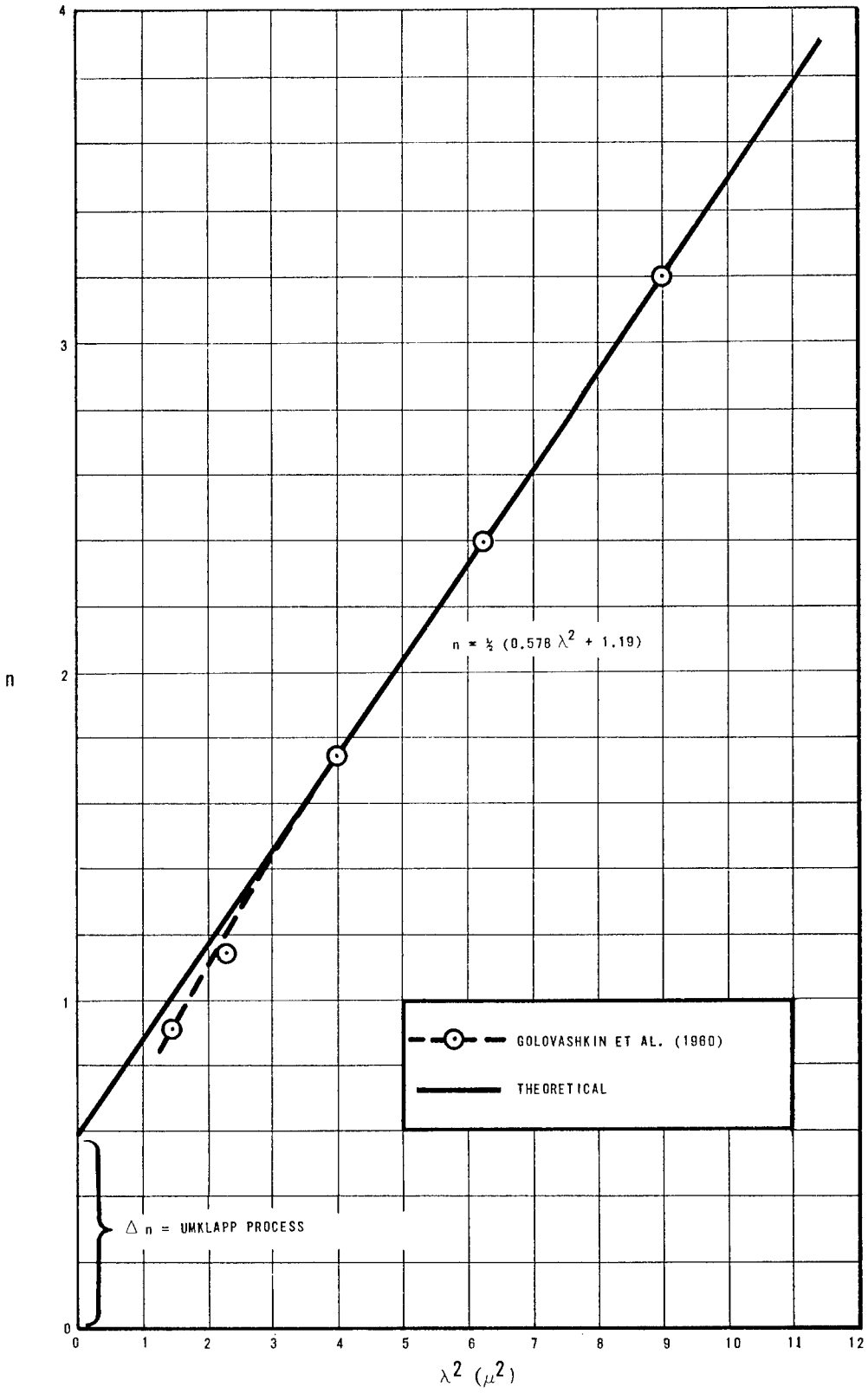

Figure 29. Aluminum (295°K) n versus λ^2

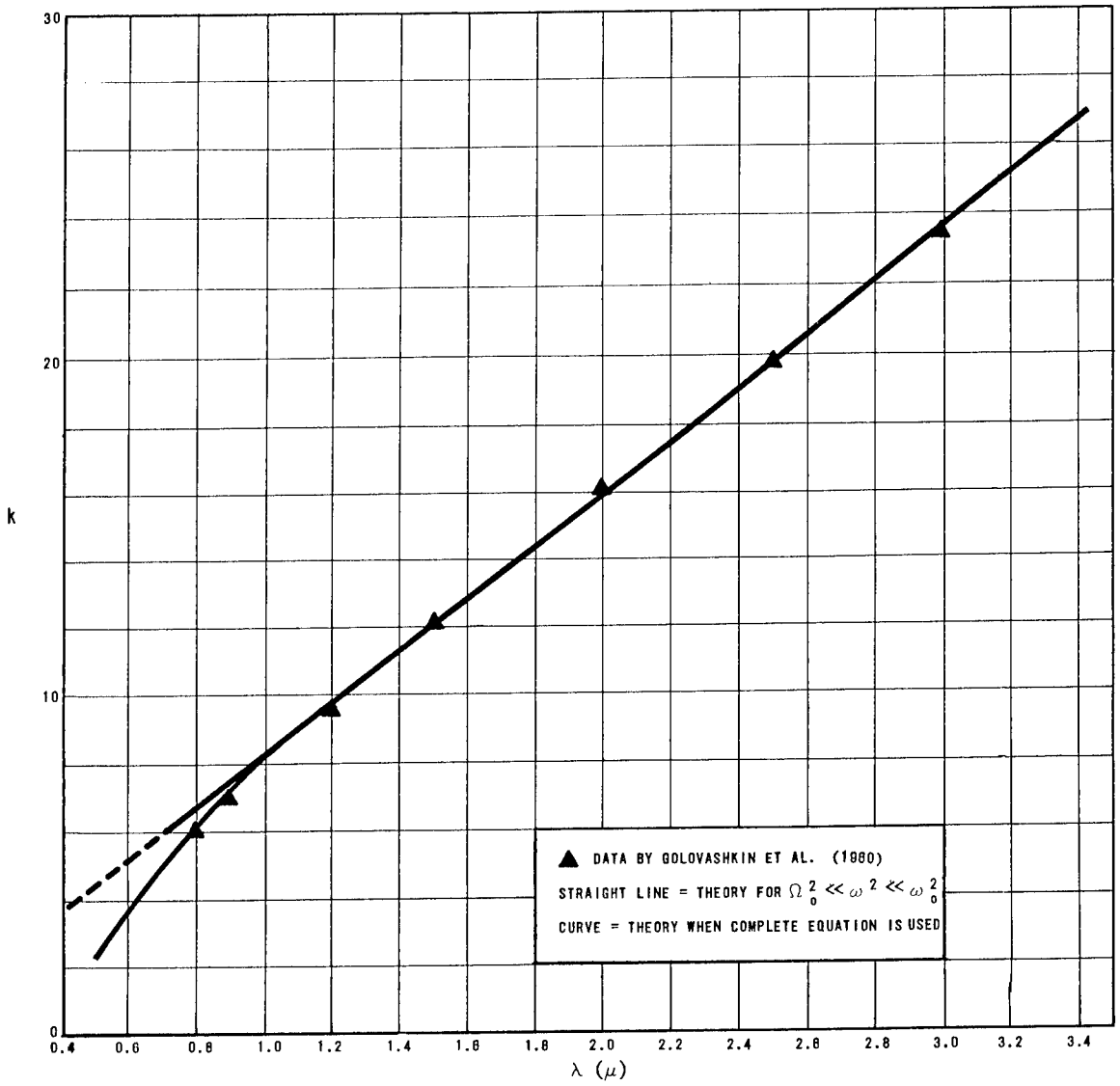

Figure 30. Aluminum (78°K) k versus λ

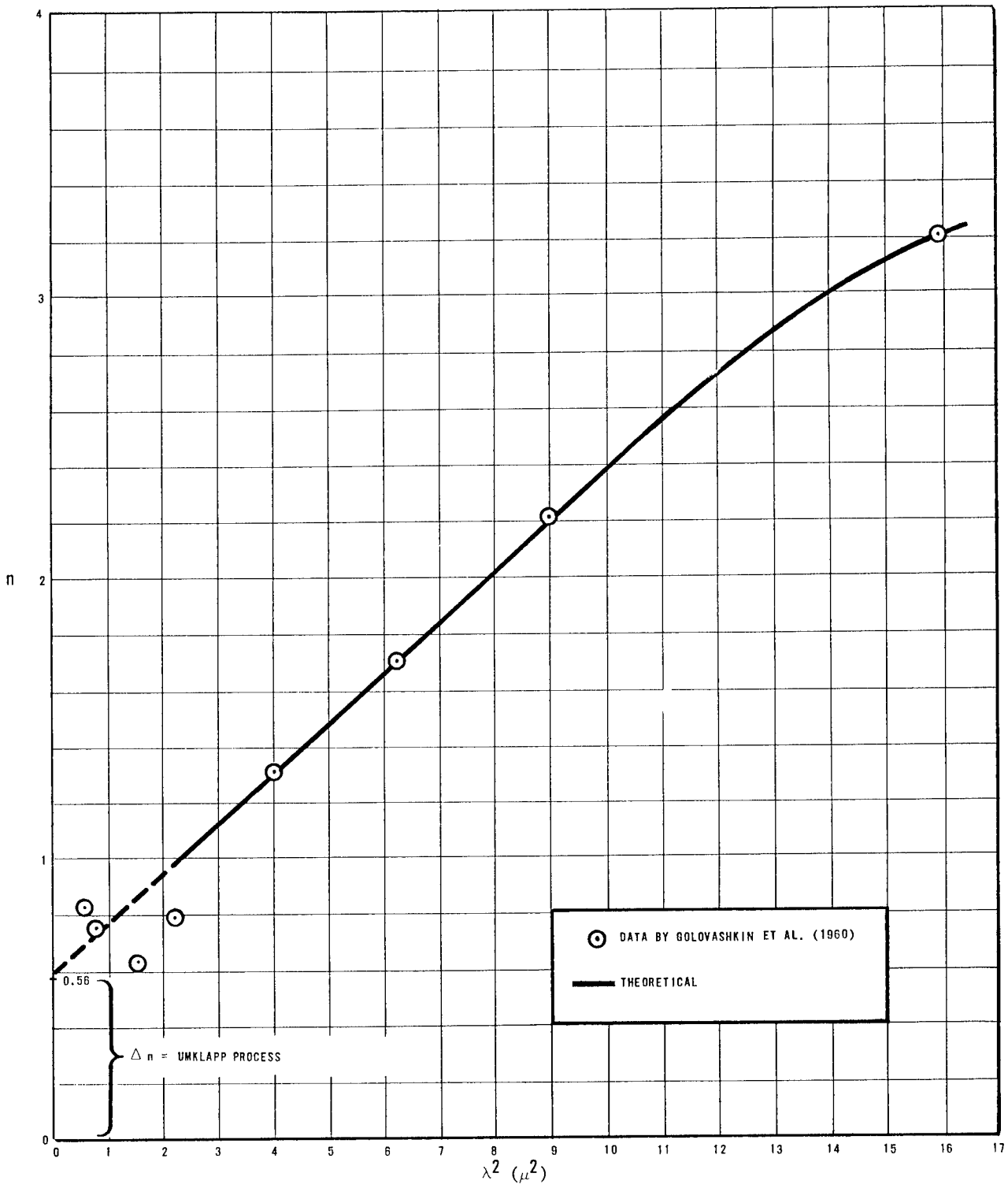

Figure 31. Aluminum (78°K) n versus λ^2

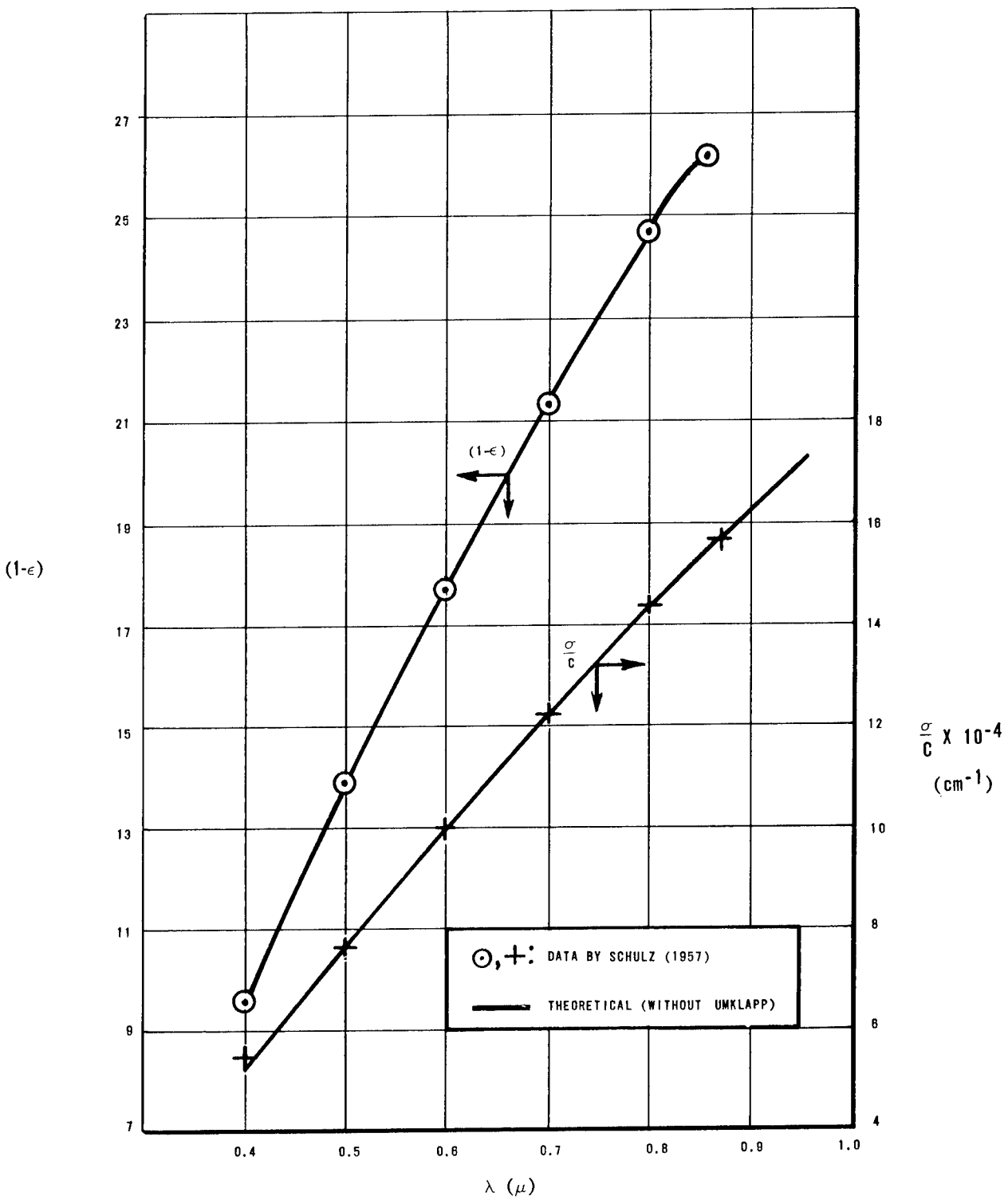

Figure 32. Mercury (~ 300°K) (1-ϵ) and $\frac{\sigma}{c}$ versus λ

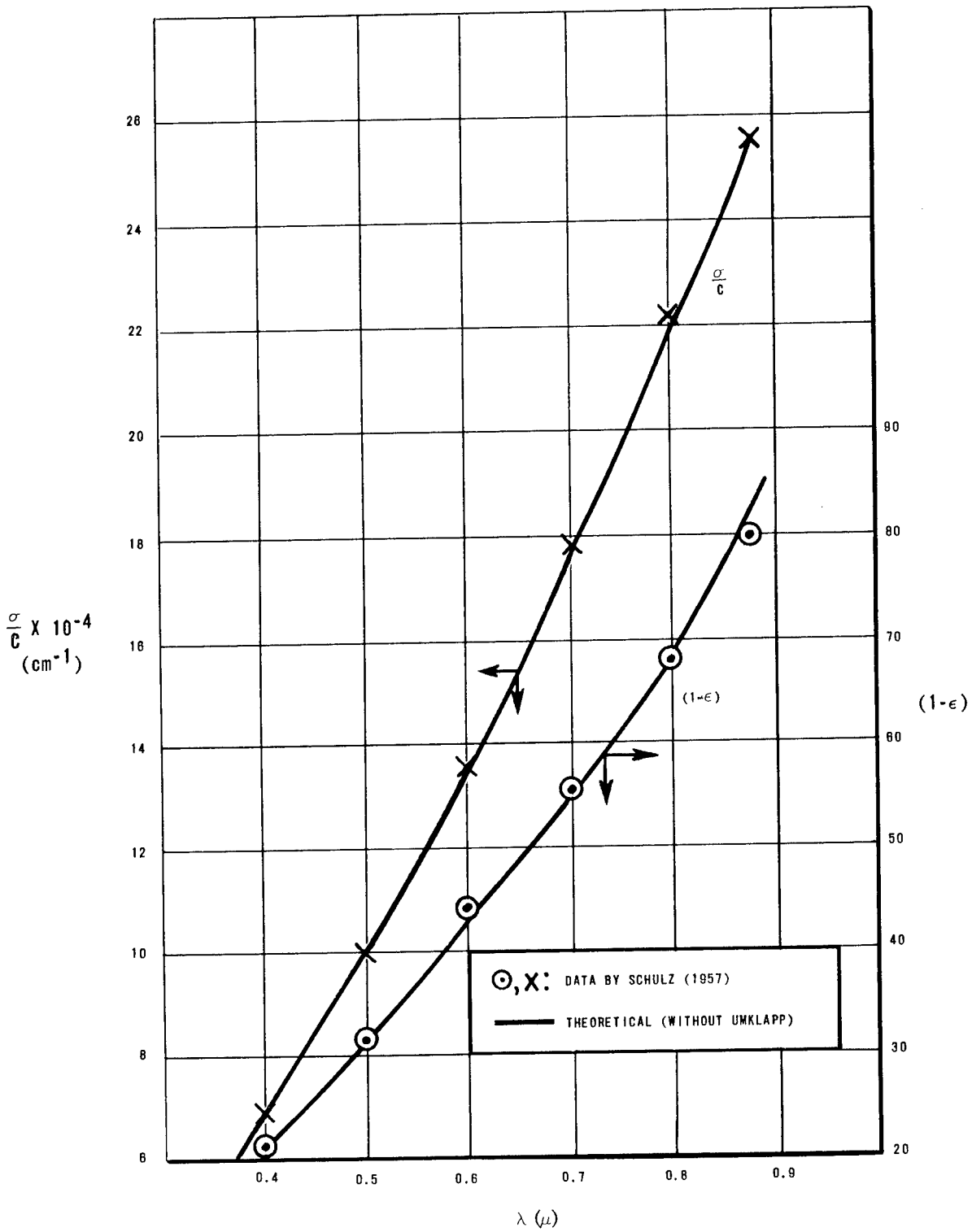

Figure 33. Gallium (~ 300°K)

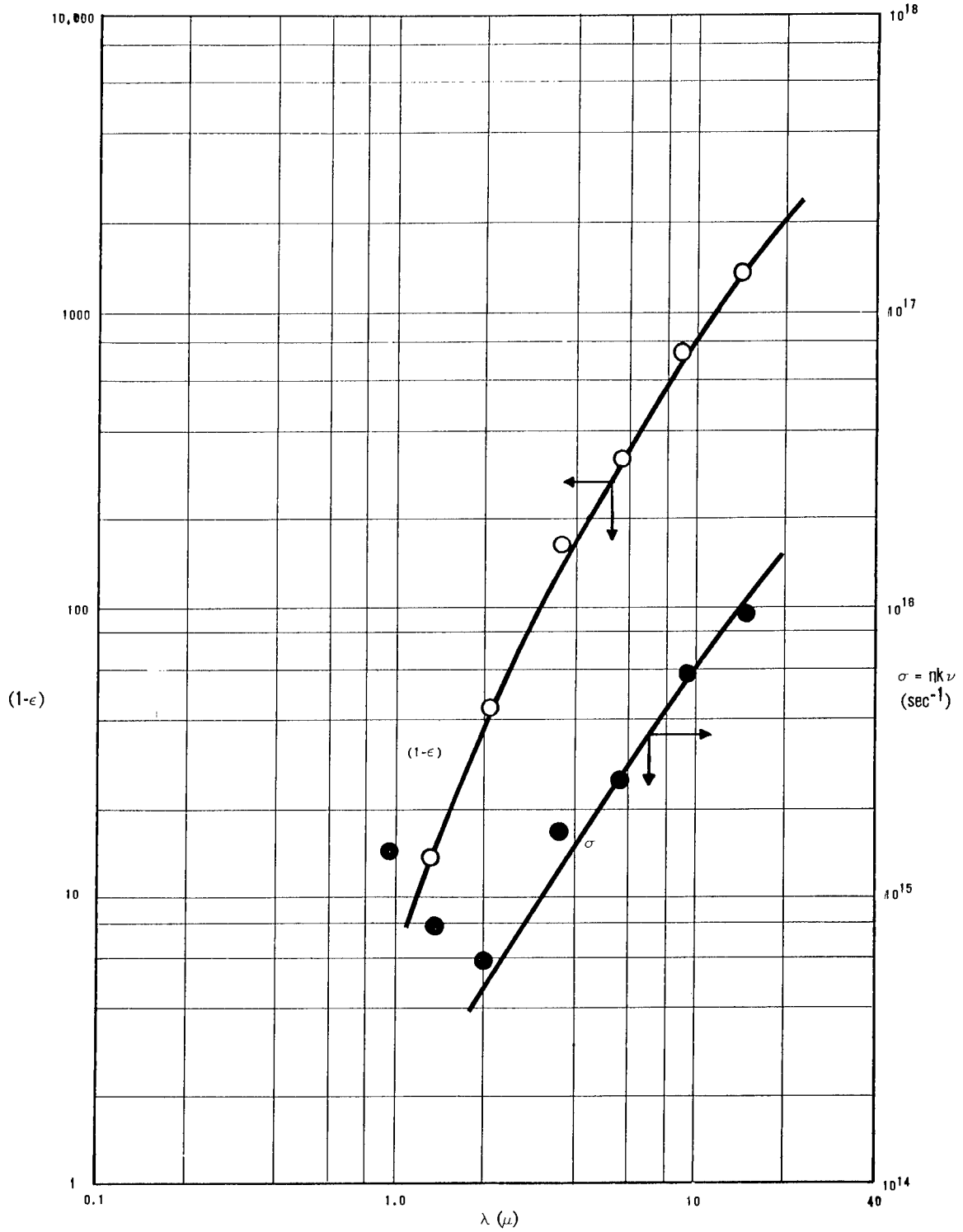

Figure 34. Zinc (without Umklapp)

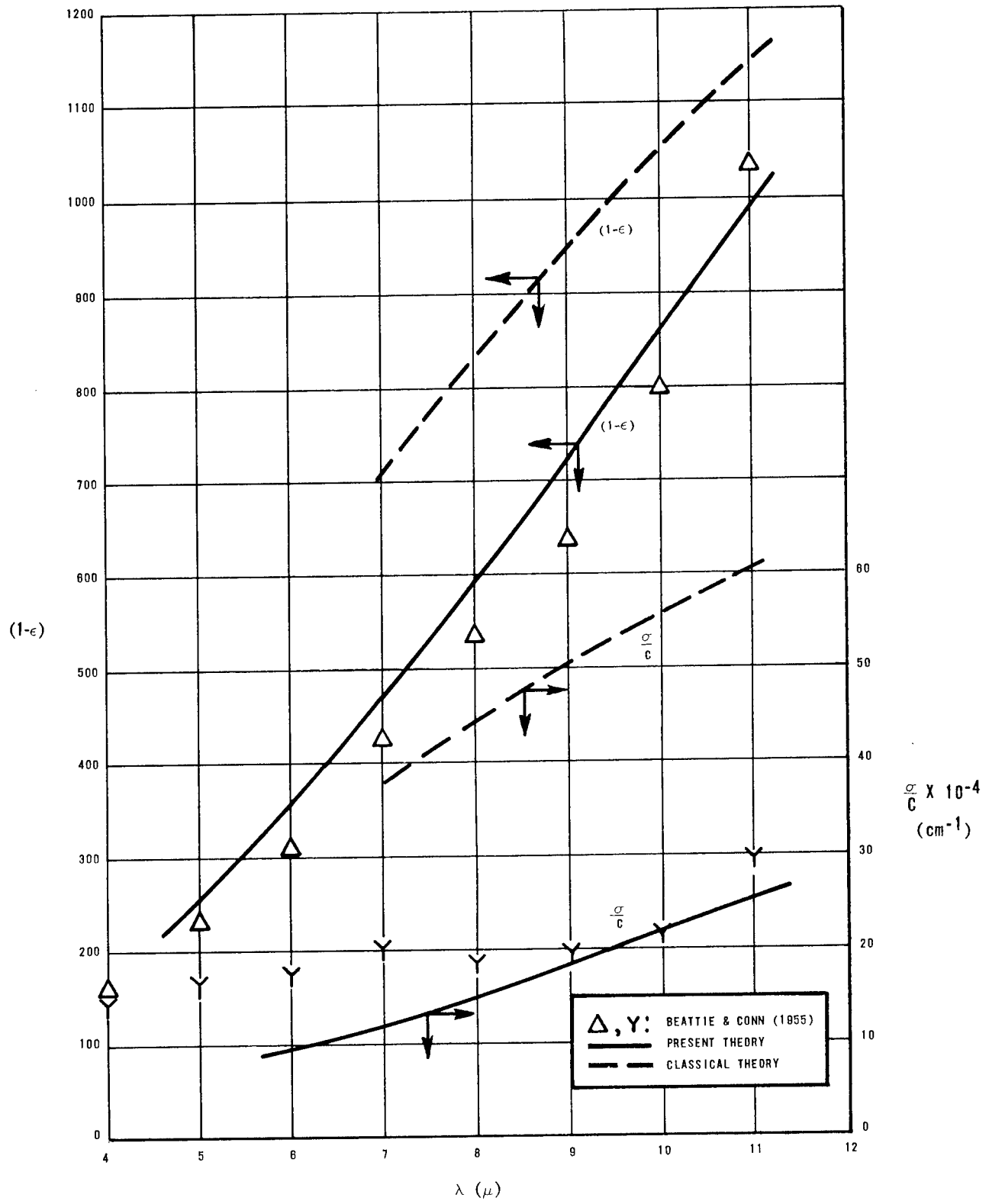

Figure 35. Nickel (~ 300°K)

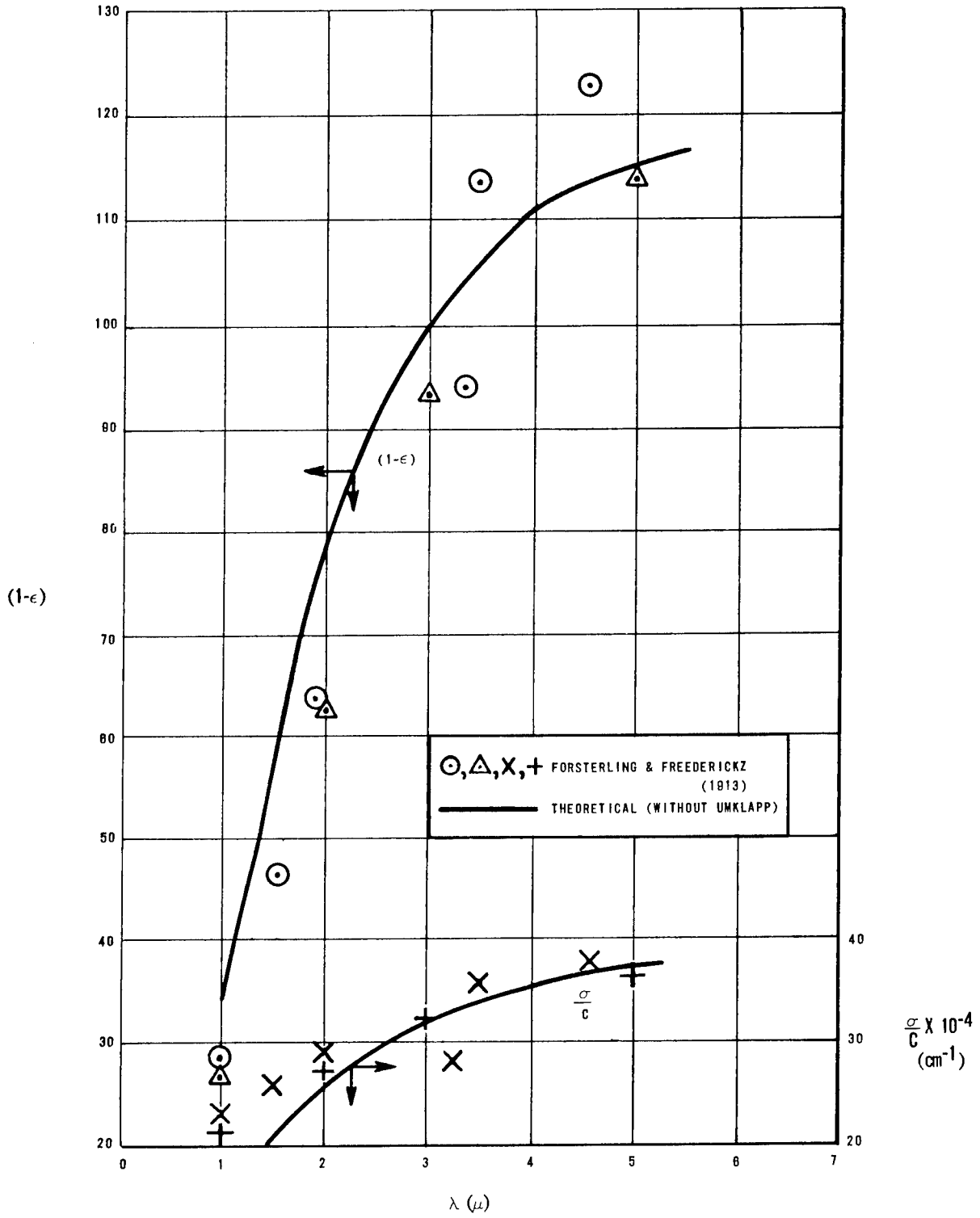

Figure 36. Platinum (~ 300°K)

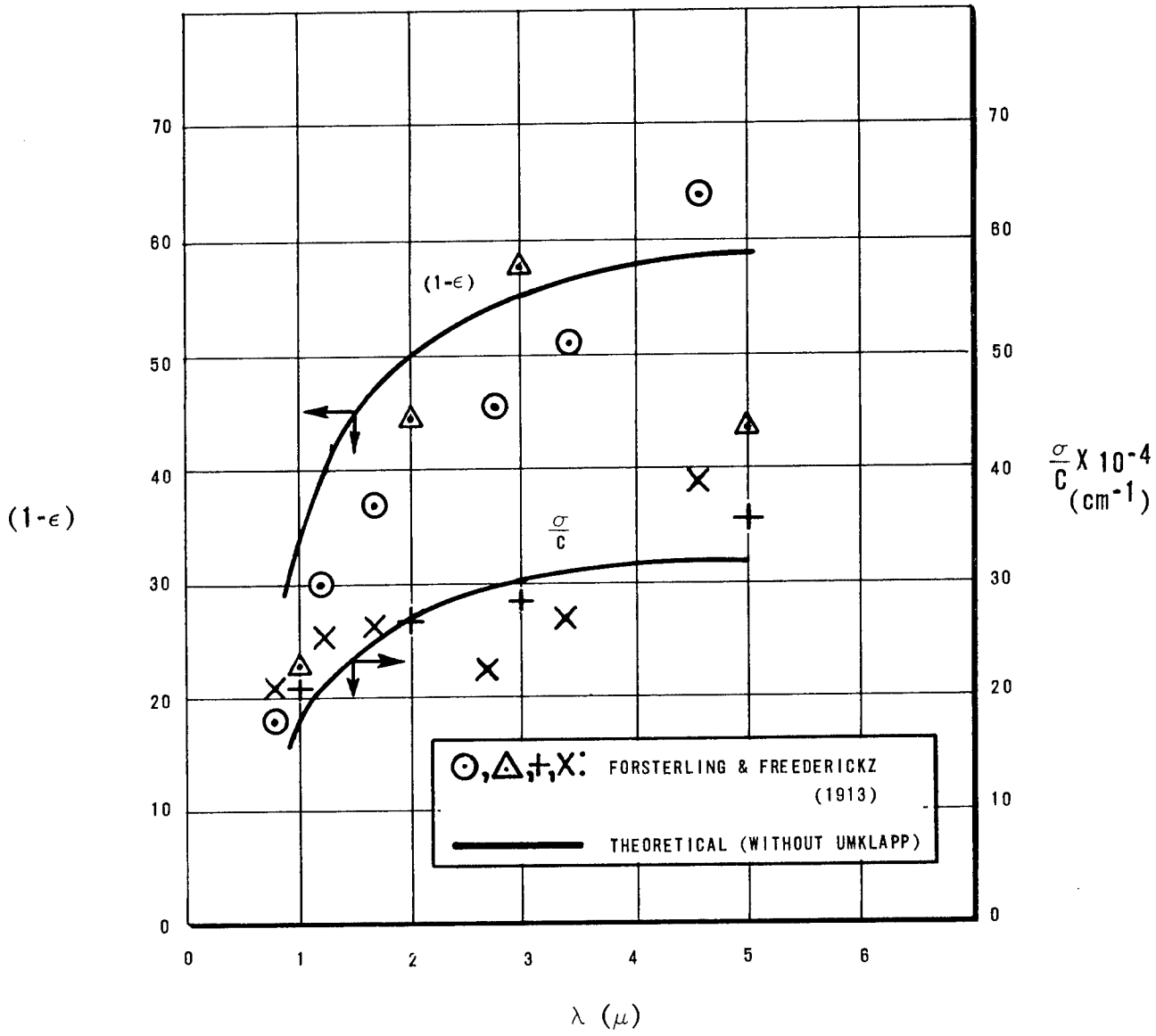

Figure 37. Iridium (~ 300°K) (1-ϵ) and $\frac{\sigma}{c}$ versus λ

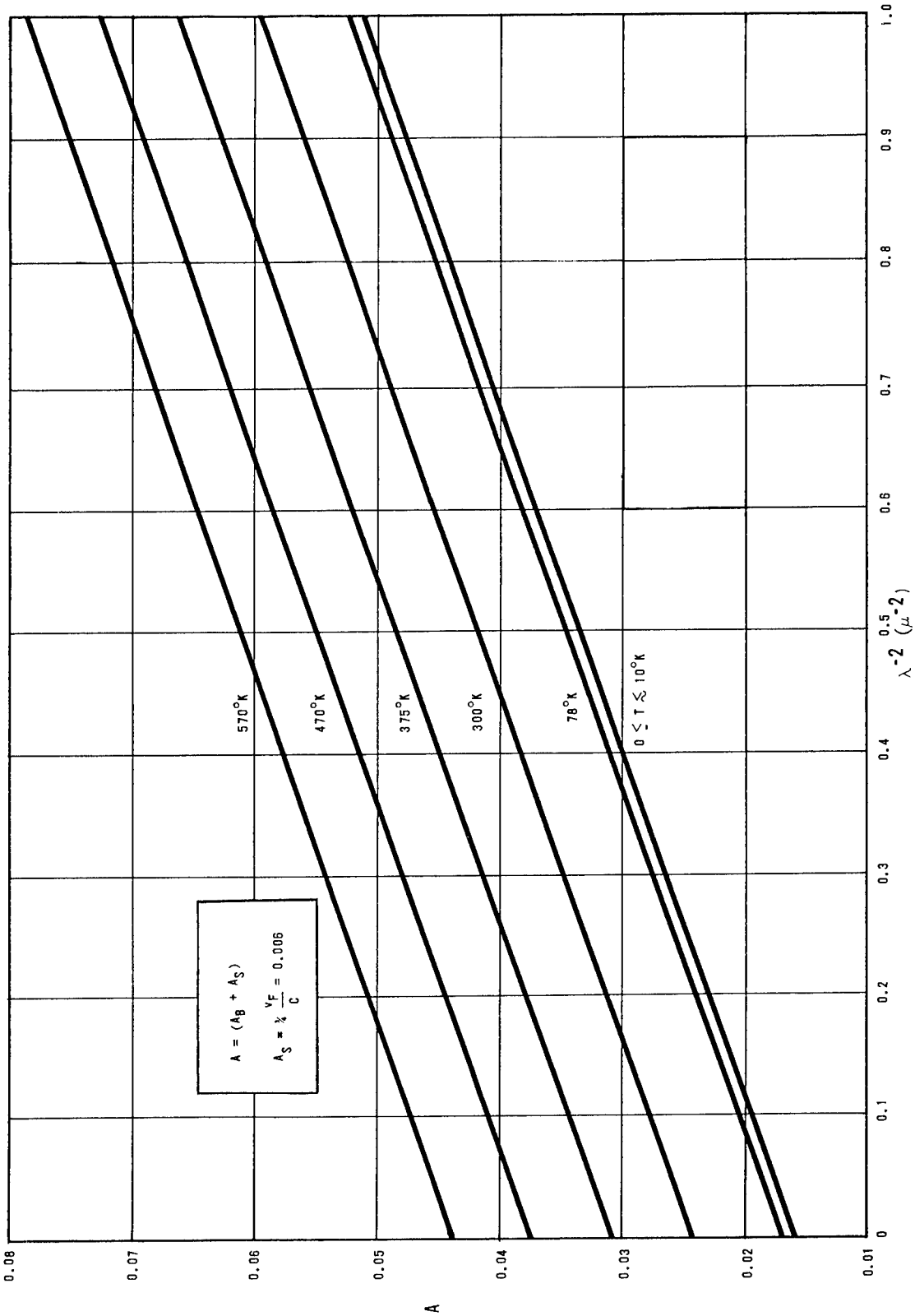

Figure 38. Aluminum - Total Absorptivity, A, versus λ^2

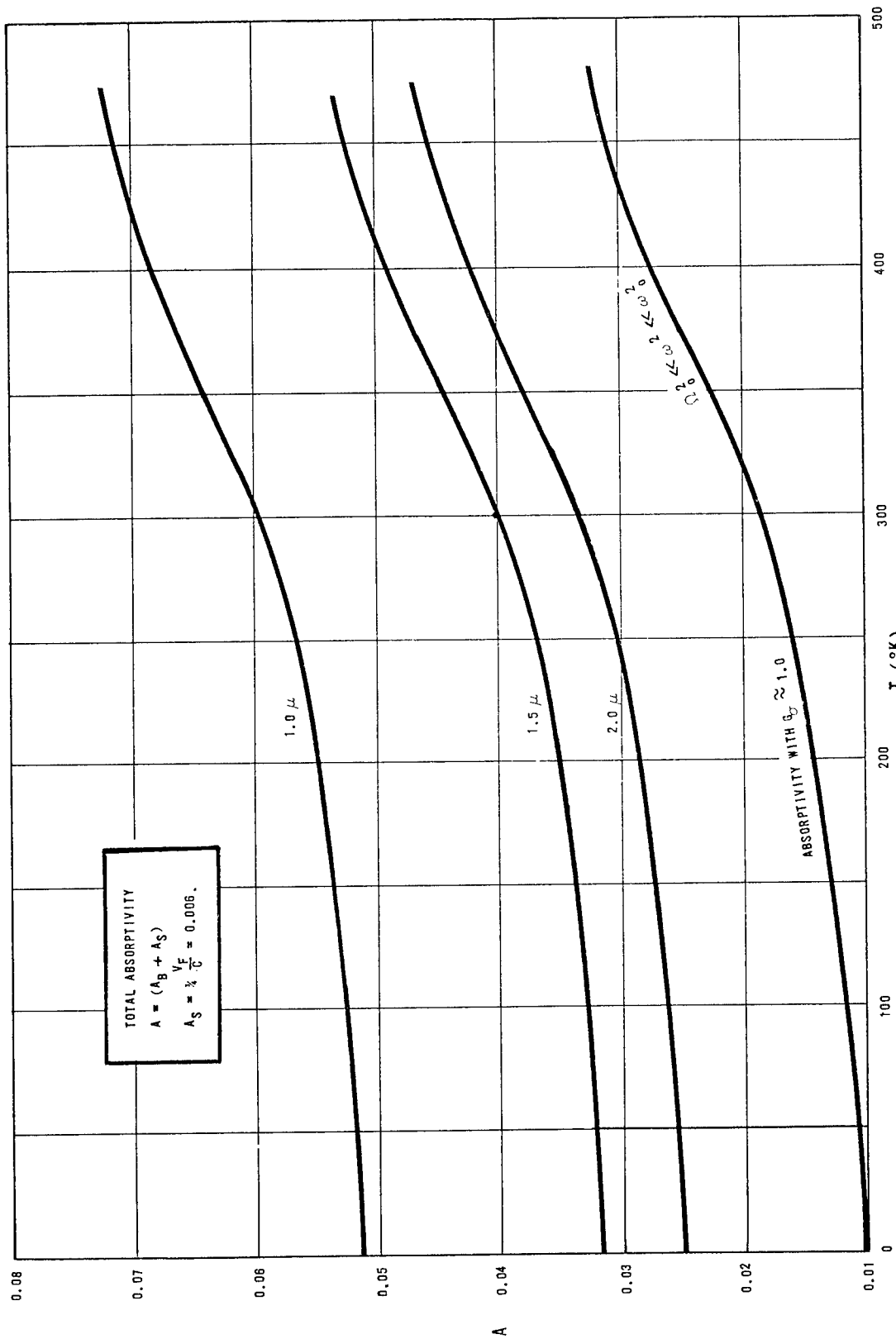

Figure 39. Aluminum

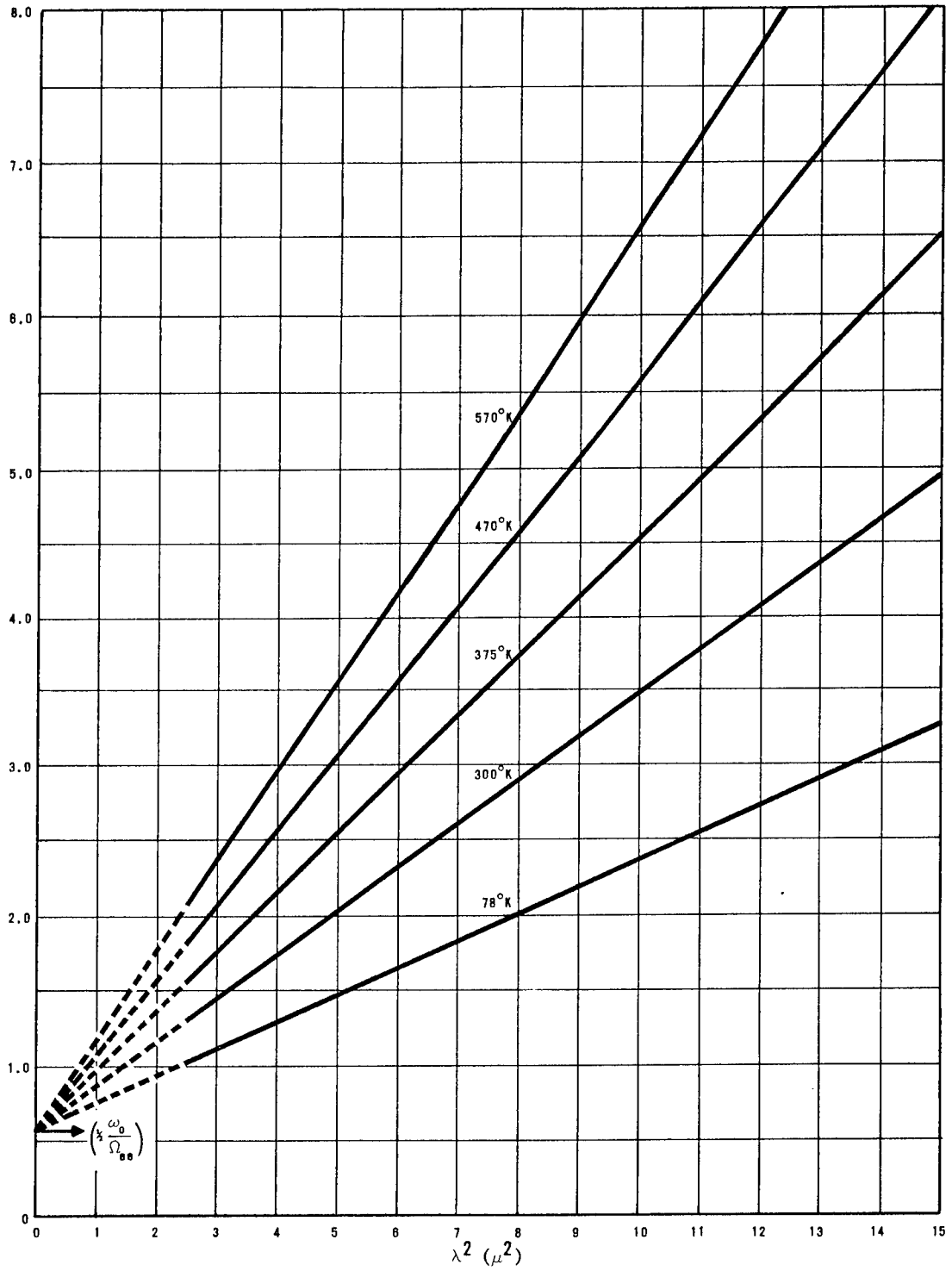

Figure 40. Aluminum n versus λ^2 (Theoretical Values at different temperatures)

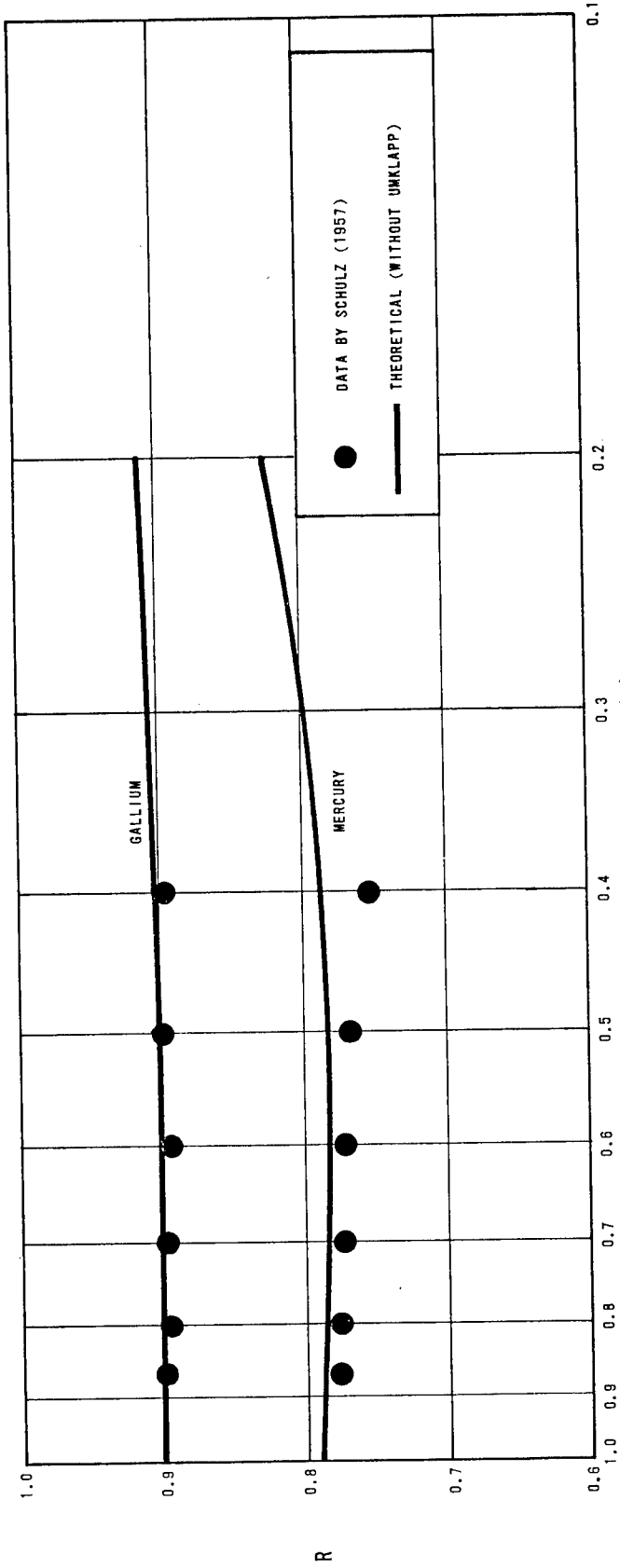

Figure 41. Reflectivity of Mercury and Gallium (300°K)

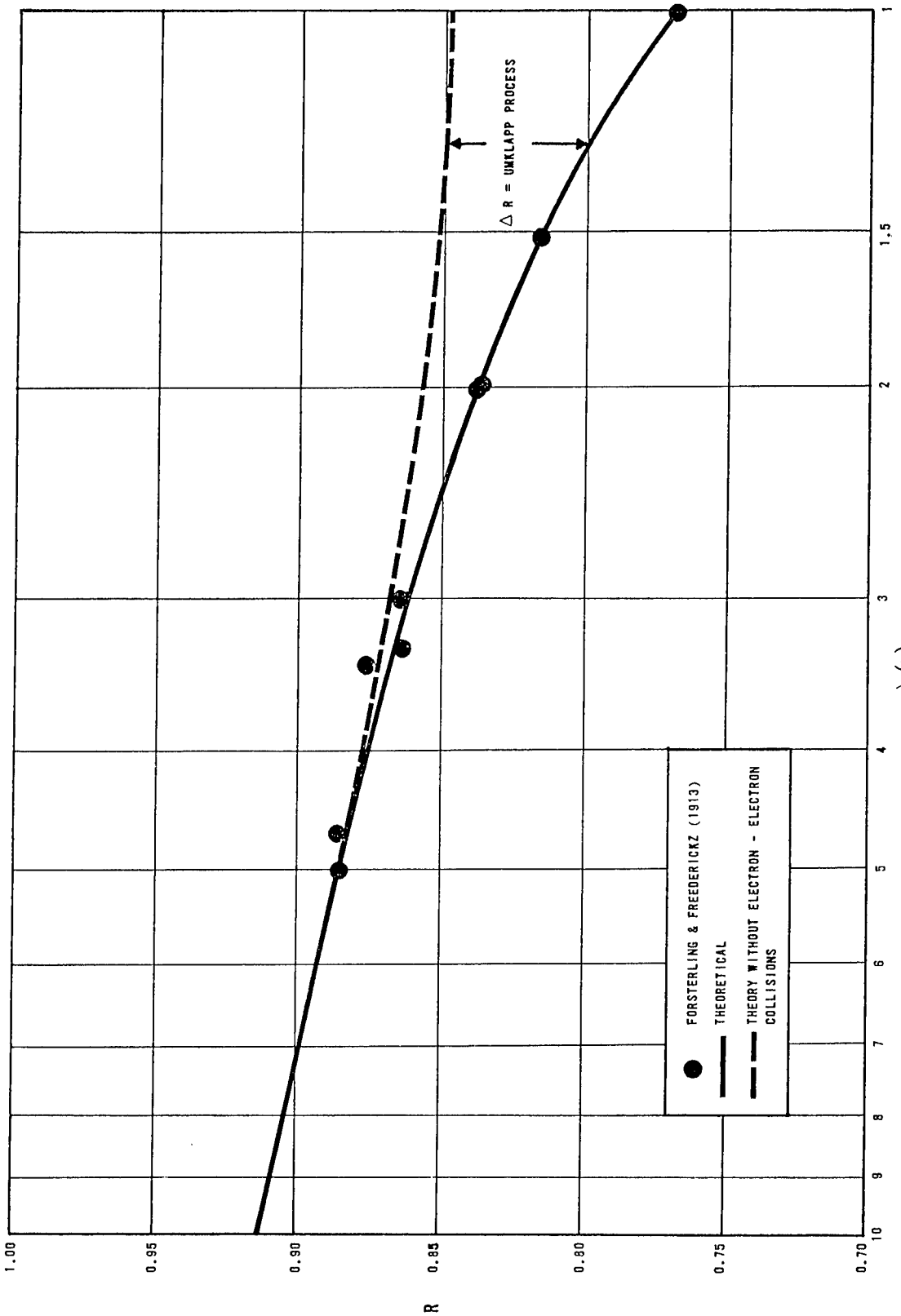

Figure 42. Platinum (~ 300°K) Reflectivity versus λ

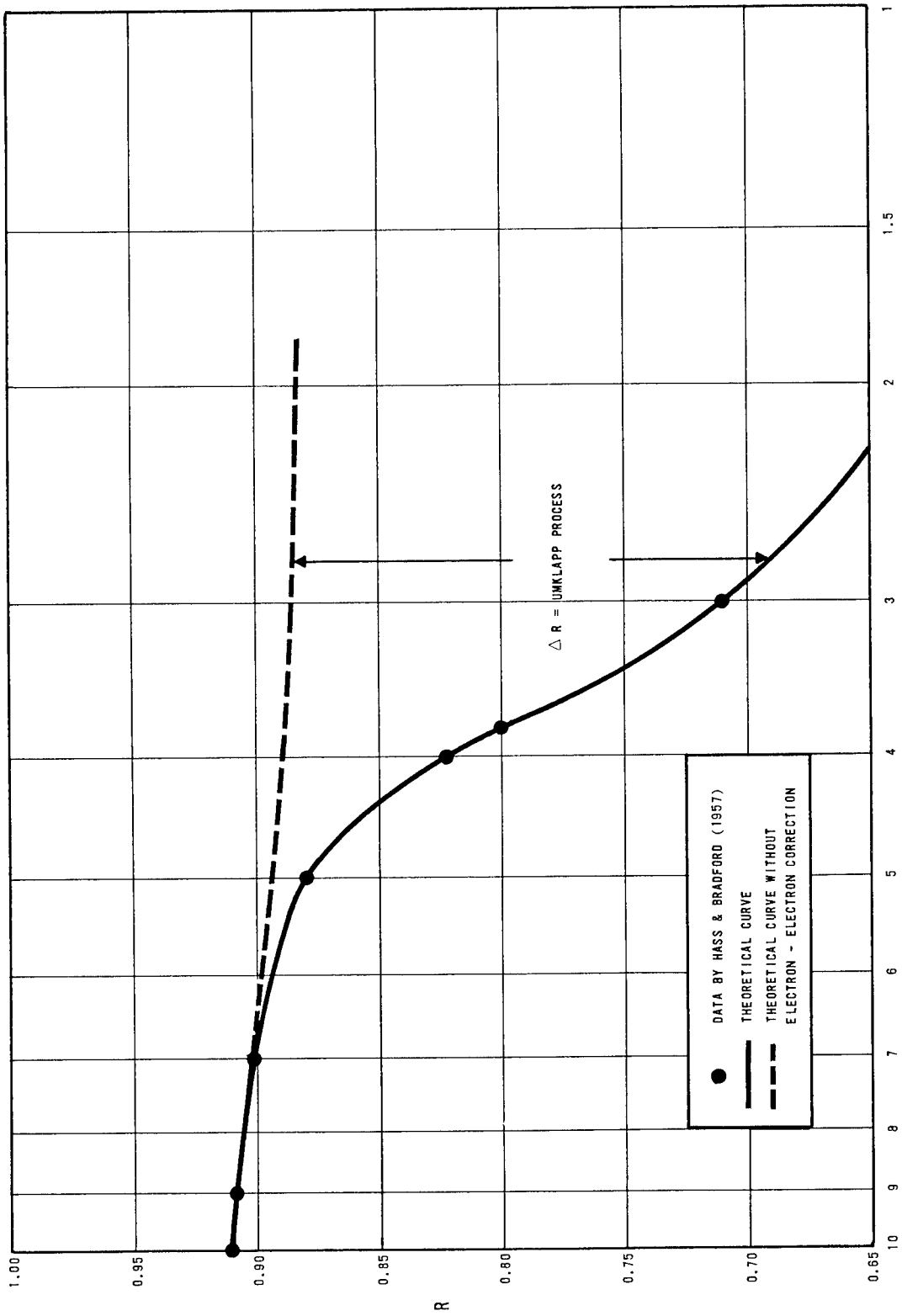

Figure 43. Titanium (~ 300°K)

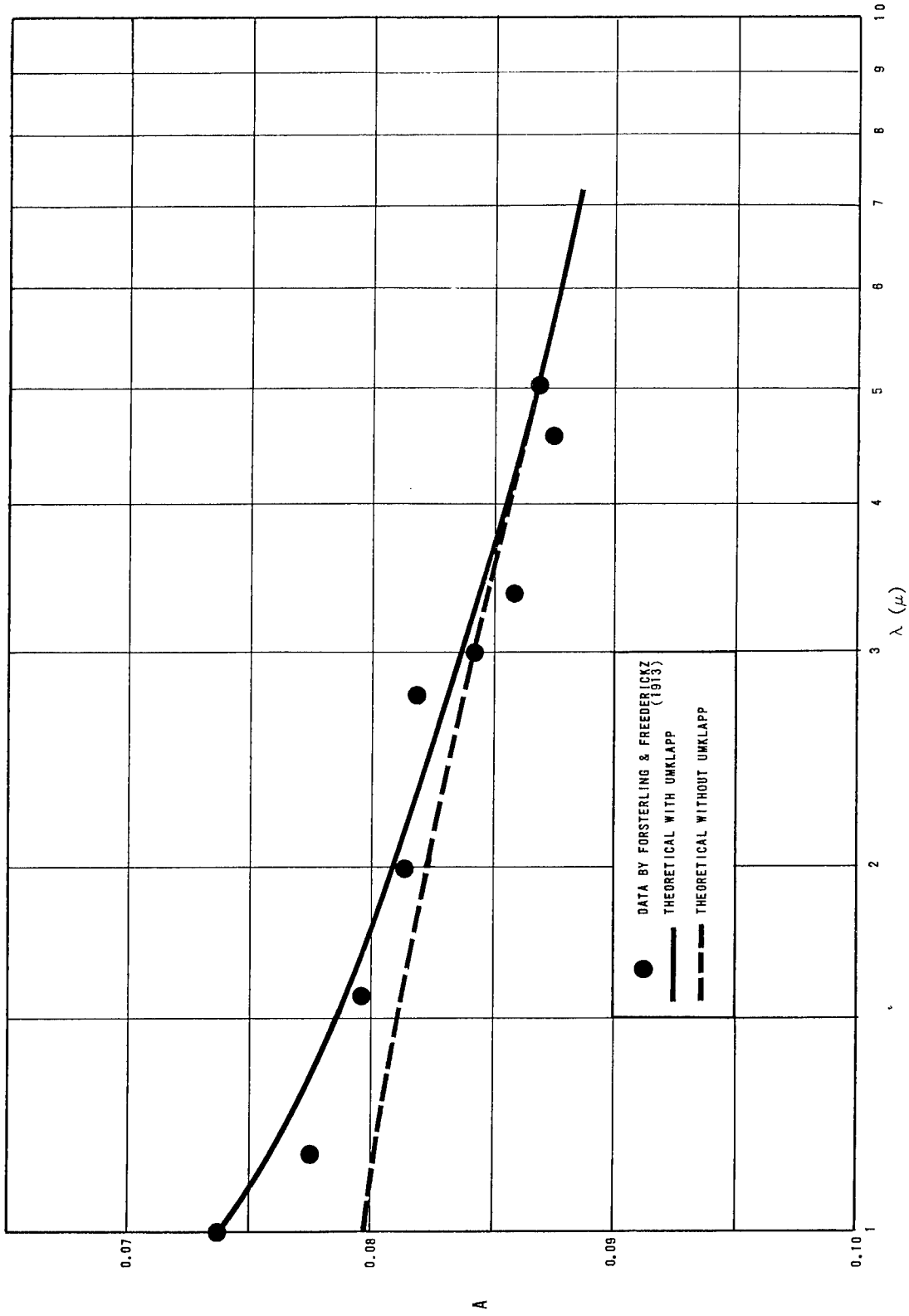

Figure 44. Tridium (~ 300°K) Absorptivity versus λ

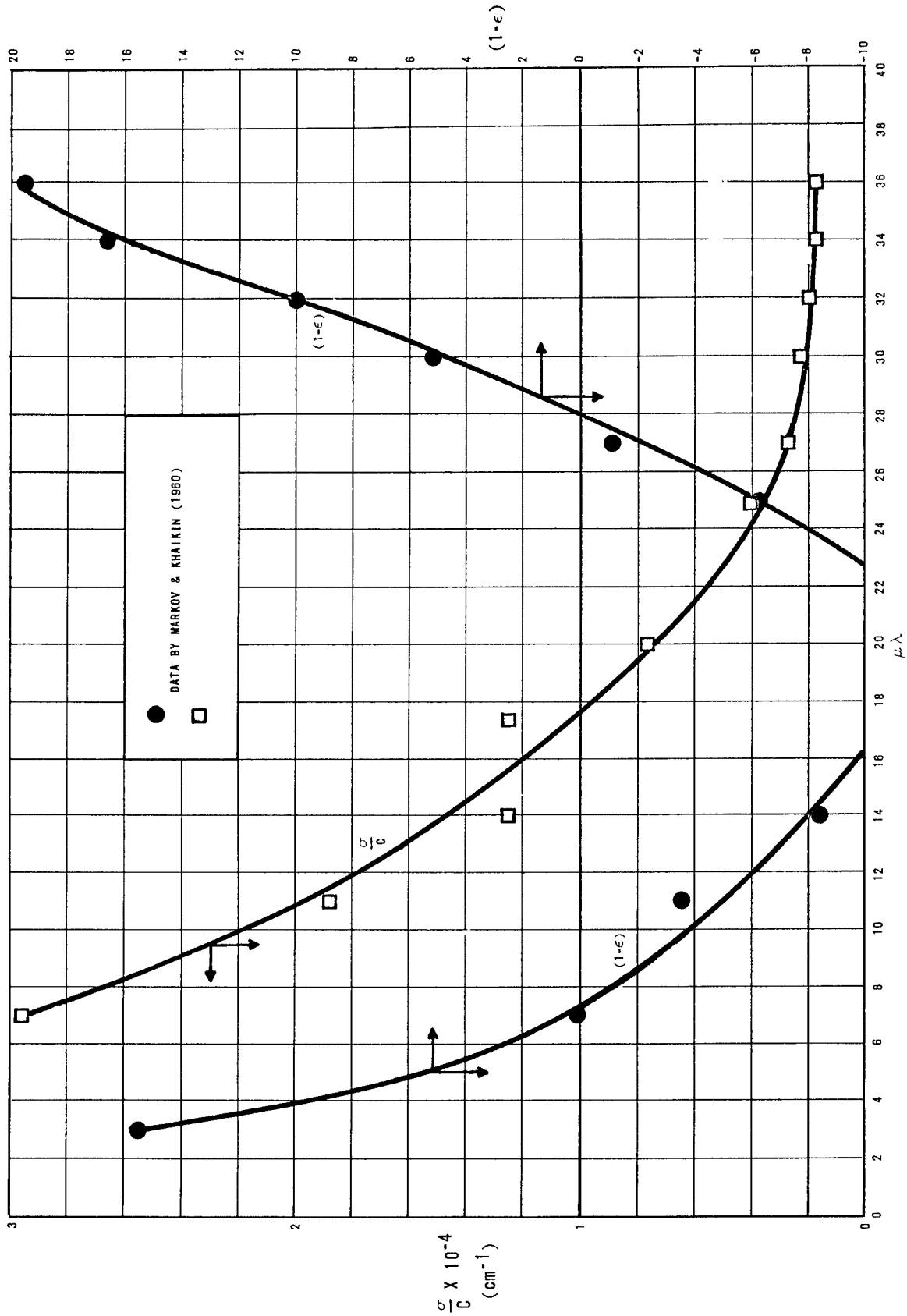

Figure 45. Bismuth (~ 300°K)

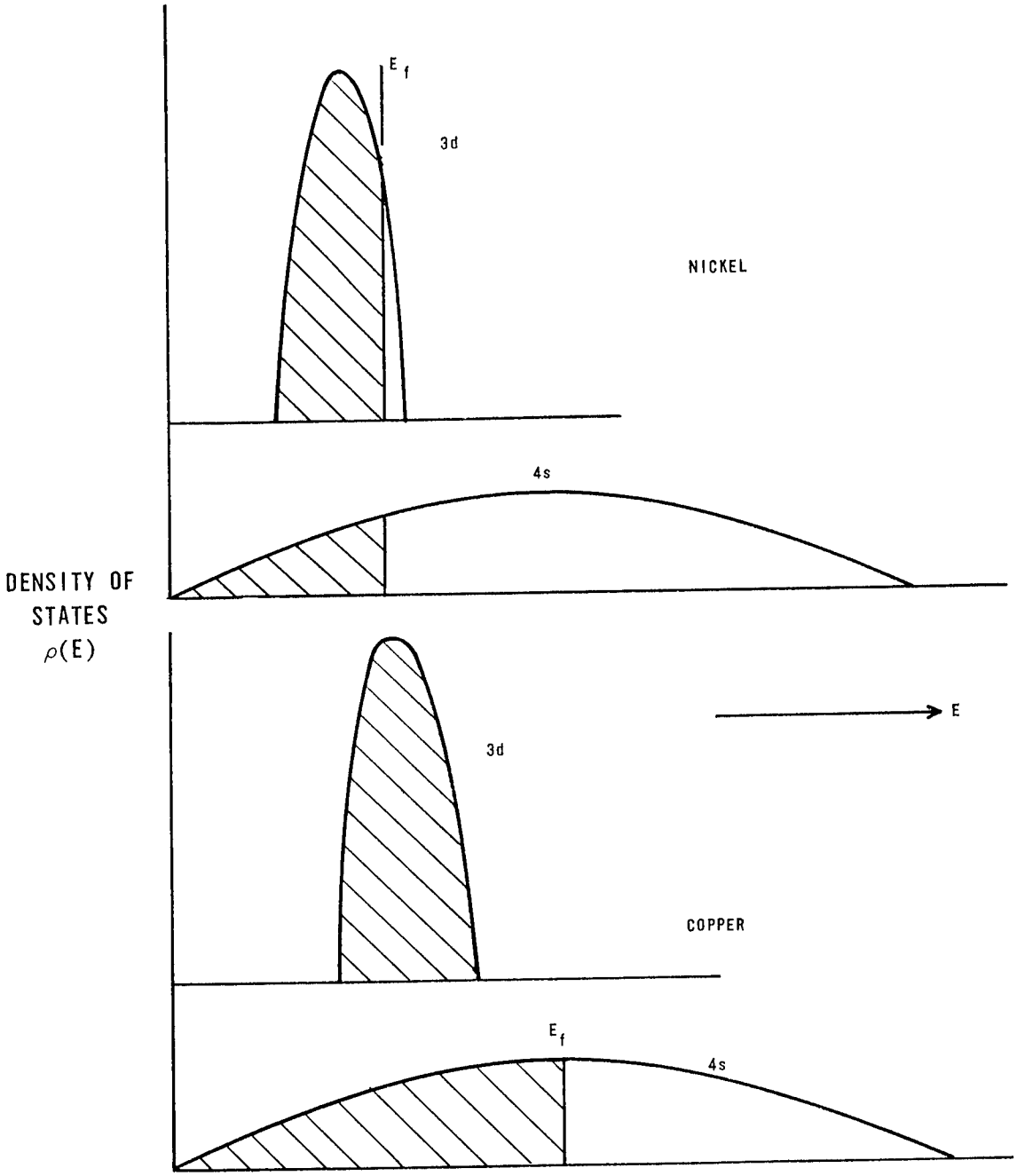

Figure 46. The Density-of-States functions of Nickel at 3d- and 4s- States Compared with those of Copper

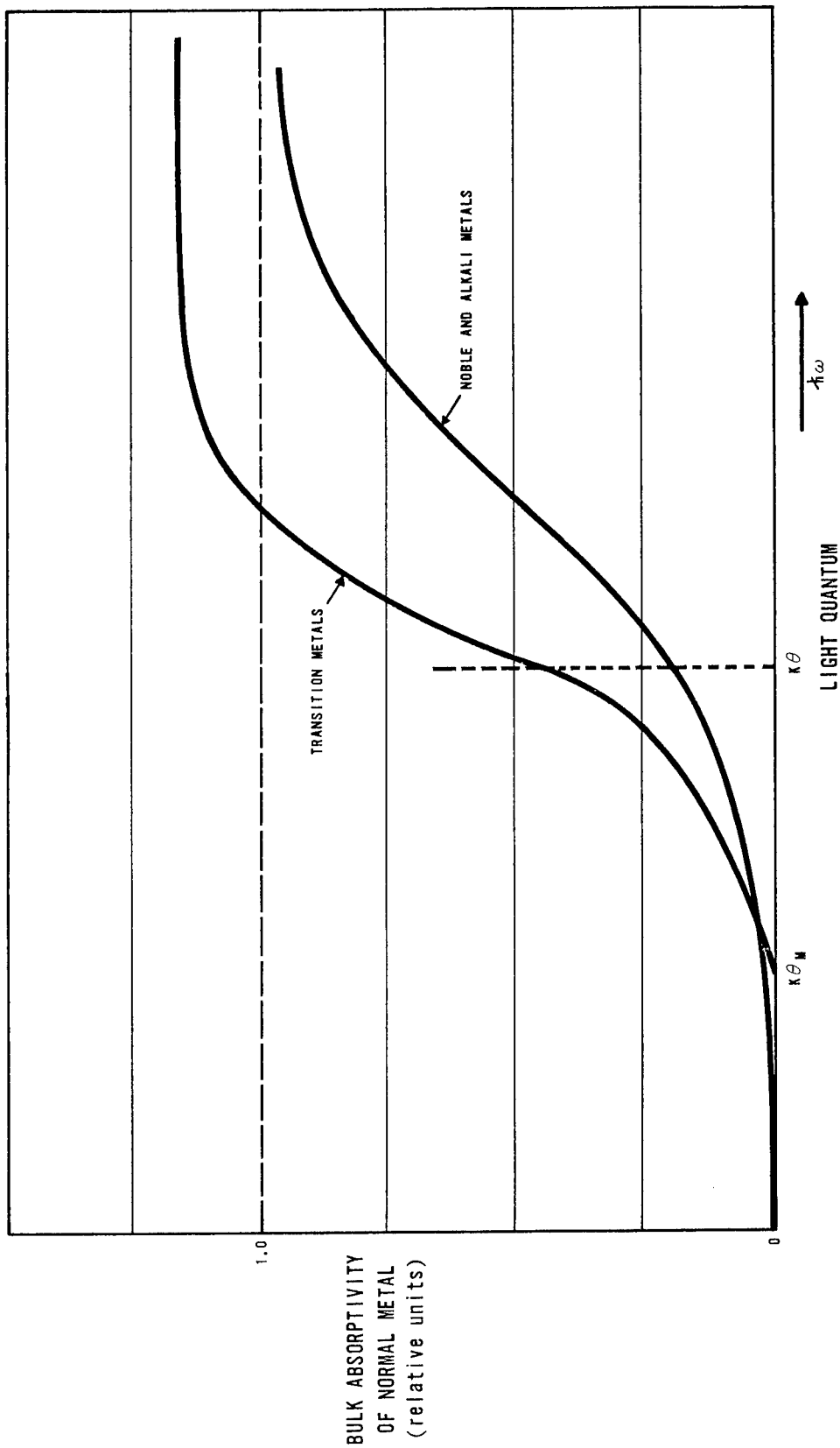

Figure 47. Bulk Absorptivity of Normal Metal at $T \cong 0°K$

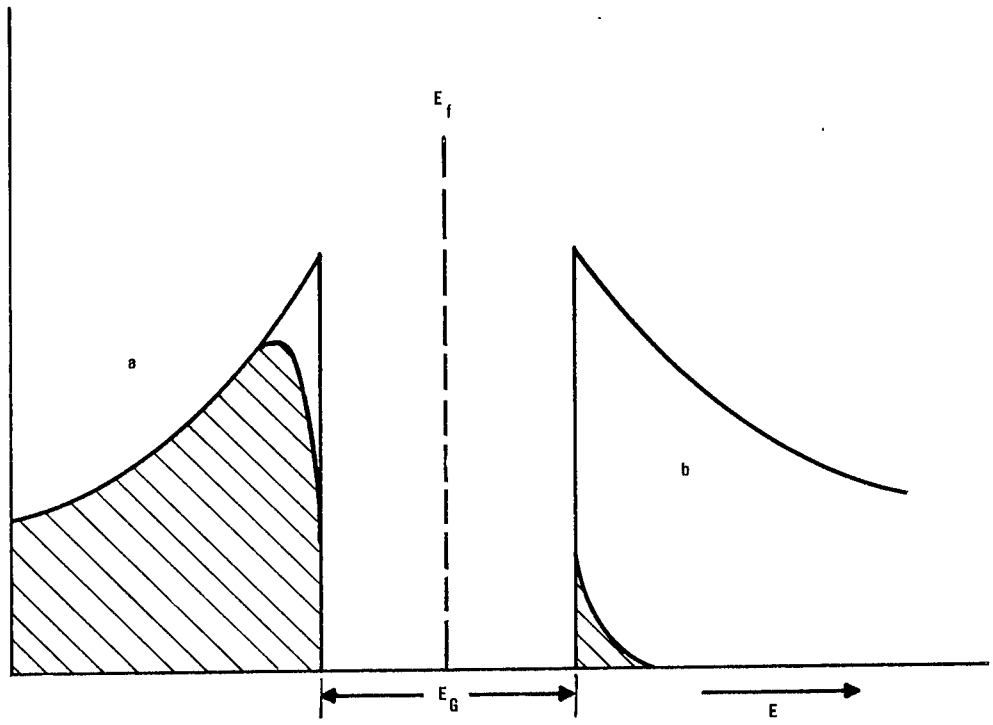

Figure 48. The BCS Density-of-States functions for Superconductors

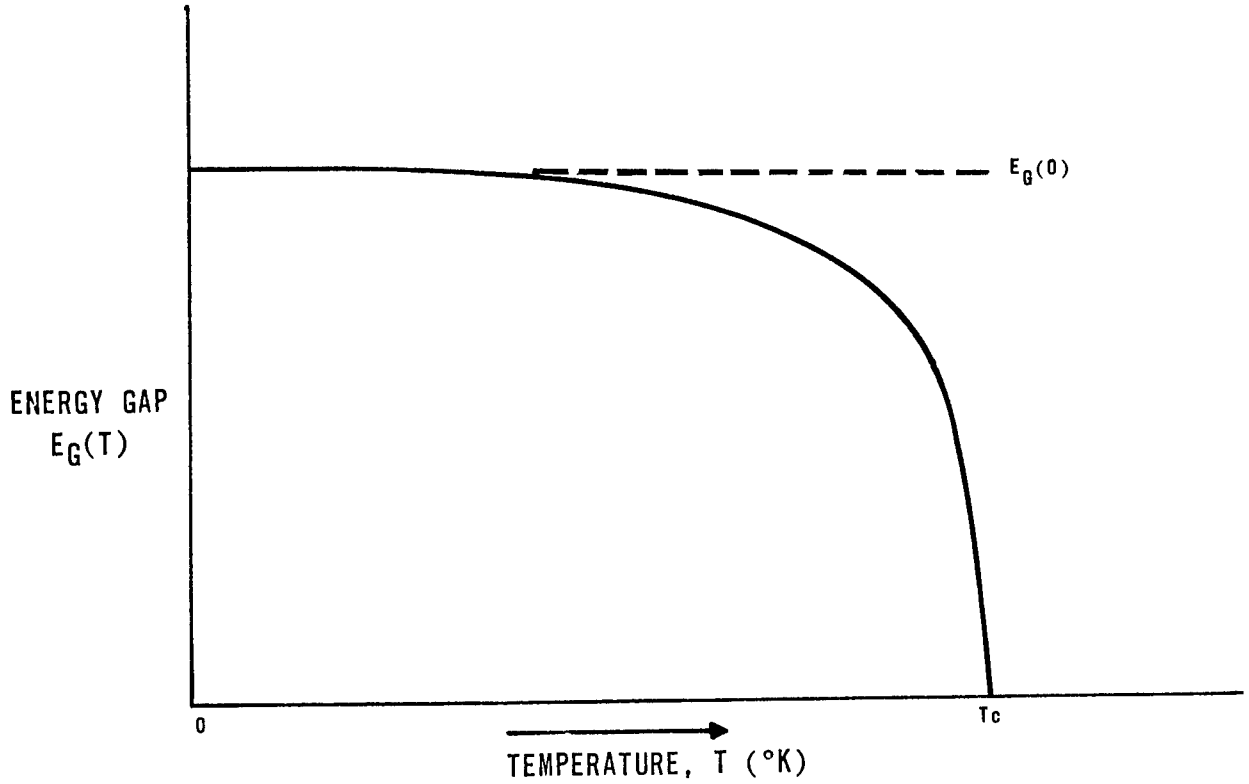

Figure 49. The Superconducting Energy Gap versus Temperature

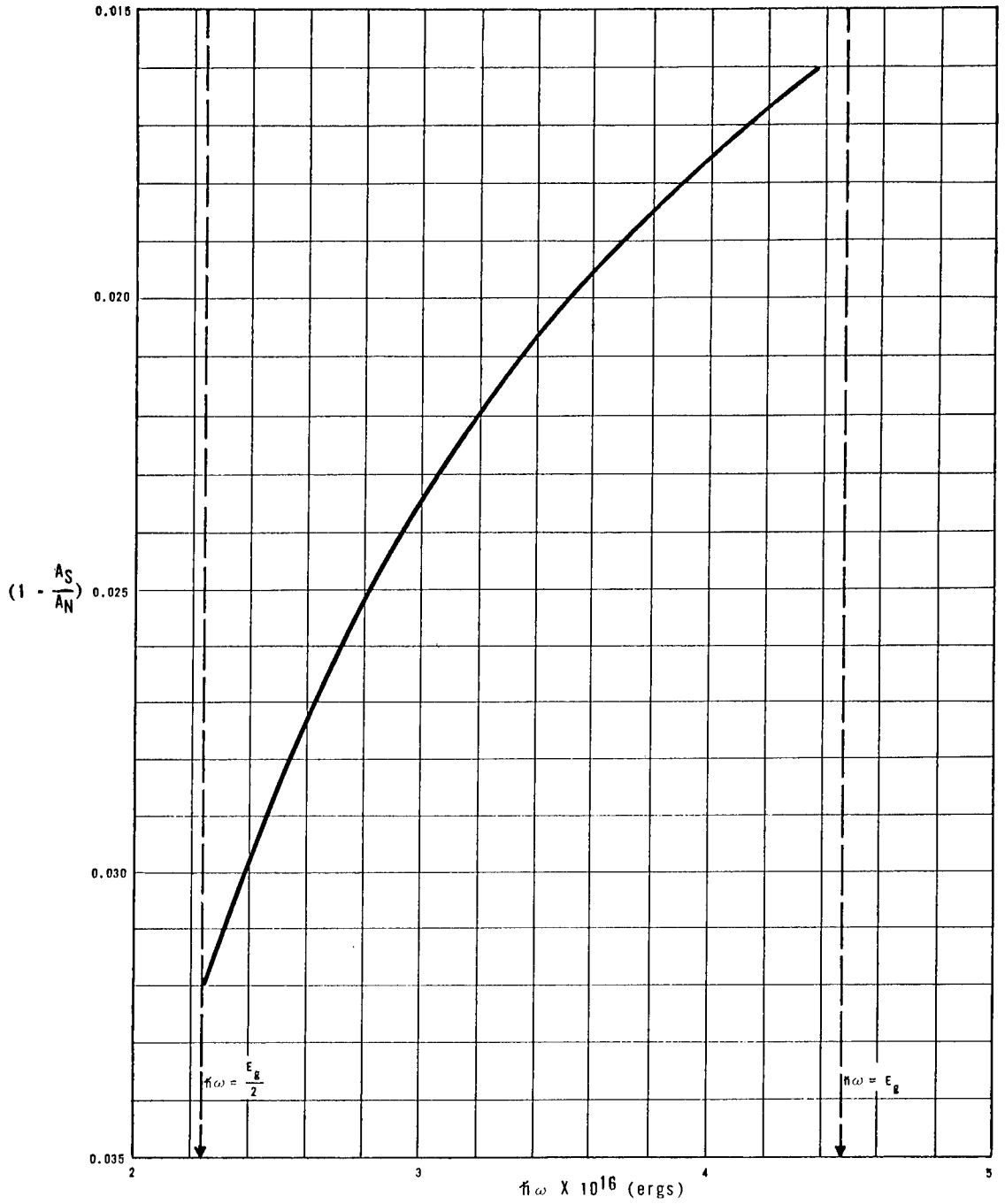

Figure 50. Absorptivity of Superconducting Aluminum for $\frac{E_g}{2} < h\omega$ from formula by Schrieffer (1960)

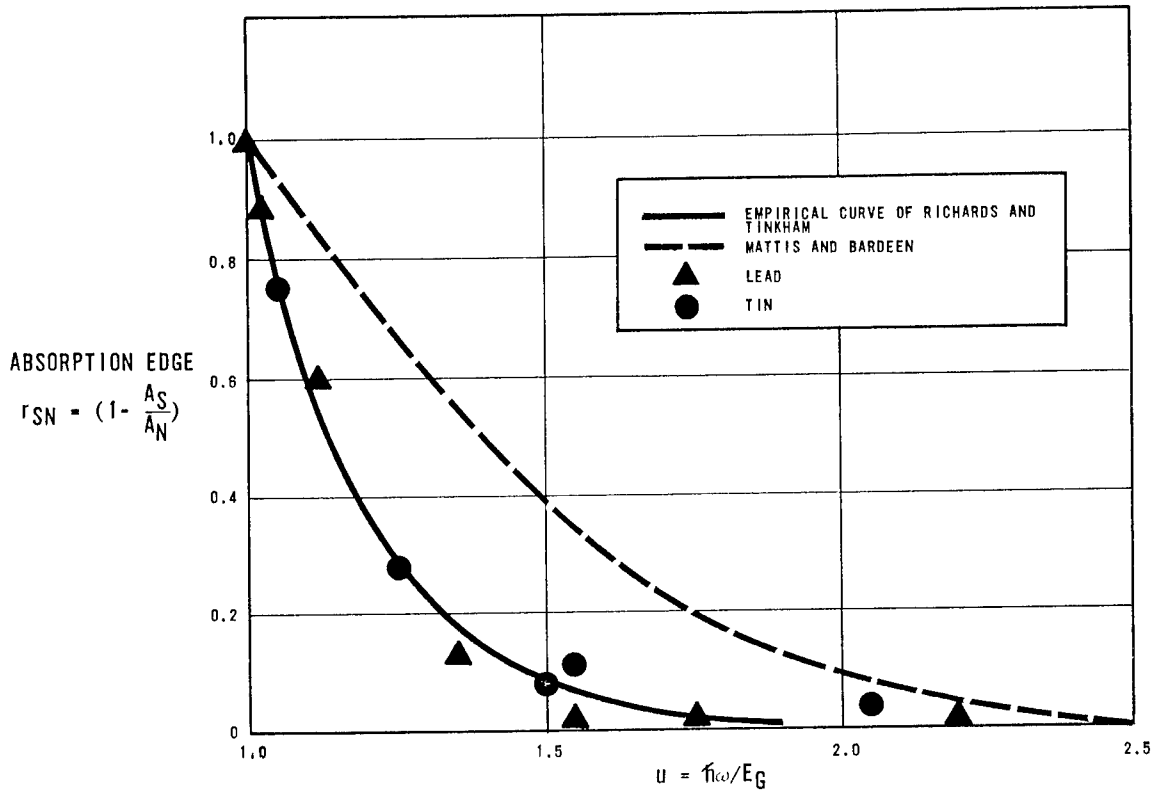

Figure 51. The Absorption Edge of Superconducting Tin and Lead

here are to be used in various dispersion formulas that are given in Section V in applying the present theory to transition metals. It must be kept in mind that some transition metals exhibit resonances at relatively long wavelengths compared with noble metals, and when this happens the resonance contribution must be substracted out of the dispersion curves, by use of the Kramers-Kronig relation or by other means, before the theory is applied. A method of substracting the contribution of the bound electrons to the infrared dispersion was illustrated in Section III where we used the Kramers-Kronig relation. When the resonance band is narrow and clearly distinguishable, separation of the free-electron part of dispersion becomes a trivial matter.

SECTION VII. THEORY APPLIED TO OPTICAL DATA

A. CALCULATION OF MICROSCOPIC PARAMETERS

The microscopic parameters that define the optical dispersion properties may be calculated from the best-fit theoretical curves of either the optical constants, (n,k) or (σ,ϵ). In general, it is much simpler to use the data on (σ,ϵ) rather than (n,k) since the general formulas for the former are less complicated than the latter. If the optical data are available in the spectral range, Ω_o^2 , $\bar{\Omega}_o^2 \ll \omega^2 \ll \omega_o^2$, which, for many metals, corresponds to $1\mu \lesssim \lambda < 10\ \mu$, it is convenient to use the best-fit theoretical curves of (n,k). In this part of the spectrum, the theoretical formula for k is exactly the same as that given by the classical Drude theory while the formula for n can differ substantially from the classical formula namely:

$$k \cong \left(\frac{\omega_o}{\omega}\right) = \left(\frac{\lambda}{\lambda_o}\right) \tag{355}$$

$$n \cong \tfrac{1}{2} \frac{\omega_o \tilde{\Omega}_o}{\omega^2} \tilde{G}_\sigma$$

$$= 1/2 \left[\frac{\omega_o \tilde{\Omega}_o}{\omega^2} + \frac{\omega_o}{\Omega_{ee}} \right]$$

$$\therefore \tilde{\Omega}_o = \left(\Gamma_{ep}^o b_{ep} + \Gamma_{ee}^o + \Gamma_M^o \right) \tag{356}$$

It is seen that k describes a straight line when it is plotted against λ, while n describes a straight line when it is plotted against λ^2. The critical frequency, ω_o, is obtained from Equation (355) and when this is used in Equation (356), the numerical values of $\tilde{\Omega}_o$ and Ω_{ee} follow immediately. The value of the electron-electron damping coefficient, Γ^o_{ee}, is obtained from Ω_{ee} when we use the relation:

$$\Omega_{ee} = \left(\frac{\hbar\beta}{2\pi}\right)^2 \Gamma^o_{ee} \left(\frac{\hbar\beta_\theta}{2\pi}\right)^2 R_{ee}$$

$$\beta = 1/KT \qquad (357)$$

$$\beta_\theta = 1/K\Theta$$

where R_{ee} is a constant which is independent of ω and T. The values of Γ^o_{ep}, and hence R_{ep} can be determined from Equation (355) and (356) only when we neglect Γ^o_M compared with Γ^o_{ee} and Γ^o_{ep}. This procedure is valid for metals which are substantially free of impurities, provided that the temperature is not too low. The method of determing the "Restwiderstand" term, Γ^o_M, from the low-temperature optical data will be explained in a later part of this section.

Once the values of ωo, R_{ep}, and R_{ee} are determined, we can predict the values of (n,k) and other dispersion quantities at any other temperature and frequency.

It is important to note that, in fitting Equation (355) to the corresponding experimental curve, the extrapolated straight line must pass through the origin at $\lambda = 0$, and that, when Equation (356) is plotted against λ^2, the non-zero value of n defined by the intersection of the straight line at $\lambda = 0$ is entirely due to the Umklapp processes which give rise to a non-zero contribution of the electron-electron collisions.

The remarkable qualities of Equations (355) and (356) are clearly demonstrated in FIGURES 20 to 23 for gold and copper, and in FIGURES 27 to 30 for the multivalent aluminum.

For many metals, it is not easy to identify the portion of the spectrum where Equations (355) and (356) are applicable, and the general equations of Section V need be used. In this case, it is more convenient to obtain the best-fit theoretical curves of (σ,ϵ) than of (n,k) using the equations:

$$\sigma = \frac{\omega_o^2}{4\pi} \quad \tilde{\Omega}_o \, \tilde{G}\sigma \Big/ (\omega^2 + \tilde{\Omega}_o^2)$$

$$\{1 - \epsilon\} = \omega_o^2 \Big/ (\omega^2 + \bar{\Omega}_o^2) \qquad (358)$$

where $\tilde{\Omega}_o$ and $\bar{\Omega}_o$ are independent of ω.

The best-fit theoretical curves of σ and $\{1-\epsilon\}$ are shown in FIGURE 19, and FIGURES 24 to 26, and FIGURES 31 to 36 for 10 different metals including the noble, multivalent, and transition metals. In particular, the multivalent metal, aluminum, is examined at two different temperatures, 78° K and 295° K.

Table XV shows the numerical values of various microscopic parameters that are calculated from FIGURES 19 to 36. These parameters are sufficient to enable us to calculate the dc electric properties and the dispersion properties at different spectral and temperature ranges.

The dc electrical conductivity, σ_o, is calculated from the formulas:

$$\sigma_o = \frac{\omega_o^2}{4\pi} \quad \frac{1}{\Gamma o}$$

$$\Gamma o = \Gamma_{ep}^{\,o} + \Gamma_{ee}^{\,o} + \Gamma_M^{\,o} \qquad (359)$$

where $\Gamma_M^{\,o}$ may be ignored at ordinary temperature. The theoretical and measured values of σ_o are shown in Table XIII for a variety of metals. For most of the metals that are examined, the theoretically calculated values agree well with the electrically measured values. Note, in particular, that the values for Ni and Al have been improved considerably from the old values of Table VI. In Table XIII, some of the measured values of σ_o are not obtained from the samples on which the optical data are available. For an accurate comparison between the calculated and measured values of σ_o, both the optical and electrical measurements must be made on the same sample, since,as was explained in Section III, the optical and electric properties vary depending on the manner in which the metallic surface is prepared. For instance, most of the available optical data are obtained from vacuum evaporated surfaces whicle the handbook values of σ_o are for bulk samples. Beattie and Conn (1955) obtained the optical data for several metals, each with several different surface preparations. The variation in the values of the electrical and optical properties among differently prepared metal surfaces was quite

substantial.

B. CALCULATION OF ABSORPTIVITY

With the help of the microscopic parameters that are given in Table XV, the absorptivity is calculated from the formula:

$$A_B \approx \frac{2}{\omega_o}\ \Omega_o\ G_\sigma \left[1 - \frac{9}{8}\left(\frac{\Omega_o}{\omega}\right)^2 + \frac{37}{32}\left(\frac{\Omega_o}{\omega}\right)^4 + \ldots \right] : \omega > \Omega_o > \bar{\Omega}_o$$

$$A_s = \frac{3}{4}\ \frac{\nu_F}{C} \qquad (360)$$

$$A = A_B + A_s$$

where A_s is the absorptivity due to the diffuse surface scattering (Dingle, 1953). The skin absorption is important when the mean free path given by:

$$\ell = \nu_F\ \tau_R \qquad (361)$$

is much larger than the skin depth than the skin depth δ_s, which was given in Section III, where τ_R, unlike the dc relaxation time τ_R^o, is now given by:

$$\frac{1}{\tau_R} = \frac{1}{\tau_R} + \Gamma_{ep}^{o} \times \left(\tilde{b}_{ep} - 1 \right) \qquad (362)$$

According to the original theory of the anomalous skin effect, the dc relaxation time, τ_R^o, was used in Equation (361) so that, at low temperatures, ℓ can be substantially larger than δ_s due to the rapid decrease Γ^o with decrease in temperature.

According to the present theory, however, τ_R does not increase so fast as might have been expected from the theory of electric conduction, since a rapid increase of $\tilde{b}_{ep}$, according to $\sim \left(\frac{\Theta}{T}\right)^5 \frac{1}{J_5^o}$, completely

counteracts the rapid decrease of Γ_{ep}^{o}, until τ_R reaches the constant low-temperature value:

$$\frac{1}{\tau_R} \approx \left(\frac{1}{10} R_{ep} + \Gamma_M^{o} \right) : \quad T \approx 0°K \tag{363}$$

This is to be compared with:

$$\frac{1}{\tau_R^{o}} \approx \Gamma_M^{o} \quad : \quad T \approx 0°K \tag{364}$$

which results when Γ_{ep}^{o} is used in place of Γ^{o}. As the result of this, the absorption due to the anomalous skin effects is not so significant in the present theory as was suggested in the original theories of Reuter and Sondheimer (1948) and Dingle (1953). For transition metals and also for multivalent metals for which interband transitions are predominant, the relation in Equation (363) is replaced by:

$$\frac{1}{\tau_R} \approx \left(\frac{R_{ep}^{s \rightarrow d}}{6} + \Gamma_M^{o} \right) \tag{365}$$

The constant, R_{ep}, can be obtained from the known values of Γ_{ep}^{o} upon using the relation:

$$\Gamma_{ep}^{o} = R_{ep} \frac{1}{\alpha^5} J_5^{o}(\alpha) \tag{366}$$

for nontransition metals, and the relation:

$$\Gamma_{ep}^{o} = R_{ep}^{sd} \frac{1}{\alpha^3} J_3^{o}(\alpha) \tag{367}$$

for transition metals, where the functions J_5^{o} and J_3^{o} are available in the appendix in calculable forms: the numerical values of $J_5^{o}(\alpha)$ are computed in Tables XI and XII. Since R_{ep} is usually $\frac{1}{10} \sim 1$ times as large as Γ_{ep}^{o} at room temperature, τ_R for both transition and nontransition metals at very low temperatures and in the near infrared is given by:

$$\tau_R \approx (10 \sim 10^2) \times \tau_R^{o} \quad (300°K) \tag{368}$$

which implies that the mean free path, 1, increases by a factor of 10 ~ 100 when T is lowered from room temperature to the absolute zero. This is in mark contrast to the low-temperature electrical properties and also to the existing theories of optical dispersion.

The absorptivity values that are computed from (360) are presented in Figures 39 to 43 and are compared with the experimental curves for the liquid metals, Hg and Ga, and for the transition metals, Pt, Ti, and Ir. The contributions by the Umklapp processes are indicated in FIGURES 40 to 43. One glance at these curves is sufficient to show that the transition metals with predominantly interband transitions exhibit a markedly greater contributions of the Umklapp processes than other metals. Table VII shows the theoretical values of the low-temperature (4.2°K) and near-infrared (1 ~ 2μ) absorptivity of eleven different metals. The theoretical values for Cu and Ag are in agreement with the experimental alues of Biondi (1956) within ~ 2 percent. Unfortunately, the experimental values are as yet unavailable on other metals, and no further comparison is possible. The relative importance of the bulk absorption as compared with the skin absorption is represented by computing the per cent value of $\left(\frac{A_B}{A}\right) = \left(1 - \frac{A_s}{A}\right)$. It is seen that for all the metals that are studied, the bulk absorption ranges from 20 percent for Ag to nearly 100 percent of the total absorption. In general, the bulk absorption is relatively more pronounced in multivalent and transition metals than in noble metals. It is hardly necessary to mention that, according to the classical theory, there should be almost no bulk contribution to the low-temperature absorption, and that the remarkable features demonstrated in Table II are entirely the consequence of the quantum correction factor, b_{ep}, of the present theory.

C. CALCULATIONS OF DISPERSION PROPERTIES AT DIFFERENT TEMPERATURES

We have already demonstrated how the microscopic parameters that are computed from the room temperature optical data can be used to compute absorptivity at very low temperatures. We may likewise calculate and hence predict the values of any dispersion property at different temperatures when the values of the fundamental microscopic parameters are available from the optical data at a particular temperature.

Before we proceed with numerical applications, we need to establish the validity of the T-dependence that is formulated in the present theory. The temperature-dependence of $\Gamma^{o}_{ee}(\alpha)$ is well established and has been popularly used in the past. Therefore, we need to concern ourselves only with the T-dependence of the electron-phonon damping coefficient, $\Gamma^{o}_{ep}(\alpha)$,

and the quantum-factor, $b_{ep}(\alpha,\mu)$. We explained previously that the T-dependence of $\Gamma^{o}_{ep}(\alpha)$ of the present theory is entirely consistent with the T-dependence of the well-known Gruneisen formula and also with that which is derived in Wilson's theory of electric conduction in metals, and that Gruneisen's formula is in excellent agreement with the observed heat capacity data: e.g., see FIGURE 15a and b. Although this enables us to conclude that our formula for $\Gamma^{o}_{ep}(\alpha)$ is valid, we have yet to establish the validity of the T-dependence $b_{ep}(\alpha,\mu)$, or equivalently of $\tilde{b}_{ep}(\alpha)$.

For this purpose, we shall use the optical data on aluminum which are obtained at two widely separated temperatures, 78°K and 295°K, by Golovashkinetal (1960). We saw previously that the theoretical curves for n,k, σ, and $(1-\epsilon)$ at the two temperatures agree well with the corresponding experimental curves,and that the calculated value of σ_o at 295°K also agrees with the electrically measured value. Table XV shows further that the values of the temperature-independent parameters which are calculated from the two separate data agree with each other within ~ 5 percent. Therefore, we only need to show that the value of $\Gamma^{o}_{ep}(78°K)$, which is obtained from the data at 78°K by using $b_{ep}(78°K) = (5.94)$, reproduces successfully the value of $\Gamma^{o}_{ep}(295°K)$ which is obtained independently from the optical data at 295°K using $\tilde{b}_{ep}(295°K) = 1.22$. From the optical data, we have:

$$\Gamma^{o}_{ep}(78°K) = 1.41 \times 10^{13} \ \text{sec}^{-1}$$

$$\Gamma^{o}_{ep}(295°K) = 1.12 \times 10^{14} \ \text{sec}^{-1} \qquad (369)$$

each of which has been obtained independently with $\Theta = 375°K$. On the other hand, Table X gives us:

$$J^{o}_{5}(295°K) = 0.5$$

$$J^{o}_{5}(78°K) = 50$$

so that:

$$\Gamma^{o}_{ep}(295°K) = \Gamma^{o}_{ep}(78°K) \times \left(\frac{295}{78}\right)^{5} \left(\frac{J^{o}_{5}(295°K)}{J^{o}_{5}(78°K)}\right) \qquad (370)$$

$$= 1.17 \times 10^{14} \ \text{sec}^{-1}$$

Comparing this with the value, 1.12×10^{14} sec $^{-1}$ of Equation (369), we find that the two values agree within 5 percent. Since use of $\tilde{b}_{ep}(\alpha)$ was essential in obtaining the values of Equation (369) optical data, the good agreement between Equations (369) and (370) automatically establishes the validity of the temperature-dependence of b_{ep}.

Now that we have verified experimentally the temperature-dependence of the dispersion formulas, we are ready to predict various dispersion properties at any arbitrary temperature. As an illustration, we shall calculate the near infrared absorptivity and the optical constants, (n,k), of aluminum at very low temperatures ($\lesssim 10°K$), 375°K, 470°K, and 570°K in addition to the values at 78°K and 295°K which are already available from the optical data of Golovashkin et al (1960).

In the spectral range defined by:

$$0.8\mu \lesssim \lambda \lesssim 3.5\mu$$

we use the formula:

$$A_B \cong \frac{2}{\omega_o} \tilde{\Omega}_o \tilde{G}_\sigma$$

$$\cong \frac{2}{\omega_o} \left[R_{ep} \frac{1}{\alpha^5} J_5^o(\alpha) \tilde{b}_{ep}(\alpha) + R_{ee} \frac{1}{\alpha^2} + \frac{\omega^2}{\Omega_{ee}} \right] \qquad (371)$$

In the same spectral range, the formula for the index of refraction is:

$$n \cong \frac{1}{2} \frac{\omega_o}{\omega^2} \left[\tilde{\Omega}_o + \frac{\omega^2}{\Omega_{ee}} \right] \qquad (372)$$

$$= \frac{1}{4} \left(\frac{\omega_o}{\omega} \right)^2 A_B$$

where Equation (371) is to be used for A_B, and K is nearly independent of temperature and is $\approx \left(\frac{\omega_o}{\omega} \right)$.

Upon using the numerical values of various parameters given in Table XV and X, we obtain:

$$R_{ee} = 7.0 \times 10^{12} \text{ sec}^{-1}$$

$$R_{ep} = 7.7 \times 10^{14} \text{ sec}^{-1}$$

$$\Omega_{ee} = 1.34 \times 10^{16} \text{ sec}^{-1}$$

and thus Equation (371) becomes:

$$A_B \cong \left\{ (0.0103) \frac{10}{\alpha^5} J_5^o(\alpha) \tilde{b}_{ep}(\alpha) + \frac{3.51 \times 10^{-2}}{\lambda^2} \right\} \qquad (373)$$

The values of $A = (A_B + A_S)$ are plotted at the temperatures, $T \lesssim 10°K$, 78°K, 295°K 375°K, 470°K, and 570°K in FIGURES 37 and 38. The values of n are plotted in FIGURE 39. The absorptivity describes a straight line when plotted against $\left(\frac{1}{\lambda^2}\right)$ while n describes a straight line as a function of λ^2. In obtaining the values of A, we have used A_S=0.004 as the skin absorptivity.

It should be noted that the Umklapp processes were completely absent, the second term of Equation (373) would vanish and A_B would be independent of λ. The curves of FIGURE 37 are then replaced by a family of horizontal lines, while the straight lines of FIGURE 39 for n should all pass through the origin.

Finally, it may be said that calculations similar to that which has been done on aluminum can be made on any other metal for which optical data are available. This applies to all the metals that have been investigated in the present chapter except for solid bismuth. The optical data on bismuth show extremely anomalous behavior, as shown by the curves of σ and $(1-\epsilon)$ in FIGURE 44. Whether the anomaly is due to oxides or due to some peculiar properties of the lattice is yet to be determined. While both the present and all the existing theories completely fail to explain the peculiar dispersion properties of solid bismuth that are observed by Markov and Khaikin (1960), Table VIII shows that the liquid bismuth is explained even by the classical Drude theory (Kent, 1919), and hence by the present theory also.

D. DETERMINATION OF IMPURITY CONTRIBUTIONS

Unlike the dc electrical properties, the optical dispersion properties are affected very little by the presence of a small amount of impurities (i.e.,$\sim 10^{-4}$ or less in concentration), except at the far infrared and low

temperatures. It is well known that the impurity contributions give rise to the finite residual resistance important at very low temperatures. The pronounced effect of the impurity scattering at very low temperature is attributed to the fact that the damping coefficients, $\Gamma_{ep}^{o}(\alpha)$ and Γ_{ee}^{o}, vanish with $\sim T^5$ (or $\sim T^3$ for transition metals) and $\sim T^2$, respectively, when T is decreased to the neighborhood of the absolute zero, while Γ_M^o, being independent of temperature, maintains its constant value even at 0°K.

In the present theory, however, the damping coefficients, Γ_{ep}^{o} and Γ_{ee}^{o}, appear multiplied by the respective quantum correction factors, $b_{ep}(\omega,T)$ and $b_{ee}(\omega)$, which, at very low temperatures and in the near infrared, increase exactly as fast as the rate at which Γ_{ep}^{o} and Γ_{ee}^{o} decrease with decrease in T. As a result, the over-all damping coefficient, (ω,T), manages to maintain a constant but relatively large value even at 0°K. For this reason, it will be senseless to attempt to determine the value of Γ_M^o from a near infrared optical data, unless the concentration of impurities is sufficiently large as to make Γ_M^o comparable with R_{ee} or R_{ep}. It was shown in Section V that, unlike σ, $(1-\epsilon)$ depends on the ω-independent damping Ω_o such that:

$$1-\epsilon \approx \frac{\omega^2}{\omega^2 + (\Gamma_M^o)^2} \qquad (374)$$

at very low temperatures. Unless the wavelength is very long, however, this is not going to improve the situation since in most of the infrared and near infrared regions of spectrum, Equation (374) is replaced by $\approx \left(\frac{\omega_o}{\omega}\right)^2$

Therefore, it is quite clear that any attempt to determine Γ_M^o can be made only when the optical data are available in the far infrared region, $1 \ll \beta h \omega \lesssim \alpha$. In this case, Equation (374) is useful, provided that ω is not much larger than Γ_M^o.

At very low temperatures ($T \lesssim 10°K$) and in the far infrared, the optical quantity which is measured with relative ease is the absorptivity, A, or the reflectivity, R =(1-A). The value of Γ_M^o can then be determined from the formulas that are given in Section VIII. For many metals, the values of Γ_{ee}^{o}, Γ_{ep}^{o} and ω_o are available from the room temperature data with an accuracy of 10 percent or less, so that if A_β is measured up to $\lesssim$ 10 percent, the value of Γ_M^o can be determined up to $\lesssim$ 10 percent. The optical estimation of Γ_M^o can be useful when a direct electrical measurement is difficult.

When the value of Γ_M^o is available, the impurity concentration N_M

can be estimated from the complete expression for Γ_M^o (Gurzhi, 1959) or qualitatively from:

$$N_M \sim (\mu_F \tilde{\ell}_M)^{-3} = \left(\frac{\Gamma_M^o}{\mu_F}\right)^3 \tag{375}$$

which gives us the order-of-magnitude estimation, where $(\mu_F\ T_M)$ is the mean free path of the electron-impurity collisions.

SECTION VIII. BULK ABSORPTION AT VERY LOW TEMPERATURES

A. NORMAL METALS AT VERY LOW TEMPERATURES

It was shown in the preceding chapters that the bulk absorptivity, A_B, of a normal metal (i.e., non-superconducting) retains a finite non-zero value even at 0°K in the spectral range given by $\mu \gg \alpha \gg 1$, and vanishes at 0°K, for a pure metal in the limit $\omega \longrightarrow 0$. It was also shown that the bulk absorptivity at 0°K, which we shall call the "zero-point bulk absorptivity," in the near infrared is independent of ω aside from the Umklapp term.

Specifically, we obtained the following formulas for the bulk absorptivity in the high frequency part of the infrared:

$$A_B \approx \frac{2}{\omega_o}\ \Omega_o\ G_\sigma \left[\ 1 - \frac{9}{8}\left(\frac{\Omega_o}{\omega}\right)^2 + \frac{37}{32}\left(\frac{\Omega_o}{\omega}\right)^4 + \ldots\right]$$

$$: \omega > \Omega_o \quad (\mu > \alpha) \tag{376}$$

and:

$$A_B \approx \frac{2}{\omega_o}\ \tilde{\Omega}_o\ \tilde{G}_\sigma : \quad \omega \gg \tilde{\Omega}_o \quad (\mu \gg \alpha) \tag{377}$$

where:

$$\begin{pmatrix} \Omega_o \\ \tilde{\Omega}_o \end{pmatrix} = \Gamma_{ep}^o \begin{pmatrix} b_{ep}(\mu,\alpha) \\ \tilde{b}_{ep}(\alpha) \end{pmatrix} + \Gamma_{ee}^o + \Gamma_M^o$$

$$G_\sigma = \left(1 + \frac{\omega^2}{\Omega_o\ \Omega_{ee}}\right)$$

$$\tilde{G}_{\sigma} = \left(1 + \frac{\omega^2}{\bar{\Omega}_o \Omega_{ee}} \right) \tag{378}$$

and $(G_{\sigma} - 1)$ and $(\tilde{G}_{\sigma} - 1)$ can differ from zero only when the Umklapp processes are present.

It is the purpose of the present work to compute the absorptivity, A_B, at very low temperatures in the spectral ranges defined by:

$$\text{(condition i)} \quad \alpha \gg \mu \gg 1$$

$$\text{(condition ii)} \quad \alpha \gg \mu, \ \mu \sim 1 \tag{379}$$

both of which are in the far infrared. At $T \approx 0°K$, the condition (i) applies for practically all frequency values of infrared, and the calculated value of A_B would then represent the far infrared zero-point bulk absorptivity.

It was explained in Section V that the generalized Hagen-Rubens formula:

$$A_B = 2 \sqrt{\frac{\nu}{\sigma_o}} \left[1 + \frac{\Gamma_{ep}^{o}}{\Gamma^{o}} (b_{ep} - 1) \right]^{\frac{1}{2}} \tag{380}$$

applies in the far infrared when the temperature is not too low. We recall that Equation (380) was obtained by taking $\omega^2 \ll \Omega_o^2, \bar{\Omega}_o^2$.

At very low temperatures, however, ω^2 may not be necessarily smaller than Ω_o^2 and $\bar{\Omega}_o^2$ in the far infrared, since $\bar{\Omega}_o$, being independent of ω, decrease in T and Ω_o^2 likewise may have a small value if the quantum correction factor, $b_{ep}(\mu, \alpha)$, does not counteract sufficiently the rapid decrease of $\Gamma_{ep}^{o}(\alpha)$ with decrease in T.

Therefore, it is quite clearly the primary task of the present work to investigate the ω-dependence of $b_{ep}(\mu,\alpha)$ in the spectral ranges of Equation (379) and also to specify the order of magnitude of Γ_M^{o} relative to the values of ω in these spectral ranges. We shall first investigate the ω-dependence of $b_{ep}(\mu,\alpha)$ for $\mu \gg 1$ and $T \cong 0°K$. We shall, for the sake of generality, calculate it for both $\mu > \alpha$ and $\mu < \alpha$.

Upon using various formulas for $J_n(\mu,\alpha)$ and $K_n(\mu,\alpha)$ in the results of Sections IV, V, and VI, we obtain the following expressions for b_{ep}

(μ,α) for both transition and nontransition metals, μ,α:

$$b_{ep}(\mu,\alpha) \approx \frac{\alpha^5}{10}\left[1 - \frac{5}{6}\frac{\alpha}{\mu}\right] \Big/ J_5^o(\alpha) \tag{381}$$

$\mu < \alpha$:

$$b_{ep}(\mu,\alpha) \approx \frac{\mu^5}{60} \Big/ J_5^o(\alpha) \tag{382}$$

for nontransition metals, and $\mu > \alpha$:

$$b_{ep}(\mu,\alpha) \approx \frac{\alpha^3}{6}\left[1 - \frac{3}{4}\frac{\alpha}{\mu}\right] \Big/ J_3^o(\alpha) \tag{383}$$

$\mu < \alpha$:

$$b_{ep}(\mu,\alpha) \approx \frac{\mu^3}{24} \Big/ J_3^o(\alpha) \tag{384}$$

for transition metals, where, for the sake of convenience, we have taken α_E to be zero.

Thus, the electron-phonon damping coefficient of nontransition metals is given by:

$$\Gamma_{ep}(\mu,\alpha) \approx \frac{R_{ep}}{10}\left(1 - \frac{5}{6}\frac{K\Theta}{\hbar\omega}\right) : \quad \mu > \alpha \tag{385}$$

$$\approx \frac{R_{ep}}{60}\left(\frac{\hbar\omega}{K\Theta}\right)^5 \quad : \quad \mu < \alpha \tag{386}$$

For transition metals with $\alpha_E \cong 0$, we have:

$$\Gamma_{ep}^{sd}(\mu,\alpha) \approx \frac{R^{sd}}{6}\left(1 - \frac{3}{4}\frac{K\Theta}{\hbar\omega}\right) : \quad \mu > \alpha \tag{387}$$

$$\approx \frac{R^{sd}}{24}\left(\frac{\hbar\omega}{K\Theta}\right)^3 \quad : \mu < \alpha \tag{388}$$

It must be remembered that, for a ferromagnetic metal, Equations (387) and (388) must be multiplied by 1/2 on the R.H.S. as the correction for the residual magnetization. Equations (383), (384), (387), and (388) will also apply to those transition metals which have $\alpha_E > 0$ provided that α_E is sufficiently smaller than α. In this case, Equations (384) and (388) are multiplied by $(1 - \frac{\alpha_E}{\mu})$ so that $\Gamma_{ep}^{sd}(\mu,\alpha)$ has non-zero values for $\hbar\omega > K\Theta_E$ only.

For both types of metals, the electron-electron damping coefficient is given by:

$$\Gamma_{ee}(\mu,\alpha) \approx \frac{1}{4\pi^2} R_{ee} \left(\frac{\hbar\omega}{K\Theta}\right)^2 \tag{389}$$

In order to write down the formulas for the bulk absorptivity, we need to compare the magnitudes of ω^2 with Ω_o^2, $\bar{\Omega}_o^2$: i.e., to find out which of the Equations (376) and (380) is applicable.

At $T \cong 10°K$, $\mu = 1$ corresponds to the values of ω which is of the order of $\sim 10^{12}$ sec^{-1} We are therefore interested in the spectral range given by:

$$10^{12} \lesssim \omega \ll \frac{K\Theta}{\hbar} \cong 10^{13} \sim 10^{14} \text{ sec}^{-1} \tag{390}$$

It was shown in preceding sections that R_{ep} (and R_{ep}^{sd}), R_{ee} and Γ_M^o (for a "pure" metal) have typical values of the order $10^{13} \sim 10^{14}$, $10^8 \sim 10^{10}$, and $\lesssim 10^{10}$, respectively. The Debye temperature is generally of the order of several hundered °K corresponding to ω of $10^{13} \sim 10^{14}$ sec^{-1}

Therefore, for $\omega \simeq 10^{12}$ sec^{-1} and $\Theta \tilde{=} 100°K$, we have:

$$\omega^2 \gg \Omega_o^2 \tag{391}$$

The same is then true for $\bar{\Omega}_o^2$ since it contains no ω-dependence and:

$$\bar{\Omega}_o \approx (\Gamma_M^o + \Gamma_{ee}^o) \ll \omega \tilde{=} 10^{12} \text{ sec}^{-1} . \tag{392}$$

This implies that Equation (376) is to be used for evaluating the absorptivity in the spectral range of $\omega \gtrsim 10^{12}$ sec^{-1} and $T < 10°K$.

Thus, we have the following formulas for the bulk absorptivity of the noble metals and the transition metals, respectively:

$\mu > \alpha$:

$$A_B \approx \frac{2}{\omega_o} \left\{ \frac{R_{ep}}{10} \left(1 - \frac{5}{6} \frac{K\Theta}{\hbar\omega} \right) + \frac{1}{4\pi^2} R_{ee} \left(\frac{\hbar\omega}{K\Theta} \right)^2 + \Gamma_M^o \right\} \tag{393}$$

$\mu < \alpha$:

$$A_B \approx \frac{2}{\omega_o} \left\{ \frac{R_{ep}}{60} \left(\frac{\hbar\omega}{K\Theta} \right)^5 + \frac{1}{4\pi^2} \left(\frac{\hbar\omega}{K\Theta} \right)^2 + \Gamma_M^o \right\} \tag{394}$$

for nontranstion metals, and:

$\mu > \alpha$:

$$A_B^{sd} \approx \frac{2}{\omega_o} \left\{ \frac{X(0)}{2} \frac{R^{sd}}{6} \left(1 - \frac{3}{4} \frac{K\Theta}{\hbar\omega} \right) + \frac{1}{4\pi^2} R_{ee} \left(\frac{\hbar\omega}{K\Theta} \right)^2 + \Gamma_M^o \right\} \tag{395}$$

$\mu < \alpha$:

$$A_B^{sd} \approx \frac{2}{\omega_o} \left\{ \frac{X(0)}{2} \frac{R^{sd}}{24} \left(\frac{\hbar\omega}{K\Theta} \right)^3 + \frac{1}{4\pi^2} R_{ee} \left(\frac{\hbar\omega}{K\Theta} \right)^2 + \Gamma_M^o \right\} \tag{396}$$

for transition metals, where $X(0) = 1$ for ferromagnetic metals and $X(0) = 2$ for paramagnetic metals.

Although R_{ee} is generally smaller than R_{ep} by a large factor, contributions of the electron-electron collisions to Equations (393) ~ (396) can be substantially large compared with the electron-phonon term because of the smaller power of $\left(\frac{\hbar\omega}{K\Theta} \right)$ in the electron-electron term. This is even more true if Equations (395) and (396), α_E is very large. The first terms inside the braces of Equations (395) and (396) must be equated to zero for $\hbar\omega \leq K\Theta_E$ when Θ_E is not zero so that the only ω-dependence appears in the Umklapp term.

Now let us investigate the case of $\mu \lesssim 1$ and:

$$\omega \simeq \left(\frac{KT}{\hbar}\right) \lesssim 10^{12} \text{ sec}^{-1} \tag{397}$$

This spectral range is of interest when one wishes to compare the absorption of a normal metal since the superconducting energy gap is generally of the order of several °K in temperature and thus, $\omega \lesssim 10^{12}$ sec.$^{-1}$ For $\omega \sim 10^{11}$ sec^{-1}, we will, in general, have $\left(\frac{\hbar\omega}{K\Theta}\right) \lesssim 10^{-2}$ for $\Theta \gtrsim 100°K$. This implies that we will have Γ_M^o as the most dominant term in both Ω_o and $\bar{\Omega}_o$ when the metal is not completely free of impurities. However, since we saw previously that $\Gamma_M^o \lesssim 10^{10}$ sec.$^{-1}$ for the most of the so-called "pure" metals samples, we still have:

$$\left(\frac{\Omega_o}{\omega}\right), \left(\frac{\bar{\Omega}_o}{\omega}\right) \lesssim \frac{1}{10} \tag{398}$$

so that Equation (376) is again applicable.

Therefore, we shall henceforth consider Equation (376) as the general formula for bulk absorptivity which is applicable in the far infrared at very low temperatures regardless of whether $\mu \gg 1$ or $\mu \simeq 1$, unless a metal has an exceptionally large value of Γ_M^o. When the sample has a large Γ_M^o, $\gtrsim 10^{12}$ sec.$^{-1}$, say, the Hagen-Rubens formula (Equation 380) should be used with $\Gamma^o(\alpha)$ equated to Γ_M^o.

For $\alpha \gg \mu$ and $\mu \lesssim 1$, we have the following formulas for $J_n(\mu,\alpha)$ and $K_n(\mu,\alpha)$:

$$J_n(\mu,\alpha) \approx \frac{2}{e^{2\mu}-1}\left[\!\left[\mu\, J_n^o(\alpha) + \mu^3 \frac{n(n-1)}{3!} J_{n-2}^o(\alpha) + \ldots\right]\!\right]$$

$$K_n(\mu,\alpha) \approx \frac{2}{e^{2\mu}-1}\left[\!\left[\mu\, K_n^o(\alpha) + \mu^3 \frac{n(n-1)}{3!} K_{n-2}^o(\alpha) + \ldots\right]\!\right] \tag{399}$$

where the first terms inside $[\![\ldots]\!]$ are the largest terms. These formulas are to be used in evaluating $b_{ep}(\mu,\alpha)$:

$$b_{ep}(\mu,\alpha) = \frac{e^{\mu}\sinh\mu}{\mu}\left[\!\left[J_5(\mu,\alpha) - \mu\frac{(e^{\mu}-1)^2}{(e^{2\mu}-1)}\left[J_4 + 2K_4\right]\right]\!\right] \tag{400}$$

for nontransition metals, and:

$$b_{ep}(\mu,\alpha) = \frac{e^{\mu}\sinh\mu}{\mu}\left[\left[\bar{J}_3(\mu,\alpha) - \mu\frac{(e^{\mu}-1)^2}{e^{2\mu}-1}\left[\bar{J}_2(\mu,\alpha) + 2\bar{K}_2(\mu,\alpha)\right]\right]\right] \tag{401}$$

for transition metals. Then, it is a trivial matter to write down the bulk absorptivity since we only need to replace b_{ep} of Equations (394) ~ (396) by (400) and (401) in the electron-phonon term.

Finally, it may be reminded that the values of the parameters R_{ep}, R_{ee}, and R_{ep}^{sd} which are required for a numerical estimation of Equations (394) ~ (396) are to be obtained from the optical data taken at higher temperatures and alternatively from the dc electrical data. The same applies to the other parameters.

B. BULK ABSORPTION BY SUPERCONDUCTORS

Compared with what are available on normal metals, very little experimental data are available on the optical and infrared absorption in superconductors. Some of the latest measurements are those of Biondi and Garfunkel (1959) and Richards and Tinkham (1960). These measurements are designed to determine the superconducting energy gap from the shape of the observed absorption curves. Specifically, these experiments include measuring the absorption of the external electromagnetic wave in a superconductor relative to that in a normal metal, and the results are embodied in the curves showing the ratio:

$$r_{sn} = 1 - \frac{A_s}{A_n} \tag{402}$$

where A_s and A_n are the absorptivities, at a given frequency and temperature, of the superconducting and normal metal, respectively. The normal state of metal is accomplished by applying a magnetic field parallel to the surface which is strong enough to reduce the gap to zero. The results are equivalently expressed in terms of the power absorbed, P_s and P_n, instead of the absorptivities, A_s and A_n. In the plot of r_{sn} versus ω, for instance, the energy gap is determined by locating the frequency ω_g where r_{sn} starts to decrease abruptly: that is, the head of the absorption tail.

The superconductor differs from the normal state in that the density-of-states function, $\rho(E)$, does not show the continuous distribution around the Fermi level in the form:

$$\rho(E) = \text{constant} \times \sqrt{E} \tag{403}$$

but possesses discontinuities exhibiting a forbidden region on both sides of the Fermi level.

In the theory of Bardeen, Cooper and Schrieffer (1957), a certain minimum energy is required to produce an excitation from the ground state. This minimum excitation energy, or the energy gap, is a central result of the BCS theory. Existence of the predicted energy gap has been fully verified, and is by now a popularly accepted fact. According to the theory of BCS, the density-of-states function, $\delta_s(E)$, of a superconductor is given by:

$$\rho_s(E) = \rho_n(o) \quad \frac{Z}{\left[Z^2 - \epsilon^2\right]^{\frac{1}{2}}} \quad : \quad |Z| > \epsilon$$

$$= 0 \quad : \quad |Z| < \epsilon \qquad (404)$$

where δ_N (0) is the density-of-states function of a normal metal evaluated at the Fermi level, ϵ is (1/2) of the energy gap E_g which is a function of temperature, and:

$$Z = (E - E_F) \qquad (405)$$

It is seen that $\rho_s(E)$ increases very sharply at the gap edges, $E = (E_F \pm \epsilon)$. The energy gap $E_g(T)$ achieves its maximum value $E_g(0)$ at $T = 0^\circ K$ and decreases to zero as T is increased to T_c, the superconducting transition temperature. In the region where $E < E_f - \epsilon$, all the electrons occur paired and this part of the band is called the paired band. On the other hand, the electrons in the region where $E > E_F + \epsilon$ are unpaired, and this part of the band is usually referred to as the unpaired band or the "normal" conduction band which bears no difference from the conduction band of a normal metal. However, at a temperature T below T_c, most of the electrons are paired, and very few are available in the unpaired band. Therefore, most of the absorption will be due to these paired electrons. When the paired electrons make transitions to the unpaired band, the energy absorbed must be at least as much as that which is required to overcome the gap E_g: otherwise, no transition of this type is possible, since electrons are forbidden in the gap. The BCS density-of-states function, ρ_s (E), is schematically illustrated in FIGURE 47. The typical temperature dependence of E_g is shown in FIGURE 48. For $T > T_c$, the metal is completely normal, and absorptivity is fully described by the results obtained in Table XIII. The curve showing the dependence of E_g on the magnetic field H bears a close resemblance to that of FIGURE 48 when we replace T by H and T_c by a certain critical field strength H_c. Thus when $H > H_c$, the metal is completely normal even if $T < T_c$, and the optical properties are

satisfactorily described by the results obtained in VIII- (A) and also in the preceding chapters.

The latest theory of optical dispersion in superconductors is due to Mattis and Bordeen (1958), who calculate the frequency dependence of the complex conductivity σ_s of superconductor on the basis of the BCS theory. Specifically, they calculate the ratios:

$$\left(\sigma\ (\omega,\ \underline{p}) \Big/ \sigma_N \right), \quad \left(\sigma_2\ (\omega, \underline{p}) \Big/ \sigma_N \right)$$

σ_N being the high frequency conductivity of normal metal and $\underline{p}$ the photon propagation momentum that is involved, and where σ_1 and σ_2 are defined as:

$$\sigma_s = \sigma_1 + i\ \sigma_2 \tag{406}$$

Based on these results, Richards and Tinkham calculate the quantity:

$$r_{sn} = 1 - \frac{A_s}{A_n} = 1 - \frac{R_s}{R_n} \tag{407}$$

from the relations:

$$\frac{Z_s}{Z_n} = \left(\sigma_n \Big/ \sigma_1 + i\ \sigma_2 \right)^{\frac{1}{3}} \tag{408}$$

$$Z_n = (1 + i\sqrt{3})\ R_n$$

$$R_n = \mathrm{Re}\ (Z_n) \tag{409}$$

$$R_s = \mathrm{Re}\ (Z_s)$$

where Z_s and Z_n are the surface impedance of superconducting and normal metals, and R_s and R_n are the respective surface resistance values.

These relations are applicable only in the extreme anomalous limit

where all the contributions to the absorption and resistance come from the surface effects in which the electrons absorb photons and collide with the surface of the metal to conserve energy and momentum. Thus, they do not include the possible contributions of the bulk where electrons might absorb photons and emit phonons to conserve energy and momentum. The bulk contribution of this kind has been found to be significant in normal metals and was fully discussed theoretically in Section VIII, paragraph A and preceding sections. That the bulk effects might also be significant in a superconductor on account of the large electron-phonon interactions that are present was suggested by Richards and Tinkham (1960) following the similar suggestion by Holstein (1952) for a normal metal.

Richards and Tinkham compared the experimental absorption-edge curves for superconducting lead and tin with the curve predicted by the theory of Mattis and Bardeen. The comparison shows that although they agree qualitatively as far as the shape of the absorption-edge is concerned, the theoretical values are much greater than the measured values. Further, the theoretical curve tails off much slower than the observed edge. This is shown in FIGURE 50 where r_{sn} is plotted against the ratio (ω/ω_g) for W greater than $\omega_g = (E_g/\hbar)$. At the present, no positive explanations are available on the discrepancy between the theoretical and experimental absorption edges shown in FIGURE 50. Since the theoretical curve of Mattis and Bradeen is obtained by considering the anomalous skin effects only, it might perhaps be worthwhile to follow the suggestion of Richards and Tinkham and compute the bulk contributions to the absorptivity. If the bulk contribution is significant at all, it could very well effect in reducing the theoretical values of Mattis and Bardeen, although it is not certain as to whether the magnitude of the bulk absoprtion is of the right order as to bridge the gap between the theory and experiment. For $\omega < \omega_g$, Schrieffer (1959) derived the formula:

$$[1- r_{sn}] \cong \frac{1}{h\omega} \int_{\epsilon}^{\infty} \frac{(E_1 E_2 + \epsilon^2)\left[F(E_1) - F(E_2)\right]}{\left[(E_1^2 - \epsilon^2)(E_2^2 - \epsilon^2)\right]^{\frac{1}{2}}} dE_1 \qquad (410)$$

from the BCS theory assuming a symmetric electron-phonon interaction coefficients. This formula applies in the spectral range of $\frac{1}{2}\omega_g < \omega < \omega_g$ and differs from zero only for $T > 0°K$. Richards and Tinkham (1960) checked this formula in the above spectral range and found good agreement with the experimental absorption data. Equation (410) is plotted in FIGURE 49. It is shown that r_{sn} rises slowly with increase in ω and is smaller than unity only by a small fraction. Experimental curves of r_{sn} shown that the rise of r_{sn} with increase in ω is pronounced in some superconductors such as the transition metals vanadium and indium while others have a nearly flat r_{sn} for $\omega < \omega_g$. At any rate, it is certain that the r_{sn} curves do have their peaks, which are very likely to be discontinuous because of the discontinuity of ρ_s at the gap edges, at $\omega = \omega_g$

and tails off rapidly as ω is increased further beyond ω_g.

In what follows, we shall do our calculations for the bulk absorptivity only for $\omega > \omega_g$ and at T= 0°K. The theoretical method is essentially the same as in the preceding sections, and the difference will be in that we now have to use the new density-of-states function, $\rho_s(E)$, that is offered by the BCS theory.

The density-of-states function, ρ_s, and the Fermi function, F(E) define the number of electrons per unit volume by the relation:

$$n^o = n_- + n_+$$

$$= 2\left[\int_{-\infty}^{-\epsilon} dz + \int_{+\epsilon}^{+\infty} dz\ \rho_s(z)\ F(z)\right]$$

$$: Z = (E - E_F) \qquad (411)$$

where n_- is the number of paired electrons per unit volume and n_+ is the number of unpaired electrons per unit volume. At 0°K, we have $n_+ = 0$ and the second integral vanishes.

Probability per unit time and per unit energy range that an electron initially at the state, E_1, makes a transition to the final states in the range, $E_2 \longrightarrow (E_2 + dE_2)$, is given by:

$$\frac{\Delta P}{\Delta E_2} \propto P(E_1 \rightarrow E_2)\ \rho_s(E_2)\left[1 - F(E_2)\right] \qquad (412)$$

and hence:

$$P(E_1) \propto \int dE_2\ \rho_s(E_2)\left[1 - F(E_2)\right] P(E_1 \rightarrow E_2) \qquad (413)$$

Similarly, the average of $P(E_1)$ over all the initial states is given by:

$$\langle P \rangle \propto \int\int dE_1\ dE_2\ \delta_s(E_1)\ \rho_s(E_2)\ F(E_1)\left[1 - F(E_2)\right] P(E_1 \rightarrow E_2) \qquad (414)$$

where it is implicit that the surface integrals have already taken care of the necessary requirements of conservation of energy and momentum.

Upon comparing Equations (413) and (414) with the corresponding equations for a normal metal in Chapter IV, it is readily shown that the expression for the power expenditure, $\overline{W}_s$, of a superconductor will involve the function $F_{(s)}^{(r)}$ in the form:

$$F_{(s)}^{(r)}(q) = \frac{1}{\beta} \frac{1}{\rho_N(0)^2} \int_{-\infty}^{+\infty} dx \frac{1}{1 + e^{x+a}} \frac{e^x}{1 + e^x} \rho_s(x) \rho_s(x+a) \quad (415)$$

where:

$$A = \beta (rE_q + s\hbar\omega)$$

We have only $F_{(-)}^{(+)}$ to consider and other three vanish at T=0°K. Further, the integrand:

$$\frac{e^x}{1 + e^x} \qquad \frac{1}{1 + e^{x+a}} \quad (416)$$

is different from zero only for those values of ω which satisfies the inequality:

$$0 < x < - a \quad (417)$$

The possible values of x are further restricted due to the presence of the energy gap: namely, the condition expressed by Equation (404):

$$\left|x + a\right| , \quad \left|x\right| > \beta \epsilon \quad (418)$$

for the product, $\rho_s(x)\ \rho_s(x+a)$, not to vanish. Combination of Equations (417) and (418) immediately yields the inequality condition:

$$\beta \epsilon < x < - (a+ \epsilon) \beta$$

$$2 \epsilon < - a \quad (419)$$

The integral (415) thus reduces to the form:

$$F_{(-)}^{(+)}(q) \approx \int_{\epsilon}^{-(a+\epsilon)} dy \; \frac{|y|\,|y+a|}{\left[(y^2-\epsilon^2)\,(y+a)^2-\epsilon)\right]^{\frac{1}{2}}} \tag{420}$$

For $\hbar\omega < K\Theta$, we obtain the following expression for the power expenditure per unit volume per unit time:

$$\overline{W}s \cong \frac{3\pi}{4} \; \frac{e^2 g^2 N_p E^2}{n_o M (K\Theta)^6 \omega^2} \; x$$

$$\int_{o}^{(\hbar\omega - E_g)} \zeta^4 \, d\zeta \int_{\epsilon}^{(\hbar\omega - \epsilon)} dx \; \frac{|x|\,|x+\zeta-\hbar\omega|}{\left\{\left[x^2-\epsilon^2\right]\left[(x+\zeta-\hbar\omega)^2-\epsilon\right]\right\}^{\frac{1}{2}}} \tag{421}$$

The absorptivity A_s is then readily obtained as:

$$A_s \approx \sqrt{\frac{m^*}{\pi n_- e^2}} \; \frac{R}{60} \left(\frac{\hbar\omega}{K\Theta}\right)^5 (1 - r_{sn}) \tag{422}$$

where:

$$(1 - r_{sn}) \simeq \frac{6}{(\hbar\omega)^5} \int_{o}^{(\hbar\omega - Eg)} \zeta^4 ds \int_{\epsilon}^{(\hbar\omega - \epsilon)} dx \; \frac{|x|\,|x+\zeta-\hbar\omega|}{\left\{\left[x^2-\epsilon^2\right]\left[(x+\zeta-\hbar\omega)^2-\epsilon\right]\right\}^{\frac{1}{2}}} \tag{423}$$

where R is exactly the same as R_{ep} if we take:

$$n_- + n_+ \simeq n_- \simeq n_o \tag{424}$$

: i.e., all conduction electrons are in the paired band at $T \simeq 0°K$.

Equation (423) is good only when the Umklapp processes and impurity scattering can be ignored in the normal metal. Otherwise, we must use the more general formula:

$$1 - r_{sn} \cong \frac{1}{1 + \frac{15}{\pi^2}\frac{R_{ee}}{R}\left(\frac{K\Theta}{\hbar\omega}\right)^3 + 60\frac{\Gamma_M^o}{R}\left(\frac{K\Theta}{\hbar\omega}\right)^5} \times$$

$$\frac{6}{(\hbar\omega)^5}\int_0^{(\hbar\omega - Eg)} \zeta^4\, d\zeta \int_{\epsilon}^{(\hbar\omega - \zeta - \epsilon)} dx \; \frac{x\;\; x + \zeta - \hbar\omega}{\left\{\left[x^2 - \epsilon^2\right]\left[(x + \zeta - \hbar\omega)^2 - \epsilon^2\right]\right\}^{\frac{1}{2}}} \qquad (425)$$

The integrals of Equations (417) and (419) are difficult to evaluate exactly because of the discontinuity in the density-of-states functions.

However, a simple, and perhaps oversimplified, approximation can be obtained upon noting that the first factor in the integrand represents the density of states of the initial states and the second factor represents that of the final states, and that, at T = 0°K, most transitions may involve only those initial states which lie at the lower edge of the gap: i.e.,

$$E_1 \cong E_F - \epsilon, \quad x \cong \epsilon \qquad (426)$$

This means that most of the contribution to the integral in Equation (421) comes from the lower limit of the integral, although the apparent form of the formula tends to show that the integrand has singularity at the upper limit as well as at the upper limit as well as at the lower limit. The singularity at the upper limit has to do with the fact that most of the electrons reaching the unpaired band as the result of transitions are likely to crowd at the upper edge of the gap, where the density-of-states function is large. We thus have:

$$F_{(-)}^{(+)}(q) \approx (\hbar\omega - E_q - \epsilon) \quad :> \; + \epsilon \qquad (427)$$

where it is implicit that the integral in q is to include only those values which make $F_{(-)}^{(+)} > + \epsilon$. After some necessary mathematical steps, we find

that r_{sn} of Equation (423) reduces to the simple formula:

$$1 - r_{sn} \approx \left(1 - \frac{E_g}{\hbar\omega}\right)^5 \left(1 + 2\ \frac{E_g}{\hbar\omega}\right)$$

$$: \hbar\omega < K\,\Theta \tag{428}$$

The expresions for A_s and r_{sn} of a transition metal may be obtained in the same manner. In particular, for those transition metals which have $\alpha_E = 0$, the formula for r_{sn} which is equivalent to Equation (428) is readily obtained as:

$$1 - r_{sn} \approx \left(1 - \frac{E_g}{\hbar\omega}\right)^2 \left(1 - \left(\frac{E_g}{\hbar\omega}\right)^2\right) \tag{429}$$

Equations (428) and (429), unfortunately, fail to improve the agreement with the experimental values of FIGURE 50. For a more rigorous comparison, however, we have to obtain a numerical solution to the complete integral of Equation (423). This would certainly improve the situation since the assumption that was adopted in obtaining the crude solutions in Equations (428) and (429), was to restrict absorptive transitions to only those pairs lying at the edge of the gap, while the complete integral takes into consideration the transitions of any electrons in the paired band, thus increasing the value of $(1 - r_{sn})$.

APPENDIX A.

CALCULATION OF $J_n^o(\alpha)$

$$J_n^o(\alpha) = \int_o^\alpha x^n \, dx/(e^x-1)\ (1-e^{-x}) \quad : \quad n > 0 \tag{1}$$

A: $\alpha \ll 1$

$$J_n^o(\alpha) \approx \int_o^\alpha x^{n-2} \, dx \left[1 - \frac{7}{12} x^2 + \ldots \right]$$

$$= \frac{1}{n-1} \alpha^{n-1} - \frac{7}{12} \frac{1}{n+1} \alpha^{n+1} + \ldots \tag{2}$$

B: $\alpha \gg 1$

$$J_n^o(\alpha) \approx n \int_o^\infty \frac{x^{n-1} \, dx}{e^x - 1} = n! \sum_{m=1}^{\infty} \left(m^{-n} \right) \tag{3}$$

e.g.,

$$J_5^o(\alpha) = 124.4$$

C: General Calculation

$$J_n^o(\alpha) = \int_o^\alpha \frac{e^x x^n \, dx}{(e^x - 1)^2} = n \int_o^\alpha \frac{x^{n-1} e^{-x} \, dx}{(1 - e^{-x})} - \frac{\alpha^n}{e^\alpha - 1} \tag{4}$$

The integral on the right-hand side can be written:

$$\int_o^\alpha \frac{x^{n-1} e^{-x}}{1 - e^{-x}} \, dx = \int_o^\infty \frac{x^{n-1} e^{-x}}{1 - e^{-x}} \, dx - \int_\alpha^\infty \frac{x^{n-1} e^{-x} \, dx}{1 - e^{-x}} \tag{5}$$

The definite integral can be evaluated by the series:

$$\int_0^\infty \frac{x^{n-1}\, e^{-x}}{1 - e^{-x}}\, dx = (n-1)! \sum_{m=1}^{\infty} \left(m^{-n}\right) \tag{6}$$

e.g.

$$= 24.8861 \; ; \; n = 5$$

The indefinite integral can also be written as a series:

$$\int_\alpha^\infty \frac{x^{n-1}\, e^{-x}}{1 - e^{-x}}\, dx = \sum_{r=1}^{n} \frac{(n-1)!}{(n-r)!}\, \alpha^{n-r} \sum_{m=1}^{\infty} \left(m^r\, e^{m\alpha}\right)^{-1} \tag{7}$$

Substitute Equations (5), (6) and (7) into Equation (4):

$$J_n^o(\alpha) = \left[n! \sum_{m=1}^{\infty} \left(m^{-n}\right) - \sum_{r=1}^{n} \frac{n!}{(n-r)!}\, \alpha^{n-r} \sum_{m=1}^{\infty} \left(m^r\, e^{m\alpha}\right)^{-1} - \alpha^n \Big/ \left(e^\alpha - 1\right) \right] \tag{8}$$

D: $J_5^o(\alpha)$

From Equation (8), we compute the numerical values of $J_5^o(\alpha)$. For small values of α:

$$\frac{1}{\alpha^4}\, J_5^o(\alpha) = B_o + B_1\alpha^2 + B_2\alpha^4 + B_3\alpha^6 + B_4\alpha^8 + B_5\alpha^{10} + \ldots \tag{9}$$

$$
\begin{aligned}
B_0 &= 0.25000000 \\
B_1 &= -.01388889 \\
B_2 &= 0.00052083 \\
B_3 &= -.00001653 \\
B_4 &= 0.00000096 \\
B_5 &= -.00000003
\end{aligned}
\tag{10}
$$

This series is good to 8 places for $\alpha = 1$, and its accuracy diminishes thereafter.

For somewhat larger values of α, let

$$u = \frac{1}{3}\ \alpha.$$

Then:

$$\frac{1}{\alpha^4}\ J_5^o(\alpha) = D_o + D_1u^2 + D_2u^4 + D_3u^6 + \ldots + D_9u^{18} \tag{11}$$

$$
\begin{aligned}
D_o &= 0.250000 \\
D_1 &= -.125000 \\
D_2 &= 0.042188 \\
D_3 &= -.012054 \\
D_4 &= 0.003164 \\
D_5 &= -.000792 \\
D_6 &= 0.000193 \\
D_7 &= -.000046 \\
D_8 &= 0.000011 \\
D_9 &= -.000003
\end{aligned}
\tag{12}
$$

This series is good for $\alpha < 2\pi$ and diverges for $\alpha > 2\pi$; and should not be used for values of α much larger than 3 so that the last terms contribute significantly.

APPENDIX B.

CALCULATION OF $\tilde{b}_{ep}(\alpha)$

In the limit of $h\omega \gg K\Theta$, the quantum correction factor $b_{ep}(\mu,\alpha)$ becomes:

$$\tilde{b}_{ep}(\alpha) = \left[\frac{1}{5} + \frac{\alpha^5}{5}\left(1/2 + \frac{1}{e^{\alpha}-1}\right) \Big/ J_5^o(\alpha)\right] \tag{1}$$

With the help of Appendix I, we evaluate $\tilde{b}_{ep}(\alpha)$ numerically for $\alpha < 2\pi$.

For small values of α:

$$\tilde{b}_{ep}(\alpha) = \frac{1}{5} + \frac{A_o + A_1\alpha^2 + A_2\alpha^4 + A_3\alpha^6 + A_4\alpha^8}{B_o + B_1\alpha^2 + B_2\alpha^4 + B_3\alpha^6 + B_4\alpha^8 + B_5\alpha^{10}} \tag{2}$$

where:

$$\begin{aligned} A_o &= 0.20000000 \\ A_1 &= 0.01666667 \\ A_2 &= -.00027778 \\ A_3 &= 0.00000661 \\ A_4 &= -.00000017 \end{aligned} \tag{3}$$

and the B-series are the same as in Equation (9).

The A series are the quantity:

$$\frac{\alpha}{5}\left(1/2 + \frac{1}{e^{\alpha}-1}\right) \cong \sum_{m=o}^{\infty} A_m \alpha^{2m} \tag{4}$$

$$: \alpha \lesssim 1$$

For somewhat larger values of α, let

$$u = 1/3\ \alpha.$$

Then:

$$\tilde{b}_{ep}(\alpha) = \frac{1}{5} + \frac{C_o + C_1u^2 + C_2u^4 + C_3u^6 + \ldots + C_8u^{16}}{D_o + D_1u^2 + D_2u^4 + D_3u^6 + \ldots + D_9u^{18}} \qquad (5)$$

$$: \alpha < 2\pi$$

$$\sum_{m=o}^{\infty} C_m\ u^{2m} = \frac{\alpha}{5}\left(1/2 + \frac{1}{e^{\alpha}-1}\right) \qquad (6)$$

$$C_o = 0.200000$$

$$C_1 = 0.150000$$

$$C_2 = -.022500$$

$$C_3 = 0.004821$$

$$C_4 = -.001085 \qquad (7)$$

$$C_5 = 0.000247$$

$$C_6 = -.000056$$

$$C_7 = 0.000013$$

$$C_8 = -.000003$$

and the D-series are the same as in Equation (11).

Similarly, it can be evaluated for $\alpha > 2\pi$ when the formulate of Appendix are used.

For $\alpha \geq 17$, for instance, we obtain:

$$\tilde{b}_{ep}(\alpha) = \left(\frac{1}{5} + \frac{\alpha^5}{1244.31}\right) \qquad (8)$$

APPENDIX C.

INTEGRALS $J_n(\mu,\alpha)$ and $K_n(\mu,\alpha)$

A: General Expression for $J_n(\mu,\alpha)$

$$J_n(\mu,\alpha) = \int_o^\alpha x^n\, dx \Big/ \left(e^x - e^\mu\right)\left(e^\mu - e^{-x}\right) : \quad n > 0 \tag{1}$$

We will use the relation:

$$\frac{1}{\left(e^x - 1\right)\left(e^{x+2\mu} - 1\right)} = \frac{e^{-x}}{\left(e^{2\mu} - 1\right)}\left[\frac{1}{e^x - 1} - \frac{1}{e^{x+2\mu}-1}\right]$$

$$\int_o^\alpha \frac{x^m\, dx}{e^x-1} = \frac{x^{m+1}}{m+1}\,\frac{1}{e^x-1}\Bigg|_o^\alpha + \frac{1}{m+1}\, J^o_{m+1}(\alpha)$$

where:

$$\left[\frac{x^{m+1}}{e^x-1}\right]_{x=o} = \begin{cases} o & : \quad m > o \\ 1 & : \quad m = o \end{cases}$$

Then, for $n > 0$:

$$J_n(\mu,\alpha) = \frac{1}{e^{2\mu}-1}\sum_{m=o}^{n}\frac{1}{m+1}\binom{n}{m}\mu^{n-m}\left[\left[\frac{(\alpha-\mu)^{m+1}}{e^{\alpha-\mu}-1}\right.\right.$$

$$+ (-1)^{n-m+1}\frac{(\alpha+\mu)^{m+1}}{e^{\alpha+\mu}-1} - (-1)^{m+1}\left\{e^\mu + (-1)^n\right\}\frac{\mu^{m+1}}{e^\mu-1} \tag{2}$$

$$\left.\left. + J^o_{m+1}(\alpha-\mu) + (-1)^{n-m+1}J^o_{m+1}(\alpha+\mu) - (-1)^{m+2}\left\{1+(-1)^{n+1}\right\}J^o_{m+1}(\mu)\right]\right]$$

B: General expression for $K_n(\mu,\alpha)$:

$$K_n(\mu,\alpha) = \int_0^{\alpha} x^n \, dx \Big/ \left(e^x - e^{\mu}\right)\left(e^{\mu} - e^{-x}\right)\left(e^x - 1\right) \tag{3}$$

We split the three factors as follows:

$$\frac{1}{\left(e^x - e^{\mu}\right)\left(e^{\mu} - e^{-x}\right)} = \frac{e^{-\mu}}{\left(e^{2\mu} - 1\right)} \left[\frac{1}{e^{x-\mu} - 1} - \frac{1}{e^{x+\mu} - 1}\right]$$

$$\frac{1}{\left(e^x - 1\right)\left(e^{x\pm\mu} - 1\right)} = \frac{e^{-x}}{\left(e^{\pm\mu} - 1\right)} \left[\frac{1}{e^x - 1} - \frac{1}{e^{x\pm\mu} - 1}\right]$$

$$\frac{1}{e^x(e^x - 1)} = \left[\frac{1}{e^x - 1} - \frac{1}{e^x}\right]$$

and use the relation:

$$\int_0^{\alpha} \frac{x^m}{e^x - 1} \, dx = \frac{x^{m+1}}{m+1} \frac{1}{e^x - 1} \Bigg|_0^{\alpha} + \frac{1}{m+1} J^o_{m+1}(\alpha)$$

Then:

$$K_n(\mu,\alpha) = \frac{e^{-\mu}}{(e^{2\mu} - 1)(e^{\mu} - 1)} \int_0^{\alpha} x^n e^{-x} dx \left[\frac{1}{e^{x+\mu} - 1} + \frac{e^{\mu}}{e^{x-\mu} - 1} - \frac{(1+e^{\mu})}{e^x - 1}\right]$$

$$= \frac{e^{-\mu}}{(e^{2\mu} - 1)(e^{\mu} - 1)} \left[\int_0^{\alpha} (x-\mu)^n \, dx \, \frac{e^{\mu - x}}{e^x - 1} + \int_{-\mu}^{\alpha-\mu} (x+\mu)^n \, dx \, \frac{e^{-x}}{e^x - 1}\right.$$

$$\left. - (1 + e^{\mu}) \int_0^{\alpha} \frac{x^n \, dx \, e^{-x}}{e^x - 1}\right]$$

From this, we have:

$$K_n(\mu,\alpha) = \frac{1}{(e^{\mu}-1)(e^{\mu}-1)}\Bigg[\sum_{m=o}^{n} \frac{1}{m+1}\binom{n}{m}\mu^{n-m}\Bigg\{e^{\mu}(-1)^{n-m}\left[\frac{(\alpha+\mu)^{m+1}}{e^{\alpha+\mu}-1} - \frac{\mu^{m+1}}{e^{\mu}-1}\right] + \frac{(\alpha-\mu)^{m+1}}{e^{\alpha-\mu}-1} - (-1)^{m+1}\frac{\mu^{m+1}}{e^{-\mu}-1}$$

$$- (m+1)\left[(-1)^{n-m}e^{\mu}\zeta_m(\alpha+\mu,\mu) + \zeta_m(\alpha-\mu,\mu)\right]$$

$$+ e^{\mu}(-1)^{n-m}\left[J^{o}_{m+1}(\alpha+\mu) - J^{o}_{m+1}(\mu)\right] + \left[J^{o}_{m+1}(\alpha-\mu)\right.$$

$$\left.+ (-1)^{m+1}J^{o}_{m+1}(\mu)\right]\Bigg\} - \frac{(1+e^{\mu})}{n+1}\frac{\alpha^{n+1}}{e^{\alpha}-1}$$

$$- \frac{(1+e^{\mu})}{n+1}J^{o}_{n+1}(\alpha) - (1+e^{\mu})\zeta_n(\alpha,0)\Bigg] \qquad (4)$$

where:

$$\zeta_n(a,b) = \int_b^a x^n e^{-x}\,dx$$

$$= -e^{-x}\sum_{r=0}^{n} x^{n-r}\,n(n-1)\ldots(n-r+1)\Bigg|_b^a \qquad (5)$$

C: $J_n(\mu,\alpha)$ and $K_n(\mu,\alpha)$ at low temperature.

We shall evaluate these integrals for two cases,

[i] $\alpha \gg \mu \gg 1$ $(K\Theta \gg h\omega \gg KT)$

[ii] $\alpha \gg \mu$, μ 0

For the other limiting case of $\mu > > \alpha$, Equation (1) of Appendix is applicable.

From Equations and , we obtain the following simplified expressions:

[i] $$J_n(\alpha,\mu) \approx e^{-2\mu}\,\mu^{n+1} \sum_{m=0}^{n} \frac{(-1)^m}{m+1} \binom{n}{m} \tag{6}$$

$$K_n(\mu,\alpha) \approx -2\mu \left[-n! \left(1 + \sum_{s=1}^{\infty} \frac{1}{s^{n+1}}\right) + \sum_{m=0}^{n} \frac{(-1)^{n+m}}{m+1} (m+1)! \binom{n}{m} \mu^{n-m} \left(\sum_{s=1}^{\infty} \frac{1}{s^{m+1}} - 1 \right) \right] \tag{7}$$

: $\alpha \gg \mu \gg 1$

[ii] $$J_n(\alpha,\mu) \approx \frac{2}{e^{2\mu}-1} \left\{ \mu\, J_n^o(\infty) + \mu^3 \frac{n(n-1)}{3!} J_{n-2}^o(\infty) + \mu^5 \frac{n(n-)(n-)(n-)}{5!} J_{n-4}^o(\infty) + \mu^7 \frac{n(n-1)\ldots(n-5)}{7!} J_{n-6}^o(\infty) + \ldots \right\} \tag{8}$$

$$K_n(\alpha,\mu) \approx \frac{1}{(e^{2\mu}-1)(1-e^{-\mu})} \left[\left[\frac{\mu^{n+1}}{e^{\mu}-1}\left\{\sum_{m=0}^{n} \frac{(-1)^{m+1}}{m+1}\binom{n}{m} \quad 1+(-1)^n\right\}\right.\right.$$

$$+ \sum_{m=0}^{n} \frac{\mu^{n-m}}{m+1} \quad (m+1)!\binom{n}{m} e^{-\mu} + (-1)^{n-m}\left(\sum_{s=1}^{\infty} \frac{1}{s^{m+1}} - 1\right)$$

$$\left.\left. - n!\ (1 + e^{-\mu}) \quad \left(1 + \sum_{s=1}^{\infty} \frac{1}{s^{n+1}}\right)\right]\right] \qquad (9)$$

: $\alpha \gg \mu, \quad \mu \gtrsim 0$

where $J^{o}_{n}(\infty)$ is given by Equation (3) of Appendix . Equations (6), (7), (8) and (9) are sufficient to enable us to calculate $b_{ep}(\mu,\alpha)$ at very low temperatures even in the very far infrared.

APPENDIX D.

ON THE QUESTION OF EXISTENCE OF $\cos^2\theta \leq 1$ AT THE SINGULARITY $\xi=0$

The theoretical calculations of the transition probability rested on the assumption that there exists a $\cos^2\theta$ which satisfies the condition:

$$\delta(\xi) = 1,$$

and hence:

$$\xi = E(\underline{k}+r\underline{q}) - E(\underline{k}) - rE(\underline{q}) - sh\omega = 0 \qquad (1)$$

$$; \; r,s = (\pm)$$

and:

$$\cos\theta = (\underline{k}\cdot\underline{q}/k\ q) \qquad (2)$$

The existence of such a $\cos\theta$ was asserted by Wilson (1936) for the processes which do not involve an external electromagnetic field.

We shall show that such a $\cos\theta$ exists also in the presence of the electromagnetic field.

From Equation (1), we have:

$$\cos\theta = \left[-sr\ \frac{m^*\omega}{h\ kq} + \left(\frac{m^*uL}{hk}\right) - r\ \frac{q}{2k}\right] \qquad (3)$$

In comparing the order of magnitude of the three terms on the R.H.S. of Equation (3), we shall use the typical values:

$$m^* \simeq 10^{-27} \quad (q)$$

$$u_L \simeq 10^5 \quad (cm/sec)$$

$$v_F \simeq 10^8 \quad (cm/sec)$$

$$q_o = \left(\frac{K}{h\ u_L}\right) \simeq 10^8 \quad (cm^{-1}) \text{ for } \sim 10^2 \ ^\circ K$$

The first term is rewritten as:

$$A = \left(\frac{m^*\omega}{hkq}\right) = 2\pi \left(\frac{c}{v_F}\right) \left(\frac{1}{\lambda\ q}\right) \tag{4}$$

and the second term as:

$$B = \left(\frac{m^* u_L}{h\ k}\right) = \left(\frac{u_L}{v_F}\right) \simeq 10^{-3} \tag{5}$$

At ordinary and higher temperatures, the phonons with $q \approx q_o$ are active, and hence we have:

$$A \lesssim (2\pi)10^{-2} \quad \text{for } \lambda \gtrsim 1\mu.$$

In this case, the third term is the only important one, and any q equal to or smaller than $(2k_F)$ gives us $\cos\theta \leq 1$ satisfying the condition (1). Thus, we have

$$\begin{aligned} &\cos^2\theta \leq 1 && : \quad q_o \geq 2k_F \\ &\cos^2\theta \leq {}^1/_4 \left(\frac{q_o}{k_F}\right)^2 && : \quad q_o < 2k_F \end{aligned} \tag{6}$$

In general, the second of the above two applies. When $q_o \geq 2k_F$, the integral over q must be cut off at $q=2k_F$.

The scattering angle ϕ is defined as:

$$\cos\phi = \left(\vec{k} \cdot \vec{k}' / k\ k'\right) \tag{7}$$

$$\vec{k}' = \left(k + r\vec{q} + s\vec{q}\right)$$

$$\simeq \left(\vec{k} + r\vec{q}\right)$$

Then, ϕ is related to θ by the relation:

$$\left(k^2 + q^2 + 2r\cos\theta\right)^{\frac{1}{2}} \cos\phi = k\left(1 + r\frac{q}{k}\cos\theta\right) \tag{8}$$

Then, upon writing:

$$q_o \cong (2\pi)\left(\tfrac{3}{4}\pi V_o\right)^{\frac{1}{3}} \tag{9}$$

$$k \cong k_F \cong (2\pi)\left(\tfrac{3}{8}\pi V_o\right)^{\frac{1}{3}}$$

we easily see that the second condition of Equation (6) corresponds to

$$\phi < 78.1$$

in agreement with the usual value of 79° for elastic scattering ($k' = k$), and that the first condition of Equation (6) corresponds to $0 < \phi < \pi$, thus scatterings are possible for all angles.

At low temperatures, the phonons with

$$h\ u_L q \approx KT \tag{10}$$

are active, and it is easily seen in Equation (3) that the first term (e.m.-phonon term) can be the most important one. For such a case, we have

$$A \lesssim \frac{1}{T} \quad \text{for} \quad \lambda \gtrsim 1\mu.$$

and hence

$$\cos^2\theta \lesssim \frac{1}{T^2} \quad ; \quad \lambda \gtrsim 1\mu \tag{11}$$

so that for $T \gtrsim 1°K$, it is assured that a $\cos^2\theta \leq 1$ exists.

REFERENCES

1. M. Minnaert, The Sun , edited by E. Kuiper, Chicago, University of Chicago Press, 1953, p 88.

2. R. Tousey, ibid, p 658.

3. C. de Jager, "Structure and Dynamics of the Solar Atmosphere," Encyclopedia of Physics, Berlin, Springer Publishing Co., Inc., 1959, vol. LII.

4. H. Friedman, T. A. Chubb, J. E. Kupperian, R. W. Kreplin and J. C. Lindsay, IGY Rocket Report Series, 1, 183 (1958).

5. J. A. Van Allen, Sci. American, 200, 39 (1959).

6. A. C. B. Lovell, "Geophysical Aspects of Meteors," Encyclopedia of Physics, Berlin, Springer Publishing Co., Inc., 1957, vol. XLVIII, p 453.

7. F. L. Whipple and G. S. Hawkins, "Meteors," Encyclopedia of Physics, Berling, Springer Publishing Co., Inc., 1959, vol. LII, p 519.

8. G. Robillard, J. Am. Rocket Soc., 29, 492 (1959).

9. H. C. van de Hulst, Light Scattering by Small Particles , New York, John Wiley and Sons, 1957.

10. E. Schmidt and E. Eckert, Forsch. Gebiete Ingenieurw., 6, 175 (1935).

11. M. Jakob, Heat Transfer , New York, John Wiley and Sons, 1959, vol. I.

12. V. Twersky, J. Appl. Phys., 22, 825 (1951).

13. W. S. Partridge, H. B. Vanfleet and G. R. Whited, J. Appl. Phys., 29, 1333 (1958).

14. G. D. Anderson, D. G. Doran, F. S. Hempy and M. C. Kells in Proc. Third Symposium on Hypervelocity Impact, Oct. 1958, vol. I, p 45; Armour Res. Found., Chicago, Ill., 1959.

15. G. H. Kinchin and R. S. Pease, Repts. Progr. in Phys., 18, 1 (1955).

16. F. Seitz and J. S. Koehler, Solid State Phys., 2, 305 (1956).

17. J. A. Brinkman, J. Appl. Phys., 961 (1954).

18. J. W. Marx, H. G. Cooper and J. W. Henderson, Phys. Rev., 88, 106 (1952).

19. H. G. Cooper, J. S. Koehler and J. W. Marx, Phys. Rev., 94, 496 (1954).

20. M. F. Kaplon, B. Peters, H. L. Reynolds and D. M. Ritson, Phys. Rev., 85, 295 (1952).

21. W. John, "Passage of Particles through Matter," Amer. Inst. Phys. Handbook, New York, McGraw-Hill Book Company, Inc., 1957, pp 8-24.

22. H. O. McMahon, J. Opt. Soc. Amer., 40, 376 (1950).

23. H. Y. Fan, "Infrared Absorption in Semiconductors," Repts. Progr. in Phys., 19, 108 (1956).

24. Conference on Radiation Effects in Semiconductors, Gatlinburg, Tenn., May 1959: J. Appl. Phys., 30, August 1959.

25. H. Y. Fan and A. K. Ramdas, ibid., p 1127.

26. F. Seitz, Revs. Modern Phys., 18, 384 (1946).

27. W. MacNevin, Chem. Eng. News, 30, 1728 (1952).

28. W. A. Weyl and T. Foerland, Ind., Eng. Chem., 42, 257 (1950).

29. C. F. Goodeve, Trans. Faraday Soc., 33, 340 (1937).

30. G. Hass, F. Drummeter and M. Schach, J. Opt. Soc. Am., 49, 918 (1959).

31. K. Sun and N. J. Kreidl, Glass Ind., 33, 589 and 651 (1952).

32. S. D. Stookey, Ind. Eng. Chem., 41, 856 (1949).

33. N. J. Kreidl and J. R. Hensler, J. Opt. Soc. Am., 47, 73 (1957).

34. Blau, H. H., Jr., "High Temperature Thermal Radiation Properties of Solid Materials," Arthur D. Little, Inc., Scientific Report No. 2, Contract AF19(604)-2639, March 31, 1960.

35. Gier, Dunkle, and Devans, J. Opt. Soc. Am., 44, 558 (1954) "Measurement of Absolute Spectral Reflectivity from 1.0-15.0 μ."

36. Weber, D., J. Opt. Soc. Am., 49, 815 (Aug. 1959) "Spectral Emissivity of Solids in Infrared at Low Temperature."

37. "Spectral Reflectance Properties of Tin-Plated Steel", Report to United States Steel Corporation, Arthur D. Little, Inc., November 8, 1960.

38. Benford, Lloyd, and Schwarz, J. Opt. Soc. Am., 88, 445 (1948) "Coefficients of Reflection of Magnesium Oxide and Magnesium Carbonate."

39. Benford, Schwarz, and Lloyd, J. Opt. Soc. Am., 38, 964 (1948) "Coefficients of Reflection in Ultraviolent of $MgCO_3$ and MgO."

40. Middleton and Sanders, J. Opt. Soc. Am., 41, 419 (1951) "Absolute Spectral Diffuse Reflectance of MgO."

41. Sanders and Middleton, J. Opt. Soc. Am., 43, 58 (1953) "Absolute Spectral Diffuse Reflectance of MgO in the Near Infrared."

42. Jaques, McKeehan, Huss, Dimitroff, and Kuppenheim, J. Opt. Soc. Am., 45, 971 (1955) "Integrating Sphere for the Measurement of Reflectance with the Beckman Model DR Recording Spectrophotometer."

43. Tegart, W. J. McG., The Electrolytic and Chemical Polishing of Metals , Pergamon Press, 1959.

44. Smithsonian Physical Tables, 9th ed., 1954, p 552, W. E. Forsythe.

45. Abeles, F., (1957) J. Opt. Soc. Am. 47, 473.

46. Beattie, J. R., and G. K. T. Conn (1955), Phil Mag. (7) 46, 989.

47. Beattie, J. R., (1955) Phil. Mag. 46, 235.

48. Benthem, C. W., and R. Kronig (1954), Physica 20, 293.

49. Biondi, M., (1956) Phys. Rev. 102, 964.

50. Bardeen, Jr., and W. Schokley (1950) Phys. Rev. 80, 69, 72.

51. Born, M., and K. Huang (1956), Dynamic Theory of Crystal Lattices, Oxford University Press.

52. Bor, J., A. Hobson, and C. Wood, Proc. Phys. Soc. (London) 51, 932.

53. Biondi, M., and M. P. Garfunkel (1959) Phys. Rev. 116, 853.

54. Bardeen, J., L. N. Cooper, and Schrieffer (1957) Phys. Rev. 108, 1175.

55. Blau, H. H. Jr., J. L. Miles, and L. E. Ashman (1958) The Thermal Radiation Characteristics of Solid Materials - A Review, Arthur D. Little, Inc., AFCRC-TN-58-132, ASTIA Document No. AD 146833.

56. Drude, P., (1902) Theory of Optics, Longmans Green and Co., New York.

57. Drude, P., (1904) Ann. Physik 14, 677, 936.

58. Dingle, R. B., (1952) Physica 18, 985 (Letter).

59. Dingle, R. B., (1953) Physica 19, 311, 348, 729.

60. Foesterling, K., and V. Freedericksz (1913), Ann. Physik 40, 200.

61. Gordon, A. N., and E. H. Sondheimer (1953), Appl. Sci. Res. B 3, 297.

62. Ginsberg, V. L., and V. P. Silin (1956), Soviet Phys JETP 2, 46.

63. Gerlach (1932), Ann. Physik 14, 589.

64. Quincke, G., (1874) Poddend. Ann. Jubelband 336.

65. Reuter, G. E. H., and E. H. Sondheimer (1948) Proc. Roy Soc. (London) A195, 336.

66. Ramanathan, K. G., (1952) Proc. Phys. Soc. A65, 532.

67. Roberts, S., (1955) Phys. Rev. 100, 1667.

68. Richards, P. L., and M. Tinkham (1960) Phys. Rev. 119, 575.

69. Seitz, F., and D. Turnbull (1958), Solid State Physics, Vol. 6, Academic Press, Inc., New York.

70. Schulz, L. G., (1951) J. Opt. Soc. Am. 41, 1047.

71. Schulz, L. G., (1954) J. Opt. Soc. Am. 44, 357.

72. Schulz, L. G., (1957) (a) Advances in Physics 6, 102 (b) J. Opt. Soc. Am. 47, 64 (c) J. Opt. Soc. Am. 47, 70.

73. Slater, J. C., (1949) Phys. Rev. 76, 1592.

74. Tool, A. Q., (1910) Phys. Rev. 31, I.

75. Van Vleck, J. H., (1959) The Theory of Electric and Magnetic Susceptibilities, Oxford University Press, 1959 edit.

76. von Wartenburg, H., (1910) Verhandl. Deut. Physik Ges. 12, 105.

77. Wilson, A. H., (1936) The Theory of Metals, Cambridge University Press, 1958 edit.

78. Wilson, A. H., (1938) Proc. Roy. Soc. A167, 580 and (1937) Proc. Camb. Phil. Soc. 33, 371.

79. Wannier, G. H., (1937) Phys. Rev. 52, 191.

80. Weiss, P., (1907) J. Phys. Radium 6, 661.

81. Wolfe, R., (1954) Proc. Phys. Soc. A67, 74.

82. Wolfe, R., (1955) Proc. Phys. Soc. A68, 121.

83. (H-No. 1) American Institute of Physics Handbook, McGraw-Hill Book Company, New York, (1957).

84. (H-No. 2) Smithsonian Physical Tables, 9th rev. edit. The Smithsonian Institution, Washington, D.C. (1954).

NASA-Langley, 1963

NASA TN D-1523
National Aeronautics and Space Administration.
OPTICAL PROPERTIES OF SATELLITE MATERIALS - THE THEORY OF OPTICAL AND INFRARED PROPERTIES OF METALS. Research Projects Division. March 1963. 253p. OTS price, $4.00. (NASA TECHNICAL NOTE D-1523)

The probable effects of solar radiation, primary cosmic rays, van Allen radiation and meteoric dust on the emissive properties of materials are reviewed in the light of recently published data. Experimental data on the spectral emittance (0.25 to 27 microns) of metals with polished and carefully abraded surfaces are presented. A quantum mechanical theory of optical and infrared dispersion in metals originally developed by T. Holstein and previously presented in unpublished Westinghouse Research Laboratories Research Reports 60-94698-3-R1 and 60-94698-3-R6 (1954 and 1955) is combined with other existing theories of Umklapp and impurity scattering processes

(over)

I. Research Projects Division
II. NASA TN D-1523

NASA

NASA TN D-1523
National Aeronautics and Space Administration.
OPTICAL PROPERTIES OF SATELLITE MATERIALS - THE THEORY OF OPTICAL AND INFRARED PROPERTIES OF METALS. Research Projects Division. March 1963. 253p. OTS price, $4.00. (NASA TECHNICAL NOTE D-1523)

The probable effects of solar radiation, primary cosmic rays, van Allen radiation and meteoric dust on the emissive properties of materials are reviewed in the light of recently published data. Experimental data on the spectral emittance (0.25 to 27 microns) of metals with polished and carefully abraded surfaces are presented. A quantum mechanical theory of optical and infrared dispersion in metals originally developed by T. Holstein and previously presented in unpublished Westinghouse Research Laboratories Research Reports 60-94698-3-R1 and 60-94698-3-R6 (1954 and 1955) is combined with other existing theories of Umklapp and impurity scattering processes

(over)

I. Research Projects Division
II. NASA TN D-1523

NASA

NASA TN D-1523
National Aeronautics and Space Administration.
OPTICAL PROPERTIES OF SATELLITE MATERIALS - THE THEORY OF OPTICAL AND INFRARED PROPERTIES OF METALS. Research Projects Division. March 1963. 253p. OTS price, $4.00. (NASA TECHNICAL NOTE D-1523)

The probable effects of solar radiation, primary cosmic rays, van Allen radiation and meteoric dust on the emissive properties of materials are reviewed in the light of recently published data. Experimental data on the spectral emittance (0.25 to 27 microns) of metals with polished and carefully abraded surfaces are presented. A quantum mechanical theory of optical and infrared dispersion in metals originally developed by T. Holstein and previously presented in unpublished Westinghouse Research Laboratories Research Reports 60-94698-3-R1 and 60-94698-3-R6 (1954 and 1955) is combined with other existing theories of Umklapp and impurity scattering processes

(over)

I. Research Projects Division
II. NASA TN D-1523

NASA

NASA TN D-1523
National Aeronautics and Space Administration.
OPTICAL PROPERTIES OF SATELLITE MATERIALS - THE THEORY OF OPTICAL AND INFRARED PROPERTIES OF METALS. Research Projects Division. March 1963. 253p. OTS price, $4.00. (NASA TECHNICAL NOTE D-1523)

The probable effects of solar radiation, primary cosmic rays, van Allen radiation and meteoric dust on the emissive properties of materials are reviewed in the light of recently published data. Experimental data on the spectral emittance (0.25 to 27 microns) of metals with polished and carefully abraded surfaces are presented. A quantum mechanical theory of optical and infrared dispersion in metals originally developed by T. Holstein and previously presented in unpublished Westinghouse Research Laboratories Research Reports 60-94698-3-R1 and 60-94698-3-R6 (1954 and 1955) is combined with other existing theories of Umklapp and impurity scattering processes

(over)

I. Research Projects Division
II. NASA TN D-1523

NASA

NASA TN D-1523

and is shown to successfully account for the optical properties of metals in the entire free electron region at all temperatures of interest. Detailed calculations are presented for monovalent and some polyvalent metals for which assumption of a symmetric Fermi surface is valid. Polyvalent and transition metals for which interband transitions are important and the Fermi surface is not spherical are also considered. In all, more than a dozen metals, for which reliable experimental data are available, have been successfully treated. Calculations of the absorption properties of super-conducting metals are also presented in an attempt to determine the extent to which bulk electron-phonon processes are responsible for infrared absorption by super-conductors.

NASA

NASA TN D-1523

and is shown to successfully account for the optical properties of metals in the entire free electron region at all temperatures of interest. Detailed calculations are presented for monovalent and some polyvalent metals for which assumption of a symmetric Fermi surface is valid. Polyvalent and transition metals for which interband transitions are important and the Fermi surface is not spherical are also considered. In all, more than a dozen metals, for which reliable experimental data are available, have been successfully treated. Calculations of the absorption properties of super-conducting metals are also presented in an attempt to determine the extent to which bulk electron-phonon processes are responsible for infrared absorption by super-conductors.

NASA

NASA TN D-1523

and is shown to successfully account for the optical properties of metals in the entire free electron region at all temperatures of interest. Detailed calculations are presented for monovalent and some polyvalent metals for which assumption of a symmetric Fermi surface is valid. Polyvalent and transition metals for which interband transitions are important and the Fermi surface is not spherical are also considered. In all, more than a dozen metals, for which reliable experimental data are available, have been successfully treated. Calculations of the absorption properties of super-conducting metals are also presented in an attempt to determine the extent to which bulk electron-phonon processes are responsible for infrared absorption by super-conductors.

NASA

NASA TN D-1523

and is shown to successfully account for the optical properties of metals in the entire free electron region at all temperatures of interest. Detailed calculations are presented for monovalent and some polyvalent metals for which assumption of a symmetric Fermi surface is valid. Polyvalent and transition metals for which interband transitions are important and the Fermi surface is not spherical are also considered. In all, more than a dozen metals, for which reliable experimental data are available, have been successfully treated. Calculations of the absorption properties of super-conducting metals are also presented in an attempt to determine the extent to which bulk electron-phonon processes are responsible for infrared absorption by super-conductors.

NASA